# Behaviour of Concrete Incorporating Ground Glass and Alkali-Reactive Aggregates

**Thèse**

**Isabelle Fily-Paré**

**Doctorat interuniversitaire en sciences de la Terre**
Philosophiæ doctor (Ph. D.)

Québec, Canada

# Behaviour of Concrete Incorporating Ground Glass and Alkali-Reactive Aggregates

**Thèse**

**Isabelle Fily-Paré**

Sous la direction de :

Benoît Fournier, directeur de recherche

Josée Duchesne, codirectrice de recherche

Arezki Tagnit-Hamou, codirecteur de recherche

# Résumé

L'objectif de cette étude doctorale était de mieux comprendre le comportement d'un ajout cimentaire alternatif à haute teneur en alcalis comme le verre broyé (VB) face au phénomène de la réaction alcalis-silice (RAS). Ainsi, des systèmes cimentaires binaires et ternaires composés de ciments de différentes teneurs en alcalis (0.63 à 1.25% $Na_2Oeq$), de VB (10 – 30%) et d'un des ajouts cimentaires suivants : fumée de silice (FS) (5 - 10%), métakaolin (MK) (5 – 15%), cendre volante (CV) (15 – 30%) ou laitier de hauts fourneaux (LHF) (20 – 40%), ont été utilisés pour la fabrication de prismes de béton et de pâtes cimentaires. Les prismes de béton incorporant un calcaire hautement réactif (Spratt) ont été conditionnés à 38°C avec une H.R.>95% et leur changement dimensionnel suivi pour une période de deux ans. Les échantillons de pâtes cimentaires ont été, quant à eux, conservés dans des contenants hermétiques à 38°C et leur solution interstitielle extraite sous pression et analysée après 28 et 182 jours de conditionnement pour en déterminer la concentration en $Na^+$ et $K^+$.

Contrairement à ce qui est attendu en fonction des connaissances actuelles, les résultats des analyses chimiques indiquent que le sodium du VB n'est pas relâché dans la solution interstitielle en proportion de son contenu original (>13% $Na_2O$), du moins pour les systèmes ternaires étudiés. L'ajout de VB réduit la $[K^+]$ de manière plus importante que ne le ferait une simple dilution du ciment, alors que la $[OH^-]$ est modestement influencée par l'ajout de VB.

L'expansion des éprouvettes fabriquées à partir des mélanges ternaires étudiés n'est pas fonction du pourcentage de VB dans le système; d'ailleurs, de nombreux mélanges se trouvent de part et d'autre de la limite de 0.040% de deux ans préconisée par la Pratique Normalisée CSA A23.2-28A. La nature et la proportion de FS/MK/CV/LHF a un impact plus important que la quantité de VB. L'ajout de NaOH au mélange, tel que recommandé pour fins d'accélération lors des essais réalisés en laboratoire, semble réduire l'expansion de nombreux mélanges ternaires incorporant du VB.

# Abstract

The aim of this Ph.D. project was to deepen the understanding of the behaviour of a high-alkali Supplementary Cementitious Material (SCM) like Ground Glass (GG) on Alkali-Silica Reaction (ASR). Thus, binary and ternary cementitious systems made of 1) cements of different alkali contents (0.63 to 1.25% $Na_2Oeq$) 2); GG (10 - 30%) and 3) one of the following supplementary cementitious materials: Silica Fume (SF) (5 – 10%), Metakaolin (MK) (5 – 15%), Fly Ash (FA) (15 – 30%) or Blast Furnace Slag (BFS) (20 – 40%), were used to manufacture concrete prisms and cement pastes. Concrete prisms incorporating a highly reactive limestone (Spratt) were stored at 38˚C with a R.H.>95% and their dimensional change monitored for a period of two years. Cement paste samples were stored at 38˚C in sealed containers and their pore solution was extracted under pressure and analyzed for their concentration of $Na^+$ and $K^+$ (28 and 182 days).

To the contrary of the expectations based on actual knowledge, the results of the chemical analysis suggest that the sodium of the GG is not released into the pore solution proportionally to its original content (13% $Na_2O$), at least for the cementitious systems studied. The addition of GG reduces the $[K^+]$ more significantly than would do a simple cement dilution, while the $[OH^-]$ is modestly influenced by the addition of GG in the system.

The expansion of the prisms cast from the ternary mixtures studied is not a function of the percentage of GG in the system and many expansion results of mixtures are found on either side of the 0.040% two-year limit proposed by CSA Standard Practice A23.2-28A.The nature and proportion of FS/MK/CV/LHF in the system is more significant that the GG content. The addition of NaOH to the mixture, as recommended for acceleration purposes in laboratory tests, appears to reduce the expansion of many ternary mixtures incorporating GG

# Table of content

# List of Figures

# List of Tables

*Cher Éric, chère famille, chers ami(e)s, chers professeur(e)s, chers mentors, vous m'avez inspiré le plaisir d'observer, l'humilité de considérer plusieurs points de vue, la patience d'écouter, le courage de s'exprimer et la résilience. Vous m'avez fait connaître la joie de partager, l'amour et la force. À vos belles qualités, je dédie cet ouvrage.*

# Remerciements

J'ai tellement de gratitude à exprimer à tous ceux qui ont directement ou indirectement participé à mon projet doctoral. Je ne l'oublierai jamais. À commencer par Benoit et Josée, qui ont été d'une disponibilité exceptionnelle pour encourager et nourrir ma curiosité intellectuelle et aussi (surtout) pour la diriger. J'ai vécu quelques moments d'épiphanie en analysant mes résultats ou en lisant des articles et j'ai eu la chance de tomber sur des portes ouvertes quand j'ai couru à leur bureau (sans aucun préavis). Vous avez répondu à l'appel quand j'étais à la recherche de gens avec qui partager les joies de la recherche. Avec beaucoup de gratitude, j'emporte avec moi ces moments où vous avez accueilli mon enthousiasme. Arezki, malgré les kilomètres et les décalages horaires qui ont complexifiés nos communications, nos moments d'échanges intellectuellement fructueux m'ont toujours laissée avec le sentiment d'être encouragée et aussi avec l'impression que si quelque chose allait mal dans mon projet, tu trouverais une manière de faire tomber les kilomètres et d'arranger ce qui cloche. J'ai eu du plaisir à faire mon travail dans un contexte de grande sécurité psychologique.

J'ai tellement de reconnaissance à exprimer à tous ceux qui y ont contribué aux nombreux moments de joie. Claudia, pour les folies comme les déguisements de licornes le jour de l'halloween et Edgardo pour m'avoir initié à je ne sais combien de podcasts à propos de tous les sujets du monde. Vous avez été d'une compagnie exceptionnelle et la rigueur avec laquelle vous m'avez assistée dans mes travaux m'a permis de faire tout ce que j'avais à faire avec tranquillité d'esprit. Combien de centaines de prismes avons-nous coulé Edgardo et combien de centaines de solutions avons-nous dilué Claudia? Je me surprends de repenser à ce laborieux travail avec joie et je vous attribue tout le mérite de ce beau sentiment! Je me dois de remercier René, P-A et Thomassin pour leur judicieux conseils et pour avoir résolu la totalité de mes problèmes d'équipements. Encore une fois, grâce à vous je retire des souvenirs étrangement chaleureux des moments difficiles liés aux travaux de laboratoires.

Benoit, tu es très humble et j'espère que tu accepteras que je mentionne avoir été inspirée par toi à bien des égards. Tes suggestions en termes de communication orale et écrite m'ont inspiré et j'ai fini par me trouver un style qui m'ouvre la porte pour de grandes tribunes. À force de te côtoyer j'ai essayé de me laisser influencer par tes aptitudes à l'écoute dans l'espoir de faire du bien autour de moi comme tu fais du bien autour de toi. Merci de m'avoir inspiré des qualités importantes sur le plan scientifique, mais aussi humain. Je remercie ta bienveillance qui t'a value quelques confidences de ma part et je remercie également tes conseils qui ont fait évoluer mon projet.

Josée, je voudrais que tu saches qu'une des fiertés de ma thèse vient de toi. J'ai appris à me connaître avec toi et tu m'as fait accomplir des choses dont je ne me serais pas crue capable. Ton souvenir m'inspirera l'audace de me dépasser pour les années à venir.

Au Plt-3755 et à tous ses habitants; Cédric, Fred, Tony, JB, Math, Mélissa, Rod et Steeve. Je voudrais vous remercier pour les évènements qui ont fait l'ambiance du bureau comme remplir des bottes de travail de brillant de bricolage, coller tous les objets du bureau sur le bureau, emballer individuellement les livres d'une bibliothèque, remplir les tiroirs de pompons et autres… La recherche est un contexte demandant de donner libre court à la créativité... et on l'avait! Dans une aussi belle ambiance, nous avons été une équipe qui s'entraide au laboratoire, qui s'échange des articles, qui s'explique des notions et qui se supporte dans tous les aspects de la vie. Merci.

Ma chère sœur, aussi loin que je me souvienne, tu étais là pour tous les moments de ma vie. J'espère que tu sais à quel point je te suis reconnaissante et t'admire. J'ai une petite sœur grande comme une géante. Merci de m'avoir permis de ventiler les moments moins évidents et aussi de féliciter le choix de couleur de mes graphiques ;). En fait, je dois partager toutes les réussites de ma vie avec ma famille qui m'a toujours supportée. À maman pour ta grande écoute et tes précieux conseils humains. À papa pour croire qu'il n'y a rien à mon épreuve. À Yann pour m'amener au spa juste parce que la vie c'est beau et François pour partager ta sagesse entre deux coups de scrabble. À mamy pour avoir valorisé l'éducation toute notre vie et à Nini qui a toujours voulu nous apprendre à ricaner. Je ne sais pas où je serais sans l'amour et le support inconditionnel de ma famille.

À mes amis qui se souviennent encore que j'existe même si ces dernières années j'étais pas mal hors du radar, Marjorie, Guillaume, Simon, Jeff, Coco, Karine, Heidi, Claudia, Marie-Mich, François, Geneviève, Maxime, William, Fernando et Olly.

Je m'excuse au lecteur d'avoir été si longuement soutenue, mais je me dois de continuer mes interminables remerciements en exprimant ma reconnaissance à ma nouvelle équipe de travail. François, Éli-Anna, Loïc, Jean-Serge, Sébastien, Vincent, Louise, Nicolas et Éric. Vous avez apporté un bouffé d'air frais dans ma vie avec vos sourires, votre enthousiasme et votre dévouement pour nos projets et notre équipe. J'aimerais rajouter Richard et Pierre, vous faites partie d'à peu près tous les projets innovants dans le domaine et je ne peux faire autrement que de vous remercier pour avoir apporté les réalités du terrain à mes essais. Michel et Marie-Josée, les conséquences de votre enthousiasme contagieux sont probablement parmi vos grandes œuvres. Finalement, Éric, ses dernières semaines, tu as pris le relais sur le reste de notre vie quand j'étais débordée, tu as pris soin de notre santé mentale avec toutes tes blagues, ta guitare et ton harmonica. Tu m'apaises et tu recharges mes batteries. Je te suis tellement reconnaissante.

Cette thèse pourrait être signée Isabelle et al., car vous y avez tous contribué. Merci du fond du cœur d'y avoir participé et d'en partager tous les mérites!

# Foreword

This thesis combines a literature review and seven articles that are first authored by the Ph. D. candidate. The experimental planning, the production and testing of specimens, the analysis of the test results and the writing of the articles were all fulfilled by the first author. The co-authors, Benoit Fournier, Josée Duchesne and Arezki Tagnit-Hamou contributed to the research work by their advises, their comments, the revisions they made to the scientific papers, the technical and financial support.

The aim of the literature review is to empower the reader for an appreciation of the research work in depth; thanks to a background of fundamental knowledge linked to the research topics. The literature review is cautious in avoiding redundancy with the content of the seven articles composing the main body of the thesis and presents the fundamental aspects of the chemical reactions that act as protagonists in the various cementitious systems studied.

The first article - *Effect of Glass Powder (GP) on the availability of alkalis in the pore solution of binary cement pastes* - elaborates on the impact of Ground Glass (GG) on the composition of the pore solution of binary cementitious pastes (i.e., cement + GG). This article was peer-reviewed, published and presented in 2017 at the *10th ACI/RILEM International Conference on Cementitious Materials and alternative binders for sustainable concrete (ICCM 2017; Montreal - Canada).*

The second and third articles explore the parameters influencing the composition of the pore solution of ternary paste specimens incorporating GG. The second article - *Response Surface Methodology (RSM) to assess the impact of Ground Glass (GG), Silica Fume (SF) and Metakaolin (MK) on the composition of the pore solution* - deals with systems incorporating the latter SCMs, while the third article - *Response Surface Methodology (RSM) to assess the impact of Ground Glass (GG), Fly Ash (FA) and Blast Furnace Slag (BFS) on the composition of the pore solution* – is about cementitious systems incorporating GG and FA/BFS. Considering the tremendous amount of data generated through the testing/analysis of pore solutions from the various cementitious systems selected, which could not be incorporated in one single article without impacting on data analysis, the authors have decided to separate the information in two articles by combining the most alike SCMs i.e. SF with MK and FA with BFS. The authors are aware that this approach results is some textual redundancy, especially in the description of the experimental program and test procedures in both papers, which is unavoidable. It is also worth mentioning that raw data and complementary information were added in Appendices of the above two papers for the benefits of the readers and research teams. These articles are expected to be submitted to the Cement and Concrete Research Journal, where the practice of adding Appendices has been used before by this research team.

The fourth article - *Impact of Ground Glass (GG) on the ASR expansion of ternary concrete prisms incorporating Silica Fume (SF), Metakaolin (MK), Fly Ash (FA) or Blast Furnace Slag (BFS)* - focuses on the expansive behavior of ternary concretes incorporating GG according to the mixture design. This article will be submitted for publication in ACI Materials Journal.

The fifth article - *Impact of NaOH addition on the ASR expansion of ternary concretes incorporating Ground Glass (GG*) – dwells on the testing methods to assess the behavior regarding ASR of ternary concretes incorporating GG. This article was peer-reviewed and will be published and presented at the *16th International Conference on Alkali Aggregate Reaction in Concrete* in 2022 (Lisbon – Portugal).

The sixth and seventh articles relate the composition of the pore solution to the expansion due to ASR of concrete specimens incorporating GG. The sixth article - *Revisiting the relation between the alkalinity of pore solution and the expansion due to Alkali-Silica Reaction (ASR) in ternary mixtures incorporating Glass Powder (GP)* – is dedicated to SF and MK and was peer-reviewed, published and presented at the *15th International Congress on the Chemistry of Cement (ICCC 2019; Prague – Czech Republic)*. The seventh article - *Relation between Alkali Silica Reaction (ASR) and pore solution composition of ternary blends incorporating Ground Glass (GG) and Blast Furnace Slag (BFS)* - is dedicated to BFS and will be submitted to Construction and Building Materials Journal.

# Introduction

## General context

Humanity evolves and its constructions as well. Indeed, the nature of construction materials changes along with human growth. Concrete is part of the signature of nowadays landscapes to the point that it is regularly claimed to be the world's most consumed material after water. Its affordability, its strength, its capacity to be shaped at will or its durability are among the reasons why this material is continually chosen.

Concrete can be chosen in construction for a myriad of reasons; however, its adaptability regarding source materials might be its major advantage over other materials. More than ever, this potential for adaptation will serve us in our effort for building a civilization with a respectful attitude regarding sustainable development, i.e. respect of our land, natural resources and air quality. As a matter of fact, the World Business Council for Sustainable Development suggests the fact that Supplementary Cementitious Materials (SCMs) will continue to be critical in the development of concrete mix designs considering they are alleged to decrease the global carbon footprint of concrete despite of the increase of global consumption (WBCSD, 2018). More precisely, SCMs are a family of materials for which the magnitude of the environmental advantages over Ordinary Portland Cement (OPC) is relative to the region of the world. Although transportation and manufacturing/processing must be considered, for most SCMs, the carbon footprint relative to their production is lower than that of OPC since it does not involve decarbonation of the raw material in a kiln at 1450°C. OPC's carbon footprint has been largely optimized already by the optimization of the energy consumption of modern kilns and the use of alternative fuels, but it can hardly be pushed further since clinker requires calcium oxide (CaO), which is obtained by heating $CaCO_3$ until $CO_2$ gets emitted and CaO remains. The use of SCMs in concrete has thus to be considered as a partial waiver to the massive production of clinker.

In the province of Québec, ground glass (GG) is an interesting SCM since it is readily available on the local market. Unfortunately, in 2012, due to the low profitability of recycling glass, the only center that was recycling 75% of the glass collected in the province stopped its activities. Outlet for post-consumed glass is still an issue and several research projects are studying the feasibility to incorporate it into concrete as an SCM. This strategy is thought to have a positive effect on concrete' environmental footprint since it involves less clinker and allows to consider post-consumed glass as a resource instead of a waste.

Although this strategy is environmentally attractive on the short term, the long-term durability of concrete incorporating GG is still facing some challenges. Because post-consumed glass has a high sodium content (about 12-14% $Na_2O$), concerns were raised about its possible contribution to the phenomenon of Alkali Silica Reaction (ASR) in concrete. ASR, indeed, reduces the lifespan of structures, thus resulting in high financial and

environmental costs for their management and repairs. The above reaction is promoted by the presence of reactive aggregates and alkalis from various sources but can be prevented using the right amounts of efficient SCM. Finely ground glass has a theoretical potential of releasing its alkalis into the concrete pore solution and thus to feed the process of ASR; however, it can also be used as an effective pozzolanic material and thus theoretically contribute at preventing this pathology. The dual potential of Ground Glass (GG) is the object of the research work, which results are presented in this thesis.

## Global objectives

The global objectives of the present work are to determine if the high sodic content of GG has the potential to fuel ASR in the presence of alkali-reactive aggregates and to understand the mechanisms involved. Also, this study aims at providing recommendations on selecting combinations of GG and SCMs that could be safely used in concrete mixtures based on their capacity to meet the proposed two-year 0.040% expansion limit of CSA Standard Practice A23.2-28A.

## Specific objectives and corresponding axes of the research

To meet the global objectives, the present research work was oriented towards three specific axes leading to the following specific objectives:

- Determining the alkali release potential of GG into the pore solution of cementitious systems. To do so, the pore solution of binary and ternary paste mixtures made with cements of various alkali ($Na_2O_{eq}$) contents, GG and either SF/MK/FA/BFS was extracted and analyzed over time (after 28 and 182 days in sealed containers at 38˚C).

- Determining the potential expansivity regarding ASR of binary and ternary concrete mixtures made with cements of various alkali ($Na_2O_{eq}$) contents and the same combinations of GG and the SCMs mentioned above. To do so, the length changes of a large number of concrete specimens stored at 38°C and R.H. > 95% was monitored up to two years.

- Developing a better understanding of the relation between the expansive behavior and the composition of the pore solution of complex ternary systems incorporating a high-alkali SCM such as GG. To do so, behavior of the pore solution was compared to the behavior of concrete.

## Originality of the work

The research work presented in this thesis claims its originality mostly by the fact that, up to date, the assessment with concrete prism testing of the behavior of ternary mixtures incorporating a high-alkali SCM, notably GG, and either SF, MK, FA or BFS is largely lacking in the literature. The present work documented the behaviour of 93 mixtures and 354 single concrete prisms to identify mixture designs that would meet the expansion requirements of CSA Standard Practice A23.2-28A (< 0.040% at two years) and then make recommendations for their use in practice.

This work is also original in the way that the analysis for [$Na^+$] and [$K^+$] of the pore solution extracted from 530 paste specimens provides a very rich database that is highly valuable when trying to predict the composition of the pore solution according to the mixture proportions of ternary cementitious systems incorporating GG and various/common types of SCMs.

This work also proposes the *Response Surface Methodology* approach to build empirical models that can be used to determine the composition of the pore solution for any given mixture compositions inside of a given experimental range. Such an approach is only scarcely found in the literature.

## Presentation of the document

Chapter 1 of this thesis presents a literature review that discusses the fundamental aspects of the chemical reactions involved in the genesis and the prevention of ASR, as well as the chemical behavior of ground glass into concrete. From the historical discovery of ASR to the most recent developments on the topic, the literature review dwells on the reactivity of siliceous phases within aggregates, the solubility of chemical species such as silica, sodium, potassium, and calcium as well as the hydrates they produce. The properties of different hydrates are also discussed to better appreciate the results and discussions proposed in the articles of Chapters two to eight. These chapters present scientific papers that were written in the context of the present research work. Chapters two to four discuss the chemical composition of the pore solution of the various paste samples made and analyzed in this study. Chapters five and six discuss the expansive behavior of concrete samples made of ternary cementitious systems and a reactive aggregate, while chapters seven and eight present the relations that were explored between the composition of the pore solution and the expansive behavior of concrete. The last chapter of this thesis presents a synthesis of the main conclusions of the seven articles comprised in this thesis. An overview of the organisation of the document is presented in Figure 1

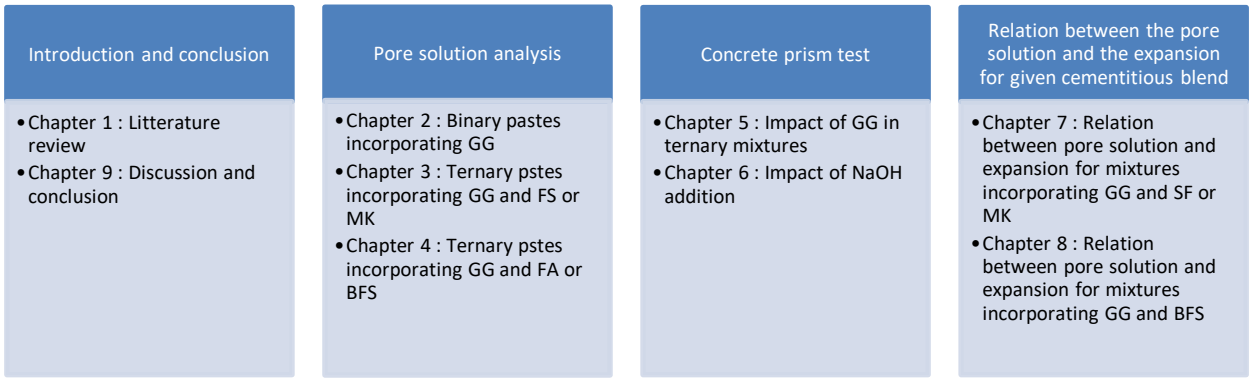


**Figure 1: Overview of the organisation of the document**

# Chapter 1. Literature review

## 1.1 Discovery of ASR

What is now known as ASR was first described by Stanton in 1940 after witnessing the failure of a concrete pavement built in California in 1936-1937 (Stanton,1940) This failure, due to excessive expansion, culminated with the premature deterioration of other concrete elements in the same area, the patterns of deterioration involving buckling at expansions joints for pavements and severe map cracking for all structures. Cases studies showed that problematic constructions had in common the use of local river sand as fine aggregates in combination with a cement with an alkali content of 1.14%. After testing in the laboratory, the expansive behavior of different sands combined with cements of different alkali contents, Stanton noticed: "*All sands in the coast area relatively high in shale and chert, […] developed expansions in few months roughly in proportion to the alkali content of the cement"* (Stanton, 1940). Thus, without naming it, Stanton provided a valuable overview of the causes and consequences of ASR.

Although the first documented cases were in California, ASR is not geographically circumscribed. For instance, in Iceland, highly-reactive volcanic rocks are frequent to the extent that ASR mitigation measures are mandatory with Icelandic cements since 1979 (Gudmundsson and Olafsson, 1999). Iceland, USA and other countries had discovered their sources of reactive aggregates after having gone through one or two decades of "unexplained'' and premature failures of structures (e.g.: Denmark in the 1950's, UK and France in the 1970's, Belgium in the 1980's and The Netherlands in the 1990's (Elsen et al., 2003)). In Canada, the first cases of alkali reactivity were reported in the 1960's and examples of potentially expansive aggregates have been identified across the entire country. The occurrence of structures affected by ASR and the alkali content of cements produced is higher in the eastern part of the country (Bérubé et al., 2000).

## 1.2 Chemistry of concrete and ASR

### 1.2.1 Reactive silica

Manifestation of ASR requires the presence of a reactive aggregate. It is worth noting that ASR does not necessarily consume the reactive aggregate as a whole, but targets particular phases such as microcrystalline, cryptocrystalline, poorly crystallized or amorphous silica phases. Those silica phases are not inexorably reactive, and the level of reactivity varies according to many macro-scale factors that will be discussed later. In this section, the reactive potential of silica is overviewed at the fundamental level, as described by chemical experts who worked on deepening the understanding of the dissolution, attack and/or corrosion of silica.

It is commonly accepted that kinetic dissolution steps are somehow common for amorphous and crystalline (quartz) silica, at the Angstrom scale. This is because dissolution and joint dislocation of silica structures are in fact a single phenomenon that corresponds to the breaking of the bonds between two silica tetrahedron. The latter phenomenon might or might not happen relatively to the crystallinity of the silica structure; it is determined by the contrast between the potential of the solid to "hold its bounds" (i.e. : to remain with a constant energy) and the potential of the contact solution to discharge its energy by binding its excess charges or ions to silica (Dove et al., 2005, Dove et al., 2008, Gao et al., 2013, Allen et al., 2017). In this case, the strength of the solid bounds corresponds to the crystallinity of the reactive phase (or the free energy barrier of the surface), while the "bound breaking potential" of the solution is the pH and the concentration of alkaline ($Na^+$, $K^+$) or earth alkaline ($Ca^{2+}$) ions.

In a siliceous structure, the free energy barrier is the energy required to break a $\equiv Si - O - Si \equiv$ bound holding silica tetrahedrons together and it is related to the number of bridging oxygens of tetrahedrons. Yet, the level of energy required to break the bounds in a $Q_3$ configuration (see Figure 1.1 for nomenclature of $Q_i$ configurations) is different than for a $Q_1$ configuration (Criscenti et al., 2006, Wallace et al., 2010). At the mineral level, an example of different dissolution rates for different configurations would be between fully polymerized silica (such as quartz) having a slower dissolution rate than a depolymerized chain of silica (like wollastonite) (Criscenti et al., 2006). An example of this principle in the ASR context would be Icelandic volcanic glass oversaturated with silica (Katayama et al., 1996), which is a disorganized silica form being more reactive than a quartz exhibiting undulatory extinction and (or) microcrystalline quartz of Quebec Laurentian shield (Bérubé et al., 2000). Other characteristics of the aggregates might also influence its reactivity, such as its silica content or its porosity, but those are not discussed in this review.

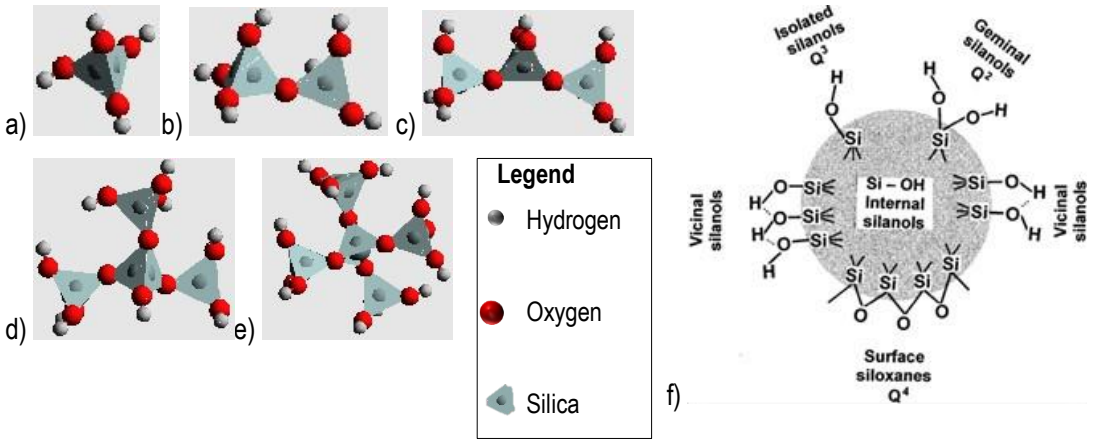


**Figure 1.1 : Configuration of silica with a) no bridging oxygen ($Q_0$), b) one bridging oxygen ($Q_1$), c) two bridging oxygens ($Q_2$), d) three bridging oxygens ($Q_3$) and e) four bridging oxygens ($Q_4$); f) Surface representation of different configurations (Zhuravlev, 2000).**

## 1.2.2 Surface Chemistry of Silica

The surface of silica involves $Q_2$ or $Q_3$ configurations and their inherent silanol sites, which is a tip of tetrahedron ending with OH atoms ($\equiv Si - OH$). A silanol site is deprotonated when an $OH^-$ ion from the solutions becomes $H_2O$ by "stealing" the hydrogen atom of the silanol that remains negatively charged (δ-). This part of reaction is illustrated in Figure 1.2 and can be written as Equation 1.1.

$$\equiv Si - OH + OH^- \longrightarrow \equiv Si - O^- + H_2O$$ **(Dent-Glasser and Kataoka, 1981)** **Equation 1.1**

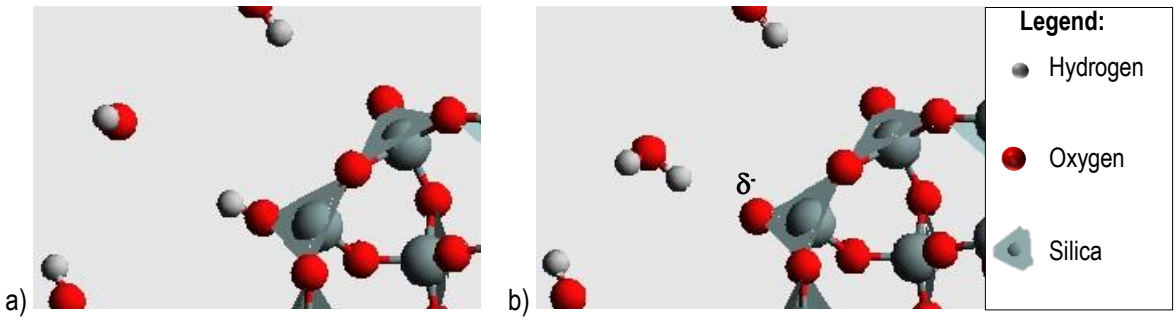


**Figure 1.2 : a) Hydroxyl ion and silanol site b) Deprotonated silanol and water molecule (adapted from Dent-Glasser and Kataoka (1981)).**

Once the deprotonated silanol is unbalanced because of the excess negative load (δ-), its lack of local electro-equilibrium can be rectified by a bound path with a cation showing an available positive charge, e.g. $Na^+$ or $K^+$. This part of the reaction is illustrated in Figure 1.3 and can be written as Equation 1.2. The nature of the "bound" in this case is not ionic nor covalent, but better described by an attraction caused by electrostatic forces.

$$\equiv Si - O^- + Na^+ \longrightarrow \equiv Si - O - Na \text{ (Yang et al., 2018)} \qquad \textbf{Equation 1.2}$$

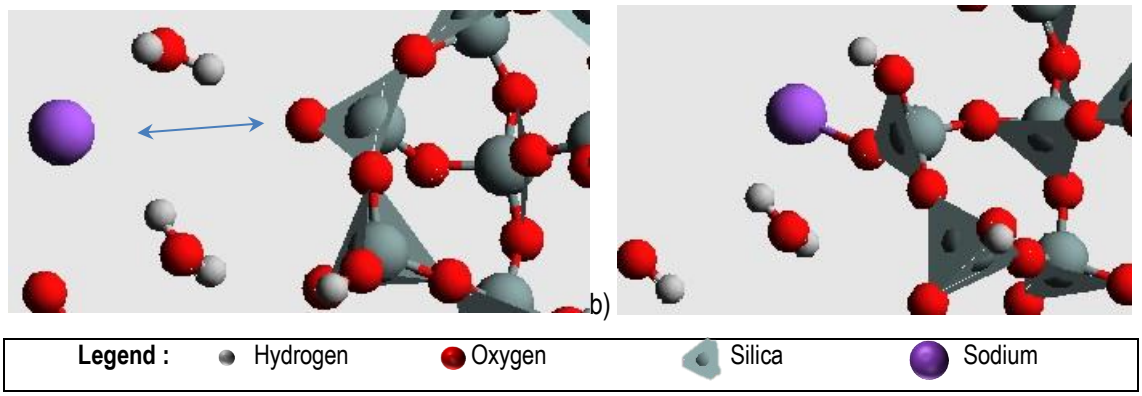


**Figure 1.3 : a) Deprotonated silanol and sodium ion ; b) bound path or electrostatic attraction between silicon and sodium (adapted from Yang et al. (2018)).**

Since the latter two reactions resulted in $OH^-$ transformed to $H_2O$, the pH was naturally affected in the sorption process of the cation. Allen et al. (2017) monitored this phenomenon by adjusting to 4.00 the pH of solution containing 0.05M and 0.17M of monovalent ("+") and divalent ("2+") cations before adding 20-25mg of ground quartz. The authors noted a pH drop to 3.44 and attributed it to the release of $H^+$ ion when the cations were adsorbed. It is also worth noticing that, inversely, cation desorption (release of bounded alkalis and bounding of a $H^+$ from the solution) leads to pH increase from 4.00 to 4.37. This study is interesting because it demonstrates the impact on the pH of adsorption and desorption of soluble alkalis in contact with a siliceous phase. More precisely, the surface adsorption of 2.5, 2.4 and 2.7 moles of respectively $Na^+$, $K^+$ and $Ca^{2+}$ leads to pH decreases from 4.00 to respectively 3.53, 3.54 and 3.50. Although this experiment happened in an acidic environment, the interaction with $H^+$, $OH^-$ and alkalis is similar in an alkaline environment, as Equation 1.1 and Equation 1.2 are frequently proposed in ASR discussions.

## 1.3 Breaking Down the Silica Network

Dove and Elston (1992) suggested that a silanol bound to $Na^+$ or $K^+$ is not as strongly connected to the silica network than the counterparts bound to $H^+$ at the tip of a tetrahedron. Understandably, they are different in their potential to attract electrons or electronegativity, (2.2, 0.93 and 0.82 for respectively $H^+$, $Na^+$ and $K^+$), their radii, and their vibration frequency; hence, the substitution involves a somewhat internal reorganization of the silicon tetrahedron which, in this case, weakens the silicate network, induces lower coordination number, and increases its solubility.

More directly, Dove and Nix (1997) measured the kinetics of quartz dissolution in the presence of alkalis and earth alkalis and suggested that the dissolution rate increases with the introduction of salts in the following order : $Mg^{2+} < Ca^{2+} \sim Li^+ \sim Na^+ \sim K^+ < Ba^{2+}$ in near neutral solutions. In contexts closer to the pore solution of concrete, Saccani and Bignozzi (2010) noted greater mass loss of glass discs stored in a 1N NaOH solution compared to a lime saturated solution (0.04 mol/L). Similarly, Maraghechi et al. (2016) measured greater dissolution rates of glass sheets stored in solutions with higher concentrations of NaOH for pH between 12 and 14. As an explanation for the increased dissolution rate in the presence of cations, Dove and Elston (1992) suggested that the substitution of $H^+$ by $Na^+$ or $K^+$ at the surface of silica affects the connectivity/reactivity of the silicate network. Indeed, a silicon tetrahedron bounded to a $Na^+$ is "stretched" at this tip, which results in a lengthened Si-O bound at his tip and smaller angles for Si-O-Si bounds of the network that are strained and "ready to break". According to computational work of Wallace et al. (2010), those weakened Si-O-Si are more prone to be attacked and broken by hydroxyl ions. Figure 1.4 illustrates the context and the end results of the reactions.

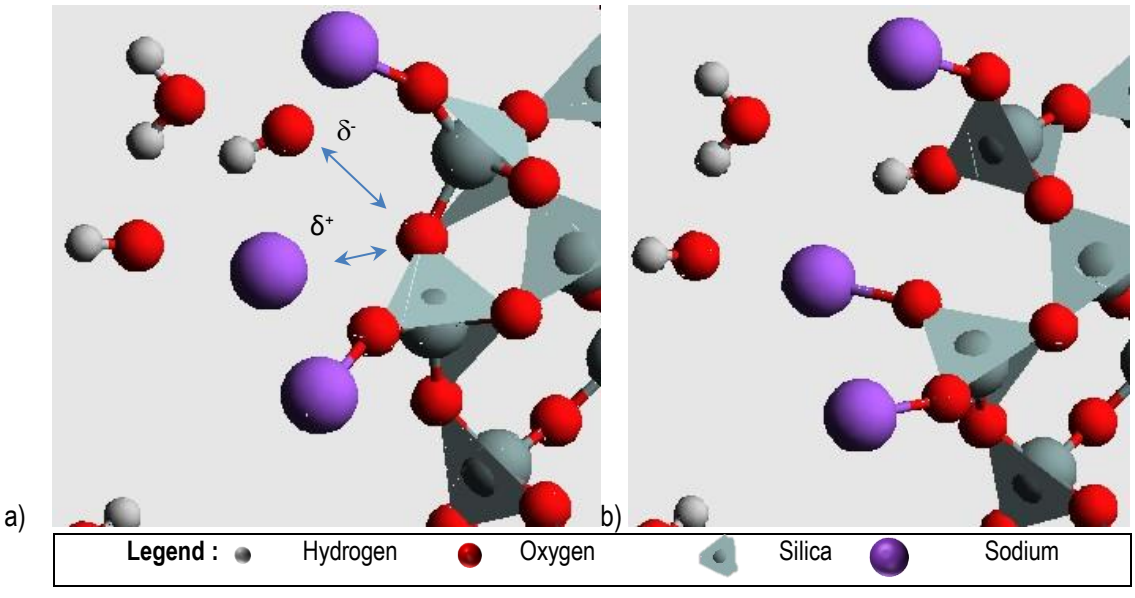


**Figure 1.4 : (a) Siloxane bridge, water molecule, hydroxyl ion and sodium ion; b) Bounded sodium, bounded hydroxyl and broken bound between silica tetrahedron. (Adapted from Helmuth et al. (1993)).**

Those steps of the mechanism are also proposed in ASR contexts by Gao et al. (2013), who assessed dissolved silica of various reactive aggregates in acidic and basic environments. The aggregates for the study were opal, siliceous limestone, quartzite and quartz aggregate containing reactive phases such as quartz with/without undulatory extinction, microcrystalline quartz, chalcedony-like spherulites and amorphous phases of silica. The authors suggested that the mechanism is suitable for both amorphous silica and crystalline silica but, for the latter, the solubility is much lower. For example, in an aqueous solution of pH = 14 at 25 °C, the solubility of amorphous silica is approximately 21 times that of quartz (≈125 mol/l for amorphous silica compared to ≈6 mol/l for quartz).

### 1.3.1 Volume Variations

Another phenomenon worth mentioning in this section focusing on the attack of silica network is the volume variation involved when downgrading the silicon configuration from $Q_4$ to $Q_3$. Garcia-Diaz et al. (2006) isolated the flint reactive aggregates of mortar bar of various expansion levels using HCl and estimated the number of $Q_3$ configuration in the reacted aggregates with thermal treatment and mass variation. The authors suggested that the absolute volume of a $Q_3$ tetrahedron is 31 $mm^3$/mmol while a $Q^4$ silicon tetrahedron occupies only 23 $mm^3$/mmole.

### 1.3.2 Contact Reaction Between Solid Silica and Calcium Solution

The preferential bounding of calcium over sodium on a silica network is well demonstrated in the experiments of Maraghechi et al. (2016) where glass sheets were stored in 1M NaOH without $Ca(OH)_2$ and in saturated $Ca(OH)_2$ solution. The authors observed reaction products on the glass sheets stored in 1N NaOH solution, which were not strongly bound to the glass and could be easily removed under running water, as illustrated in Figure 1.5. This reaction product had a Ca/Si around 1.05 and Na/Si ratio around 0.05. Since the Ca/Si ratio of the glass sheet is only 0.09 and that the glass sheet is the only source of calcium in that system, the authors proposed that the increased Ca/Si of the reaction product is not caused by external calcium, but rather by the dissolution of the silica of the glass sheet. Leemann et al. (2011) also observed that the presence of calcium plays a role in silica dissolution by precipitating silica as calcium silicate, lowering the silica concentration and promoting further dissolution of silica to reach equilibrium concentration. On the other hand, the reaction products observed on the glass sheet stored in 1M NaOH saturated in $Ca(OH)_2$ were strongly bounded to both glass surfaces in the way that it could not be removed; its Ca/Si was 1.84 while the Na/Si was approximately 0.22. This experiment of Maraghechi et al. (2016) demonstrated the stronger bound between Ca and Si compared to Na and Si but also that the presence of calcium remarkably lowers the glass dissolution. The mass loss of the glass sheet stored in 1N NaOH was indeed more than 5 mg/$cm^2$ after 28 days while it was less than 1mg/$cm^2$ for the glass sheet in the lime saturated NaOH solution The low glass solubility in presence of calcium was also observed by

Saccani and Bignozzi (2010) who measured ≈-7% weight change for sodalime glass disc stored in 1NaOH and only about 0.5% for sodalime glass disc stored in a 1M NaOH solution saturated in $Ca(OH)_2$, both after 28 days.

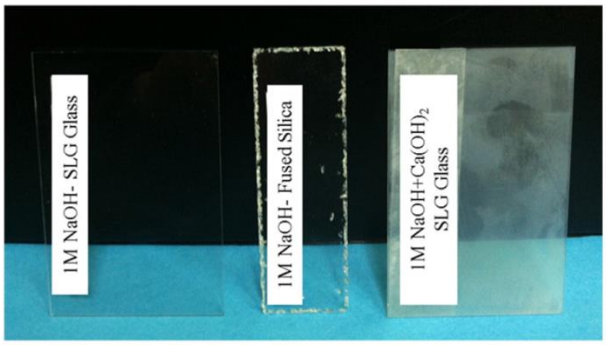


**Figure 1.5 : Clear washed glass after exposition to NaOH solution (left) and calcium and sodium visible to glass surface after exposition to NaOH + $Ca(OH)_2$ (right) (Maraghechi et al., 2016).**

Barnes et al. (1978) reported the presence of a "duplex film" at the surface of a glass aggregate particle in concrete; they noticed that : "In some areas, the $Ca(OH)_2$ part seemed to be thin or missing entirely, with C-S-H gel particles deposited directly on the glass surface." The work of Barnes et al. (1978) is worth mentioning since the authors assessed the glass passivation in a concrete context and suggested that other elements might be included in the passivation layer. The authors mentioned: "Relatively large well-formed hexagonal crystals developed in largely open space adjacent to the duplex film and extending back into the paste, […], and with suspiciously high contents of sulfur and aluminum." Interestingly, Wilson et al. (2018) also observed, with semi-quantitative EDS technique, a sulfur rich phase to the proximity of glass particles in cementitious pastes.

### 1.3.3 Calcium Silicate Uptake

While the latter section proposed unlabeled reaction products on the siliceous surface that are mainly composed of Ca and Si, this section presents a short summary of certain properties of calcium silicate hydrate (C-S-H) phase. Labbez et al. (2011) produced synthetic C-S-H and measured their electrokinetic potential ($\zeta$) by electrophoresis in different pH conditions. As presented in Figure 1.6, the results suggest that, at higher pH, the C-S-H has higher content of deprotonated silanol, which are silanols "seeking" to be electrostatically bound with alkaline species, as detailed in the previous sections. In other words, the reactive sites of silica ($\equiv Si - O^-$) are not only found on reactive aggregates but also in C-S-H and the occurrence of those sites tend to be enhances by higher pH conditions.

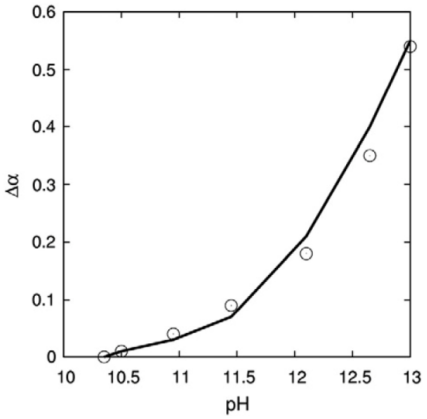


**Figure 1.6 : Comparison between experimental (points) and simulated (line) net increase of the ionization fraction (Δα) as a function of the pH for C-S-H nano-particles dispersed in solution containing a low bulk calcium concentration (Labbez et al., 2011).**

The results presented above suggest that the higher the pH, the greater is the potential for C-S-H to adsorb positively charged species. The authors also suggested that $Ca^{2+}$ and $Na^{+}$ cations are in competition to balance the negatively charged surface of C-S-H; the presence of divalent cations, such as calcium, would then switch the charge of the surface, which tends to repel other positively charged ions such as sodium on the surface of C-S-H. $Ca^{2+}$ balances the negative surface more efficiently than $Na^{+}$ and the authors indeed found that $Ca^{2+}$ is 5 times more concentrated in the vicinity of the C-S-H surface compared to $Na^{+}$. The authors also observed that C-S-H richer in calcium have lower electrokinetic potential ($\zeta$) and adsorbed few $Na^{+}$ ions compared to C-S-H poorer in calcium. This is explainable by the fact that adsorption of $Ca^{2+}$ balanced the negative charge of the silanols and those somewhat "balance" silanols have lower potential to "attract" charged ions such as $Na^{+}$. Similar observations were reported by Ke-rui et al. (2004) who also synthetized C-S-H, measured the $\zeta$ potential by electrophoresis and analysed the composition of washed C-S-H after immersion in solution containing different concentrations of $Ca^{2+}$ and $Na^{+}$ ions. These authors also observed that Ca-rich C-S-H had lower $\zeta$ potential as well as lower adsorbed $Na^{+}$. Those studies demonstrated well that the potential of C-S-H to adsorb alkali ions, such as $Na^{+}$ or $K^{+}$, is related to the availability of the silanol sites and the later are controlled by both the pH of the contact solution and the Ca/Si of the C-S-H.

Hong and Glasser (1999) studied the sorption of alkalis by C-S-H of different Ca/Si synthetized and stored in solutions of various concentrations of NaOH or KOH. The alkali uptake by C-S-H was assumed to be equal to the concentration drop of the solution at the end of the experiment. As illustrated in Figure 1.7, C-S-H with low Ca/Si are more efficient to sorb $Na^{+}$ and $K^{+}$ ions into/onto the solid phase. Also, the results of the study are coherent with previously presented studies in the way that solutions with higher concentrations of $K^{+}$ or $Na^{+}$ have higher pH, which favor sorption.

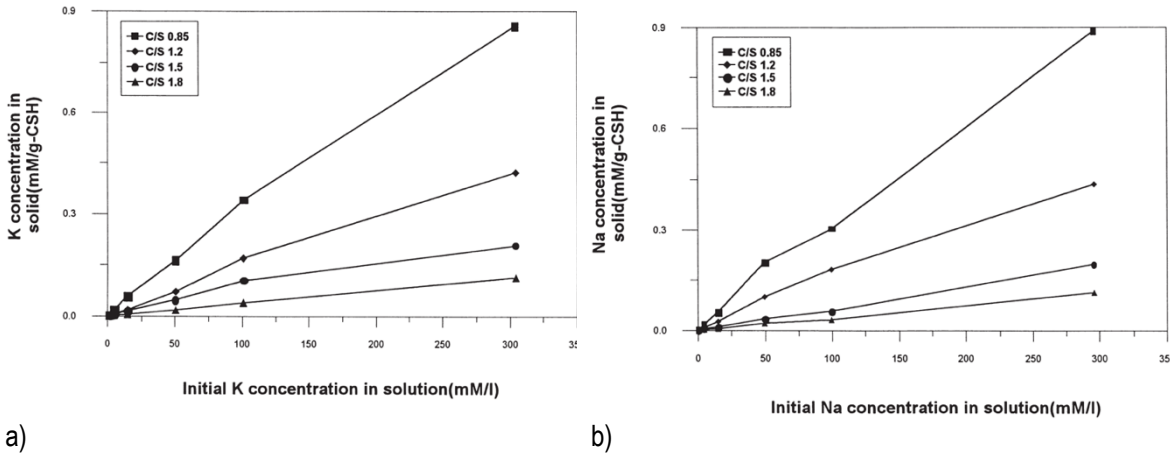


a) b)

**Figure 1.7 : Alkali uptake of synthetic C-S-H immersed in solutions of various alkali concentrations a) $K^+$, b) $Na^+$ (Hong and Glasser, 1999).**

Stade (1989) observed that synthetized C-S-H with lower Ca/Si incorporates more $K^+$ ions and also that C-S-H immersed 1 to 3 days in more concentrated KOH solutions tend to incorporate more $K^+$. Viallis et al. (1999) also observed that the alkali interaction with the surface of the C-S-H is modulated by the concentration of the contact solution.

### 1.3.4 Pozzolanic Reaction

Pozzolanic materials typically contain a high percentage of amorphous silica and are finely ground/disseminated materials, which provide an important surface of contact and available silanol sites for equations 1.1 to 1.2 to occur, thus lowering the concentration of $OH^-$ and cations (such as $Na^+$, $K^+$ and $Ca^{2+}$) in the pore solution as explained earlier in this review. Since the binding of the latter cations by silicon tetrahedrons might happen either in solution, in/on C-S-H or in/on reactive silica of pozzolanic materials, it might be interesting to consider that those reactions are similar to ASR (despite of the fact that the first mitigates expansion due to ASR while the second promotes it). Gudmundsson and Olafsson (1999) mentionned that before introducing SF, Icelandic engineers used their ground rhyolite as a preventive measure against ASR although this rock is considered alkali reactive. Carles-Gibergues et al. (2008) suggested that reactive aggregates can be converted to pozzolanic materials through pulverization. Indeed, Reactive Aggregate Powder (RAP) acts as a pozzolan for many properties of concrete, such as durability or compressive strength. The authors obtained RAP from crushing and sieving, through an 80μm sieve, reactive aggregates of various types and with $SiO_2$ contents ranging between 88% and 15%. For each reactive aggregate, concrete samples were made with 100% non-reactive (NR) sand and a mixture of 80% NR sand and 20% RAP. The specimens were then stored at 60°C and 100% RH for expansion measurements up to 88 weeks. The expansion of the test prisms made with siliceous limestone containing 15% $SiO_2$ was reduced by 36% through the use of siliceous limestone RAP while the expansion of test prisms incorporating aggregates with $SiO_2$ contents ranging between 66 and 87% was reduced by 89% and

96% by the use of RAP. Other investigations showed that concrete with RAP had their compressive strength increased from 15% to 58% and that no ASR products were visible by SEM. Davraz and Gündüz (2008) also suggested the pozzolanic behavior of RAP and its potential to reduce expansion due to ASR.

Ground glass (GG) is another material with overlapping properties in promoting or inhibiting expansion due to ASR. As for RAP, the particle size was found to be critical in predicting the expansion of concrete or for determining which reaction will be dominant between ASR and pozzolanic reaction. Idir et al. (2011) observed by EDX the composition of reaction products of glass particles and suggested that both fine and coarse particles produced C-S-H with Ca/Si between 0.6 and 1.4. Particles roughly coarser than 1mm produced ASR gel with chemical composition that varies according to its location. Inner products have Ca/Si below 0.3 and (Na+K)/Si between 0.2 and 0.4, while outer products have a Ca/Si between 0.2 and 0.8 and (Na+K)/Si between 0.1 and 0.3, as presented in Figure 1.8.

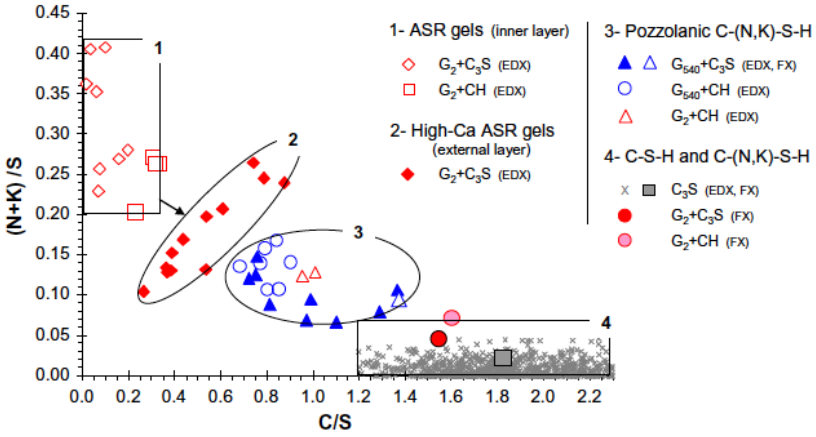


**Figure 1.8: Composition of newly-formed hydrates produced by the reaction of glass particles of various dimensions in $C_3S$-KOH solutions (154 days at 60°C) and $Ca(OH)_2$-KOH solution (129 days at 60°C) (Idir et al., 2011).**

Hints on the difference between the behavior of alkali-rich ($Na^+$, $K^+$) or calcium-rich ($Ca^{2+}$) siliceous products are presented at the fundamental level in Figure 1.9. It shows that divalent $Ca^{2+}$ ions tend to link two silicon tetrahedrons while monovalent $Na^+$ ions tend to isolate the ends of the tetrahedron and make it available to attract water molecules. Those products could thus be considered as pozzolanic reaction products that are richer in calcium and composed of a somewhat stiff siliceous network with limited swelling properties or ASR reaction products that are rich in hygroscopic monovalent ions ($K^+$,$Na^+$) with higher swelling potential.

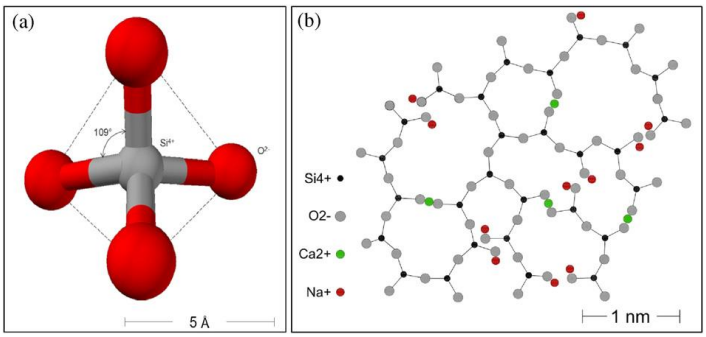


**Figure 1.9 : a) Silicon tetrahedron and b) siliceous structure incorporating $Ca^{2+}$ and $Na^{+}$ (Maraghechi et al., 2016).**

## 1.4 ASR Gel

Despite of the seriousness of the issue induced by the dissolution of metastable phases in reactive aggregates, alkalis trigger even more noticeable issues within concrete due to the presence of ASR products. Indeed, deformations and cracks caused by the swelling of the ASR gel is a primary source of concerns for concrete durability.

### 1.4.1 Impact of Water on the Swelling Properties of ASR Gel

The swelling of the gel is thought to be caused by water molecules migrating into the above secondary reaction products. Movement of water molecules towards the gel can be explained by:

a) Imbibition, which consists in water moving from a lower concentration (pore solution) to higher concentration (ASR gel) of chemical species such as $Na^{+}$, $K^{+}$;
b) osmotic pressure which, technically speaking, differs from imbibition in the fact that ASR gel surface acts as a semi-permeable membrane (Glasser, 1979);
c) hygroscopic properties of atomic constituents of the gel. For example, as shown in Figure 1.10, a sodium ion tends to “carry” water molecules around it. In water, sodium and potassium ions tend to be weakly bound by electrostatic forces to respectively 17 and 11 water molecules around them (Jiang, 1997));
d) Volume change properties of water. Indeed, Imberti et al. (2005) who worked on the microscopic structure of concentrated hydroxide solution mentioned that :”*the solvation of alkali hydroxides in water strongly disturbs the water-water coordination and that the disturbances depends on the solute species as well as on its concentration*.” Indeed, the species in solution destroy the H-bound network of water, which results in “denser water”, as illustrated in Figure 1.11. Interestingly, the shrinkage of water caused by alkali ions can be translated into equivalent disturbance on pure water caused by an applied pressure in MPa, as presented in Figure 1.12. The latter also suggests that the volume occupied by water molecules of the aqueous solution is related to the concentration and the nature of the species

in solution. The phenomena related to the swelling properties and increased water content of ASR gel are not mutually exclusive, and it is probable that they happen simultaneously but with different impacts on the expansion of the ASR gel.

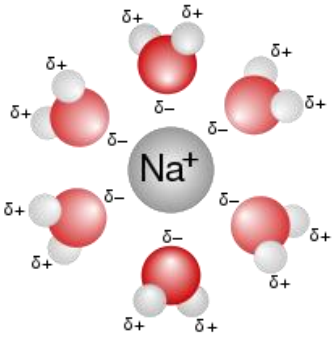


**Figure 1.10 : Schematization of hydration number of a sodium ion with six water molecules around (Wikipedia article on Aqueous solution, 2019)**

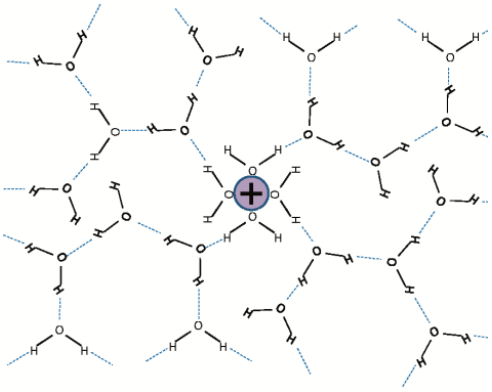

**Figure 1.11: Cation surrounded by water molecules disturbed in their organisation by other water molecules because of broken hydrogen bridges (Mahler and Persson, 2012).**

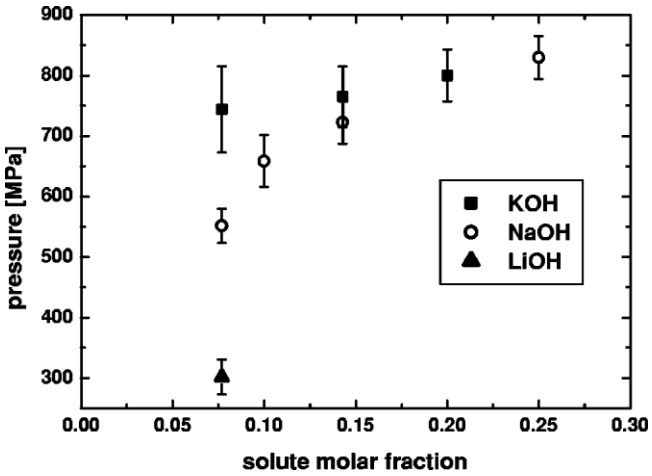


**Figure 1.12 : Pressure on pure water equivalent to volume changes induced by solvation of different chemical species in various concentrations (Imberti et al., 2005).**

The water content of a silica gel and its relation to its chemical composition was studied by Diamond and Barneyback Jr (1981), who prepared eight synthetic silica gels of various sodic contents and monitored their water content. The authors observed that the gel with highest water content also had a high $Na^+$ content; however, no relation between the chemical composition and the swelling properties or water content of the gel could be established. Further analyses conducted by Struble and Diamond (1981) could not correlate the free swelling behavior and the water content or the chemical composition of the gel. For example, as presented in Table 1.1 out of the eight gels synthetized, five showed swelling pressure below 4% and their Na/Si were between 0.28 and 0.46; on the other hand, the three gels that swelled showed volumetric variations between 60% and 80% and had Na/Si between 0.27 and 0.53. The swelling pressure of the gel also failed to correlate with their chemical composition and free swelling behavior.

**Table 1.1 : Gels composition and properties (Struble and Diamond, 1981).**

| Na/Si | Ca/Si | $H_2O$ | Free swelling pressure /osmotic pressure | Swelling pressure |
|---|---|---|---|---|
| 0.27 | | 1.93 | 81.6 | 0.4 |
| 0.27 | 0.17 | 1.16 | 8.0 | 0.3 |
| 0.28 | | 1.32 | 3.6 | 0.14 |
| 0.30 | | 1.77 | 2.5 | 0.27 |
| 0.33 | | 1.98 | 0.5 | 0.06 |
| 0.34 | | 2.24 | 1.3 | 10.89 |
| 0.35 | 0.18 | 1.57 | 3.1 | 0.51 |
| 0.42 | | 1.99 | 63.2 | 3.09 |
| 0.46 | | 1.84 | 2.0 | 0.09 |
| 0.53 | | 2.10 | 69.8 | 2.22 |

Gholizadeh-Vayghan and Rajabipour (2017) used Response Surface Methodology to obtain a broader picture of the hydrophilic properties and free swelling behavior of ASR gel. For this purpose, the authors casted mini bars (½" x ½" x 5") of gel with Ca/Si, Na/Si and K/Si ranging between 0.05 and 0.5, 0.1 and 1.0, and 0.0 and 0.3, respectively. The length and the weight of the bars were measured after 1, 4, 7, 14, 21 and 28 days of storage in a 95% RH environment at 25+/-1°C. The authors observed that length and weight changes are reasonably related together, as illustrated in Figure 1.13.

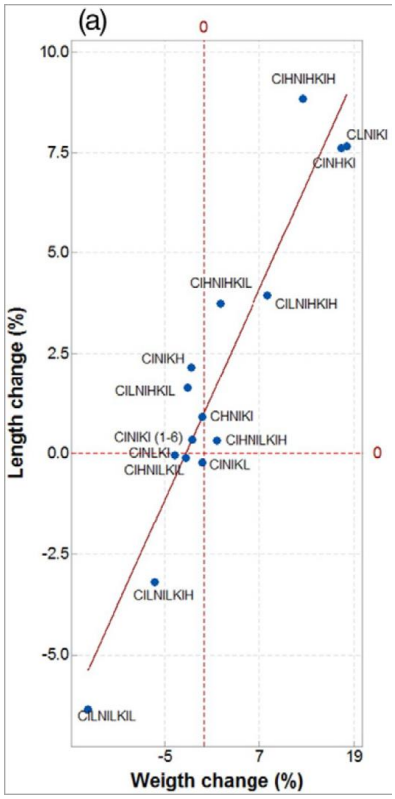


**Figure 1.13: Correlation between length and weight changes of minibar of ASR gel of various compositions (Gholizadeh-Vayghan and Rajabipour, 2017).**

Yet, as presented in Figure 1.14, the chemical composition showed that, on one hand, an increase in Na/Si or K/Si is related to greater expansion and weight gain, which was explained by the fact that those chemical species in silica network were often identified as "network modifiers/breakers" that promote volumetric instability. Also, the increased presence of the above monovalent cations increases charge density and osmotic pressure of the gel's pore solution, which promote the gel's water affinity. In counterpart, the effect of Ca/Si was found to be non-monotonic. At low and high levels (i.e. Ca/Si below 0.18 and above 0.40), a decrease of length and weight was observed, while between 0.18 and 0.40, an increase in Ca/Si was related to increased length and weight of the gel minibars. The hypothesis proposed for the different behaviors is that at low Ca/Si (<0.18), numerous Si-$O^-$ bounds are available at the surface of the gel, thus allowing the uptake of monovalent ions ($K^+$, $Na^+$); in other words, there is no competition between the cations to occupy "vacant" ends of Si-$O^-$ at that stage, and increasing the Ca/Si results in more calcium on the surface of the gel, which decreases its water affinity and results in reduced swelling. For Ca/Si between 0.18 and 0.4, the hypothesis suggested by the authors is that $Ca^{2+}$, $Na^+$ and $K^+$ compete for silanol sites. Hence, higher Ca/Si tend to have Si-$O^-$ $Ca^{2+}$ $^-$O-Si that could even replace Si-$O^-$ $Na^+$ bounds; "alkali recycling" is thus thought to occur and free $Na^+$ increases osmotic pressure into the gel, which promotes weight and length gain. The hypothesis proposed by the authors for Ca/Si above 0.4, is that Si-$O^-$ $Ca^{2+}$ $^-$O-Si reach a somewhat "network", which has a very low swelling property since calcium ions allow the

gel to “hold himself” and remain stiff. The hypothesis proposed by Gholizadeh-Vayghan and Rajabipour (2017) remains coherent with the results of other studies proposed in the present work. Thomas (2001) suggested that the Ca/Si of ASR gel in aggregate particles is actually below 0.40 (Figure 1.15), which supports the fact that expansion occurs more severely into the aggregate particles than in the cement paste.

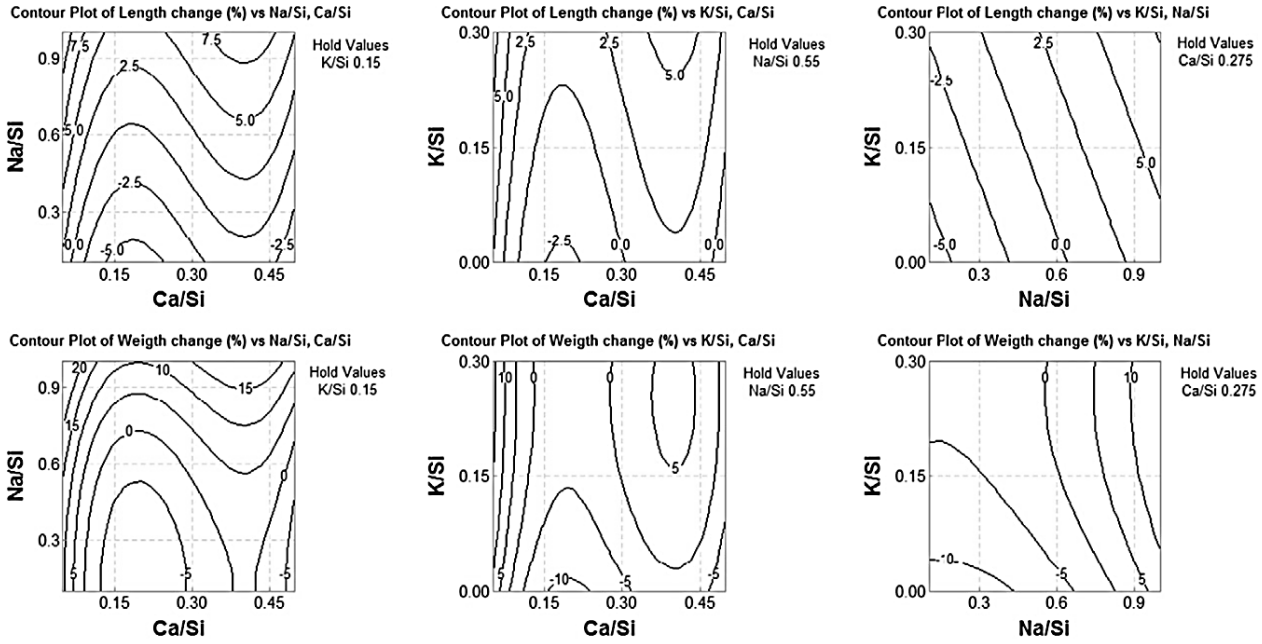


**Figure 1.14 : Surface response of the length and weight changes of ASR gel minibars according to the compositions of the gel (Gholizadeh-Vayghan and Rajabipour, 2017).**

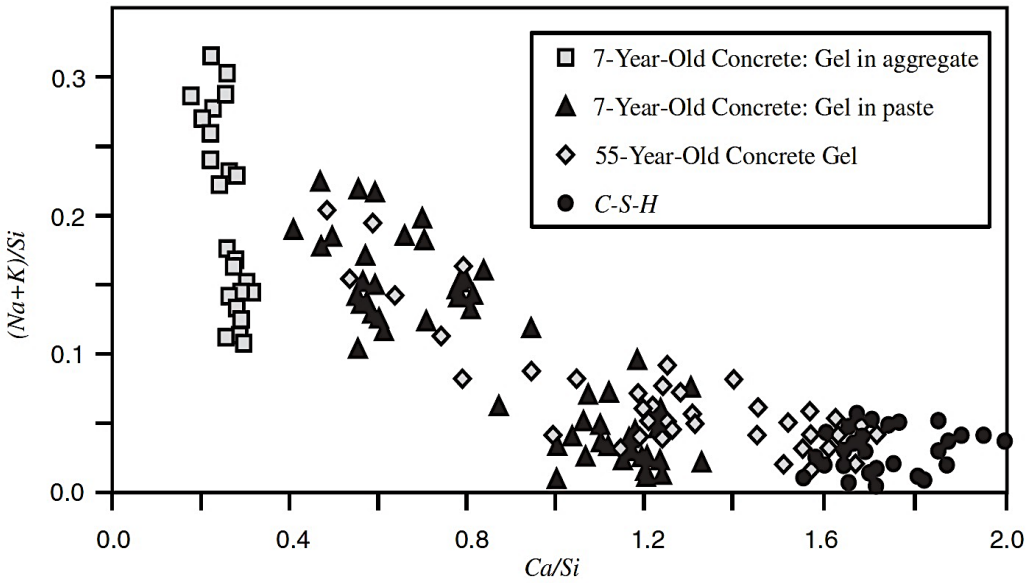


**Figure 1.15: Chemical ratios of ASR gel located in aggregate particles and in the cement paste of 7 and 55 years old concretes (Thomas, 2001, Rajabipour et al., 2015).**

### 1.4.2 K+ vs Na+ Into ASR Gel

Hu et al. (2018) produced concrete prisms incorporating the highly-reactive Spratt aggregate from Canada and that were stored at 95% RH for six months at room temperature and six months at 50°C. The authors then conducted Scanning Electron Microscopy (SEM) investigations through which they obtained Backscattered electron (BSE) images and elemental gel compositions with Energy-dispersive X-ray (EDX) analyses. ASR products similar to those described by Katayama (2012), such as rosette-like shapes, appeared to be dominant in cracks within reactive aggregate particles while granular or more amorphous ASR products were prevailing elsewhere. The authors observed that, as illustrated in Figure 1.16, Ca/Si and K/Si of both types of reaction products were somewhat similar, i.e. between 0.20 and 0.25 and between 0.17 and 0.30, respectively. However, the reaction products greatly differed in the way that rosette-like ASR products hardly contained any sodium. Indeed, the Na/Si of rosette-like products was found to be below 0.05, while the Na/Si of the granular products was between 0.10 and 0.23.

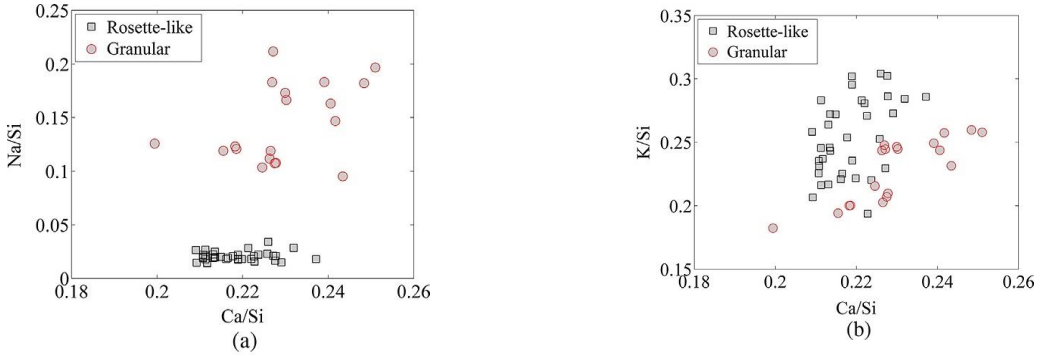


**Figure 1.16 : Chemical composition of ASR gel according to the morphology of the gel a) Na/Si against Ca/Si and b) K/Si/Ca/Si (Hu et al., 2018).**

According to the calculations of Katayama (2012), the expansive behavior of the rosette-like products of ASR cannot be attributed to crystallisation, but rather to hydrostatic swelling pressure.

As mentioned by Leemann et al. (2016), rosette-like products where frequently reported in cracks within reactive aggregate particles while granular products were reported along the particle edge and in the cement paste. Those observations are coherent with the results of other studies reported in the literature, as presented in Figure 1.17 (Leemann and Lothenbach, 2008, C. Hu et al., 2018).

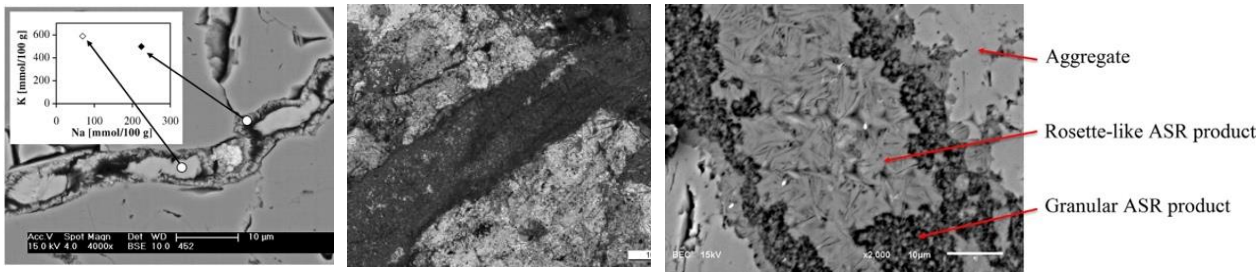


a) b) c)

**Figure 1.17: a) Central gel with a low sodium content and near aggregate gel with higher sodium content (Leemann and Lothenbach, 2008) b) Crystalline-called ASR product in medium grey at the center of the crack and amorphous ASR product near the paste and on the gel/aggregate interface (Leemann et al., 2016) and c) Rosette-like product at the center of the crack and granular product in the gel/aggregate interfacial zone (Hu et al., 2018).**

According to the observations of Leemann and Lothenbach (2008), the reaction product at the center of the cracks (within reactive aggregate particles) forms earlier and has a higher K/Na than the product at the edge (i.e. close to the cement paste), which exhibits lower K/Na. Visser (2018) mentions that potassium ions require lower concentration for gelation compared to the sodium ion since the $K^+$ ion has a stronger "effective charge" (see Figure 1.18 to better figure out hydration rules of Visser (2018) which are: 1) An unhydrated cation has a charge similar in proportion to its valence ($ve$), with $e$ the elemental charge and v its valence; 2) A hydrated cation has a charge that is reduced by the presence of the hydration layer, which can be depicted as having a charge of $\delta-$. The net charge of the hydrated cation is therefore $ve-\delta-$; 3) Small cation (lower ionic radius) binds water more strongly and has a smaller effective charge than a larger cation with the same valence: $ve-\delta-$.) in aqueous solution than sodium. This makes the $K^+$ more efficient in reducing repulsion between soluble ions, thus promoting gelation at lower concentration. To strengthen the latter hypothesis, Imberti et al. (2005), who studied interactions between molecules of monovalent earth ions (Li, Na and K) in concentrated basic solutions, suggests that the solvation entropy of $K^+$ has to be higher than that of $Li^+$ and $Na^+$.

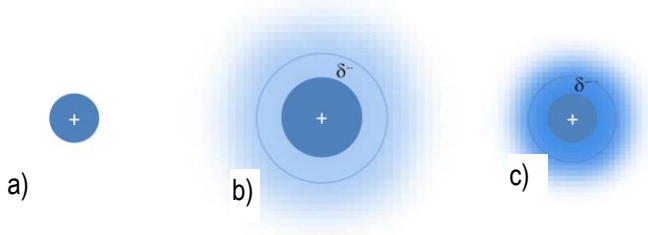


a) b) c)

**Figure 1.18: Illustration of the "hydration 'rules" according to Visser (2018) a) unhydrated cation with smallest radius but largest effective charge; b) larger cation hydrated with a weakly bonded hydration layer with a smaller effective charge than the unhydrated cation, c) and same cation as in a) but hydrated with strongly-bonded water resulting in the smallest effective charge.**

$K^+$ is a relatively large cation that does not attract the negative dipole of the water molecule tangentially. This results in a single layered cluster of water molecules "tied" by hydrogen with somehow weak bound that forms a closed structure (called *clarthate*) in which $K^+$ is located at the center (Imberti et al., 2005, Mahler and Persson, 2012, Cooper et al., 2013). Visser (2018) explains that $K^+$ is not strongly tied to its water molecule and might not "carry" them while displacing, thus improving its mobility. Relative to $Na^+$, Imberti et al. (2005) suggest that the hydration layer of $Na^+$ attracts tangentially the water molecules, which make the shell somewhat organised or defined, thus implying longer residence. Another study that underlines the different properties of those ions comes from the 2003 Nobel prize of chemistry (The nobel prize of chemistry 2003), Peter Agre and Roderick MacKinnon, who demonstrated that a channel lined by oxygen atoms with a specific width might allow the transportation of $K^+$ but not $Na^+$. In other words, it is possible to create an ion specific filter by using the steric properties of the hydrated ions.

Unfortunately, very few studies are available on the properties of ASR gel according to their chemical composition regarding Na and K. However, according to Gholizadeh-Vayghan and Rajabipour (2017), the equilibrium relative humidity of an ASR gel is much more related to its Na/Si, which is over 95% for Na/Si of 0.3, while K/Si is poorly related to relative humidity at the equilibrium. The latter observation is in accordance with the hydration shell study, which suggests that $Na^+$ is more strongly bound to its water molecule than $K^+$ when considering the steric aspect. The two cations have different "transport properties" as well as different affinity to water; also, because they induce gelation of siliceous solutions at different concentrations, there is no surprise that they produce gel with different properties. However, specific properties of the expansive potential of K-rich gel vs Na-rich gel remain to be clarified by further studies.

## 1.5 Impact of the Pore Solution on the Reactivity of C-S-H Surface

According to Hong and Glasser (1999), the composition of the solid reaction products in cementitious systems is influenced by the composition of the contact pore solution, as they found that C-S-H incorporated more $K^+$ or $Na^+$ when soaked in solutions of higher concentrations in those ions. This fact is corroborated by the study of Ke-rui et al. (2004) in which sodium-bearing C-S-H were synthetized after mixing saturated $Ca(NO_3)_2$ and $NaSiO_3$ solutions. Throughout the experimental process, the $\zeta$ potential and the $Na^+$ content of the C-S-H were determined by electrophoresis and XRD, respectively. The $\zeta$ potential approach translates the somewhat negative charge of the C-S-H or its potential to attract cations. Before each measurement, C-S-H were washed with distilled water until the $Na^+$ content of the C-S-H remained stable between the washes.

Table 1.2 presents the data collected for the freshly synthetized C-S-H ($t_0$), after a two-hour immersion in a solution of NaOH + $Ca(OH)_2$ ($t_1$) and after immersion in a saturated $Ca(OH)_2$ solution for two hours. The

experiments suggest that the $Na^+$ content of C-S-H increases after being immersed in a solution containing $Na^+$ ions and that solutions richer in NaOH resulted in C-S-H richer in $Na^+$. Indeed, the original $Na^+$ content of the C-S-H that was 11.40% after their synthesis was enhanced to 15.00% and 17.80% after being immersed in a solution containing respectively 0.1 and 1.0 mol of $Na^+$. When the same C-S-H that were immersed in NaOH + $Ca(OH)_2$ solution were immersed in sodium free solution saturated in $Ca(OH)_2$, the $Na^+$ content of the C-S-H was reduced (11.30 and 15.30%). This suggests that the composition of the C-S-H is not a static property that is set at the synthesis/formation of the C-S-H by is rather dynamic and evolves along with the composition of the contact solution.

Table 1.2 also present the measurements taken to characterize the surface charge of the C-S-H. Indeed, $Na^+$ is less efficient than $Ca^{2+}$ in "balancing" the negatively charged silicon tetrahedrons, which is translated in higher $\zeta$ potentials (in mV). C-S-H with higher content of $Na^+$ (compared to $Ca^{+2}$) are associated to higher $\zeta$ potentials. Ke-rui et al. (2004) experiment shows that calcium uptake on a certain area of the C-S-H lowers the potential of the surrounding areas to attract other positive ions (such as $Na^+$ or $K^+$). On the other hand, the uptake of $Na^+$ ion (that substituted $Ca^{2+}$ ion) tends to increase the potential of the C-S-H to attract positive charges.

**Table 1.2 : $Na^+$ % and $\zeta$ potential of C-S-H prior to treatment ($t_0$), after 2 h of treatments A or B ($t_1$) and after 2h of treatment C ($t_2$). Treatments A, B and C consist in immersing the C-S-H for two hours in solutions saturated in $Ca(OH)_2$ and respectively, 0.1, 1.0 and 0 mol/L of NaOH . (Ke-rui et al., 2004).**

| Treatments | Measure ↓ Time→ | $t_0$ (0h) | $t_1$ (2h) | $t_2$ (4h) |
|---|---|---|---|---|
| A and C | $Na^+$ in C-S-H | 11.40% | 15.00% | 11.30% |
| | $\zeta$ potential of C-S-H | -15.02 | -17.44 | -14.40 |
| B and C | $Na^+$ in C-S-H | 11.40% | 17.80% | 15.30% |
| | $\zeta$ potential of C-S-H | -15.02 | -21.43 | -15.54 |

In accordance with the results presented previously, Labbez et al. (2011) calculated that the charge density of the C-S-H decreases exponentially against the concentration of $Ca(OH)_2$ and experimental results showed that Na/Si increases along with $Na^+$ concentration of the solution, as presented in Figure 1.19.

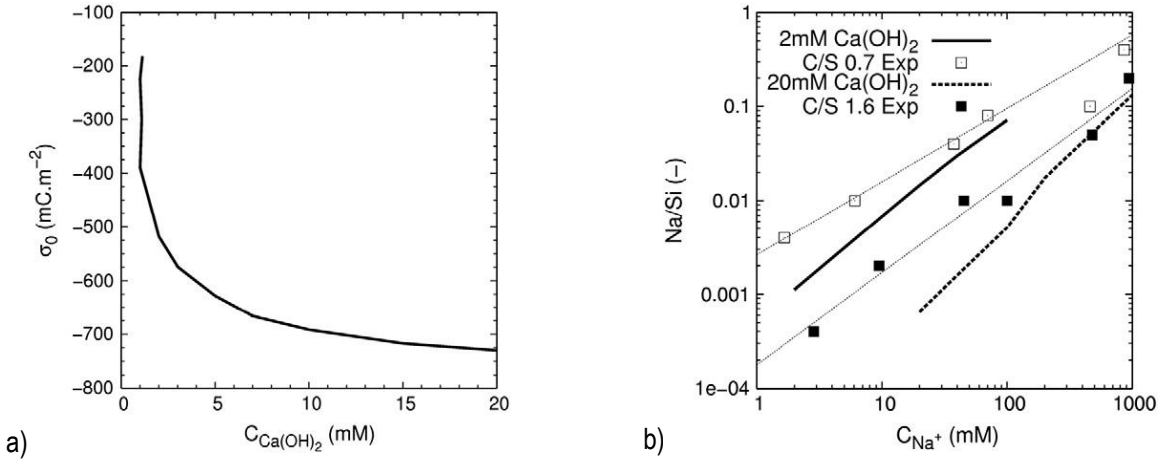


**Figure 1.19 : a) Predicted surface charge density (σ0) as a function of the bulk $Ca(OH)_2$ for C-S-H nano-particles Experimental and simulated amounts of sodium ions "adsorbed" per silica (Na/Si) versus bulk sodium concentration for two C/S and $Ca(OH)_2$ / NaCl mixtures (Labbez et al., 2011).**

Those studies show that the pore solution composition impacts on the C-S-H capabilities of binding alkalis. As a matter of fact, higher pH, higher concentrations of monovalent ions ($Na^+$, $K^+$), and lower concentrations of $Ca^{2+}$ are all factors that increase the alkali binding potential of the C-S-H.

### 1.5.1 Chemical Equilibrium

In cementitious systems, portlandite or $Ca(OH)_2$ is considered to be a regulator of the $[OH^-]$ of pore solution that maintains a high pH. According to the solubility of $Ca(OH)_2$, the activity of the $Ca^{2+}$ ion is inversely proportional to the square of $[OH^-]$. When silica is attacked or dissolved, $OH^-$ are inherently consumed, which results in a pH drop and which in turn promotes dissolution of $Ca(OH)_2$ (release of $Ca^{2+}$). However, the solubility of $Ca(OH)_2$ is not only affected by $[OH^-]$ but also by the presence of monovalent ions such as $Na^+$ and $K^+$. As proposed by Duchesne and Reardon (1995), the presence of alkali hydroxides tends to lower the solubility of $Ca(OH)_2$ (Figure 20). Indeed, in 1M solutions of KOH or NaOH, the solubility of $Ca(OH)_2$ is below 0.001 M, as presented in Figure 1.20. This suggests that when monovalent Na and K ions are present in sufficient amounts, portlandite might not play its regulator role and the pH drop associated to silica attack (and $OH^-$ consumption) might not be compensated by $Ca(OH)_2$ solubilization.

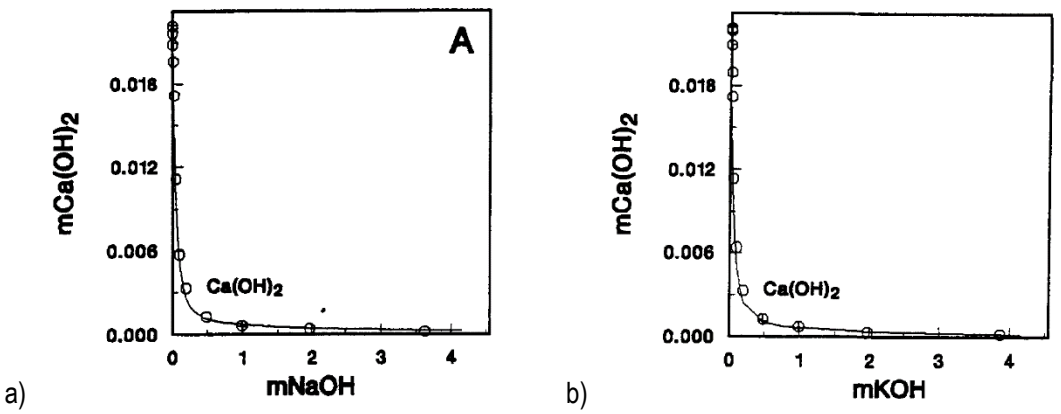


**Figure 1.20 : Comparison of model-calculated and experimental measurements of $Ca(OH)_2$ solubility in a) NaOH and b) KOH solution at 25°C. Circles are data from undersaturation while plus signs are from supersaturation. (Duchesne and Reardon, 1995).**

Maraghechi et al. (2016) presented the solubility of sodium silicates as a function of the pH (Figure 1.21), while the influence of alkali hydroxides on the solubility of silica and the pH of the solution has been investigated by Dent Glasser and Kataoka (1981) (Figure 1.22). The latter study suggests that, in the presence of alkali hydroxides, silica dissolves (which lowers the pH) until the solubility curve is reached.

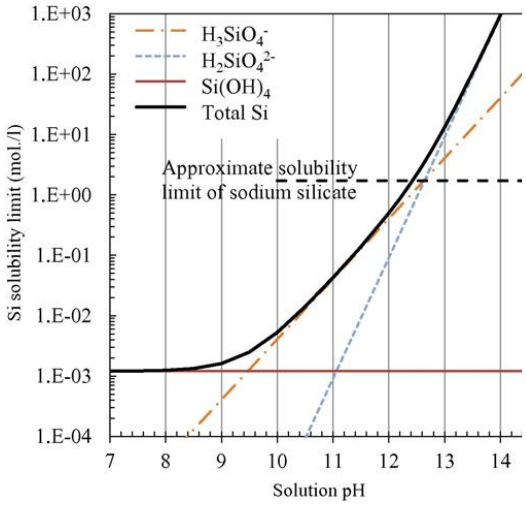


**Figure 1.21 : Speciation graph of vitreous silica at 25 °C using the thermodynamic data presented by (Maraghechi et al., 2016).**

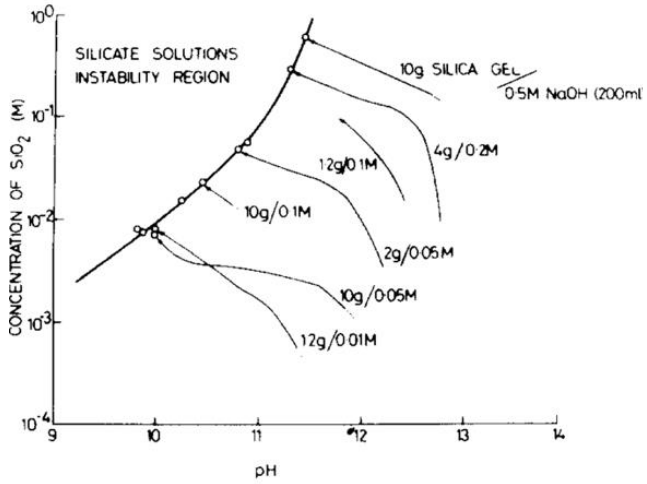


**Figure 1.22: The final concentration of dissolved silica against pH (heavy line) and the paths by which individual solutions approach it (light lines). (Dent Glasser and Kataoka, 1981).**

There is a complex equilibrium between $OH^-$, $Na^+/K^+$, $Ca^{2+}$ and silica, where $Ca^{2+}$ is released to enhance pH and Si is released to lower the pH. Meanwhile, $Na^+$ and $K^+$ act as catalyzers for the dissolution of silica as well as for calcium precipitation (Dove and Nix, 1997, Viallis et al., 1999). $Na^+$ and $K^+$ in solution tend to induce gelation of silica, while an alkali siliceous gel in contact with a $Ca^{2+}$-bearing solutions can exchange its $Na^+/K^+$ for $Ca^{2+}$.The ionic exchange with siliceous (solid) structures are closely related to the contact solution. Altogether, those interactions draw a very complex picture, which has been roughly drafted by Brown (1990) (Figure 1.23); however, the whole picture remains incomplete and requires further work and research.

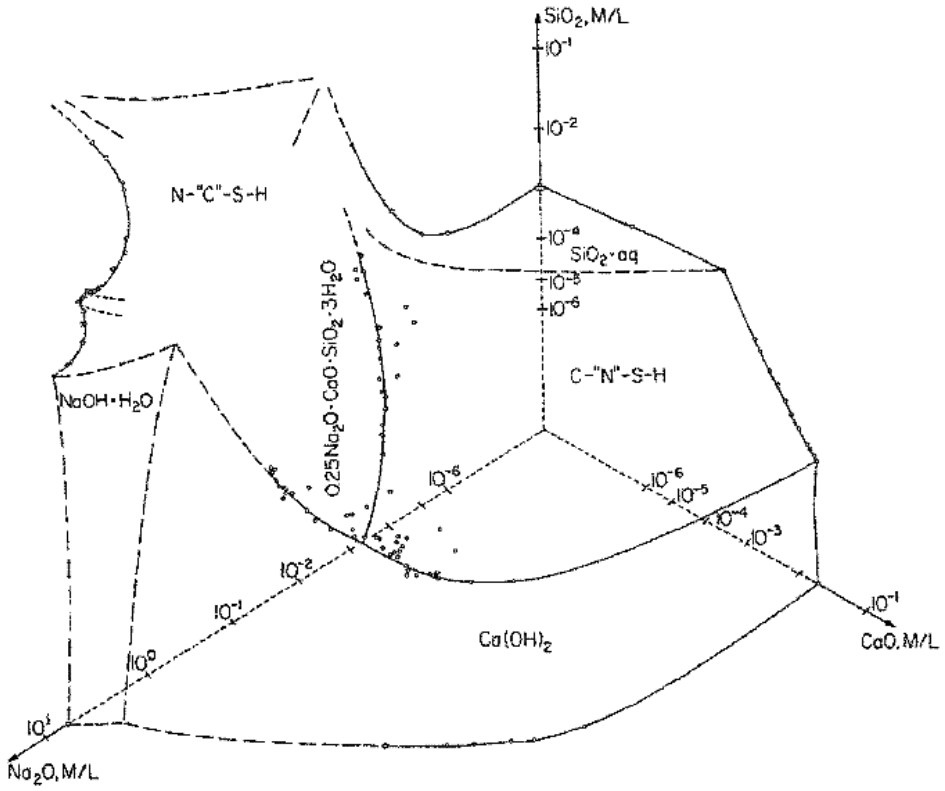


**Figure 1.23 : Quaternary system $Na_2O$-CaO-$SiO_2$-$H_2O$. Six "precipitation surfaces" are shown. Phases boundaries and invariant points indicated by dashed lines are uncertain (Brown, 1990).**

Furthermore, other species might interfere, such as $Al^{3+}$, which is suspected to bind to siliceous surfaces and prevent its dissolution (Chappex and Scrivener, 2013) or to promote the dissolution of metastable sulfoaluminates releasing anions ($SO_4^{2-}$), which "balance" the solution equilibrium instead of $OH^-$ (Shao et al., 2019). Diamond and Ong (1994) suggested that the sulfate concentration is, indeed, another element that is in equilibrium with the $Na^+$ and $K^+$ concentration of the pore solution, as presented at Figure 1.24. This underlines the importance of avoiding the oversimplification of the chemistry of concrete by labeling the effect of chemical species without considering all other species that interact with one another.

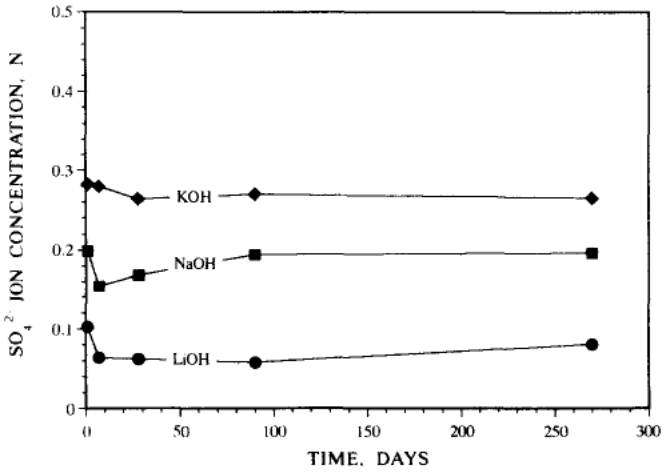


**Figure 1.24 : Changes in $SO_4^{2-}$ ion concentration with time in pore solution expressed from mortars made with cement to which LiOH, NaOH and KOH were added in the mixture water at level equivalent to 1% $Na_2O$ in the cement (Diamond and Ong, 1994).**

All the studies mentioned above highlight the importance of $Na^+$ and $K^+$ concentrations since those species interfere in the dissolution, the precipitation of reactive silica, pozzolanic materials, C-S-H, C-A-S-H, CH, ASR gel and possibly sulfate phases. $Na^+$ and $K^+$ are unavoidable to understand ASR since their concentrations in the pore solution is reflected in the amount and the composition of the main reaction products of concrete.

## 1.6 Ground Glass (GG)

### 1.6.1 Glass-Paste Interface

Lu et al. (2017) produced mortar bars containing recycled glass as fine aggregate and replaced 0 (control) or 20% of the cement by GG of various fineness. The authors measured the expansion of the mortar bars immersed in a 1N NaOH solution at 80°C up to 28 days and examined the reaction products by SEM-EDX. Figure 1.25 a) shows a glass fine aggregate particle in a mortar containing no GG and a reaction product (labeled 2) between the cement paste and the glass aggregate particle that is cracked like typical ASR gel. SEM-EDX indicates Na/Si and Ca/Si of 0.461 and 0.323, respectively, for the ASR gel. The ground glass (GG) presented in Figure 1.25 b) had a distinct reaction product on its surface, which was described as a pozzolanic material with Na/Si and Ca/Si of 0.758 and 1.152, respectively. Those results are in good agreement with the work of Idir et al. (2010) who also observed that the size of the glass particles is determinant in the nature of the reaction product.

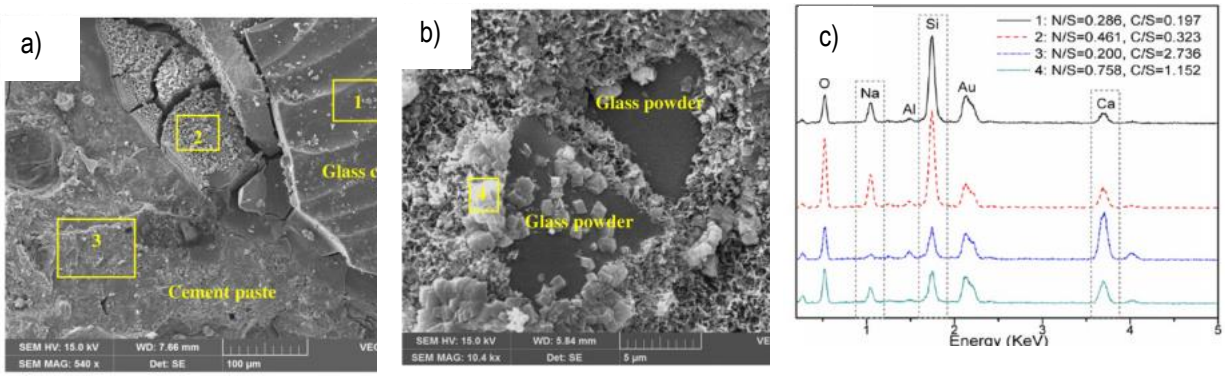


**Figure 1.25 : SEM images and EDX spectra of cement-based mortars: a) ASR damage in control mortar; b) pozzolanic reaction of GP c) compositions of zones 1, 2, 3 and 4 by EDX (Lu et al., 2017).**

Maraghechi et al. (2014) studied the reaction products of glass particles by making paste samples of CH : GP : water / 1 N NaOH solution with the accurate mass ratio of 1 : 4 : 5. The pastes were hand mixed for 1 minute, poured in plastic containers, sealed and cured at 60°C for up to 60 days. Pastes were vacuumed “dried” at 60°prior to SEM-EDS examination and analyses. The study allowed to find that the glass dissolution was stopped after 28 days, which suggests that CH was consumed and pH dropped to the point that the dissolution of glass was interrupted. For pastes made with 1 N NaOH, dissolution continued between 28 and 60 days and the glass particle was progressively replaced by “a third phase”. Figure 1.26 presents a chemical composition profile from the core to the rim of a glass particle, which shows a rim poorer in silica and sodium with steady calcium content. This suggests that silica and sodium diffuse out of the glass grain while calcium remains in place to form a reaction product with a Ca/Si close to that of a typical pozzolanic C-S-H. Such a rim was also identified in mortar bars containing 30%GP immersed for 30 days in a 1N NaOH solution, as presented in Figure 1.27, and in concrete specimens with 60% of cement replacement by GP (w/b of 0.49, binder, coarse and fine aggregate contents of 380, 825 and 913 kg/m$^3$, respectively) as presented in Figure 1.27. Other authors observed such glass rims, as presented in Figure 1.27 and Figure 1.28 (Rajabipour et al., 2010, Du and Tan, 2017).

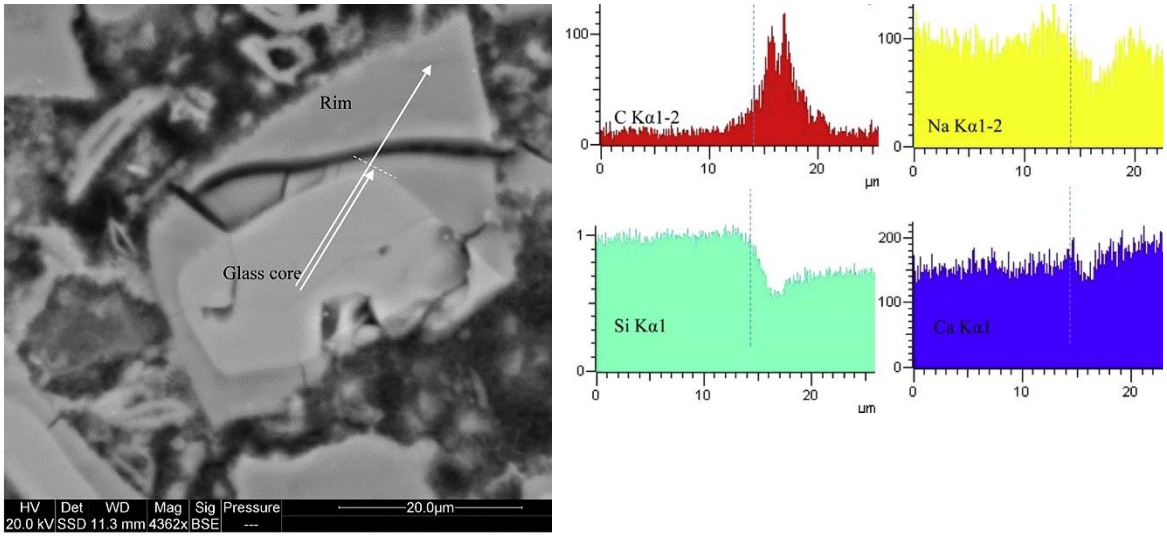


a) b)

**Figure 1.26 : a) Reaction rim around a glass particle and b) qualitative chemical composition of the grain and the rim (Maraghechi et al., 2014, Du and Tan, 2017).**

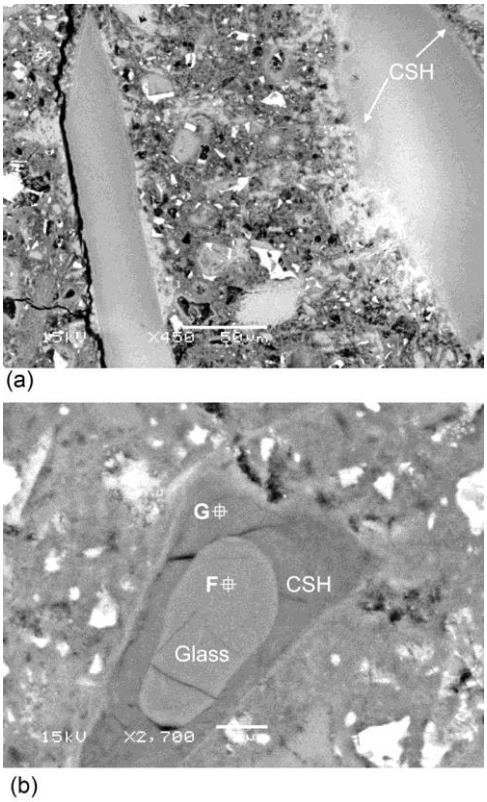


**Figure 1.27: Glass-paste interface in mortar bar prepared and conditioned as per ASTM 1260 at a) 14 days and b) 30 days (Rajabipour et al., 2010).**

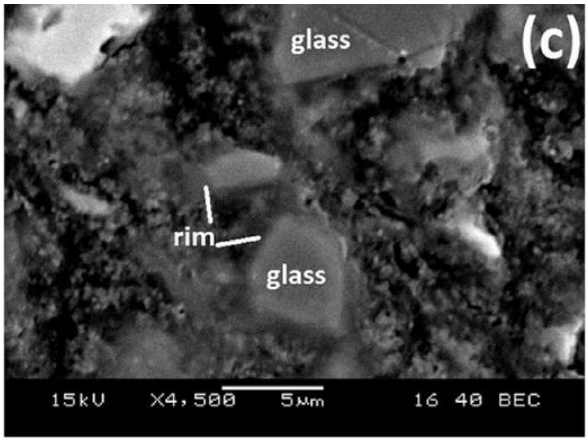


**Figure 1.28 : SEM image of 60%GP paste aged one year (Du and Tan, 2017).**

### 1.6.2 Inside of a Glass Particle

Maraghechi et al. (2012) used SEM to investigate, after 14 and 28 days, the formation of ASR products into preexisting cracks of glass particles used in mortar bars immersed in a 1N NaOH solution at 80°C. The authors suggested that ASR products do not form at the glass-paste interface nor inside small cracks of the particles (<2.5μm). Instead, ASR products were observed in cracks wider than the "critical width" of 2.5μm, as presented in Figure 1.29.

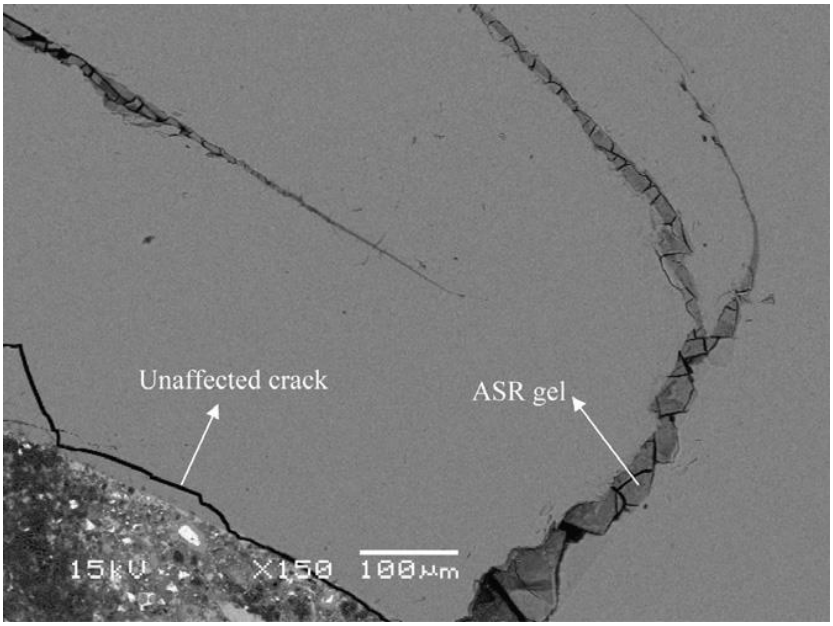


"

**Figure 1.29 Affected and unaffected cracks in mortars with 1.18–2.36 mm glass particles after exposure to ASTM C1260 condition for 14 days (Maraghechi et al., 2012).**

To strengthen the hypothesis that glass particles do not produce ASR products at their surface but rather in their interior, other authors heated crushed glass until its viscosity is reduced to the point that cracks are "healed"; then compared the expansion of mortar bars made with "healed" and "normal" crushed glass. At 14 days, mortar bars made with "normal" crushed glass showed expansion of approximately 0.8%, while those made with the glass heated at 650°C for 40 min had an expansion below 0.05% (Maraghechi et al., 2014). According to the authors, the coarser glass is crushed, the higher is the proportion of wide cracks, which is suggested to promote ASR product formation and expansion. The authors suggested that ASR occurs in wide cracks while pozzolanic reaction occurs at the glass/paste interface, as presented at Figure 1.30.

In addition, the study of Rajabipour et al. (2012) suggests no expansion nor the formation of ASR product in mortar bars incorporating crack free glass beads, as presented in Figure 1.31.

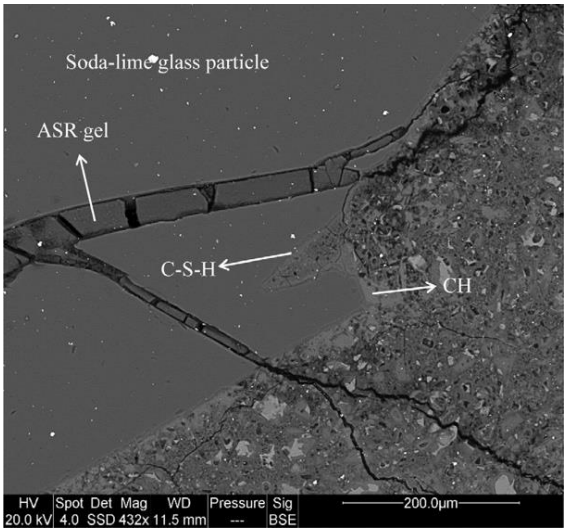


**Figure 1.30 : Alkali silica reaction occurring in the interior of a soda lime glass particle, while the particle surface undergoes a pozzolanic reaction (Maraghechi et al., 2014).**

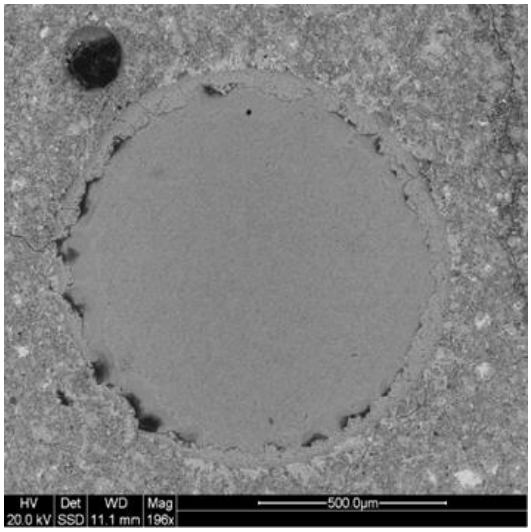


**Figure 1.31 : Glass dissolution and C-S-H rim around a glass bead (Rajabipour et al., 2012).**

## 1.7 Reference

(2003). "Nobel Price in chemistry 2003." Retrieved June 29th 2022, from https://www.nobelprize.org/prizes/chemistry/2003/summary/

Allen, N., M. L. Machesky, D. J. Wesolowski and N. Kabengi (2017). "Calorimetric study of alkali and alkaline-earth cation adsorption and exchange at the quartz-solution interface." Journal of Colloid and Interface Science 504: 538-548.

Barnes, B., S. Diamond and W. Dolch (1978). "The contact zone between Portland cement paste and glass "aggregate" surfaces." Cement and Concrete Research 8(2): 233-243.

Bérubé, M.-A., B. Durand, D. Vézina and B. Fournier (2000). "Alkali-aggregate reactivity in Quebec (Canada)." Canadian Journal of Civil Engineering 27(2): 226-245.

Brown, P. W. (1990). "The System Na2O-CaO-SiO2-H2O." Journal of the American Ceramic Society 73(11): 3457-3461.

Carles-Gibergues, A., M. Cyr, M. Moisson and E. Ringot (2008). "A simple way to mitigate alkali-silica reaction." Materials and Structures 41(1): 73-83.

Chappex, T. and K. L. Scrivener (2013). "The effect of aluminum in solution on the dissolution of amorphous silica and its relation to cementitious systems." Journal of the American Ceramic Society 96(2): 592-597.

Cooper, R. J., T. M. Chang and E. R. Williams (2013). "Hydrated alkali metal ions: spectroscopic evidence for clathrates." Journal of Physical Chemistry A 117(30): 6571-6579.

Criscenti, L. J., J. D. Kubicki and S. L. Brantley (2006). "Silicate Glass and Mineral Dissolution: Calculated Reaction Paths and Activation Energies for Hydrolysis of a Q3 Si by H3O+ Using Ab Initio Methods." The Journal of Physical Chemistry A 110(1): 198-206.

Davraz, M. and L. Gündüz (2008). "Reduction of alkali silica reaction risk in concrete by natural (micronised) amorphous silica." Construction and Building Materials 22(6): 1093-1099.

Dent Glasser, L. S. and N. Kataoka (1981). "The chemistry of 'alkali-aggregate' reaction." Cement and Concrete Research 11(1): 1-9.

Diamond, S. and R. Barneyback Jr (1981). Physics and chemistry of alkali-silica reactions. Master, Purdue University.

Diamond, S. and S. Ong (1994). "Effects of added alkali hydroxides in mix water on long-term SO42− concentrations in pore solution." Cement and Concrete Composites 16(3): 219-226.

Dove, P. M. and S. F. Elston (1992). "Dissolution kinetics of quartz in sodium chloride solutions: Analysis of existing data and a rate model for 25°C." Geochimica et Cosmochimica Acta 56(12): 4147-4156.

Dove, P. M. and C. J. Nix (1997). "The influence of the alkaline earth cations, magnesium, calcium, and barium on the dissolution kinetics of quartz." Geochimica et Cosmochimica Acta 61(16): 3329-3340.

Dove, P. M., N. Han and J. J. De Yoreo (2005). "Mechanisms of classical crystal growth theory explain quartz and silicate dissolution behavior." Proceedings of the National Academy of Sciences 102(43): 15357-15362.

Dove, P. M., N. Han, A. F. Wallace and J. J. D. Yoreo (2008). "Kinetics of amorphous silica dissolution and the paradox of the silica polymorphs." Proceedings of The National Academy of Sciences 105(29): 9903-9908.

Du, H. and Tan, K. H. (2017). "Properties of high volume glass powder concrete." Cement and Concrete Composites 75: 22-29.
Duchesne, J. and E. J. Reardon (1995). "Measurement and prediction of portlandite solubility in alkali solutions." Cement and Concrete Research 25(5): 1043-1053.

Elsen, J., J. Desmyter and E. Soers (2003). "Alkali-Silica reaction in concrete in Belgium-a review." Aardkundige Mededelingen (Industrial minerals: resources, characteristics and applications) 13: 73-79.

Gao, X. X., M. Cyr, S. Multon and A. Sellier (2013). "A comparison of methods for chemical assessment of reactive silica in concrete aggregates by selective dissolution." Cement and Concrete Composites 37(0): 82-94.

Garcia-Diaz, E., J. Riche, D. Bulteel and C. Vernet (2006). "Mechanism of damage for the alkali–silica reaction." Cement and Concrete Research 36(2): 395-400.

Gholizadeh-Vayghan, A. and F. Rajabipour (2017). "The influence of alkali–silica reaction (ASR) gel composition on its hydrophilic properties and free swelling in contact with water vapor." Cement and Concrete Research 94 (Supplement C): 49-58.

Glasser, L. S. D. (1979). "Osmotic pressure and the swelling of gels." Cement and Concrete Research 9(4): 515-517.

Gudmundsson, G. and H. Olafsson (1999). "Alkali-silica reactions and silica fume: 20 years of experience in Iceland." Cement and Concrete Research 29(8): 1289-1297.

Helmuth, R., D. Stark, S. Diamond and M. Moranville-Regourd (1993). "Alkali-silica reactivity: an overview of research." Contract 100: 202.

Hong, S.-Y. and F. Glasser (1999). "Alkali binding in cement pastes: Part I. The CSH phase." Cement and Concrete Research 29(12): 1893-1903.

Hu, C., B. P. Gautam and D. K. Panesar (2018). "Nano-mechanical properties of alkali-silica reaction (ASR) products in concrete measured by nano-indentation." Construction and Building Materials 158: 75-83.

Idir, R., M. Cyr and A. Tagnit-Hamou (2010). "Use of fine glass as ASR inhibitor in glass aggregate mortars." Construction and Building Materials 24(7): 1309-1312.

Idir, R., M. Cyr and A. Tagnit-Hamou (2011). "Pozzolanic properties of fine and coarse color-mixed glass cullet." Cement and Concrete Composites 33(1): 19-29.

Imberti, S., A. Botti, F. Bruni, G. Cappa, M. A. Ricci and A. K. Soper (2005). "Ions in water: The microscopic structure of concentrated hydroxide solutions." The Journal of Chemical Physics 122(19).

Jiang, W. (1997). Alkali-activated cementitious materials: Mechanisms, microstructure and properties, ProQuest LLC.
Karamberi,A., Chaniotakis,E., Papageorgiou, D.and Moutsatsou, A. (2006). "Influence of glass cullet in cement pastes." China Particuology 4(5): 234-237.

Katayama, T. (2012). ASR gels and their crystalline phases in concrete—universal products in alkali–silica, alkali–silicate and alkali–carbonate reactions. Proceedings of the 14th International Conference on Alkali Aggregate Reactions (ICAAR), Austin, Texas.

Katayama, T., T.S. Helgason, and H. Olafsson (1996). Petrography and alkali reactivity of some volcanic aggregates from Iceland. Proceedings of the10th International Conference, Melbourne, Australia.

Ke-rui, Y., Z. Cai-wen Z., Zhi-gang, G. Zhi and N. Cong (2004). A study on alkali-fixation ability of CSH gel. Proceedings of the 12th International Conference on Alkali-Aggregate Reaction in Concrete (ICAAR), Beijing, China 120: 2.

Labbez, C., Pochard,I. Jönsson, B. and Nonat, A, (2011). "C-S-H/solution interface: Experimental and Monte Carlo studies." Cement and Concrete Research 41(2): 161-168.

Leemann, A., T. Katayama, I. Fernandes and M. A. T. M. Broekmans (2016). Types of alkli–aggregate reactions and the products formed." Construction Materials 169(CM3): 117-178.

Leemann, A., G. Le Saout, F. Winnefeld, D. Rentsch and B. Lothenbach (2011). "Alkali-Silica Reaction: the Influence of Calcium on Silica Dissolution and the Formation of Reaction Products." Journal of the American Ceramic Society 94(4): 1243-1249. .

Leemann, A. and B. Lothenbach (2008). "The influence of potassium–sodium ratio in cement on concrete expansion due to alkali-aggregate reaction." Cement and Concrete Research 38(10): 1162-1168.

Lu, J.-X., B.-J. Zhan, Z.-H. Duan and C. S. Poon (2017). "Using glass powder to improve the durability of architectural mortar prepared with glass aggregates." Materials & Design 135: 102-111.

Mahler, J. and I. Persson (2012). "A study of the hydration of the alkali metal ions in aqueous solution." Inorganic Chemistry 51(1): 425-438.

Maraghechi, H. (2014). "Development and assessment of alkali activated recycled glass-based concretes for civil infrastructure."

Maraghechi, H., M. Maraghechi, F. Rajabipour and C. G. Pantano (2014). "Pozzolanic reactivity of recycled glass powder at elevated temperatures: Reaction stoichiometry, reaction products and effect of alkali activation." Cement and Concrete Composites 53(0): 105-114.

Maraghechi, H., F. Rajabipour, C. G. Pantano and W. D. Burgos (2016). "Effect of calcium on dissolution and precipitation reactions of amorphous silica at high alkalinity." Cement and Concrete Research 87: 1-13.

Maraghechi, H., S. Salwocki and F. Rajabipour (2017). "Utilisation of alkali activated glass powder in binary mixtures with Portland cement, slag, fly ash and hydrated lime." Materials and Structures 50(1): 16.

Maraghechi, H., S.-M.-H. Shafaatian, G. Fischer and F. Rajabipour (2012). "The role of residual cracks on alkali silica reactivity of recycled glass aggregates." Cement and Concrete Composites 34(1): 41-47.

Mukherjee, P.K. and J.A. Bickley (1986). Performance of glass as a concrete aggregate. 7th international conference on alkali aggregate reaction. Ottawa.

Rajabipour, F., E. Giannini, C. Dunant, J. H. Ideker and M. D. A. Thomas (2015). "Alkali–silica reaction: Current understanding of the reaction mechanisms and the knowledge gaps." Cement and Concrete Research 76: 130-146.

Rajabipour, F., H. Maraghechi and G. Fischer (2010). "Investigating the alkali-silica reaction of recycled glass aggregates in concrete materials." Journal of Materials in Civil Engineering 22(12): 1201-1208.

Rajabipour, F., H. Maraghechi and S. Shafaatian (2012). ASR and its mitigation in mortar containing recycled soda-lime glass aggregates. . Proceedings of the 14th International Conference on Alkali Aggregate Reactions (ICAAR), Austin, Texas.

Redden, R. and N. Neithalath (2014). "Microstructure, strength, and moisture stability of alkali activated glass powder-based binders." Cement and Concrete Composites 45: 46-56.

Saccani, A., and Bignozzi, M.C. (2010). "ASR expansion behavior of recycled glass fine aggregates in concrete." Cement and Concrete Research 40(4): 531-536.

Shao, Q., K. Zheng, X. Zhou, J. Zhou and X. Zeng (2019). "Enhancement of nano-alumina on long-term strength of Portland cement and the relation to its influences on compositional and microstructural aspects." Cement and Concrete Composites 98: 39-48.

Stade, H. (1989). "On the reaction of C-S-H(di, poly) with alkali hydroxides." Cement and Concrete Research 19(5): 802-810.

Stanton, T. E. (1940). "Expansion of Concrete through Reaction between Cement and Aggregate." Proceedings of the Americain Society of Civil Engineer 66(10): 1871-1811.

Struble, L. J. and S. Diamond (1981). "Swelling properties of synthetic alkali silica gels." Journal of the American ceramic society 64(11): 652-655.

Viallis,H., Faucon, P., Petit,J.C. and Nonat, A.(1999). "Interaction between Salts (NaCl, CsCl) and Calcium Silicate Hydrates (C−S−H)." The Journal of Physical Chemistry B 103(23): 5212-5219.

Visser, J. H. M.(2018). "Fundamentals of alkali-silica gel formation and swelling: Condensation under influence of dissolved salts." Cement and Concrete Research 105: 18-30.

Wallace, A. F, G.V. Gibbs and P.M. Dove (2010). "Influence of Ion-Associated Water on the Hydrolysis of Si−O Bonded Interactions." The Journal of Physical Chemistry A 114(7): 2534-2542.

Wikipedia (2019), https://en.wikipedia.org/wiki/Aqueous_solution

Wilson, W., L. Sorelli and A. Tagnit-Hamou (2018). "Automated coupling of NanoIndentation and Quantitative Energy-Dispersive Spectroscopy (NI-QEDS): A comprehensive method to disclose the micro-chemo-mechanical properties of cement pastes." Cement and Concrete Research 103: 49-65.

Yang, Y., T. Ji, X. Lin, C. Chen and Z. Yang (2018). "Biogenic sulfuric acid corrosion resistance of new artificial reef concrete." Construction and Building Materials 158: 33-41.

Zhuravlev, L. T. (2000). "The surface chemistry of amorphous silica. Zhuravlev model." Colloids and Surfaces A: Physicochemical and Engineering Aspects 173(1): 1-38.

# Chapter 2. Effect of Ground Glass (GG) on the Availability of Alkalis in the Pore Solution of Binary Cement Pastes


## Résumé

Le verre broyé (VB) produit à partir d'installations de recyclage du verre post-consommation est un autre matériau cimentaire alternatif qui est souvent considéré pour des conceptions écologiques de mélanges de béton. Cependant, l'expérience sur son comportement dans le béton est limitée ou quelque peu contradictoire. De nombreuses études suggèrent que le verre broyé peut supprimer l'expansion du béton associable à la réaction alcali-silice (RAS), tandis que d'autres suggèrent que sa teneur élevée en alcalis maintient le potentiel expansif du béton face à la RAS et limite par conséquent son caractère préventif en présence de granulats réactifs.

Les travaux réalisés dans le cadre de cette étude visent à clarifier la disponibilité globale des alcalis dans la solution interstitielle de matrices cimentaires incorporant le VB. À cette fin, l'extraction de solutions interstitielles a été réalisée sur des pâtes contenant 0%, 20% et 40% de VB et des ciments de 0,25%, 0,63%, 0,94% et 1,25% $Na_2Oe$, et leur composition analysée après 28 et 91 jours de conditionnement. Les résultats ont montré que l'effet du VB sur la concentration en ions hydroxyles de la solution interstitielle est limité pour le ciment à haute teneur en alcalis mais plutôt important dans le cas du ciment à basse teneur. Aussi, une augmentation du niveau de remplacement du ciment par le VB (0, 20 et 40%) a un impact sur la composition en alcalis de la solution interstitielle, soit une réduction de la concentration en potassium et une augmentation de la concentration en sodium. L'impact sur la $[Na^+]$ est visible autant à 28 qu'à 91 jours mais une distinction par rapport à la composition du ciment est plus évidente à plus long terme.

## Abstract

Finely ground glass (GG) produced from recycling facilities is an alternative supplementary cementing material that is often considered for eco-friendly concrete mix designs. However, documentation on its behaviour in concrete is limited or somewhat contradictory. Many studies suggest that GG can suppress the expansion of concrete due to alkali-silica reaction (ASR), while others suggest that its high alkali content maintains the expansive potential in concrete due to ASR and consequently limits its preventive character in the presence of reactive aggregates.

The present work seeks to clarify the overall availability of alkalis in the pore solution of cementitious matrices incorporating GG. For this purpose, pore solution extraction had been conducted on pastes containing 0%, 20% and 40% of GG and cements of alkali levels of 0.25%, 0.63%, 0.94% and 1.25% $Na_2O$eq. After up to 91 days of conditioning, the concentration of alkalis available in the pore solution was analysed. Results showed that the effect of GG on the hydroxyl concentration of the pore solution is limited for cement with high alkali content and important for low alkali cement. Also, GG tends to reduce the potassium concentration and to increase the sodium concentration of the pore solution.

## 2.1 Introduction

Whether or not post-consumer Ground Glass (GG) is safe to incorporate into concrete is a frequently debated question. Understandably, GG can raise enthusiasm because of its environmental and economic potential as a portland cement replacement, thus contributing at reducing the gas emissions that are part signature of concrete. However, a closer look at its chemical composition leads to contradictory behavioral expectations; on one hand, GG is a material that reacts through a pozzolanic reaction in concrete (Shi et al., 2005, Shi and Zheng, 2007, Taha and Nounu, 2008, Idir et al., 2011), which is known to be beneficial for improving several mechanical and durability properties of concrete. On the other hand, GG is a supplementary cementing material (SCM) with very high alkali content (≈13% $Na_2Oeq$), which may be problematic regarding durability because of its chemical potential to "fuel" Alkali-Silica Reaction (ASR). Furthermore, unpublished concrete prism test results (Fily-Paré and Lafrenière, 2017) with moderately-reactive limestone aggregate conducted at Université Laval provide hints to anticipate the behaviour of GG into concrete. As shown in Figure 2.1, expansions of concrete prisms incorporating GG (GP in Figure 2.1) are similar to those made with a high alkali (HA) fly ash (FA) ($Na_2Oeq$ = 9.70% and CaO = 16.8%).

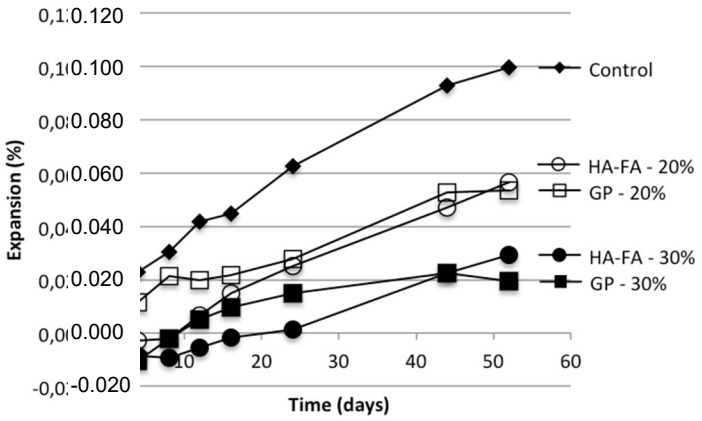


**Figure 2.1 : Expansion of concrete prisms at 52 weeks for a moderately reactive limestone aggregates. The testing was performed in accordance with Standard Practice CSA A23.1-28A (Fily-Paré and Lafrenière, 2017).**

The majority of SCMs, e.g. FA, BSF, SF, MK, natural pozzolans, can efficiently reduce/prevent deleterious expansion due to ASR provided they are used in appropriate amounts in concrete; however, Fournier et al. (2008) found that HA FA were significantly less effective for ASR control. Based on the results obtained on FA from 29 different sources, Thomas et al. (2006) showed that, for a 25% replacement level in concrete incorporating a highly-reactive aggregate (Spratt limestone), FA with low to moderate alkali (≤ 4% $Na_2Oeq$) and calcium oxide contents (≤ 20% CaO) are generally effective in controlling concrete prism expansion at < 0.040% at 2 years. Concrete prism expansion was however found to increase significantly for FA with a CaO content >

20%, while ashes with an alkali content > 5% $Na_2Oe$ were found ineffective at that replacement level, regardless of the CaO content of the FA. Duchesne and Bérubé (1994a) showed that a HA FA used at 20 and 40% cement replacement was not efficient in reducing the expansion of concrete prisms incorporating two different highly-reactive aggregates under the two-year 0.040% performance criterion. To extend the knowledge on the topic, Shehata (2001) suggested that, for a given replacement level of 25%, the two-year concrete prism expansion can be roughly estimated to be below the 0.040% expansion limit if the result of the following equation 2.1 is respected after plotting the chemical composition of the FA.

$$(10Na_2Oe + 4.45CaO)/SiO_2 < 2 \qquad (r^2=0.74) \qquad \text{Equation 2.1}$$

Furthermore, Shehata (2001) observed that the same parameters influence the concentration of hydroxyl ions in the pore solution, as follows (Equation 2.2):

$$OH^- = 0.185 + 0.44\,(10Na_2Oe + CaO)/SiO_2 \qquad (r^2 = 0.93) \qquad \text{Equation 2.2}$$

Such observations point out that higher alkali content in FA will result in greater concrete prism expansion, as well as greater concentration of $OH^-$ in the concrete pore solution.

### 2.1.1 Alkali Release of High Alkali FA

The impact on the pore solution composition of cement replacement by HA FA was explored by Duchesne and Bérubé (1994b) who prepared pastes with FA of different alkali contents (2.34%, 3.07% and 8.55% $Na_2Oeq$). After 1 year of curing in sealed conditions at 38°C, the pore solution was extracted from the paste specimens under a high pressure of 560 MPa (≈ 80 000 psi) and the chemical composition was determined. They showed that, greater alkali content of the dry raw material leads to higher alkali concentration. Indeed, for the 40% replacement level, the three FA-based binders contained more alkalis than the control by 149.1%, 177.0% and 385.7%, respectively, while the pore solution had greater alkali content by 42.1%, 36.1% and 174.1% than the control, respectively. An increase of alkalis in the cementitious material leads to an increase of alkalis in the pore solution, but the relation was not proportional considering that increasing the alkali of the dry material by almost 4 folds only increased the alkali content in the pore solution by less than 2 folds. This indicates that the increase of alkali released into the pore solution cannot be predicted by taking into consideration exclusively the alkali content of the dry material in the mix.

Also, Duchesne and Bérubé (1994b) calculated that for a 20% substitution of the high-alkali cement by an HA FA in pastes sample, 88% of the total alkali of the FA are available in the pore solution at 28 days and only 62% at 1.5 years. For a 40 % substitution, 52% of the alkalis are available at 28 days and 36% at 1.5 year. The reduction observed as a function of time suggests that once released, alkalis do not necessarily stay available over time in the pore solution.

### 2.1.2 Alkali Release of GG

Schwarz and Neithalath (2008) studied the potential alkali release of GG in a basic solution. They observed that, when 5g (≈ 0.18oz) of GG is put in a 200 ml (6.8 liquid oz) saturated $Ca(OH)_2$ solution (pH of about 12.4), the alkali concentration measured using flame atomic absorption corresponds to only 5.15% of the total alkali content of the GG. This result suggests that there is only a small fraction of the GG alkalis that is released in the solution. Moreover, a saturated lime solution does not accurately represent the concrete pore solution, which also contains alkalis and has an increased pH (often greater than 13) compared to a saturated lime solution. According to Dove and Elston (1992), the presence of alkali ions are known to weaken bounds between silica tetrahedrons and greatly enhance dissolution of amorphous silica in a highly basic environment. This behaviour can have an important impact on the solubility of GG in a real concrete pore solution. Saccani and Bignozzi (2010) also showed that solubility of glass is very low in a saturated lime solution. The found that weight changes of GG specimens are negligible after 28 days of immersion in the above solution, but when 1N NaOH is added to the solution, the weight changes are above 5% for borosilicate glass specimens and around 0.5% for soda-lime glass specimens. In addition, for a 1N NaOH solution only (i.e. no lime), all glass specimens show weight changes ranging between 7% and 20%.

Schwarz and Neithalath (2008) conducted effective electric conductivity testing on paste specimens (w/b of 0.8), made with 5%, 10% and 20% replacement of portland cement (0.73% $Na_2Oe$) by GG. The samples were stored in saturated calcium hydroxide solution up to almost 42 days. Results showed that increasing the GG contents results in effective conductivity values of 2.3, 2.0, 1.8, and 1.7 S/m for 0, 5, 10 and 20% GG replacement levels, respectively. The authors suggested that the alkali released by GG does not compensate for the alkalis released by the cement. In other words, according to them, cement replacement by GG dilutes the “available” alkali level in a cement matrix and does not increase alkalinity of the pore solution. It is worth noting that the samples possibly underwent a considerable alkali leaching during the long immersion period in saturated lime solution prior to conductivity measurements.

Saeed (2008) studied the alkali release by GG in the pore solution using the hot water extraction procedure described by Vézina et al. (2002) or Rogers and Hooton (1991). In this work, a cement with an alkali content of 0.79% $Na_2Oeq$ was used to produce paste specimens of various GG contents and that were kept sealed up to

28 days at various temperatures. At selected ages, the specimens were ground to powder and the powders were boiled, filtered and the solution analysed. The results showed that the influence of the various GG contents on pH is a weak parameter compared to the curing period. Indeed, for GG contents of 0 to 30%, pH varies from 12.3 to 12.5 at one day but from 13.2 to 13.4 at 28 days. Saeed (2008) also concluded that GG only releases a small amount of its alkalis at the early stage of hydration, i.e. between 0.7% and 1.3% at 3 days and between 1% and 1.7% at 28 days.

Based on the above studies, one could conclude that GG does not release much of its alkalis in a high alkali environment. This conclusion is different from what would be expected when comparing the behaviour of GG to that of HA FA.

## 2.2 Scope and Objective

The aim of this study is to contribute to the understanding of the effect of GG on the concrete pore solution composition. In order to do so, paste specimens of four different "cement alkali loadings" (from 0.25 to 1.25% $Na_2Oeq$) were made with 0, 20 and 40% GG replacement. The paste specimens were kept in sealed containers and their pore solution extracted under high pressure after 28 and 91 days, from which the alkali concentration was analyzed.

## 2.3 Materials and Methods

### 2.3.1 Material and Specimen Fabrication

Paste samples were made using GG and cements of various alkali contents. The chemical composition of each material used is presented in Table 2.1. Twelve mixtures were made where each cement with alkali contents of 0.25%, 0.63%, 0.94% and 1.25% $Na_2Oeq$ was replaced by GG in mass proportions of 0%, 20% and 40%. The 1.25% alkali content was actually reached using NaOH added to the 0.94% cement. The w/b was 0.50 for all mixtures. The mix proportions are presented in Table 2.2**.**

Paste samples were cast in sealed plastic container, 30 mm (1" 3/16.) by 55 mm (2" 1/8) in size, agitated for the first 24h at 23°C (73°F) and conditioned at 38°C (100°F) afterwards. After 28 or 91 days of curing, the pore solution of three replicates was extracted under high pressure (maximum of 180 MPa or ≈26 000 Psi). Collected solutions were diluted in nitric acid solution (5%) and then analysed by atomic absorption spectroscopy (AAS).

**Table 2.1 : Chemical composition of GG and cements.**

| Elements (oxides) | GG | Cement 0.25% | Cement 0.63% | Cement 0.94% |
|---|---|---|---|---|
| $SiO_2$ (%) | 70.53 | 19.74 | 19.58 | 18.7 |
| $Fe_2O_3$ (%) | 0.35 | 3.45 | - | 3.7 |
| $Al_2O_3$ (%) | 2.06 | 4.56 | 4.58 | 5.0 |
| CaO (%) | 10.77 | 64.79 | 62.09 | 60.8 |
| MgO (%) | 1.14 | 0.91 | 2.91 | 2.7 |
| $SO_3$ (%) | - | 2.45 | 4.02 | 3.8 |
| $Na_2O$ (%) | 12.49 | 0.14 | 0.22 | - |
| $K_2O$ (%) | 0.66 | 0.16 | 0.62 | - |
| $Na_2Oe$ (%) | 12.92 | 0.25 | 0.63 | 0.94 |

**Table 2.2 : Mixture proportions for w/b of 0.50**

| Mixture | GG | Cement | | | Cement | |
|---|---|---|---|---|---|---|
| | | 0.25% | 1.25% | 0.94% | 1.25% (Cement 0.94% + NaOH | Water |
| | (g) | (g) | (g) | (g) | NaOH (g) | (ml) |
| 0-GG-%A | 0 | 840 | 840 | 840 | 2.69 | 420 |
| 20-GG-%A | 178 | 672 | 672 | 672 | 2.69 | 420 |
| 40-GG-%A | 346 | 504 | 504 | 504 | 2.02 | 420 |

### 2.3.2 Statistical Data Treatment

Data treatment was performed using R software. The variability of the chemical composition results was calculated using the standard deviation of a set of three replicates for each mix at two ages; however, for data analysis and the computation of the error on a regression, the mean of the three points was used. As explained by Vaux et al. (2012), that choice was made since only one observation can be made for a given set of parameters. In our case, one single batch was made for each mixture and three repeated measurements (i.e. three replicates / paste specimens) were made and then tested at two ages (28 and 91 days). Thus, only two observations were possible per mixture since only the time parameter was independent

In this document, the error bars reflect the variation between the three replicates of a single measurement and the error of numerical computations reflects the deviation between the measurements and the proposed model analysed. The error bars represent the Standard Error (SE), which is the ratio of the standard deviation to the square root of the number of samples.

The computed analysis presented in the paper takes the form expressed by Equation 2.3

$$y=\beta_0+\beta_1 x_1+\beta_2 x_2+\beta_3 x_3+\beta_{12} x_1 x_2 \qquad \text{Equation 2.3}$$

Where $y$ is the response of $[OH^-]$, $[K^+]$ or $[Na^+]$; $\beta_0$ is the intercept; $\beta_1$ is the coefficient associated to the age parameter ($x_1$); $\beta_2$ is the coefficient of percentage of GG replacement ($x_2$) ); $\beta_3$ is the coefficient of the alkali content of cement ($x_3$) and $\beta_{12}$ is the coefficient for the interaction between %GG and "cement" $Na_2Oe$ ($x_1$ $x_2$).

The significance of the variables to predict the response parameters of the performed analysis is evaluated using the t-test: a comparison between a critical t-value and the t-ratio of the coefficient defined by the absolute value of the coefficient divided by the standard error. If the *t-ratio* of a coefficient is above the *critical t-value*, then the variable is considered significant to predict the response. The *critical t-value* for the analysis performed in this paper is defined by t ($\alpha$/2; n-p-1), where $\alpha$ is for a confidence interval of 95%, n is the number of observations and p is the number of factors and/or interactions. For $n$=24 and $p$=3 or 4, the *critical t-value* = 2.09 and for $n$=12 and $p$=3, the *critical t-value* = 2.31.

The t-test of the intercept has little or no significance in this study since the computed models are not meant to predict the response of mixtures but to discuss the effect of the parameters.

The overall significance of the analysis is also checked by the F-test, which is the comparison to a *critical F-value* and the *F-ratio* of the model. F-ratio is calculated as follows: regression mean square / residual mean square. This test is also an asset to verify the independence of variables against one another. If the *F-ratio* of the analysis is above the *critical F-value*, the proposed variable is then considered significant to predict the response. The *Critical F-value* is defined as F: ($\alpha$; p; n-p-1), where $\alpha$ is for a confidence interval of 95%, n is the number of observations and p is the number of factors and/or interactions. For $n$=24 and $p$=3, the *critical F-value* = 1.48; for $n$=24 and $p$=4, the *critical F-value* =1.47, and for $n$=12 and $p$=3, the *critical F-value* 1.63.

Finally, the $r^2$, which is defined as the sum of the squared prediction error of the predicting data to the total sum squared, is also indicated to express the validity of the model.

## 2.4 Results and Discussion

The compositions (i.e. $[Na^+]$ and $[K^+]$ of the pore solutions extracted at 28 and 91 days are presented in table 2.3.

**Table 2.3 : Chemical composition of pore solutions and the standard errors (SE) at 28 and 91days.**

| Mix | 28 days | | | | 91 days | | | |
|---|---|---|---|---|---|---|---|---|
| | [$Na^+$] | | [$K^+$] | | [$Na^+$] | | [$K^+$] | |
| | mmol/l† | SE | mmol/l†† | SE | mmol/l† | SE | mmol/l†† | SE |
| 0-GG-0.25A | 102 | 6 | 77 | 6 | 127 | 1 | 92 | 4 |
| 0-GG-0.63A | 145 | 9 | 233 | 6 | 198* | 8 | 282* | 17 |
| 0-GG-0.94A | 187 | 7 | 444 | 1 | 242 | 19 | 581* | 17 |
| 0-GG-1.25A | 291 | 35 | 588 | 66* | 460* | 17 | 548* | 47 |
| 20-GG-0.25A | 478 | 23 | 55 | 3 | 551 | 1 | 51* | 3 |
| 20-GG-0.63A | 473 | 13 | 135 | 5 | 600 | 13 | 155 | 2 |
| 20-GG-0.94A | 478 | 20 | 209 | 9 | 615 | 21 | 240 | 18 |
| 20-GG-1.25A | 625 | 26 | 254 | 7 | 683 | 18 | 280 | 7 |
| 40-GG-0.25A | 493 | 14 | 35 | 0 | 575 | 23 | 34 | 0 |
| 40-GG-0.63A | 483 | 23 | 78 | 2 | 663* | 6 | 79* | 5 |
| 40-GG-0.94A | 546 | 6 | 157 | 1 | 783 | 21 | 179 | 8 |
| 40-GG-1.25A | 669 | 5 | 169 | 14 | 803 | 52 | 217* | 33 |

* Only two out of three samples provided enough pore solution to conduct chemical analysis.

† 1mol/l=22.9g/l for sodium ions

†† 1mol/l=39.1g/l for potassium ions

The concentration of hydroxyl ions in the pore solution [$OH^-$] can be estimated using the Equation 2.4. Calculated values are presented in Table 2.4.

$$[OH^-] \approx [Na^+] + [K^+] \qquad \text{Equation 2.4}$$

**Table 2.4 : Estimated [$OH^-$] in the pore solution and standard error (SE) at 28 & 91 days.**

| Mix | 28 days | | 91 days | |
|---|---|---|---|---|
| | mmol/l† | SE | mmol/l† | SE |
| 0GG-0.25A | 179 | 11 | 219 | 4 |
| 0GG-0.63A | 378 | 8 | 662 | 23 |
| 0GG-0.94A | 631 | 3 | 745 | 19 |
| 0GG-1.25A | 885 | 6 | 1008 | 30 |
| 20GG-0.25A | 532 | 24 | 601 | 3 |
| 20GG-0.63A | 607 | 16 | 756 | 14 |
| 20GG-0.94A | 687 | 20 | 855 | 28 |
| 20GG-1.25A | 879 | 24 | 977 | 22 |
| 40GG-0.25A | 527 | 14 | 610 | 24 |
| 40GG-0.63A | 561 | 24 | 798 | 1 |
| 40GG-0.94A | 703 | 7 | 954 | 24 |
| 40GG-1.25A | 839 | 9 | 1069 | 66 |

†1mol/l=17.0 g/l for hydroxyl ions

Figure 2.2 shows the trends, both at 28 and 91 days, of increasing [$OH^-$] in the pore solution in the control specimens with increasing "cement" alkali content. Interestingly, such increasing trends are also obtained for the GG mixes. However, the [$OH^-$] in GG mixes is significantly higher than that of controls at low "cement" alkali contents, but the difference is decreasing progressively as the "cement" alkali content increases. It is also noticeable in Figure 2.2 that at each measuring point, the difference in [$OH^-$] between 20% and 40% GG mixes is low.

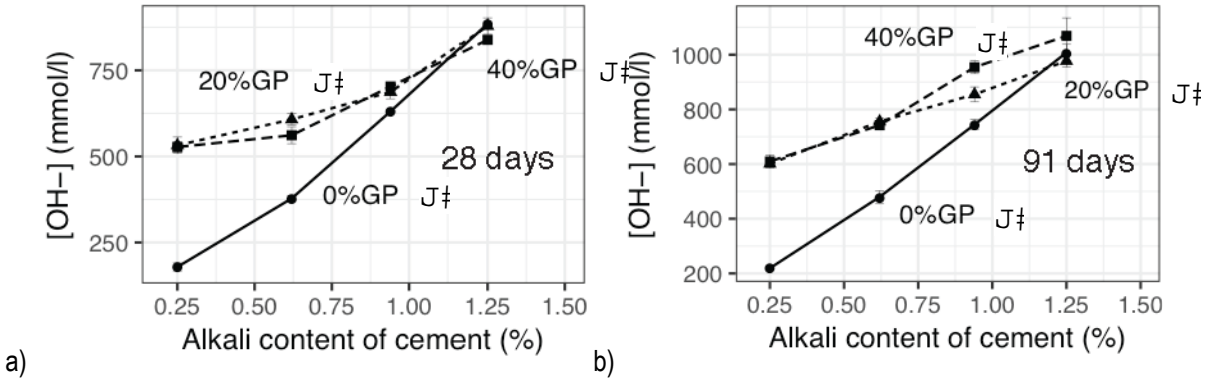


**Figure 2.2 a) [$OH^-$] in the pore solution for paste specimens incorporating portland cements of different alkali contents and various replacement levels of GG (0,20,40%). a) data at 28 days; b) data at 91 days.**

A linear regression was performed to determine the significance of three variables (%GG, Age and "cement" $Na_2Oeq$ content) on the prediction of the [$OH^-$] in the pore solution. The results of the analysis are presented in Table 2.5**;** the overall significance information for the computed model are F-ratio = 44.96 and $r^2$ = 0.87. The computed analysis indicates that the three variables (%GG, cement $Na_2Oeq$ content and age) have a significant impact on the [$OH^-$] (because their t-ratios are all above the *critical t-value*). Also, the effect of the "cement" alkali content has a marginally heavier impact on the alkali content of the pore solution compared to the %GG or the age (larger coefficient). This agrees with the first visual analysis of Figure 2.2**.**

**Table 2.5 : Coefficients of the model to predict [$OH^-$] in the pore solution and the corresponding t-ratio. Note that the critical t-value is 2.09.**

| | | Coefficient | t-ratio | > critical t-value |
|---|---|---|---|---|
| Intercept | ($\beta_0$) | 83.61 | N/A | N/A |
| Age | ($\beta_1$) | 2.31 | 3.97 | Yes |
| %GG | ($\beta_2$) | 4.55 | 4.08 | Yes |
| "cement" $Na_2Oeq$ | ($\beta_3$) | 469.50 | 10.04 | Yes |

The matrix of correlation coefficients presented in Table 2.6 indicates a weak correlation of the parameter %GG for the prediction of [OH-] (i.e. 0.33); this does not always represent observations on the Figure 2.2 as mixtures

incorporating GG behave differently from the control. Therefore, a numerical model evaluating the interaction between %GG and "cement" Na2Oeq content is proposed. A significant interaction between these parameters would suggest that the impact of %GG on the [OH-] in the pore solution is modulated by the alkali content of the cement. The results of this analysis are presented in Table 2.7; the overall significance information for the mode l are F-ratio=59.04 and r2=0.93. This analysis shows that the interaction between %GG and the alkali content of cement is significant (because their t-ratios are all above the critical t-value).

This finding explains why the parameter %GG alone is only weakly correlated to [$OH^-$] since the effect is not sta ble for different "cement" alkali content. In fact, the higher the cement alkali content, the lower is the impact of GG on the [$OH^-$] in the pore solution. For a deeper understanding of the observed phenomenon, the next sec tion proposes to examine the two elements computed, (i.e. [$K^+$] and [$Na^+$]), to obtain the response on the [$OH^-$] of the pore solution. Table 2.8 and Table 2.9 show the correlation between the same three parameters (%GG, Cement $Na_2O$eq and Age) and the measured concentrations of the two alkali ions of interest.

**Table 2.6 : Correlation coefficient (r2) between all pairs of variables to predict [OH-] in the pore solution.**

| | Age | "Cement" $Na_2O$e | [$OH^-$] | %GG |
|---|---|---|---|---|
| Age | 1 | | | |
| "Cement" $Na_2O$e | 0 | 1 | | |
| [$OH^-$] | 0.32 | 0.81 | 1 | |
| % GG | 0 | 0 | 0.33 | 1 |

**Table 2.7 : Coefficient of the model to predict [$OH^-$] in the pore solution and the corresponding t-ratio. Note that the critical t-value is 2.09.**

| | | Coefficient | t-ratio | > critical t-value |
|---|---|---|---|---|
| Intercept | ($\beta_0$) | -49.75 | N/A | N/A |
| Age | ($\beta_1$) | 2.31 | 5.13 | Yes |
| %GG | ($\beta_2$) | 11.21 | 5.65 | Yes |
| "Cement" $Na_2O$eq | ($\beta_3$) | 668.88 | 11.10 | Yes |
| %GG- $Na_2O$eq | ($\beta_4$) | -8.71 | -3.69 | Yes |

**Table 2.8 : Correlation coefficient ($r^2$) between all pairs of variables to predict [$K^+$] in the pore solution.**

| | Age | "Cement" $Na_2O$eq | [$K^+$] | %GG |
|---|---|---|---|---|
| Age | 1 | | | |
| "Cement" $Na_2O$eq | 0 | 1 | | |
| [$K^+$] | 0.09 | 0.68 | 1 | |
| %GG | 0 | 0 | -0.6 | 1 |

**Table 2.9 : Correlation coefficient between variables to predict the [$Na^+$] in the pore solution.**

| | Age | "Cement" $Na_2Oeq$ | [$Na^+$] | %GG |
|---|---|---|---|---|
| Age | 1 | | | |
| "Cement" $Na_2Oeq$ | 0 | 1 | | |
| [$Na^+$] | 0.28 | 0.34 | 1 | |
| %GG | 0 | 0 | 0.81 | 1 |

## 2.4.1 Potassium Ion Concentration [$K^+$] of the Pore Solution

The 28- and 91-day potassium concentrations [$K^+$] in the pore solution for the different mixtures made in this study are presented in Figure 2.3. The results show that for all types of cement, mixtures with GG have a lower [$K^+$] in the pore solution compared to the control mixtures (0GG). The response of [$K^+$] to the parameter "cement $Na_2Oeq$" follows the same trend as the response of [$OH^-$]: a higher cement alkali content will lead to more concentrated pore solution (in $K^+$ and $OH^-$).

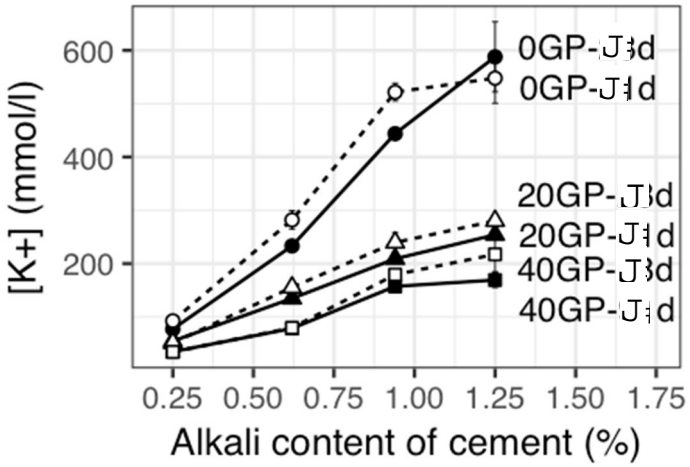


**Figure 2.3 : [$K^+$] in the pore solution of paste specimens relative to cement alkali content for different ages (28 and 91 days) and different %GG (0, 20 and 40%).**

Analytical informations presented in Table 2.8 are in accordance with results presented in Table 2.3 on the fact that the "cement" alkali content is an influent factor on [$K^+$] in the pore solution. In addition, the negative correlation obtained between [$K^+$] and %GG means that an increase in the %GG actually leads to an opposite response on the [$K^+$] in the pore solution. As Figure 2.3 shows, higher %GG leads to lower [$K^+$] for given time and alkali content of cement.

Numerical analyses presented in Table 2.10 permit a more accurate appreciation of the effect of GG on the $[K^+]$ in the pore solution. The overall significance information for the models are F-ratio = 42.01 and $r^2$ = 0.94 at 28 days, and F-ratio = 25.02 and $r^2$ = 0.87 at 91 days. The computations show that, as for $[OH^-]$, the interaction between %GG and the cement $Na_2Oe$ is significant (t-ratio (|-4.21|) > *Critical t-value (2.09), 28 days*). Yet, the %GG itself is no longer a predictor of the response of $[K^+]$ in the pore solution (t-ratio (0.84) < *Critical t-value (2.09), 28 days*) when the interaction is considered between %GG and the cement alkali content. Additionally, the negative sign of the coefficient of the interaction suggests that the reduction in the $[K^+]$ in the pore solution is increasing with increasing GG content in the system. This fact is partially noticeable on Figure 2.4 where the $[K^+]$ in the pore solution of paste specimens made with cement of low $Na_2Oe$ content exhibits almost no variation for different % GG whereas greater variations for different %GG are observed for higher $Na_2Oe$ cements.

**Table 2.10 : Coefficients of the model to predict $[K^+]$ in the pore solution and the corresponding t-ratio. Note that the critical t-value is 2.09.**

| | | 28 days | | | 91 days | | |
|---|---|---|---|---|---|---|---|
| | | **Coefficient** | **t-ratio** | **> to critical t-value** | **Coefficient** | **t-ratio** | **> to critical t-value** |
| **Intercept** | ($\beta_0$) | -51.76 | NA | NA | 21.00 | NA | NA |
| **%GG** | ($\beta_1$) | 1.60 | 0.84 | No | -0.77 | -0.31 | No |
| **"Cement $Na_2Oeq$"** | ($\beta_2$) | 480.15 | 8.27 | Yes | 435.81 | 5.74 | Yes |
| **%GG- Cement $Na_2Oeq$** | ($\beta_{12}$) | -9.46 | -4.21 | Yes | -6.99 | -2.37 | Yes |

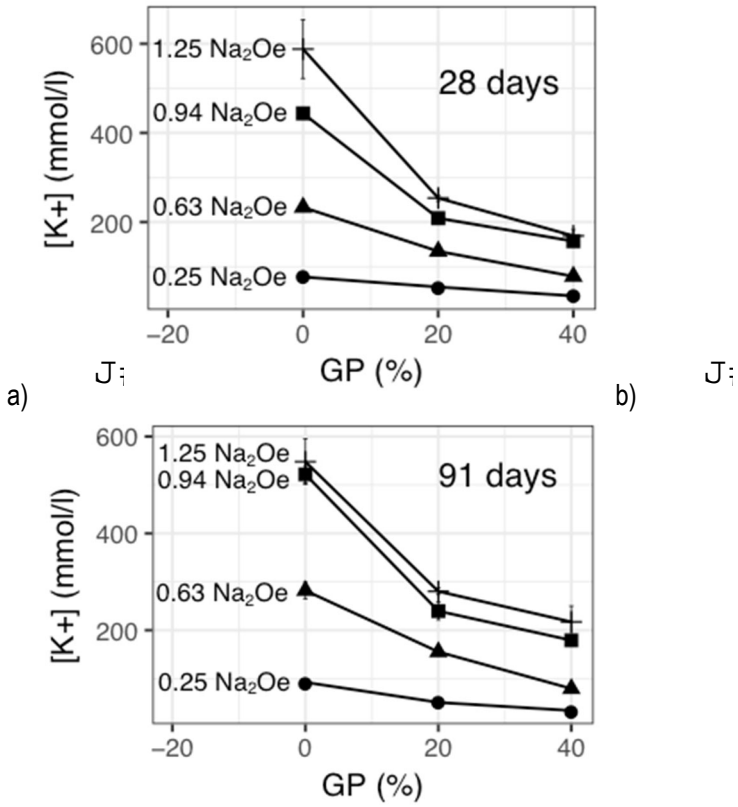


**Figure 2.4 : [$K^+$] in the pore solution of paste specimens relative to cement alkali content for different ages (28 and 91 days) and different %GG (0, 20 and 40%).**

## 2.4.2 Sodium Ion Concentration of the Pore Solution

Table 2.3 shows that, for the control pastes made without GG, there is a steadily increasing trend of [$Na^+$] in the pore solution with increasing cement alkali content (i.e. from 0.25% to 0.94% $Na_2Oeq$). The change in the trend observable for the 1.25% $Na_2Oeq$ "cement" is presumably due to a spontaneous release of sodium in the pore solution due to the use of NaOH powder to boost the alkali content in the paste.

Figure 2.5 also shows that GG contributes to the sodium ion concentration in the pore solution since higher percentages of GG lead to higher sodium concentrations. The mixtures with 20% or 40% of GG do not exhibit important difference in [$Na^+$] at 28 days, except for cement with 1.25% $Na_2O_e$. This suggests that GG covers the impact of the cement alkalis on the [$Na^+$] since the slope for 20%GG is flatter than that of plain cement (0GG). At 91 days, this effect is less obvious and computed analysis would be more appropriate.

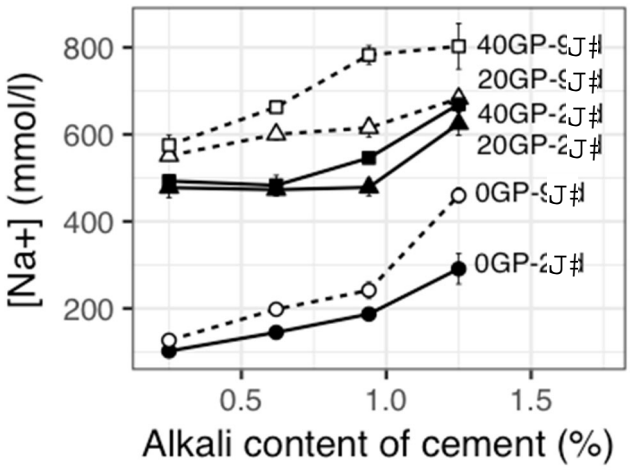


**Figure 2.5 : [$Na^+$] in the pore solution of paste specimens relative to cement alkali content for different ages (28 and 91 days) and different %GG (0, 20 and 40%).**

The correlation coefficient presented in Table 2.9 differs from the coefficient of the analysis performed in Table 2.6 for [$OH^-$] since the response of [$Na^+$] is only weakly correlated to the cement alkali content with an $r^2$ of 0.34; however, the correlation of [$Na^+$] to %GG has an $r^2$ of 0.81.

Table 2.11 presents the results of the computed analysis of the overall significance information for the models, where F-ratio=42.01 and $r^2$=0.94 at 28 days and F-ratio=25.02 and $r^2$= 0.88 at 91 days. At 28 days, the t-test indicates that %GG content is barely significant as a parameter to predict [$Na^+$] (its *t-ratio* (2.39) is just above the *critical t-value (2.09)*). Figure 2.6**a** shows that the relation between [$Na^+$] and %GG is obvious when %GG is from 0 to 20% and less clear from 20% to 40%. This observation makes more explicit the barely significant result of the t-test for the parameter %GG at this age. At 91 days, %GG is clearly a significant predictor in the numerical analysis as the *t-ratio* (3.74) is above the *Critical t-value* (2.09), while Figure 2.6 b) shows that the [$Na^+$] differs for GG replacement of 20% and 40%. Also, in addition to %GG, another significant parameter over time is the "cement" alkali content (*t-ratio* of 2.37).

Interestingly, the effect of the interaction between %GG and the cement alkali content is not significant for the [$Na^+$], which is different from its effect on the [$K^+$] response.

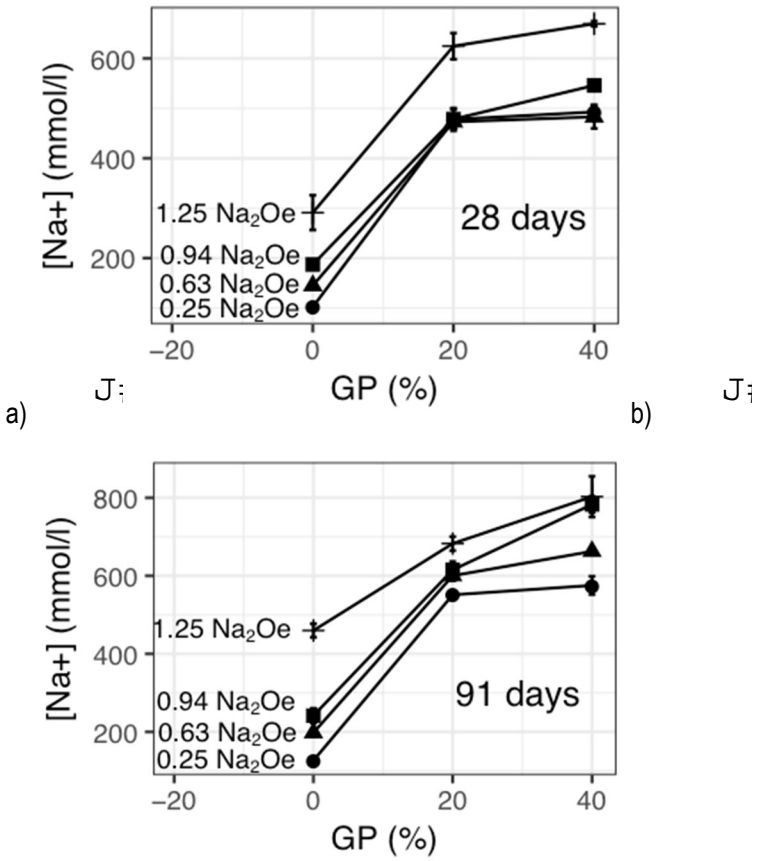


**Figure 2.6 : [$Na^+$] for different cement alkali (0.25 to 1.25 $Na_2Oeq$) and GG (0, 20 and 40%) contents at a) 28 days and b) 91 days.**

**Table 2.11 : Coefficient of the model to predict [$Na^+$] in the pore solution and their respective t-ratio. Note that the critical t-value is 2.09.**

| | | 28 days | | | 91 days | | |
|---|---|---|---|---|---|---|---|
| | | Coefficient | t-ratio | > critical t-value | Coefficient | t-ratio | > critical t-value |
| Intercept | ($\beta_0$) | 104.85 | N/A | N/A | 118.41 | N/A | N/A |
| %GG | ($\beta_2$) | 9.30 | 2.39 | Yes | 12.60 | 3.74 | Yes |
| "Cement" $Na_2Oe$ | ($\beta_3$) | 165.83 | 1.41 | No | 243.86 | 2.37 | Yes |
| %GG- "Cement" $Na_2Oeq$ | ($\beta_{12}$) | -0.18 | -0.04 | No | -1.66 | -0.42 | No |

## 2.5 Conclusion

The partial replacement of portland cement by post-consumer ground glass has a significant effect on the composition of the pore solution of the corresponding cementitious systems. On the one hand, increasing the GG content tends to lower the potassium concentration of the pore solution and its effect is affected by the cement alkali content (i.e. higher %GG leads to lower $[K^+]$ for given time and alkali content of cement).

Increasing the GG content up to 40% in the paste specimens raises the sodium concentration of the pore solution and its effect seems to be related to the cement alkali content only at later ages (91 days in the case of this study).

When the effect on both $[Na^+]$ and $[K^+]$ is translated to $[OH^-]$, it seems that the impact of up to 40% GG is limited for cementitious systems incorporating high alkali cements, but much more significant for systems made with low alkali cements.

## 2.6 Acknowledgement

The authors would like to thank the Centre de Recherche des Infrastructure en Béton (CRIB) for the space, equipment and technical support provided. Also, the authors are grateful to the Chaire de recherche de la SAQ and the Centre de Recherche en Sciences Naturelles et en Génie (CRSNG) for their financial support.

## 2.7 References


Dove, P. M. and S. F. Elston (1992). "Dissolution kinetics of quartz in sodium chloride solutions: Analysis of existing data and a rate model for 25°C." Geochimica et Cosmochimica Acta 56(12): 4147-4156.

Duchesne, J. and M. A. Bérubé (1994a). "The effectiveness of supplementary cementing materials in suppressing expansion due to ASR: Another look at the reaction mechanisms part 1: Concrete expansion and portlandite depletion." Cement and Concrete Research 24(1): 73-82.

Duchesne, J. and M. A. Bérubé (1994b). "The effectiveness of supplementary cementing materials in suppressing expansion due to ASR: Another look at the reaction mechanisms part 2: Pore solution chemistry." Cement and Concrete Research 24(2): 221-230.

Fily-Paré, I. and Lafrenière, C. (2017), Unpublished

Fournier, B., Nkinamubanzi, P.C., Chevrier, R., Ferro, A. (2008): “Evaluation of the effectiveness of high-calcium fly ashes in reducing expansion due to alkali-silica reaction in concrete”. Electric Power Research Institute (EPRI), Palo Alto (USA), 1014271.

Idir, R., M. Cyr and A. Tagnit-Hamou (2011). "Pozzolanic properties of fine and coarse color-mixed glass cullet." Cement and Concrete Composites 33(1): 19-29.

Rogers, C. A. and R. D. Hooton (1991). "Reduction in mortar and concrete expansion with reactive aggregates due to alkali leaching." Cement, Concrete and Aggregates 13(1): 42-49.

Saccani, A. and M. C. Bignozzi (2010). "ASR expansion behavior of recycled glass fine aggregates in concrete." Cement and Concrete Research 40(4): 531-536.

Saeed, H. (2008). Glass powder blended cement hydration modelling. PhD Thesis, Université de Sherbrooke.

Schwarz, N. and N. Neithalath (2008). "Influence of a fine glass powder on cement hydration: Comparison to fly ash and modeling the degree of hydration." Cement and Concrete Research 38(4): 429-436.

Shehata, M. H. (2001). The effects of fly ash and silica fume on alkali-silica reaction in concrete. Ph.D PhD Thesis, University of Toronto.

Shi, C., Y. Wu, C. Riefler and H. Wang (2005). "Characteristics and pozzolanic reactivity of glass powders." Cement and Concrete Research 35(5): 987-993.

Shi, C. and K. Zheng (2007). "A review on the use of waste glasses in the production of cement and concrete." Resources, Conservation and Recycling 52(2): 234-247.

Taha, B. and G. Nounu (2008). "Using lithium nitrate and pozzolanic glass powder in concrete as ASR suppressors." Cement and Concrete Composites 30(6): 497-505.

Thomas, M., B. Fournier, K. Folliard, J. Ideker and M. Shehata (2006). "Test methods for evaluating preventive measures for controlling expansion due to alkali–silica reaction in concrete." Cement and Concrete Research 36(10): 1842-1856.

Vaux, D. L., F. Fidler and G. Cumming (2012). "Replicates and repeats—what is the difference and is it significant?" EMBO reports 13(4): 291-296.

Vézina, D., J. Frenette, M.-A. Bérubé and M. Rivest (2002). "Measurement of the alkali content of concrete using hot-water extraction." Cement, concrete and aggregates 24(1): 28-36.

# Chapter 3. Response Surface Methodology (RSM) to Assess the Impact of Ground Glass (GG), Silica Fume (SF) and Metakaolin (MK) on the Composition of the Pore Solution of Paste Systems


## Résumé

Le présent travail cherche à clarifier si la teneur élevée en sodium du verre broyé (VB) se reflète dans la composition de la solution interstitielle des matrices ternaires incorporant également de la fumée de silice (FS) ou du métakaolin (MK). Pour cette fin, le plan expérimental mis en place pour la conception des mélanges de pâtes ternaires inclus les composants suivants : ciment avec différentes teneurs en $Na_2Oeq$ (0,63% à 1,25%), VB et FS ou MK en remplacement du ciment : 10% à 30%, 5% à 10% et 5% à 15%, respectivement. Les pâtes produites avaient un rapport eau - liant de 0,50 et les solutions interstitielles ont été extraites à 28 et 182 jours. Les concentrations en ions alcalins des solutions ont été déterminées par absorption atomique à flamme et traitées selon la méthodologie de réponse de surface.

Les résultats obtenus dans cette étude suggèrent que le paramètre le plus influent sur la $[Na^+]$, $[K^+]$ et $[OH^-]$ est le pourcentage de FS ou de MK et que le contenu en VB n'augmente que faiblement ou négligemment ces concentrations. En outre, l'ajout de NaOH au système, afin d'atteindre la valeur de 1,25% $Na_2Oeq$, conduit à une contribution réduite du VB à la $[OH^-]$. La présence d'interactions (ou de synergie) entre le contenu VB, FS/MK et la teneur en $Na_2Oeq$ du mélange indique qu'un seul paramètre ne peut à lui seul être utilisé pour expliquer le comportement des systèmes ternaires étudiés et que la prédiction du comportement de ces systèmes nécessite des modèles multivariables.

## Abstract

The present work seeks to clarify if the high sodium content of Ground Glass (GG) is reflected in the composition of the pore solution of ternary matrices incorporating Silica Fume (SF) or Metakaolin (MK). For this purpose, the experimental plan considered the following elements for the mix design of ternary pastes: cement with various $Na_2Oeq$ content (0.63% to 1.25%), GG and either SF or MK as cement replacement, i.e. 10% to 30%, 5% to 10% and 5% to 15%, respectively. Pastes were produced with a water-to-binder ratio of 0.50 and the pore solutions were extracted at 28 and 182 days. The alkali concentrations of the solutions were determined through flame atomic absorption and processed with a Response Surface Methodology (RSM) approach.

Results obtained in this experimental program suggested that the most influential parameter for $[Na^+]$, $[K^+]$ and $[OH^-]$ is the percentage of SF or MK and that the content of GG is weakly or negligibly rising those species. Also, the addition of NaOH to the cement mixture, to reach 1.25% $Na_2Oeq$, leads to reduced contribution of GG to $[OH^-]$ of the pore solution. The presence of interactions (or synergy) between GG, FS/MK and cement $Na_2O_{eq}$ content indicates that one single parameter cannot, in itself, represent the behavior of ternary systems and that predicting the behaviour of such systems requires accurate multivariable models.

## 3.1 Introduction

Members of the Canadian Standards Association (CSA) Technical Committee on Cementitious Materials Compendium introduced ground glass (GG) as a new type of Supplementary Cementitious Material (SCM) in CSA A3000-18 (CSA 2018) i.e., types $G_H$ (GG with high alkali content) and $G_L$ (GG with low alkali content). The Canadian standards is evolving along with the cement industry in its efforts in reducing the carbon footprint of cement/concrete using alternative cementitious materials – such as GG. Numerous research and field implementation projects have shown that GG can be used for manufacturing concrete with appropriate workability, mechanical and durability properties (Shayan and Xu 2006, Idir et al. 2010, Rajabipour et al. 2010, Carsana et al. 2014, Liu et al. 2015, Omran and Tagnit-Hamou 2016, Omran et al. 2017, Omran et al. 2017). However, the suitability of combining GG and reactive aggregates in concrete is still a source of controversy. Where one can predict that GG can reduce expansion due to Alkali Silica Reaction (ASR) because of its pozzolanic properties, another one is concerned that GG could promote expansion due to ASR because of its high sodium content that often reach up to 13% $Na_2Oeq$ (in this study) or even higher. Although recent works consolidate these two perspectives by suggesting that both reactions can relate to GG into concrete and that the availability of calcium hydroxide (CH) around the GG particle will determine which of the reaction will take place (Mejdi et al. 2019), further research is still required.

### 3.1.1 Relation Between the Expansion and the Composition of the Pore Solution

Previous research suggested that the use of high alkali fly ash (FA) results in high $[OH^-]$ in the pore solution and a mild decrease of concrete prism expansion due to ASR (Duchesne and Bérubé 1995, Shehata et al. 1999, Fournier et al. 2008). Such a behavior is well highlighted by the work of Shehata and Thomas (2000) who brought to light the potential for high alkali FA to reduce expansion (mildly) due ASR by a mechanism other than by decreasing the pH, as shown in Figure 3.1.

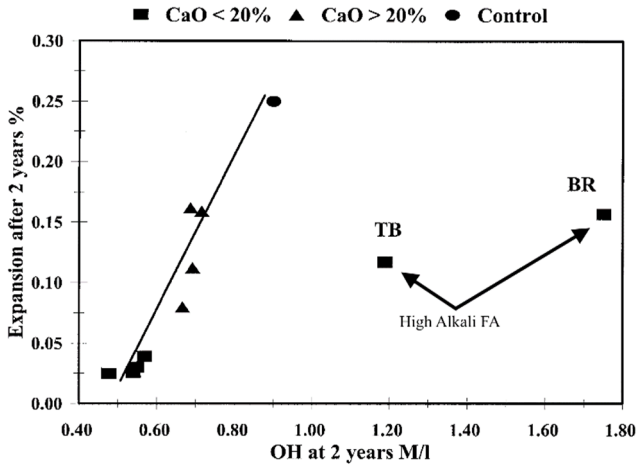


**Figure 3.1 : Two-year expansions of concrete prisms incorporating the highly-reactive Spratt limestone from Canada (testing as per Standard Practice CSA 23.2-28A) for FA of various chemical compositions (25% replacement level of the high-alkali cement), as a function of the $OH^-$ concentration in the pore solution of paste specimens made with the same FA and cement replacement levels (Shehata and Thomas 2000). The alkali content of FA TB and BR is given in Table 3.1.**

More details about the pore solution extracted from paste specimens (w/b = 0.50) made with the high alkali FA BR and TB of Figure 3.1 (25% replacement of the high-alkali cement) are presented in Table 3.1. The data suggest that the use of these FA is effective in lowering $[K^+]$ but not $[Na^+]$ compared to the control specimen made with OPC only (Shehata 2001). It is worth mentioning that the two FA contained less potassium than the OPC, which likely explains the lower $[K^+]$ in the pore solution of FA-bearing pastes. The data suggest that the effect goes beyond that of a dilution effect in the case of the $[K^+]$ reduction because the ternary cementitious mixture containing 25% of the TB FA has 13% less $K_2O$ in its elemental composition but results in 44% less $K^+$ in the pore solution of the paste specimens at 91 days. Similarly, the mixture containing 25% of the BR FA contains 8.5% less $K_2O$ in its elemental composition but 36% less $K^+$ in the pore solution of the paste specimens at 91 days.

**Table 3.1 : Composition of pore solution at different ages for paste specimens containing 25% of the two high alkali fly ashes (BR and TB) presented in Figure 3.1. "Cont" corresponds to a control paste made of 100% portland cement (Shehata 2001).**

| Ionic specy | Concentration (mole/L) | | | | | | | | |
|---|---|---|---|---|---|---|---|---|---|
| | 28 days | | | 91 days | | | 2 years | | |
| | Cont.* | BR** | TB*** | Cont.* | BR** | TB*** | Cont.* | BR** | TB*** |
| $OH^-$ | 0.839 | 1.529 | 1.189 | 0.982 | 1.950 | 1.418 | 0.9 | 1.751 | 1.188 |
| $Na^+$ | 0.280 | 1.137 | 0.846 | 0.366 | 1.413 | 1.148 | - | 1.444 | 1.010 |
| $K^+$ | 0.551 | 0.436 | 0.385 | 0.734 | 0.469 | 0.411 | - | 0.412 | 0.296 |
| $K^+/Na^+$ | 1.968 | 0.383 | 0.455 | 2.005 | 0.332 | 0.358 | - | 0.285 | 0.293 |

* Cement: $Na_2O$ = 0.41; $K_2O$ = 1.03; ** Fly ash BR: $Na_2O$ = 8.38; $K_2O$ = 0.68; *** Fly ash TB : $Na_2O$ = 8.14; $K_2O$ = 0.49;

Similarly, Duchesne and Bérubé (2001) and Duchesne and Bérubé (1995) showed that the use of 40% of the high alkali FA PFA-C contributed at reducing expansion in concrete specimens due to ASR compared to the control (Figure 3.2a)) despite the fact that the above ash replacement level raised the $[Na^+]$ but reduced the $[K^+]$ in the pore solution compared to the control paste specimens made with the OPC only (fixed w/b of 0.50) (Figure 3.2b). The effect of replacing 40% of the OPC containing 1.16% of $K_2O$ by a FA containing 0.72% of $K_2O$ resulted in a dilution of 15% in the $K_2O$ content of the dry cementitious mixture; however, the reduction of $K_2O$ in the pore solution of the PFA-C mixture compared to the control was about 173%. This suggests that the composition of the pore solution is not systematically a reflection of the composition of the cementitious material.

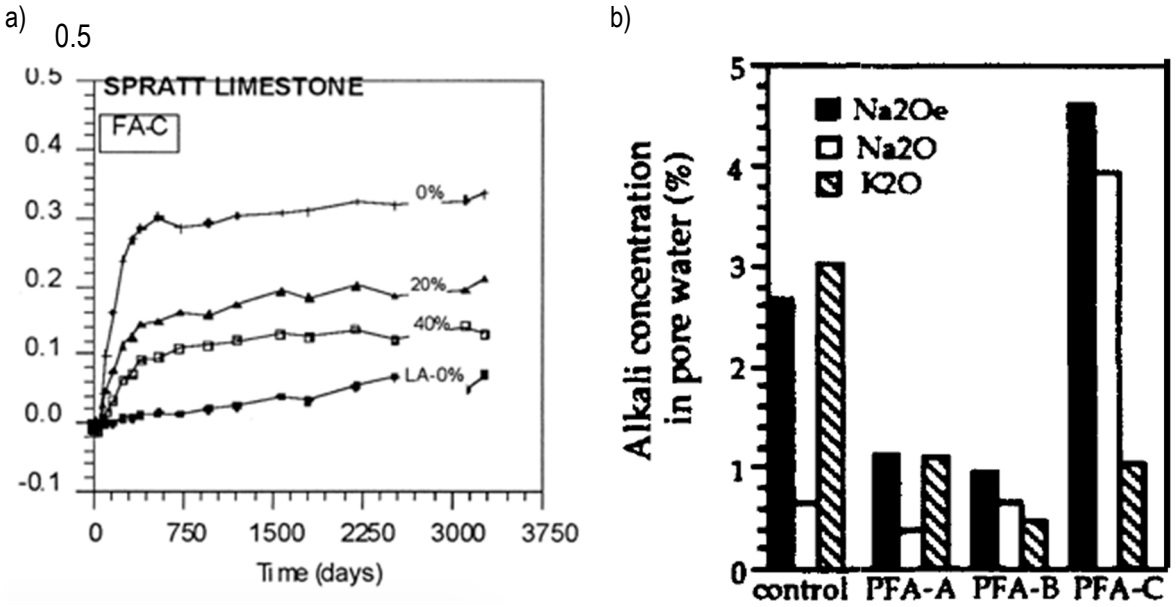


**Figure 3.2 : a) Expansion of concrete prisms incorporating the highly-reactive Spratt limestone from Canada after 9 years of testing as per Standard Practice CSA 23.2-28A. The concretes include control mixtures made with high and low alkali (LA) cements, and concretes incorporating 20 and 40% FA as replacement, by mass, of the HA cement (Duchesne and Bérubé 2001); b) alkali concentration in the pore solution after one year for paste specimens (w/b = 0.50) containing 40% of high alkali FA (PFA-C) and lower alkali FA PFA-A and PFA-B (Duchesne and Bérubé 1995). The alkali content of the cementitious materials presented in a) and b) is the following: HA OPC: $Na_2O$ = 0.29, $K_2O$ = 1.16, $Na_2Oeq$=1.05; LA OPC: $Na_2O$ = 0.26, $K_2O$ = 0.42, $Na_2Oeq$=0.54; PFA-A: $Na_2O$ = 0.66, $K_2O$ = 2.55, $Na_2Oeq$=2.33; PFA-B: $Na_2O$ = 2.74, $K_2O$ = 0.50; $Na_2Oeq$= 3.01; PFA-C: $Na_2O$ = 8.08, $K_2O$ = 0.72, $Na_2Oeq$=8.55.**

### 3.1.2 Pore solution of Binary Systems Incorporating GG

Most studies on the pore solution of cementitious systems incorporating GG referred to pH only. For instance, Kamali and Ghahremaninezhad (2016) analyzed the pH of stabilized solutions of distilled water and ground cement pastes incorporating ground glass of two $Na_2O_{eq}$ contents (0.62 and 6.2%); the authors reported that, after 91 days, the systems incorporating GG with higher alkali content resulted in solutions of higher pH (12.6 vs 12.4). Shevchenko (2012) centrifuged and analyzed the pH of slurries/pastes made with cement and different amounts of GG; he noticed that, at early ages (few hours to few days), mixtures with more GG were showing significantly higher pH than control mixtures without GG.

Fily-Paré et al. (2017) reported the results of the chemical analysis of pore solutions extracted from binary cementitious pastes (w/b = 0.5) incorporating GG ($Na_2Oeq$ = 13.11%) and portland cements of various alkali contents (0.25 to 1.25% $Na_2Oeq$); the authors found that at 28 and 91 days : 1) the incorporation of GG contributes at raising the pH of the pore solution, which was mainly due to $Na^+$ released from the GG, and 2) the impact of GG on the alkalinity of the pore solution is largely modulated by the alkali content of the cement (Figure 3.3). This study also highlighted that the presence of GG in a cementitious mixture can lower $[K^+]$ in the pore solution, which effect is also altered by the $Na_2Oeq$ content of the cement as presented in Figure 3.3 c).

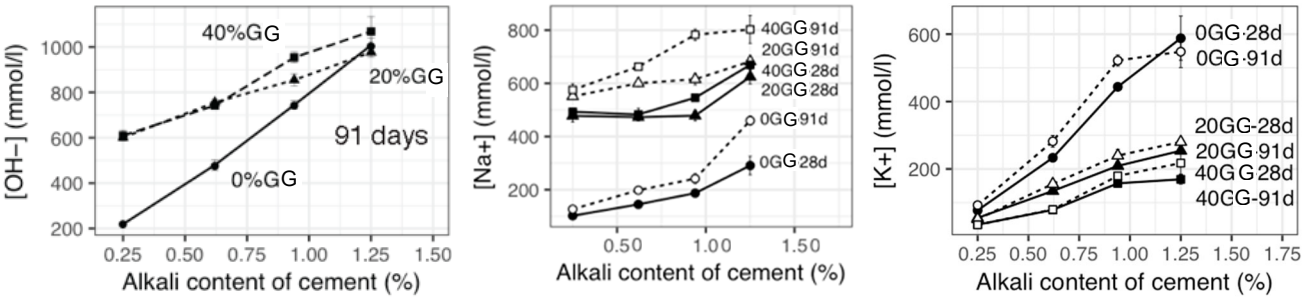


a) b) c)

**Figure 3.3 : a) $[OH^-]$ in the pore solution for paste specimens incorporating portland cements of different alkali contents and various replacement levels of GG (0,20,40%) at 91 days. b) $[Na^+]$ and c) $[K^+]$ in the pore solution relative to cement alkali content for different ages and different %GG. (%$K_2O$ of GG and of the cements are respectively 0.66, 0.16, 0.62, 1.06 and 1.06). The alkali content of the 1.25% system was obtained with the 0.94% $Na_2Oeq$ cement + NaOH addition (Fily-Paré et al. 2017).**

### 3.1.3 Pore Solution of Ternary Cementitious Systems

Thomas et al. (2006) observed that the addition of 5% SF in concrete incorporating 20% of a high alkali FA (10.45% $Na_2O_{eq}$) contributes at reducing expansion due to ASR. Analyzing the composition of the pore solutions of pastes incorporating an high-alkali FA, Shehata and Thomas (2002) showed that the synergetic effect obtained from combining fly ash and 5% silica fume is actually more important than the sum of the individual contributions of the SCMs in most cases. Indeed, Figure 3.4 shows that the addition of 5% SF to a high-alkali cement paste (HAPC 1) lowers the alkalinity by approximately 0.2 mol/L (i.e., 0.9 to 0.7 mol/L), while about 15 (FM) to 35% (OK) fly ash are required to induce the same effect. Additionally, 5% SF coupled to only 10 or 20% high-alkali FA lowers the alkalinity by 0.5 mol/L (i.e., 0.9 to 0.4 mol/L).

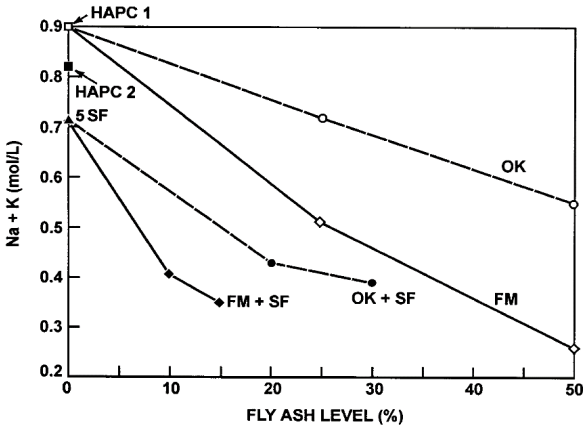


**Figure 3.4 :[$Na^+$]+[$K^+$] of pore solution at the age of two years for ternary mixtures incorporating 5%SF and different types/ contents of FA (Shehata and Thomas 2002). OK = 1.15% $Na_2O$, 0.21% $K_2O$, 1.65% $Na_2Oeq$; FM = 0.60% $Na_2O$,1.23% $K_2O$, 1.41% $Na_2Oeq$.**

Other work by the same authors suggests that combining 5% SF to high-alkali FA has a rapid effect in reducing the alkali concentration in the pore solution (i.e., by 28 days) and the effect remains stable, i.e., without any significant reductions afterwards (Figure 3.5). These observations are aligned with the work of Vollpracht et al. (2015) who reported little variation between 100 and 1000 days for [$Na^+$], [$K^+$] and [$OH^-$] variation in mixtures incorporating 5 to 10% SF.

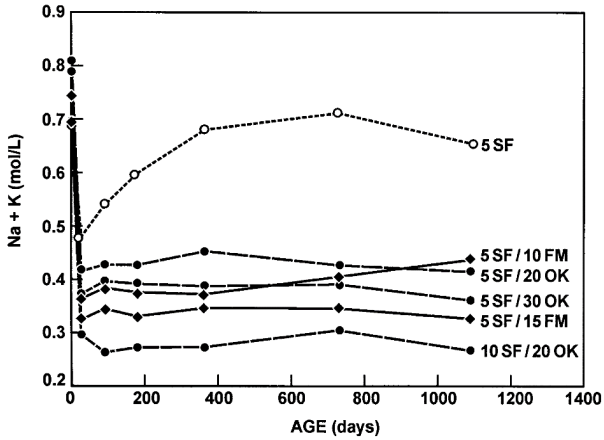


**Figure 3.5 : [$Na^+$]+[$K^+$] of pore solution over time, for ternary mixtures incorporating 5%SF and different types/contents of FA (Shehata and Thomas 2002). OK = 1.15% $Na_2O$, 0.21% $K_2O$, 1.65% $Na_2Oeq$; FM = 0.60% $Na_2O$,1.23% $K_2O$, 1.41% $Na_2Oeq$.**

### 3.1.4 Objectives and Scope of Work

The primary objective of this work was to determine if GG releases its alkalis in the pore solution; the second objective was to assess the potential synergy on the composition of pore solution that could develop between GG and a third SCM, such as SF or MK; and the third objective of this study was to evaluate the potential impact of artificially boosting the concrete alkali content with sodium hydroxide in the case of a high-alkali SCM, such as GG, as recommended in practice for evaluating the effectiveness of SCMs in preventing expansion due to ASR in the laboratory (CSA 2014 (e.g. Standard Practice CSA A23.2-28A), ASTM 2014 (ASTM C 1778).

In this study, ternary paste systems were made with various percentages of GG and SF/MK, as replacement by mass of portland cements containing different levels of $Na_2O_{eq.}$ The pore solutions were then extracted under pressure from the pastes after 28 and 182 days of storage in hermetic plastic containers at 38°C. Solutions were analyzed with flame atomic absorption for their content in $Na^+$ and $K^+$ and the data were processed using a Response Surface Methodology (RSM) approach.

## 3.2 Materials and Methods

### 3.2.1 Materials Characteristics

Paste samples were made using post consumed GG from a recycling facility located in the Province of Québec (Canada), silica fume (SF) from a ferro-silicon plant also located in Quebec, a high-purity metakaolin (MK) from Georgia (USA) and two Canadian type GU portland cements (C1 and C2) with respective $Na_2O_{eq}$ of 0.63% and 0.94%. Pastes with $Na_2O$eq of 1.08% and 1.25% were prepared using NaOH added to portland cement C2. The chemical composition of each material used in this study is presented in

**Table 3.2 : Chemical composition of binders.**

| | Portland Cements | | SCMs | | |
|---|---|---|---|---|---|
| Oxide | C1 | C2 | GG | SF | MK |
| $SiO_2$ | 19.58 | 18.7 | 70.53 | 94.27 | 51.6 |
| CaO | 62.09 | 60.8 | 10.77 | 0.54 | 0.02 |
| $Al_2O_3$ | 4.58 | 5.0 | 2.06 | 0.30 | 43.97 |
| $Fe_2O_3$ | 2.85 | 3.7 | 0.35 | 0.10 | 0.49 |
| $Na_2O$ | 0.22 | 0.25 | 12.49 | 0.12 | 0.27 |
| $K_2O$ | 0.62 | 1.05 | 0.66 | 0.65 | 0.25 |
| $Na_2O$eq | 0.63 | 0.94 | 12.92 | 0.55 | 0.43 |
| $SO_3$ | 4.02 | 3.8 | 0.11 | 0.02 | 0.00 |
| MgO | 2.91 | 2.7 | 1.14 | 0.28 | 0.04 |
| $TiO_2$ | 0.23 | - | 0.07 | 0.01 | 1.40 |
| $P_2O_5$ | 0.10 | - | 0.03 | 0.12 | 0.09 |
| MnO | | | 0.02 | 0.03 | 0.01 |
| L.O.I | 2.45 | 1.9 | 1.71 | 3.2 | 1.84 |

### 3.2.2 Design of Experiment

### 3.2.3 Mix Design

The proportions of the components of the different mixtures investigated in this study were chosen according to a $3^3$ -factorial plan with the following three variables of three levels each:

1) GG as cement replacement levels, by mass, of 10, 20 and 30%;
2) either SF or MK used as cement replacement, by mass, with levels of respectively 5, 7.5 and 10% or 5, 10 and 15%;
3) $Na_2Oeq$ of the cement or cement with alkali levels of 0.63%, 0.94 and 1.25% (0.94 + NaOH). The "check point", excluded from the data base to build the model in order to test its accuracy, is 1.08% (0.94% + NaOH).

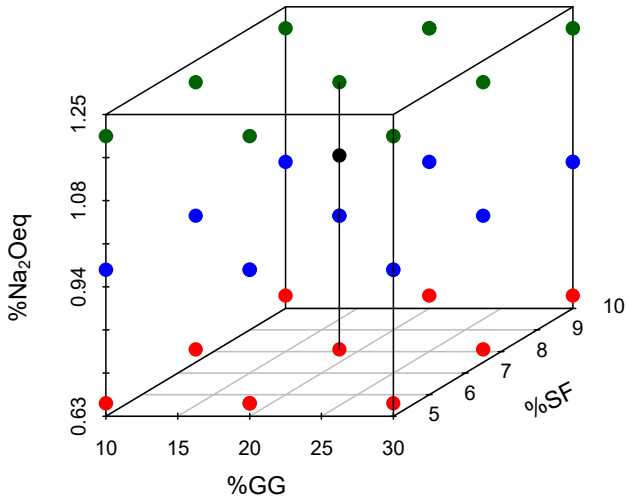


**Figure 3.6 : Mixture design for the experimental plan of SF and "check point" with an alkali content of 1.08%.**

The design is well balanced with three equally distant levels. For numerical analysis, variables are coded between -1 and 1 in order to rescale and balance their effect on the response according to their typical range of use. For instance, the effect of a 1% addition of the $Na_2Oeq$ content of cement is disproportionally high compared to that of a 1% addition of GG if the range is not "rescaled".

Table 3.2 presents the coding of the variables for both SF and MK plans, while coded parameters of the design are presented in Table 3.3. The centre point is replicated in order to estimate the variance of this cuboidal region of interest, as proposed by Montgomery (2012), while other replicated points are also included to calculate more confidently the typical coefficient of variation that is used to estimate the standard deviation of single measurements. The analyzed results of the extraction replicates are presented in Annex A.

**Table 3.2 : Value of uncoded and coded parameter.**

| Uncoded | | | | Coded |
|---|---|---|---|---|
| GG | SF | MK | Cement $Na_2Oeq$ | |
| 10 | 5 | 5 | 0.63 | -1 |
| 20 | 7.5 | 10 | 0.94 | 0 |
| 30 | 10 | 15 | 1.25 | 1 |

**Table 3.3: Coded values of the experimental plans**

| GG = -1 | | GG = 0 | | GG = 1 | |
|---|---|---|---|---|---|
| SF or MK | Cement $Na_2Oeq$ | SF or MK | Cement $Na_2Oeq$ | SF or MK | Cement $Na_2Oeq$ |
| -1 | -1 | -1 | -1 | -1 | -1 |
| -1 | 0 | -1 | 0 | -1 | 0 |
| -1 | 1 | -1 | 1 | -1 | 1 |
| 0 | -1 | 0 | -1 | 0 | -1 |
| 0 | 0 | 0 | 0 | 0 | 0 |
| 0 | 1 | 0 | 1 | 0 | 1 |
| 1 | -1 | 1 | -1 | 1 | -1 |
| 1 | 0 | 1 | 0 | 1 | 0 |
| 1 | 1 | 1 | 1 | 1 | 1 |

### 3.2.3.1 Time Repeated Measurements

Pore-solution extraction and chemical analyses were carried out for 28 and 182-day old paste specimens. Since *Time* is expected to influence the composition of the pore solution, this fourth parameter ("Day") is also part of the numerical processing.

### 3.2.3.2 Mixture Experiment

As spelled out by Myers et al. (2011) and Lawson (2014), a dependent variable is inherent to RSM mixture experiments because the proportions of the components are interrelated. In our case, the proportion of portland cement in the system corresponds to the dependent variable since this material is replaced, by mass, by different amounts of GG, SF or MK. Thus, "Cem" is added as a fifth variable ($x_5$). Like the other variables, Equation 1 allows coding this variable between --1 and 1 using the max and min values for each of the SF and MK dataset. The correspondence for "Cem" variable is presented in Table 3.4.

$$x_5 = \frac{Cem\% - {(Max_{Cem} + Min_{Cem})}/{2}}{{(Max_{Cem} - Min_{Cem})}/{2}} \qquad \text{Equation 1}$$

**Table 3.4: Coded values and corresponding cement contents for the SF and MK systems.**

| Cement content (%) | 55 | 60 | 62.5 | 65 | 70 | 72.5 | 75 | 80 | 82.5 | 85 |
|---|---|---|---|---|---|---|---|---|---|---|
| SF | | -1.00 | -0.80 | -0.60 | -0.20 | 0.00 | 0.20 | 0.60 | 0.80 | 1.00 |
| MK | -1.00 | -0.67 | | -0.33 | 0.00 | | 0.33 | 0.67 | | 1.00 |

### 3.2.4 Manufacturing of Paste Specimens

After a series of trials, a modified version of ASTM C 305-12 was adopted to properly incorporate SCMs in the paste specimens. This approach was preferred to prevent agglomerates for a fixed water-to-binder ratio of 0.50 without chemical admixtures. SF or MK was thus added to the mixing/hydration water in the first place and mixed at slow speed (140 $\pm$ 5 r/min) for 15 sec; the cement and GG were then added to the mixture and the remaining standard procedure was followed : cementitious materials resting for 30 sec to allow absorption of water; mixing for 30 sec at slow speed; stop mixing for 15 sec to allow scraping down the paste stuck to the side of the bowl and, finally, mixing at medium speed (285 $\pm$ 5 r/min) for 60 sec. The pastes were then poured in plastic containers, 30 mm by 55 mm in size, and gently agitated for the first 24 h at 23 ± 2°C. The specimens were then stored in a sealed plastic bag at 38°C for 28 or 182 days before pore solution extraction was carried out.

### 3.2.5 Pore Solution Extraction Process

Before extraction, the paste specimens were stored at 23 ± 2°C for a period of 24 h. The specimens remained in their sealed plastic bottles until they were ready to be placed in the extraction cell in order to prevent water loss and carbonation.

The pore solution was extracted under a pressure of 1600 MPa (200 kN), thus typically providing between 0.5 and 1 ml of pore solution. The set-up incorporates a sealed tube connecting the base of the extraction cell to a syringe. Immediately after completion of the extraction, the syringe was separated from the extraction cell and the end of the syringe was sealed with proper plastic cap and wax tape to prevent carbonation or evaporation of the solution. The syringes were then placed in a refrigerator (4$^{o}$C) until the chemical analyses were carried out.

### 3.2.6 Replicates

Replicates for a given mixture correspond to paste samples casted in different containers and extracted separately. Pore solution extracted from the replicates were collected and analysed independently. Detailed results of the replicates are presented in Annex A.

### 3.2.7 Chemical Analysis

All solutions were diluted with 5%V/V nitric acid and analyzed for sodium and potassium with a PerkinElmer AAnalyst 100 atomic absorption spectrophotometer (AAS) at wavelengths of respectively 589 and 766.5 nm using an air-acetylene flame. A releasing agent consisting of cesium chloride was added to the solutions to a concentration of 1.5g/L in order to avoid ionization.

The above dilution in nitric acid was also used to ensure full solubility of the species in solution and to match the detection ranges of the apparatus, which range from 0.04 to 0.133 mmol/l (Na) and from 0.05 to 0.15 mmol/l (K). The following dilution protocol was found to drastically lower variability between replicates and provided coherent results between paste specimens analyzed at different times (28 and 182 days): a) the solutions were consistently diluted no more than two times; b) the first dilution was of similar magnitude for all samples (typically about 150); c) the second dilution targeted the same portion of the calibration curve +/- 10% for replicates or time repeated measurements; d) the second dilution also had to reach the centre +/- 25% of the range of the calibration curve ; e) calibration standard solutions were prepared in large volumes (1 L) to maximize precision and to test all samples of the SF or MK mixtures at a given age with identical calibration standard solutions; f) the calibration standard solutions, as well as the analyzed solutions, were gently shaken for a few seconds before their analysis to avoid concentration gradients, and g) every two specimens, standard solutions were reanalyzed to either confirm or re-establish the accuracy of the calibration curve.

$[Na^+]$ and $[K^+]$ were measured directly with the AAS and $[OH^-]$ concentration was estimated by electro neutrality and calculated with Equation 2:

$$[OH^-] \approx [Na^+] + [K^+] \qquad \text{Equation 2}$$

### 3.2.8 Response Surface Methodology (RSM)

The *RSM* described by Myers et al. (2011) and Lawson (2014) was used to develop linear regressions, thus creating a numerical model for the responses that are $[Na^+]$, $[K^+]$ and $[OH^-]$. The results of the numerical analyses take the general quadratic form expressed by Equation 3 and the matrix form expressed by Equation 4 and Equation 5 presents the matrix formula to solve the systems, as proposed by Myers et al. (2011).

$$[y] = b_0 + b_1x_1 + \cdots + b_5x_5 + b_6x_1x_2 + \cdots + b_{15}x_4x_5 + b_{16}{x_1}^2 + + \cdots b_{20}{x_5}^2 \qquad \text{Equation 3}$$

$$[y] = [X] \times [b] \qquad \text{Equation 4}$$

$$[b] = ([X'] \times [X])^{-1} \times [X'] \times [y] \qquad \text{Equation 5}$$

In Equation 5, [b] is the vector of the regression coefficients or the "slope" of each parameter, [X] is the matrix bearing the information for each mixture or the levels of the variables (as presented in Table 3.3 and Table 3.4), and finally [y] is the vector of the observations or the results measured with the AAS or Equation 2. For example, the first two lines of [X] and [y] for the numerical model of [K+] for the SF mixtures are presented in Table 3.5. Those lines are related to the mixture 10GG-5SF-0.63A at 28 and 182 days; the measured [K+] are 114.17 (28 days) and 92.93 (182 days) mmol/L, respectively. After construction of [X] and [y], [b] is obtained through Equation 5.

**Table 3.5 : Example of the first two lines of the matrix [X] and [y] for a first order model neglecting the interactions.**

| Uncoded parameters [X] | | | | | Coded parameters [X] | | | | | [y] |
|---|---|---|---|---|---|---|---|---|---|---|
| GG | SF | Alk | Day | Cem | x1 | x2 | x3 | x4 | x5 | [$K^+$], in mmol/L |
| 10 | 5 | 0.63 | 28 | 85 | -1 | -1 | -1 | -1 | 1 | 114.17 |
| 10 | 5 | 0.63 | 182 | 85 | -1 | -1 | -1 | 1 | 1 | 92.93 |

The parameter [b] is calculated from coded [X] for the purpose of comparing the effect of the variables against each other and their impact on the answer. When [b] is calculated from uncoded [X], it is often referred as [$\beta$], and its purpose is to give the "natural equation" used to present the surface response on a ternary diagram, as well as to predict new data by plotting the proportion of any mixture design.

### 3.2.8.1 Variable Selection for Numerical Model

In this study, the significant variables are selected for the numerical model using a backward stepwise technique and $R^2_{adj}$ as the decision criterion, as proposed by Montgomery and Runger (2010). The elimination process starts with the effects of lower t-values, which correspond to the effects with a coefficient (b) of smaller magnitude and/or higher variance (i.e. high *Sum Squared Error* (SSE)) in the data set. For example, a low t-value, as expressed in Equation 6, indicates a less significant effect.

$$t - value = \frac{b_i}{Average\ SSE} \qquad \text{Equation 6}$$

The PRESS (*Prediction Error Sum Square*) statistic was also computed during the iteration process to confirm that the selected variables are not overly sensitive to single data points. According to Montgomery and Runger (2010), the PRESS statistic also9 provides a measure of how well the model is likely to perform when predicting new data. The PRESS number was divided by the Sum Squared Total (SST), as per Equation 7, to estimate the predictive capability of the regression model, as suggested by Myers et al. (2011).

$$R^2_{prediction} = 1 - PRESS / SST \qquad \text{Equation 7}$$

### 3.2.9 Model Validation

The reliability of the model is first validated by an $R^2$ above 0.90. $R^2_{adj}$ was only used in the iterative process to discard insignificant variables and select "the best model". Once the model with the highest $R^2_{adj}$ was selected, as proposed by Montgomery and Runger (2010), the near-normality and the homogeneity of the residual error were graphically assessed (see Annex B) to confirm that the regression model is uniformly accurate and that no specific "area" or group of data are particularly well or badly represented by the model. Models with errors or residuals failing the later tests were rejected.

The *Variance Inflation Factor* (VIF) was also used to verify that $R^2$ had not been inflated by multicollinearity, since a dependent variable is inherent to the mixture models, or by biased variables. Montgomery and Runger (2010) suggested that a VIF below 10 indicates a model with no multicollinearity issue. In this study, when "biased" variables were identified by a VIF over or near 10, they were eliminated from the regression model and the computations were then redone from the variable selection described in 3.2.8.1.

The hypothesis that the mean of all samples represents the observations better than the model is verified by computing $F_0$ and comparing it to a p-value, as described by Montgomery (2012). In this study, p-values lower than 0.05 for $F_0$ invalidate the last hypothesis. The final check for the multivariate model is made by plotting the predicted data against the experimental values and verifying the residuals between the equity lines and the plotted values. In this study, the correlation between the regression and the experimental data was found to be over 0.95 and are presented in Annex B.

#### 3.2.9.1 Software

The R software (Team 2013) was used for all computations, while the methodology, functions and packages proposed by Lenth (2009), Lawson (2014) and Lawson and Willden (2016) were followed. R software was also used to build the matrix, compute Equation 5 (and other statistic tests) and to double-check the good use of the functions proposed by the authors mentioned above.

#### 3.2.9.2 Confidence Interval for the Regression Model

Equation 8 is used to compute a confidence interval corresponding to an "$\alpha$" level of confidence; it holds for the confidence interval of new data within the range of the data set, while Equation 9 is appropriate for new data outside of the range of data set.

$$C.I. = \widehat{Y_0} \pm t_{\frac{a}{2}:n-k-1}\sqrt{MSE\left(x_0{}'(X'X)\right)^{-1}x_0} \qquad \text{Equation 8}$$

$$C.I. = \widehat{Y_0} \pm t_{\frac{a}{2}:n-k-1}\sqrt{MSE\left(1 + x_0{}'(X'X)\right)^{-1}x_0} \qquad \text{Equation 9}$$

where MSE is the *Mean Square Error* (MSE), $t_{\frac{a}{2}:n-k-1}$ is the percentage point on a Student distribution for a confidence of interval $\alpha$, n observations and k degrees of freedom; $x_0$ and X are respectively the matrix of the parameters and their values and $\widehat{Y_0}$ is the estimate. Annex C presents a table with the model values and their confidence interval of 95%.

## 3.3 Results of the Testing Program and of the Numerical Treatment of Data

### 3.3.1 Chemical Analyses of the Pore Solutions

The Annex C provides the detailed results of the chemical analyses of the pore solutions extracted from the ternary paste systems incorporating portland cements (C1 or C2), GG, and SF or MK, after 28 and 182 days of storage at 38°C. Standard deviation (SD) values are calculated from replicates presented in Annex A and a constant coefficient of variation was assumed to estimate the SD of the non-replicated analyses.

Figure 3.7 presents [$Na^+$] in the pore solution of paste systems incorporating GG, cements of different alkali contents and SF (Figure 3.7a to c) or MK (Figure 3.7d to f). The data presented in this figure suggest that [$Na^+$] generally increases significantly between 28 and 182 days, and that lower [$Na^+$] are associated with higher dosages of MK or SF (although the trend is not as distinct for SF). Also, for a given SF/MK-$Na_2O$eq (cement) combination, increasing the GG content generally results in higher [$Na^+$] in the pore solution. A general overview suggests that the highest [$Na^+$] were obtained when C2+NaOH (1.25% $Na_2O$eq) was used, which was expected considering that $Na^+$ ions from NaOH are readily available in solution. Actually, for SF-containing pastes, changing from a low-alkali (C1 0.63%) to a high-alkali (C2 0.94%) cement in paste systems results in relatively small differences in the [$Na^+$] of the pore solutions (at the same age and same SCM composition) compared to that of passing from the high-alkali (C2 0.94%) to the "boosted" systems (C2 + NaOH 1.25%). The difference is however not as marked in the case of MK-bearing systems.

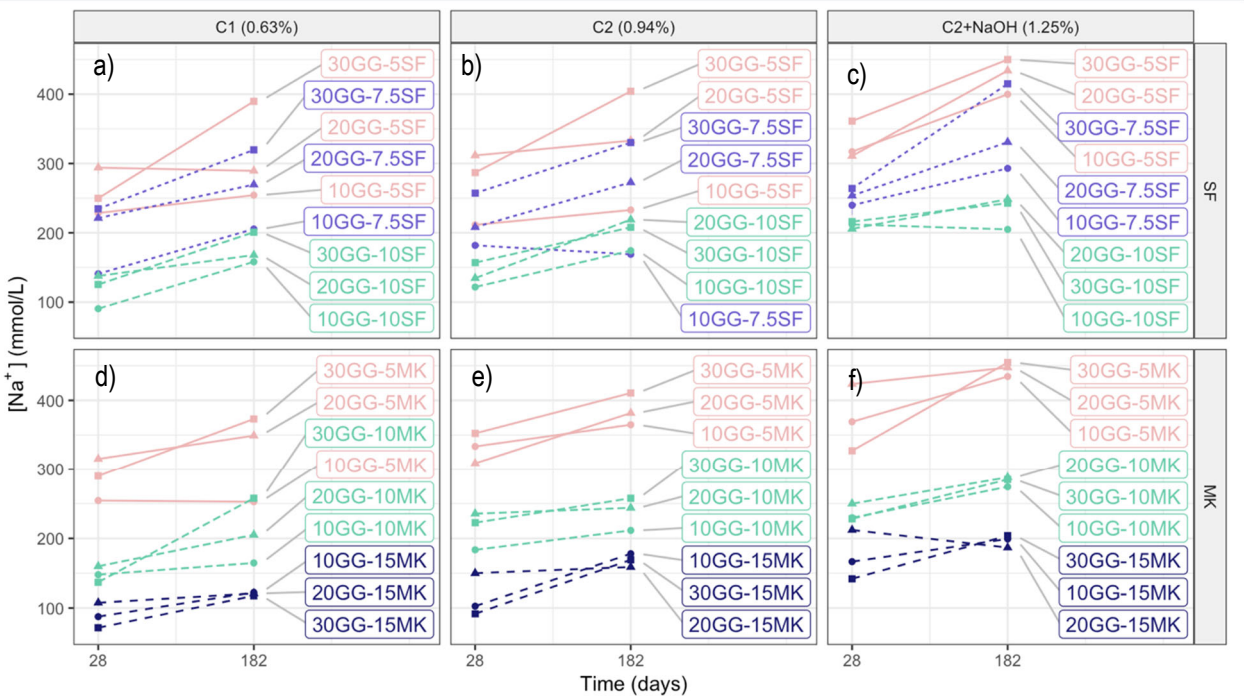


**Figure 3.7 : Evolution of [$Na^+$] between 28 and 182 days for pastes with various contents of GG, SF or MK and cements of different alkali contents.**

Figure 3.8 presents [$K^+$] in the pore solution of paste systems incorporating GG, cements of different alkali contents and SF (Figure 3.8a to c) and MK (Figure 3.8d to f). For both SF and MK systems, the lowest [$K^+$] were obtained for the pastes made with the low-alkali cement C1 and a decrease in [$K^+$] is generally observed with increasing SCMs contents in the pastes, i.e.: GG + SF or GG + MK. In the case of the MK-bearing pastes, the

[$K^+$] is found to decrease from 28 to 182 days for all cements of different alkali contents (Figure 3.8d to f). A similar trend is generally observed, but not always as pronounced, in the case of the SF-bearing pastes; actually, the [$K^+$] shows a relatively more stable behaviour between 28 and 182 days in the case of SF pastes with an alkali content of 1.25%. Also, for given cement and SF / MK contents, higher [$K^+$] are associated to lower GG content. An unexpected trend presented in Figure 3.8 is that the NaOH "boost" impacts [$K^+$], which is often higher compared to the same mixture without NaOH.

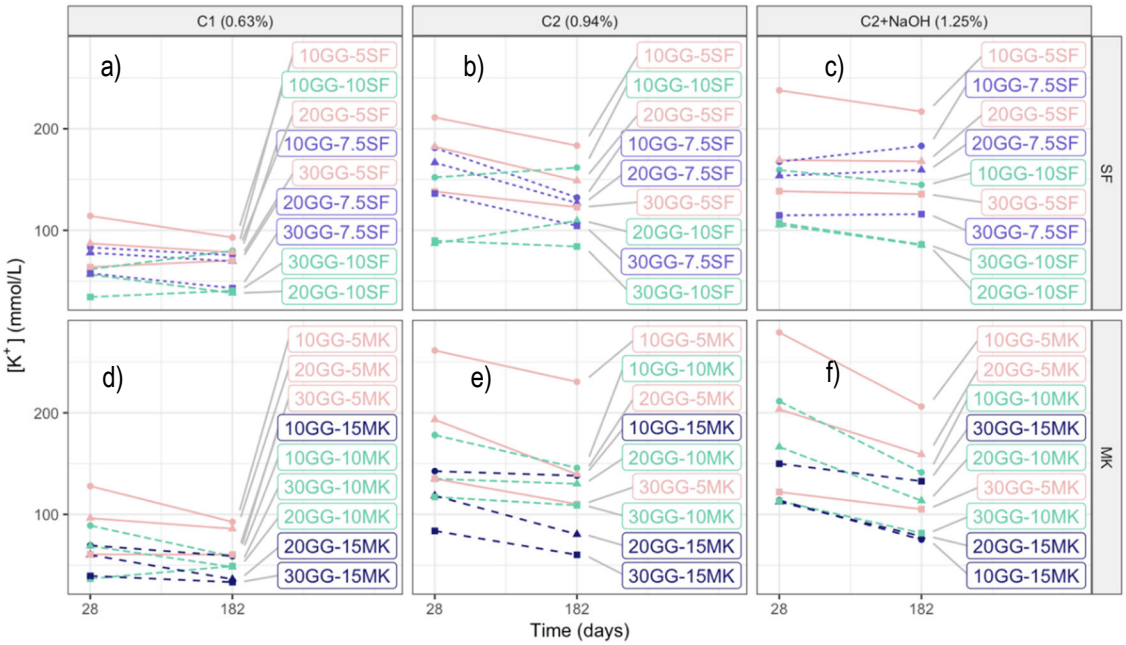


**Figure 3.8 : Evolution of [$K^+$] between 28 and 182 day for pastes with various contents of GG, SF or MK and cements of different alkali contents.**

The overall picture for the alkalinity, estimated by $[OH^-] \approx [Na^+] + [K^+]$, for pore solutions extracted at 182 days from paste systems incorporating GG and cements of different alkali contents, are presented in Figure 3.9 (a to c) for SF-bearing pastes and in Figure 3.9 (d to f) for MK-bearing pastes. For a given GG content, increasing the SF or MK content results in significant [$OH^-$] reductions of the pore solution; also, increasing the $Na_2O_{eq}$ of cement leads to an increase of the [$OH^-$] content in the pore solution. Pastes containing ≥10% SF or MK seem to be less sensitive to alkali boosting as they generally show similar or even lower [$OH^-$] for C2 and C2+NaOH (1.25%). In all cases, for a given SF or MK content and a given cement, increasing the GG content from 10 to 30% has no major effect on the [$OH^-$] of the pore solution.

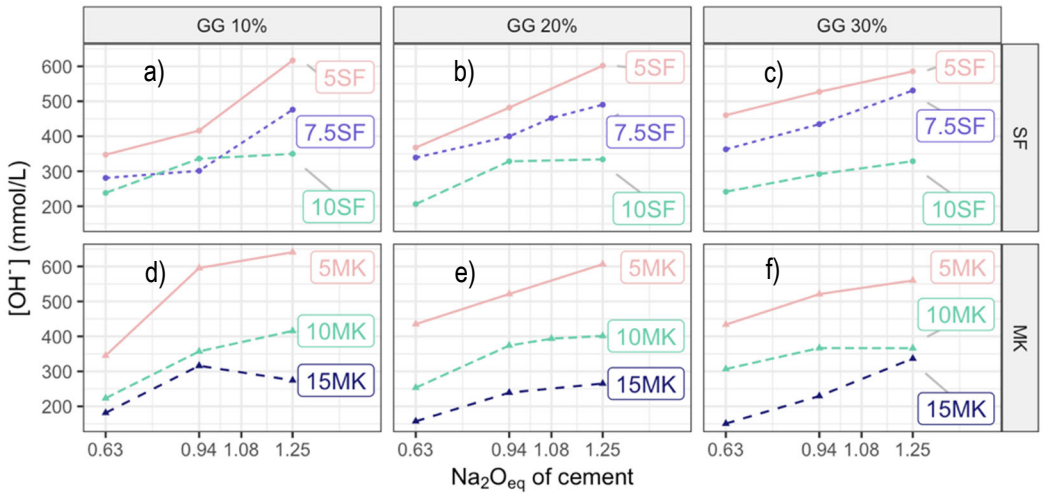


**Figure 3.9 : [$OH^-$] at 182 days, as a function of the $Na_2O_{eq}$ content of cement, for various GG and SF/MK contents.**

### 3.3.2 Numerical Treatment

Table 3.6 and Table 3.7 present the regression models proposed to better represent the data sets for the combinations of GG with SF and MK, respectively. Coefficients and other model information presented in Table 3.6 and Table 3.7are related to the coded variables, which provide a scale that is more suitable for comparing the effects of different variables. It is worth noting that the intercept of a coded regression model corresponds to the average value of the data set. The coefficients of the first order variables are proportional to their effect; consequently, most influent or less significant variables are associated with coefficients of higher or lower absolute values, respectively. Also, a negative coefficient indicates that the variable contributes at reducing the concentration. For example, in Table 3.6, the coefficients -72 for SF and 36 for GG in the model proposed for [$Na^+$] indicate that the addition of SF tends to lower [$Na^+$] because its coefficient is negative, while the use of GG tends to enhance [$Na^+$] because its coefficient is positive; the impact on [$Na^+$] is twice as much for SF compared to GG (i.e. 72 compared to 36 in absolute values). In Table 3.6 and Table 3.7, the effects are also labelled as “Main”, “Low” or “Optimum/Pessimum” to indicate in what extent the variable influences the response and a description relative to the labels is presented in the next section. The accuracy of the model is assessed in Table 3.8 by comparing the prediction to experimental data excluded from the dataset used to build the regression. Equations 10 to 15 were used to compute the predicted values presented in Table 3.8.

**Table 3.6: Regression model of SF (coded) and significant information of coefficients.**

| Type of effect | | $Na^+$ | | | $K^+$ | | | $OH^-$ | | |
|---|---|---|---|---|---|---|---|---|---|---|
| | Uncoded variable | Coeff | t-value | Prob. | Coeff | t-value | Prob. | Coeff | t-value | Prob. |
| | Intercept | 246 | 39 | 0 | 141 | 42 | 0 | 387 | 46 | 0 |
| Main | GG | 36 | 9 | 0 | -27 | -12 | 0 | 8 | 2 | 13 |
| | SF | -72 | -19 | 0 | -25 | -11 | 0 | -97 | -18 | 0 |
| | Alk | 38 | 10 | 0 | 40 | 18 | 0 | 79 | 15 | 0 |
| | Day | 30 | 9 | 0 | -6 | -3 | 0 | 23 | 5 | 0 |
| Low | GG*Alk | -7 | -1 | 17 | -9 | -3 | 0 | -16 | -2 | 2 |
| | GG*Day | 12 | 3 | 0 | - | - | - | 14 | 3 | 1 |
| | GG*Cem | 14 | 2 | 7 | -4 | -1 | 35 | 12 | 1 | 27 |
| | SF*Alk | - | - | - | -8 | -3 | 1 | -11 | -2 | 9 |
| | SF*Day | -4 | -1 | 31 | 3 | 1 | 16 | - | - | - |
| | SF*Cem | 13 | 2 | 5 | - | - | - | 10 | 1 | 25 |
| | Alk*Day | 5 | 1 | 24 | - | - | - | - | - | - |
| Optimum/Pessimum | $Alk^2$ | 24 | 4 | 0 | -36 | -10 | 0 | -10 | -1 | 26 |
| Model information | | $R^2$=0.92, N=64, $R^2_{prediction}$=0.87 | | | $R^2$=0.94, N=59 $R^2_{prediction}$=0.91 | | | $R^2$=0.92, N=59 $R^2_{prediction}$=0.88 | | |
| Model significance | | p. for $F_0$ < 2.2e-16, Cor.= 0.96 | | | p. for $F_0$<2.2e-16, Cor.= 0.97 | | | p. for $F_0$ < 2.2e-16, Cor.= 0.96 | | |

**Table 3.7: Regression model of MK (coded) and significant information of coefficients.**

| | | $Na^+$ | | | $K^+$ | | | $OH^-$ | | |
|---|---|---|---|---|---|---|---|---|---|---|
| Type of effect | Uncoded variable | Coeff | t-value | Prob. | Coeff | t-value | Prob. | Coeff | t-value | Prob. |
| | Intercept | 238 | 72 | 0 | 130 | 27 | 0 | 378 | 44 | 0 |
| Main | GG | 9 | 2 | 2 | -28 | -10 | 0 | -17 | -3 | 1 |
| | MK | -107 | -27 | 0 | -30 | -11 | 0 | -137 | -22 | 0 |
| | Alk | 43 | 10 | 0 | 39 | 14 | 0 | 83 | 13 | 0 |
| | Day | 25 | 8 | 0 | -13 | -6 | 0 | 10 | 2 | 5 |
| Low | GG*Alk | -8 | -2 | 10 | -4 | -1 | 23 | -15 | -2 | 6 |
| | GG*Day | -12 | -2 | 2 | 6 | 2 | 5 | 13 | 2 | 4 |
| | GG*Cem | 9 | 2 | 0 | -7 | -1 | 30 | - | - | - |
| | MK*Alk | - | - | - | -8 | -2 | 3 | -14 | -2 | 7 |
| | MK*Day | - | - | - | 3 | 1 | 35 | - | - | - |
| | MK*Cem | -5 | -1 | 3 | -27 | -5 | 0 | - | - | - |
| | Alk*Day | - | - | - | -7 | -3 | 1 | -6 | -1 | 32 |
| Optimum/Pessimum | $Alk^2$ | - | - | - | -36 | -7 | 0 | -33 | -3 | 0 |
| Model information | | $R^2$=0.95, N=66 $R^2_{prediction}$=0.94 | | | $R^2$=0.92, N=64 $R^2_{prediction}$=0.85 | | | $R^2$=0.94, N=58 $R^2_{prediction}$=0.91 | | |
| Model significance | | p. for $F_0$ < 2.2e-16, Cor.=0.98 | | | p. for $F_0$ < 2.2e-16, Cor.=0.96 | | | p. for $F_0$ < 2.2e-16, Cor.=0.97 | | |

**Table 3.8 : Predicted values compared to experimental "check point" excluded from the dataset but used to build/validate the models.**

| Mixture | Age | $[Na^+]$ (mmol/L) | | | $[K^+]$ (mmol/L) | | | $[OH^-]$ (mmol/L) | | |
|---|---|---|---|---|---|---|---|---|---|---|
| | | Predict. | Exp. | Diff. | Predict. | Exp. | Diff. | Predict. | Exp. | Diff. |
| 20GG-7.5SF-1.08Alk | 28 | 236 | 221 | 7% | 157 | 150 | 5% | 383 | 372 | 3% |
| | 182 | 299 | 315 | -5% | 145 | 137 | 6% | 429 | 452 | -5% |
| 20GG-10MK-1.08Alk | 28 | 249 | 240 | 4% | 157 | 138 | 13% | 401 | 379 | 6% |
| | 182 | 297 | 273 | 8% | 124 | 121 | 2% | 416 | 393 | 6% |

Equations 10 to 12 are proposed to predict new data for paste systems incorporating SF, while equations 13 to 15 are proposed for pastes made with MK. "GG", "SF", "MK" and "Cem" represent respectively the content (in percentages) of ground glass, silica fume, metakaolin (i.e. 0.1 for 10%) and cement in the systems; "Alk" represents the cement alkali content in $Na_2O_{eq}$ (i.e. between 0.63 and 1.25) and "Day" is the age (in days) of the paste sample.

Equation 10

$$[Na^+] = 303 + 96.1GG - 5069SF - 324Alk - 219GP * Alk + 1.6GG * Day + 1153GG * Cem - 2.1SF * Day + 4072SF * Cem + 0.2\ Alk * Day + 250Alk^2$$

Equation 11

$$[K^+] = -265 + 178GG - 280SF + 956Alk - 0.2 * Day - 288GG * Alk - 330G * Cem - 1002SF * Alk + 1.6SF * Day - 370Alk^2$$

Equation 12

$$[OH^-] = 14.3 + 104GG - 4440SF + 655Alk - 0.1 * Day - 517GG * Alk + 1.8GG * Day + 994GG * Cem - 1446SF * Alk + 3255SF * Cem - 106Alk^2$$

Equation 13

$$[Na^+] = 1547 - 1188GG - 313MK + 24Alk + 0.1 * Day - 374GG * Alk + 1.2GG * Day + 2581GG * Cem - 2145MK * Cem$$

Equation 14

$$[K^+] = -111 - 306GG + 1811MK + 915Alk - 0.1 * Day - 134GG * Alk + 0.7GG * Day - 568GG * Cem - 486MK * Alk + 0.7MK * Day - 3581MK * Cem - 0.3Alk * Day - 364Alk^2$$

Equation 15

$$[OH^-] = -52 - 102GG + 1874MK + 1132Alk - 476GG * Alk + 1.7GG * Day - 919MK * Alk - 0.3 * Alk * Day - 345Alk^2$$

### 3.3.3 Model Information, Significance and Coefficient Information

The "$R^2$" given in Table 3.6 and Table 3.7 indicates how accurately the model represents the experimental data, "N" indicates the number of observations used to build the regression model, "$R^2_{Prediction}$" indicates how accurately the regression model is expected to perform with new data, "p. for $F_0$" indicates the probability that the mean of the experimental measurements represents more accurately the observations than the model, and "Cor." indicates the correlation between the numerical model and the experimental measurements presented in Annex B. The "t-value" informs about the reliability of the detected effect; higher absolute t-values indicate that the effect is reliable and significant over the model. What is mentioned as "Prob." is the probability that the coefficient is indeed 0 and the coefficient computed is an artefact caused by some sort of variance alignment within the measurements.

## 3.4 Discussion

### 3.4.1 Interpretation of the Effect

The "Main" effects are the first order linear relations and they are useful to draw the major trends revealed by the data. When plotting the "main" effect on a 2D graph, the relation between the variable and the response shows a straight line and the "Main" coefficient is the slope of the linear first order regression. When plotting the "main" effect as part of a surface response expressed by contour lines on a 3D or ternary graph, the relation between the variable and the response shows contour lines parallel to each other's. Also, the "Main" effect provides a somewhat "rough analysis" of the data because it neglects the interactions.

For example, Table 3.9 shows that, for 28-day old pastes containing 7.5% SF, the "average" effect of increasing the $Na_2Oeq$ content of the cement (i.e. using C1, C2 and C2+NaOH) is a 18% increase in $[Na^+]$, ranging from 31% for the 10% GG system to 6% for the 30% GG system. The effect of increasing the $Na_2Oeq$ content of cement is thus less pronounced with 30% GG, which suggests an interaction between "GG" and "Alk" where increasing the "GG" content lowers the impact of the $Na_2Oeq$ content of cement. Therefore, in the case of interactions between the variables, a regression model considering only the "main" effects will lack accuracy when "averaging" the effect, like it would for the example presented in Table 3.9.

**Table 3.9: [$Na^+$] at 28 days for pastes containing 7.5% SF, various contents of GG and $Na_2O$eq contents of cements.**

| | | [$Na^+$] in the pore solution (mmoles/L) | | | Increase of [$Na^+$] between C1 and C2 | Increase of [$Na^+$] between C2 and C2+NaOH) | Average increase in [$Na^+$] | |
|---|---|---|---|---|---|---|---|---|
| "Alk" ($Na_2O$eq%) → | | 0.63 (C1) | 0.94 (C2) | 1.25 (C2+NaOH) | | | | |
| "GG" content | 10% | 141 | 182 | 240 | 29% | 32% | 31% | 18% |
| | 30% | 235 | 257 | 264 | 9% | 3% | 6% | |
| Increase of [$Na^+$] caused by increasing GG from 10 to 30% | | 67% | 41% | 10% | | | | |

A powerful element of the RSM approach for mixture experiments is that it takes into account the dilution. Indeed, the effect of cement dilution can be legitimately confused with a "chemical" interaction between "GG" and "Alk" because their trends are similar when analyzing the same data. However, the numerical approach allows quantifying those trends and differentiating them by comparing their order of magnitude. In Table 3.9, the effect of alkali boosting is approximately 10 times more important on [$Na^+$] for the 10% GG system (32%) than for the 30% GG system (3%), and this effect cannot be explained only by the dilution of the "boosted" cement (as can be seen in Table 3.10). Therefore, the numerical analysis suggests an interaction. Yet, the dilution effect remains worthy to keep in mind in the interpretation of the trends observed, but will be discussed further, as the graphical displays presented later are more appropriate to confirm or not the significance of the dilution effect.

**Table 3.10 : Total $Na_2O$eq of cementitious mixtures (dry composition) containing 7.5%SF, various contents of GG and cements with a $Na_2O$eq "unboosted" (0.63, 0.94%) and "boosted" (1.25%).**

| | | Alkali content of the mixture, $Na_2O$eq | | | Increase of $Na_2O_{eq}$ between C1 and C2 | Increase of $Na_2O_{eq}$ between C2 and C2+NaOH | Average increase in $Na_2O_{eq}$ | |
|---|---|---|---|---|---|---|---|---|
| "Alk" ($Na_2O_{eq}$) → | | 0.63% (C1) | 0.94% (C2) | 1.25% (C2 +NaOH) | | | | |
| "GG" content | 10% | 1.9% | 2.2% | 2.4% | 13% | 10% | 12% | 9% |
| | 30% | 4.4% | 4.6% | 4.9% | 4% | 6% | 5% | |
| Increase of $Na_2O$eq caused by increasing GG from 10 to 30% | | 128% | 110% | 102% | | | | |

Table 3.6 and Table 3.7, the "interaction" effects are classified as "low-type" effect and they increase the accuracy of the model. For example, in Table 3.6, the numerical analysis suggests that "GG" and "Alk" interfere with each other in the [$Na^+$] model and the negative coefficient (-7) for "GG*Alk" suggests that the presence of GG in the system lowers the impact of the variable "Alk", which agrees with the trends presented in Table 3.6. In addition, this interaction also means that the higher value for "Alk" lowers the impact of increasing the GG content, which also agrees with the data in Table 3.6 Indeed, for "cement" $Na_2Oeq$ contents of 0.63%, 0.94% and 1.25%, increasing the GG content from 10% to 30% increases [$Na^+$] by 67%, 41% and 10%, respectively (Table 3.9). The "low" effects detected by the numerical analysis is alternatively called "synergy" or "interaction" and are insightful for further discussions. When plotted, the surface response of a regression model including "low" effects shows curved surfaces and/or contour lines that are "tighter" or "looser" in certain areas of the plot.

The Optimum/Pessimum effect is a second order relation between the variable and the response and translates a specific value for which the response is maximal or minimal. In this study, the "Alk" variable was found to exhibit a specific value for which the [$K^+$] and the [$OH^-$] are maximal (negative coefficients for $Alk^2$) and also a specific value for which the [$Na^+$] is minimal (positive coefficient of +24 in Table 3.6) for the SF-containing pastes. The second order effect gives a parabolic shape to the response surface. Also, it is worth noting that the optimum/pessimum effects theoretically detected by the regression model were not always observed in the range of the laboratory-generated data.

### 3.4.2 Graphical Layout of the Results

The satisfactory accuracy of the experimental data to the surface response (correlations ($R^2$) ranging between 0.96 and 0.98, Annex B) indicates that the surface response reasonably represents the experimental data obtained and also fill the gap between them. Consequently, the equation of the surface response and the shape of the contour lines on ternary diagrams were considered the best tools to discuss the trends revealed by the experimental data.

The surface response on a ternary diagram is the results of the model representing the experimental data on a continuous range of mixture proportions. The ternary graph includes contour lines representing the computed [$Na^+$], [$K^+$] and [$OH^-$] that, altogether, compose the surface responses resulting from data treatment. Indications on the accuracy of the computed data against the experimental data, as well as the confidence interval of the surface responses, can be found in the Annex C (i.e. *Data from the model*, i.e. [$Na^+$], [$K^+$] or [$OH^-$] and min / max values).

In the following sections, the ternary diagrams are constructed with decreasing proportions of a given component when moving towards the opposite side of the tips and the corresponding gradations appear on the side located clock ward to that tip. For example, in Figure 3.10, the GG parameter ranges from values of 0.35 (35%) at the top to 0.10 (10%) at the bottom of the diagram ; the "working range" for GG in this study ranges between 10 and 30% and is indicated with dashed lines in the graphs, which also are the borders of the experimental region. The latter is delimited by a parallelogram.

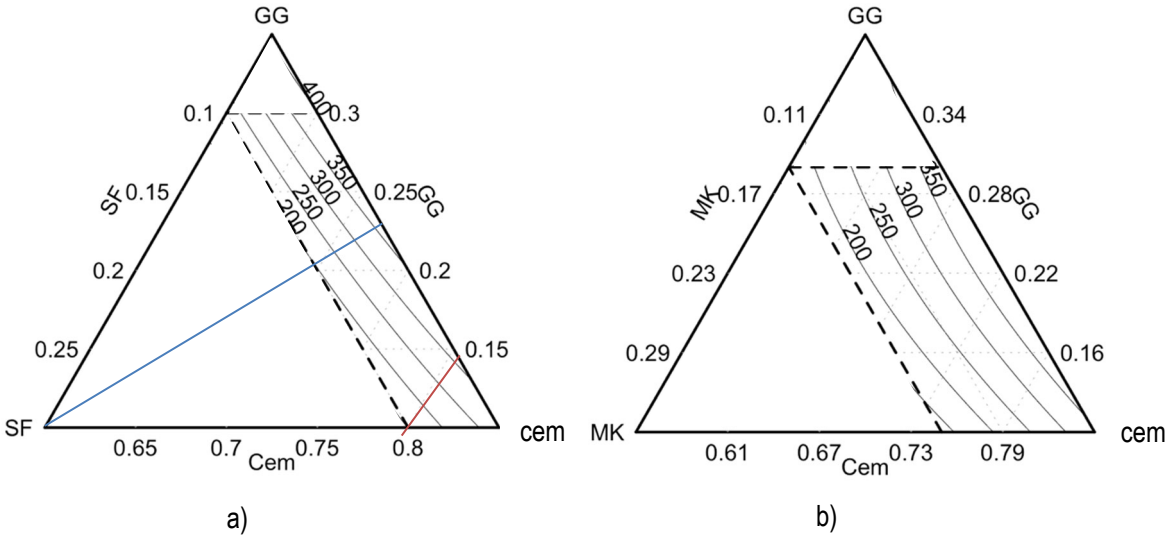


**Figure 3.10 : Surface response for the [$Na^+$] of the pore solution of 182-day old pastes made with cement C2 (0.94%, $Na_2Oeq$) and containing various proportions of GG and a) SF and b) MK. The dashed lines are the border of the experimental region and the axes indicate the proportions of the components in the mixtures.**

### 3.4.3 Impact of the Mixture Proportions on [$Na^+$]

Figure 3.10a shows the [$Na^+$] at 182 days in the pore solution of pastes made with the cement C2 without added NaOH and various contents of GG and SF. The graph reveals that [$Na^+$] is mainly influenced by the SF content in the paste. Indeed, moving along the blue line arising from the SF tip shows that the [$Na^+$] ranges from over 350 to about 150 mmol/L for pastes with SF contents between 5% and 10% (i.e. range covered in this study). Also, contours lines nearly parallel to the SF gradation lines (e.g. the 10% SF dashed line), indicate that for any given SF content, [$Na^+$] is relatively stable, and this stands for various contents of GG or cement.

The biggest impact of the SF compared to the GG component on the [$Na^+$] in the pore solution can be appreciated by following the GG gradation lines in Figure 3.10a. For example, by following horizontal lines corresponding to systems with different GG contents, e.g. the upper 30% GG dashed line, one can notice that the [$Na^+$], for any given GG content, is greatly influenced by the SF content in the system. Similarly, following lines corresponding to different cement contents in the system, e.g. the red 80% cement line, also confirms that

the SF content greatly influences [$Na^+$] in the pore solution. The strong impact of the SF content is confirmed by the numerical analysis with a negative coefficient of higher magnitude (-72) (Table 3.6), which indicates that higher SF contents lower [$Na^+$] in the pore solution for any given GG content.

A second observation in Figure 3.10a is that the contour lines are slightly tilted compared to the SF gradation lines. This suggests that although the SF content has a major influence on [$Na^+$], another parameter has a minor influence on [$Na^+$], which is actually the GG content. Indeed, for a given SF content, the incorporation of higher percentages of GG leads to higher [$Na^+$]. For instance, when moving up along the 10% SF dashed line from the 10 to the 30% GG content in Figure 3.10a, the [$Na^+$] increases steadily from 150 to about 220 mmoles/L. In the numerical analysis, the coefficient for GG is 36 (Table 3.6), which is half of the effect of SF (-72). In other words, the removal of $Na^+$ ions in the pore solution related to the addition of 5% SF (i.e. from 5% to 10%) is two times bigger than the $Na^+$ release caused by increasing the GG content in the system from 10% to 30%, or, said differently, 2.5% SF are required to "counteract" the sodium release in the pore solution of 20% GG.

Figure 3.10b illustrates the [$Na^+$] at 182 days for pastes made with the C2 (0.94%) cement (without added alkali) and various contents of GG and MK. The contour lines being nearly parallel to the MK gradation indicate that, similarly to SF, the MK content mainly controls [$Na^+$] in the pore solution and its effect is largely superior to that of the GG or the cement contents. Data in Table 3.7 suggest that the curved shape of the contour lines is partly related to the "low" effect of the interaction "GG*Cem" (9; Table 3.7) and "MK*Cem" (-5; Table 3.7).

In the MK-bearing pastes, "GG" has only a minor influence on the [$Na^+$] in the pore solution with a coefficient of only 9 (Table 3.7), whereas in SF-bearing pastes, the effect of "GG" is computed with a coefficient of 36 (Table 3.6).

The relatively small impact of the GG content on [$Na^+$] in the ternary pore solution, remains somewhat unexpected; a few studies on pore solution composition in binary paste systems incorporating GG concluded that the latter contributes significantly in raising the [$Na^+$] (Fily-Paré et al. 2017), while other studies suggested that the rise in pH of solutions or slurries correlated with the high $Na_2O_{eq}$ content of GG in the systems (Shevchenko 2012, Kamali and Ghahremaninezhad 2016). The present study suggests that the extrapolation of the contribution of GG to the [$Na^+$] in the pore solution of binary systems is probably not appropriate to predict the contribution of GG in ternary systems.

Figure 3.11 shows the measured [$Na^+$] in the pore solution of the various pastes plotted against the total $Na_2O$ in the mixture. It suggests that the GG content influences the $Na_2O$ content of the cementitious mixture; however, it is clear that an increase in the GG content of the ternary mixtures does not result in a proportional increase in the [$Na^+$] in the pore solution of the corresponding paste specimens.

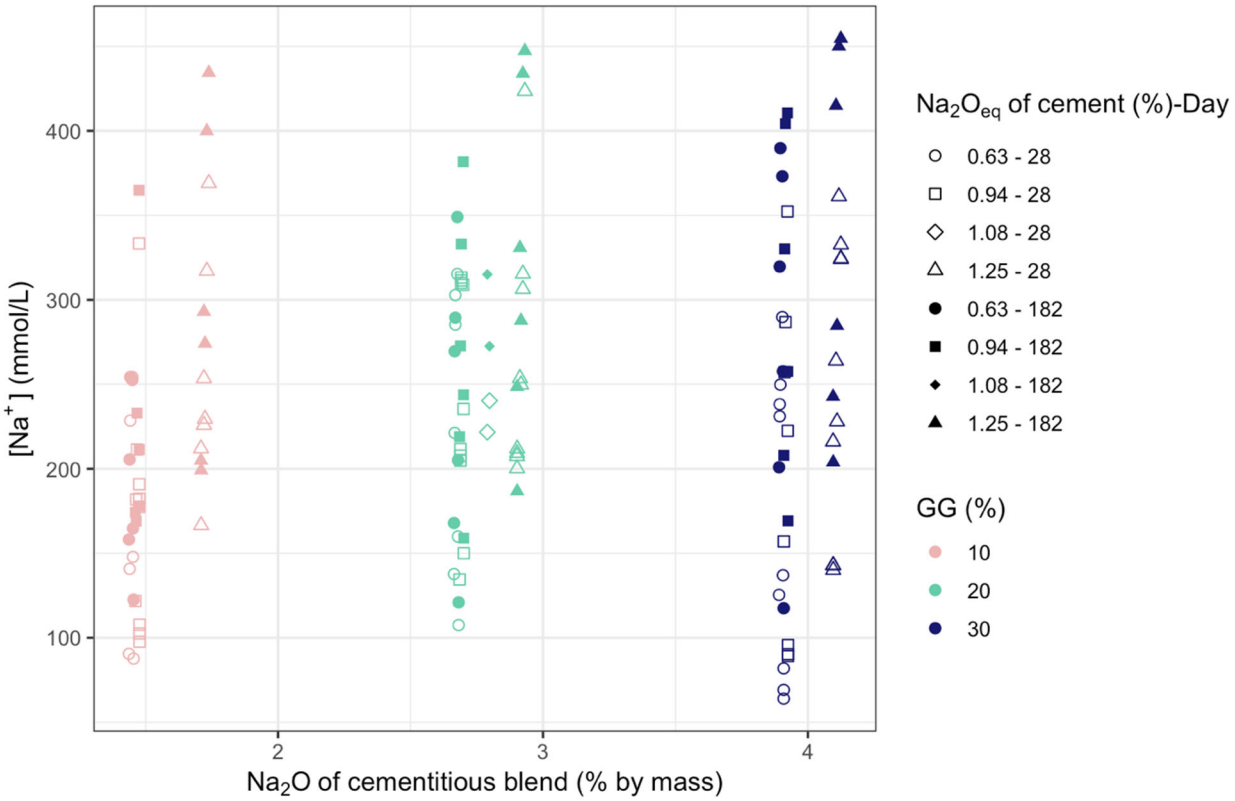


**Figure 3.11 : [$Na^+$] in the pore solution and its relation to the $Na_2O$ content of the cementitious mixture at 28 and 182 days for all ternary mixtures selected for this study (SF 5% to 10%; MK 5% to 15%; GG 10 to 30%).**

### 3.4.4 Impact of the Mixture Proportions on [$K^+$]

Figure 3.12 shows the [$K^+$] in the pore solution at 182 days for pastes made with different proportions of GG, SF and cements with three $Na_2O$eq contents. The contour lines are neither parallel nor perpendicular to a specific axis, which suggests that the [$K^+$] is controlled by more than one parameter. In Table 3.6, the coefficient for "SF" is -25, while that of GG is -27, which indicate that an increase in SF from 5% to 10% lowers [$K^+$] similarly to an increase of GG from 10% to 30% (see experimental data in Table 3.11). Hence, both GG and SF have similar potential to reduce [$K^+$] in their usual range of use; however, this implies that, by mass, SF is relatively more efficient since an increase of 5% in cement replacement by SF (5 to 10%) is equivalent to an increase of 20% in cement replacement, by mass, of GG (10 to 30%) in Table 3.11.

.

**Table 3.11: [$K^+$] in the pore solution of 182-day old pastes made with "boosted" cement C2 (1.25%) for various contents of GG and SF.**

| | [$K^+$] in the pore solution (mmoles/L) | | [$K^+$] decrease due to increase of "SF" |
|---|---|---|---|
| "SF" content → | 5% | 10% | |
| Low "GG" content (10%) | 217 | 145 | 33% |
| High "GG" content (30%) | 136 | 116 | 37% |
| [$K^+$] decrease due to increase of "GG" | 37% | 41% | |

Figure 3.13 shows the [$K^+$] in the pore solution at 182 days of various pastes made with different proportions of GG, MK and cements with three $Na_2O$eq contents. In the case of the MK-containing pastes, the contour lines are nearly vertical, but show some curvatures towards higher GG contents. Such vertical contour lines, parallel to the axis extending down from the GG tip, indicate that the overall effect of the GG content is low on the [$K^+$] of the pore solution, while the curvatures indicate that some "low" effects are present. In Table 3.7, the coefficients for "GG", "MK" and "MK*Cem" are similar at -28, -30 and -27, thus suggesting similar effects for both variables "GG" and "MK" and the interaction "MK*Cem". This is highlighted in Table 3.13 where, for example, increasing the MK proportion from 5 to 15% in a system with 10% GG has a similar reducing effect on the [$K^+$] in the pore solution (i.e. 37%) than increasing the GG proportion from 10 to 30% in a system with 5% MK (i.e. 35%).

For pastes made with cement C1, which has a $K_2O$ content of 0.62 (similar to that of GG with value of 0.66%), the incorporation of GG does not contribute to the dilution of the $K_2O$ content of the cementitious mixture, as shown in Table 3.12, since increasing the GG content is associated to a 0% decrease of the $K_2O$ content (dry composition) of the cementitious mixture. Moreover, Figure 3.14 shows a cluster of data points for pastes made with the low alkali cement C1 at the bottom left side of the plot, where the lowest [$K^+$] in the pore solution were generally obtained for 30% GG-bearing pastes while higher [$K^+$] were obtained for pastes made with 10% GG. This is interesting because, although the $K_2O$ content of GG is similar to that of cement C1, increasing GG contents still contributes at reducing [$K^+$] in the pore solution; this agrees with the regression model that suggested that the use of GG lowers [$K^+$], i.e. negative coefficient of -28 in Table 3.7.

As presented in Table 3.12, the effect of the MK content on the reduction of [$K^+$] in the pore solution is partially due to dilution because the $K_2O$ content of MK is only 0.25%, and a 10% cement replacement by mass of MK results in a decrease of $K_2O$ content by 6%. However, since the observed reduction effects of MK on [$K^+$] are 37% and 45% when 10% and 30% of GG are used, respectively, it is suggested that their impact on [$K^+$] goes beyond that of a simple cement dilution.

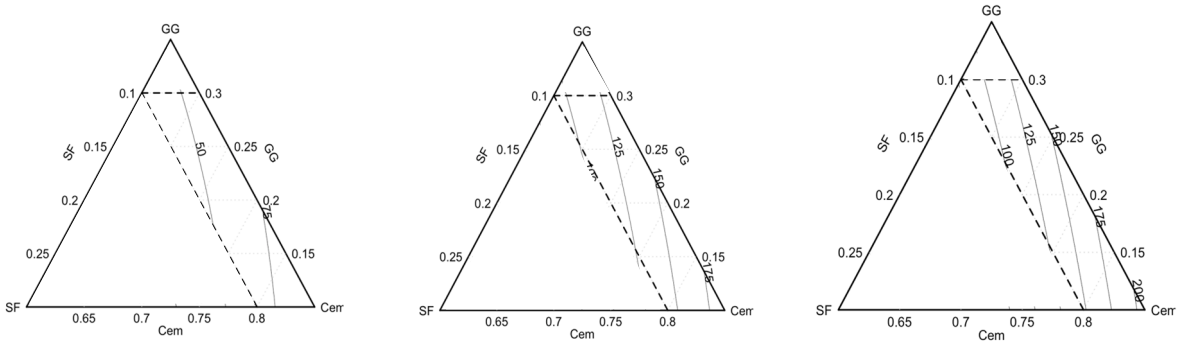


a) b) c)

**Figure 3.12 : Surface response for the [$K^+$] of the pore solution of 182-day old pastes made with various proportions of GG, SF and cements of various alkali contents ($Na_2Oeq$): a) 0,63%, b) 0.94%, and c) 0.94% boosted to 1.25% ($Na_2Oeq$) with NaOH. The dashed lines are the border of the experimental region and the axes indicate the proportions of the various components in the mixture.**

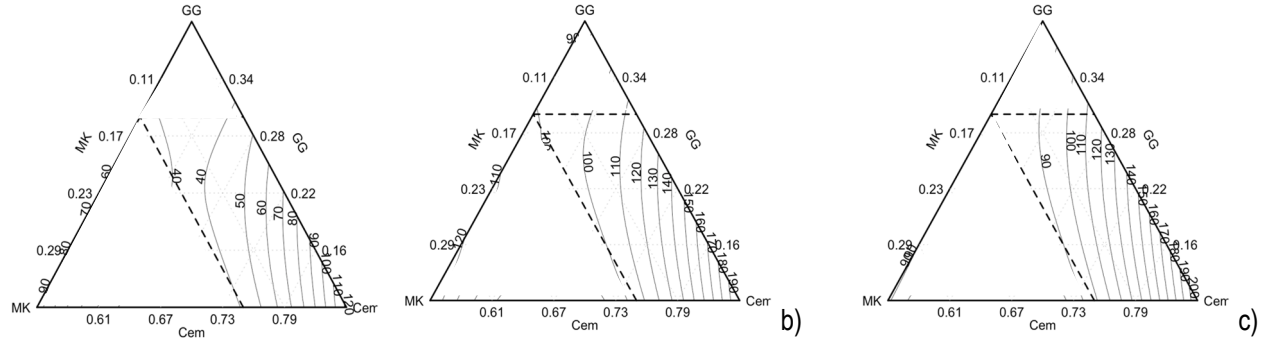


a) b) c)

**Figure 3.13 : Surface response for the [$K^+$] of the pore solution of 182-day old pastes made with various proportions of GG, MK and cements of various alkali contents ($Na_2Oeq$): a) 0,63%, b) 0.94%, and c) 0.94% boosted to 1.25% ($Na_2Oeq$) with NaOH. The dashed lines are the border of the experimental region and the axes indicate the proportions of the various components in the mixture.**

**Table 3.12 : [$K^+$] of the pore solution of 182-day old pastes made with various contents of GG and MK and cement C1 and the $K_2O$ content of the cementitious mixture (dry composition).**

| | [$K^+$] in the pore solution (mmoles/L) | | $K_2O$ content of the mixture (%) | | Decrease of [$K^+$] between 5 and 15% MK for C1 | Decrease of $K_2O$ between 5 and 15% MK for C1 |
|---|---|---|---|---|---|---|
| "MK" content → | 5% | 15% | 5% | 15% | | |
| Low "GG" content (10%) | 93 | 59 | 0.61 | 0.57 | 37% | 6% |
| High "GG" content (30%) | 60 | 33 | 0.61 | 0.58 | 45% | 6% |
| Decrease of [$K^+$] or $K_2O$ caused by increasing GG from 10 to 30% | 35% | 44% | 0% | 0% | | |

Table 3.13 presents the effect on [$K^+$] in the pore solution and on the $K_2O$ content of the cementitious mixtures (dry composition) of increasing MK and GG contents in pastes made with the C2 cement ($K_2O$ content of 1.05%). The data indicate that increasing the GG content from 10 to 30% in MK-bearing pastes (5 to 15%) contributes in a slight reduction of the $K_2O$ content of the mixture (7 or 8%); however, the effect of increasing MK and GG contents on [$K^+$] in the pore solution is of a much greater magnitude than that related to simple cement dilution (ranging from 40 to 57%). In Figure 3.14, which compares the $K_2O$ content of the blends (dry composition) and the [$K^+$] in the pore solution of the corresponding paste mixtures, the cement dilution effect is observable from the cloud of data on the right side of the figure where cementitious mixtures with higher $K_2O$ are associated to higher [$K^+$] in the pore solution and inversely. However, pastes of similar $K_2O$ content can lead to a relatively wide range of [$K^+$] in the pore solution, which suggests that the components of those mixtures (GG, MK and the cement) do not necessarily release their potassium in pore solution proportionally to their $K_2O$ content. For example, mixtures with a $K_2O$ content of 0.89% can result in [$K^+$] in the pore solution ranging between approximately 75 mmol/l and 175 mmol/l. Again, the effect of GG and MK in lowering [$K^+$] is undoubtedly due to cement dilution but probably also to some binding effects through the pozzolanic or even other reaction for which further work is needed. The effect of GG in reducing [$K^+$] was already observed in other studies in which the pore solution of binary pastes incorporating GG were investigated (Zheng 2016, Fily-Paré et al. 2017).

**Table 3.13 : [$K^+$] in the pore solution of 182-day old pastes made with various contents of GG and MK and cement C2 and the $K_2O$ content of the cementitious mixture (dry composition).**

| | [$K^+$] in the pore solution (mmoles/L) | | $K_2O$ content of the mixture (%) | | Decrease of [$K^+$] between 5 and 15% MK for C2 | Decrease of $K_2O$ between 5 and 15% MK for C2 |
|---|---|---|---|---|---|---|
| "MK" content → | 5% | 15% | 5% | 15% | | |
| Low "GG" content (10%) | 231 | 138 | 0.94 | 0.86 | 40% | 8% |
| High "GG" content (30%) | 110 | 60 | 0.87 | 0.79 | 45% | 8% |
| Decrease of [$K^+$] or $K_2O$ caused by increasing GG from 10 to 30% | 52% | 57% | 7% | 8% | | |

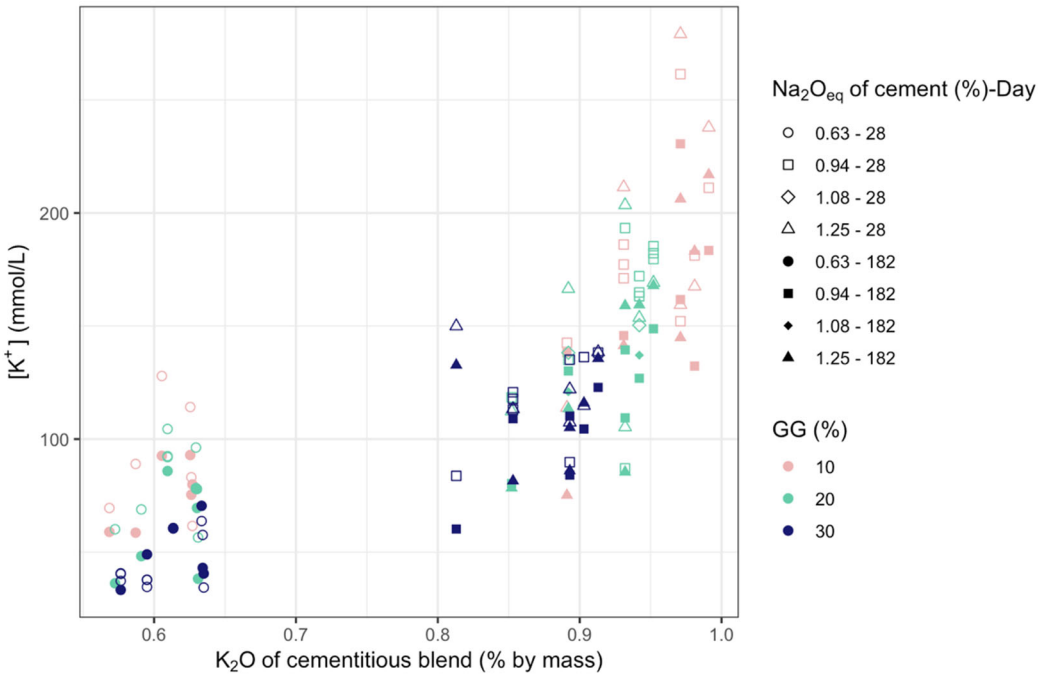


**Figure 3.14 : [$K^+$] in the pore solution at 28 and 182 days and its relation to the $K_2O$ content of the cementitious blends (dry composition) for all mixtures selected in this study (SF from 5% to 10%, MK from 5% to 15% and GG from 10% to 30%).**

### 3.4.5 Impact of the Mixture Proportions on [$OH^-$]

Figure 3.15 shows [$OH^-$] calculated by electro neutrality (see Equation 2) for pastes containing various proportions of GG and SF, as well as the low-alkali cement C1 (Figure 3.15a) and cement C2 "boosted" to 1.25% $Na_2Oeq$ with NaOH (Figure 3.15b).

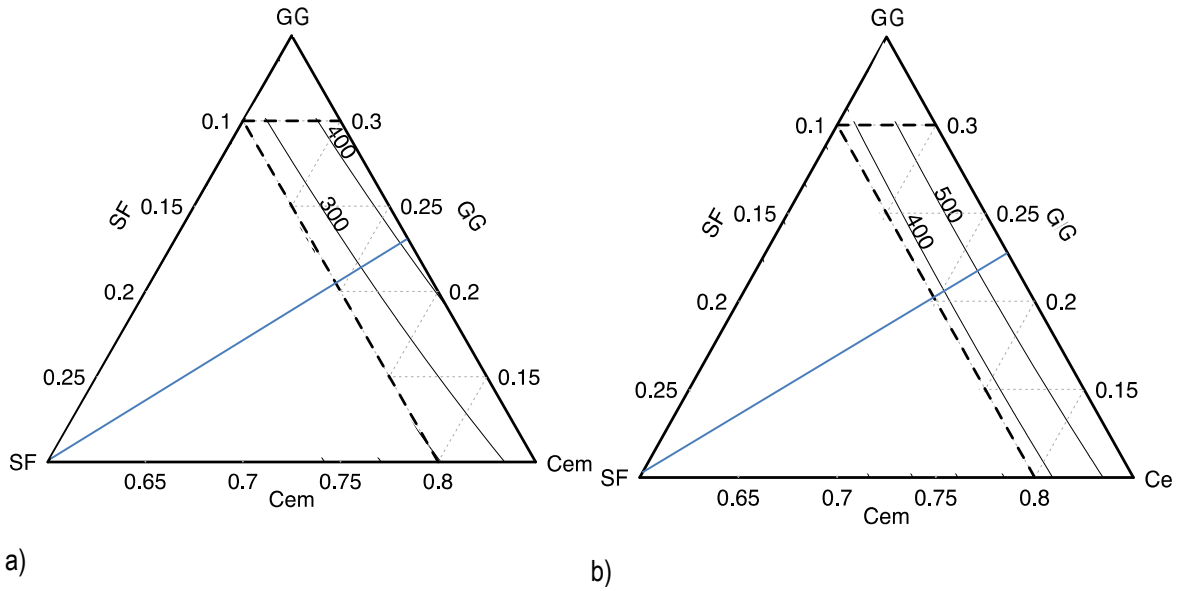


**Figure 3.15 : Surface response for the [$OH^-$] of the pore solution of 182-day old pastes made with various proportions of GG and SF, and a) cement C1 (0.63% $Na_2Oeq$), and b) cement C2 + NaOH (1.25% $Na_2Oeq$). The dashed lines are the border of the experimental region and the axes indicate the proportions of the various components in the mixtures.**

The contour lines of the [$OH^-$] response are perpendicular to the SF axis drawn in blue in Figure 3.15, which suggests that the major component influencing [$OH^-$] is the proportion of SF in the system. This was expected since SF has a major influence in [$Na^+$] (e.g. Figure 3.10a) and also, to some extent, on [$K^+$] (Figure 3.12), which are used to calculate [$OH^-$]. In the regression model of Table 3.6, the main coefficient SF for [$OH^-$] is -97, which indeed confirms the dominant influence of this parameter on the (calculated) [$OH^-$] in the pore solution. It is also interesting to note that the cement C2 with NaOH addition (to 1.25%) generally shows higher [$OH^-$]. The contour lines in Figure 3.15b for pastes made with C2 + NaOH are indeed fully parallel to SF gradations, which suggest that neither the GG nor the cement contents play an influential role on the [$OH^-$]. This is however not the case for pastes made with C1 cement as contour lines in Figure 3.15a are slightly tilted (similarly to Figure 3.10a). This suggests that GG has a slight but significant contribution to the [$OH^-$] of the pore solution for the low alkali C1 cement. The fact that the contribution of GG is modulated by the cement alkali content is also suggested by the numerical analysis, with a coefficient of -16 for the interaction “GG*Alk” (Table 3.6); this indeed suggests that the contribution of GG is less in the case of high alkali pastes in which NaOH was added.

Figure 3.16 shows [$OH^-$] calculated by electro neutrality for pastes containing various contents of GG and MK, as well as the low alkali cement C1 (Figure 3.16a) and high-alkali boosted cement (C2+NaOH) (Figure 3.16b). Similarly to SF-bearing pastes, the alkalinity of the pore solution of MK-bearing pastes is controlled by the MK content in the paste system (i.e. contour lines perpendicular to the MK axis drawn from the MK tip). The latter

observation agrees with the numerical processing results presented in Figure 3.16 since the coefficient of "MK" is -137 (Table 3.7), which suggest that the use of MK greatly reduces [$OH^-$].

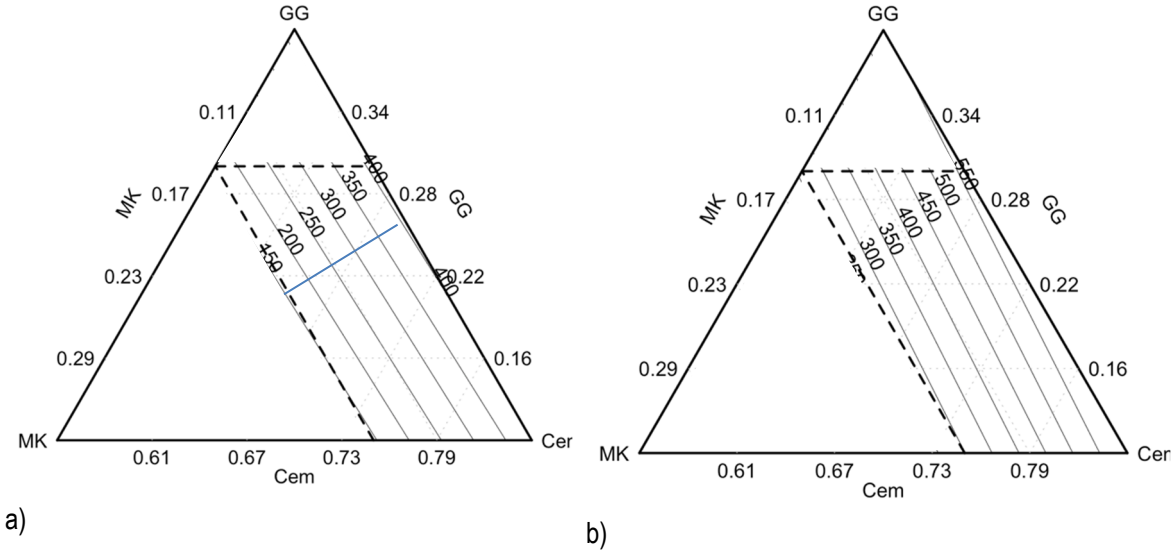


**Figure 3.16 : Surface response for the [$OH^-$] of the pore solution of 182-day old pastes made with various proportions of GG and MK, and a) cement C1 (0.63% $Na_2Oeq$), and b) cement C2 + NaOH (1.25% $Na_2Oeq$). The dashed lines are the border of the experimental region and the axes indicate the proportions of the various components in the mixtures.**

### 3.4.6 Influence of Cement's $Na_2Oeq$ Content (or "Alk) on Pore Solution Composition

Figure 3.17 presents the [$Na^+$] at 182 days for the pore solution of pastes made with different cements, various contents of GG and various contents of SF (a to c) and MK (d to f). Figure 3.18 presents the [$K^+$] at 182 days for the same pastes. A general trend of increasing ionic concentrations in the pore solutions with increasing "cement" alkali content can be seen in both Figure 3.17 and Figure 3.18.

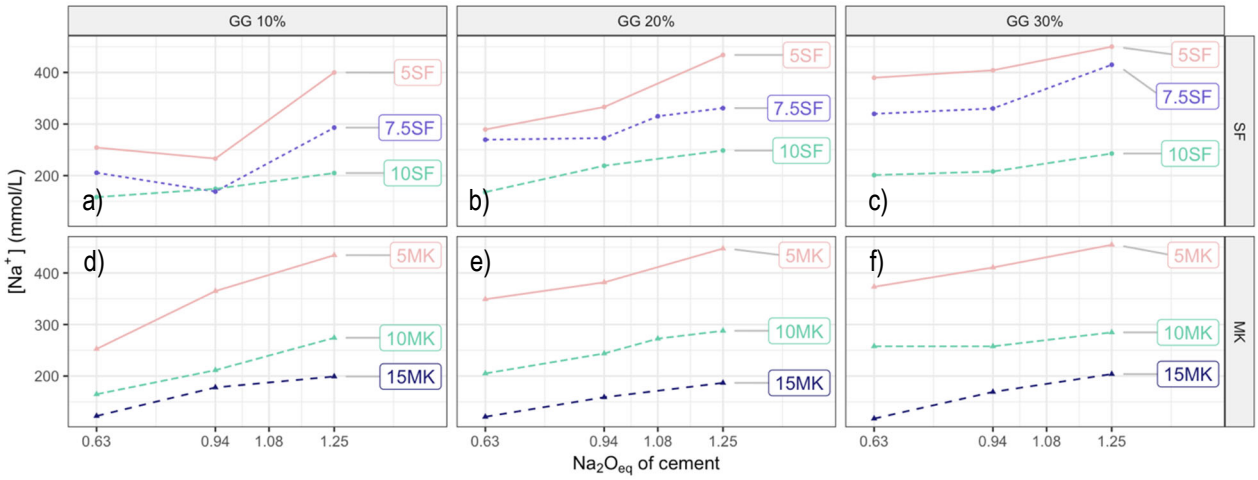


**Figure 3.17 : [$Na^+$] at 182 days for pastes made with different cements, containing various proportions of GG and various proportions of SF (a to c) and of MK (d to f).**

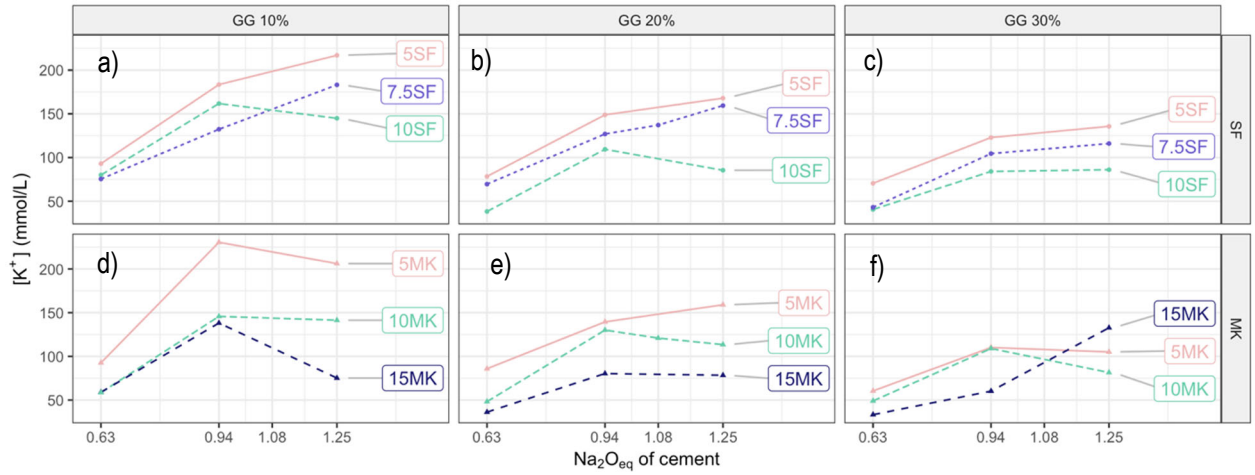


**Figure 3.18 : [$K^+$] at 182 days for pastes made with different cements, containing various proportions of GG and various proportions of SF (a to c) and of MK (d to f). A peculiar behavior was observed with mixture 30GG-15MK-1.25 in all steps of the experimentation and although the mixture was batched twice to discard the risk of an experimental error no further investigations were conducted at this stage in relation to that specific mixture.**

Data from the numerical treatment presented in Table 3.6 and Table 3.7 also corroborate this general trend, with "Alk" coefficients of relatively high magnitude, as well as of positive sign.

In SF-bearing pastes, the contribution of "Alk" with a coefficient of 38 is similar to that of "GG" (36) (Table 3.6), which suggests that an increase of the GG content from 10% to 30% has a similar effect at increasing [$Na^+$] in the pore solution as increasing cement's alkali content from 0.63% to 1.25% $Na_2Oeq$. Interestingly, the contribution of GG in raising [$Na^+$] in the pore solution could not be transposed to [$OH^-$], probably because an increase in GG content also contributes in lowering [$K^+$] (coefficient of -27). Indeed, the impact of GG on [$OH^-$] is only 8, which is 10 times less than that of coefficient "Alk" (79) (Table 3.6). The impact of "Alk" on [$OH^-$] is discussed later in the paper.

In MK-bearing systems, a value of 43 was computed for the "Alk" coefficient for [$Na^+$], which is almost 5 times greater than that computed for "GG" (9) (Table 3.7). This indicates that the effect on [$Na^+$] in the pore solution of increasing the GG content from 10 to 30% is significantly less important in MK-bearing pastes compared to SF-bearing pastes. Also, in MK-bearing systems, increasing the GG content has a much lower effect at increasing the [$Na^+$] in the pore solution than increasing the cement $Na_2O_{eq}$ content of the cementitious mixture. This can be seen from the curves in Figure 3.17 (d to f), where, for a given percentage of MK and a given $Na_2Oeq$ content of cement, somewhat similar [$Na^+$] concentrations are obtained for pastes made with 10%, 20% or 30% GG.

An interesting observation, in Figure 3.18 (a to c), is that for pastes containing low and intermediate values of SF (5 and 7.5%) and GG (10 and 20%), the [$K^+$] in the pore solution increases relatively steadily with increasing $Na_2Oeq$ content of cement (i.e. from 0.63 to 1.25% $Na_2Oeq$); this trend was unexpected, especially for pastes at 1.25% $Na_2Oeq$ because no additional $K_2O$ is provided to the system by increasing the alkali content from 0.94 to 1.25% (1.25% = C2 + NaOH). On the other hand, for pastes containing the largest amounts of those SCMs, i.e. 10%SF or 30%GG, increasing the $Na_2Oeq$ content of cement in the system from 0.94 to 1.25% $Na_2Oeq$ (i.e. *alkali boosting* effect) results in a stabilization or reduction of [$K^+$] in the pore solution. This reduction actually goes beyond that of cement dilution at the highest SCM replacement levels, and it is possibly related to some "activation-like phenomenon" of GG by NaOH, as proposed by Maraghechi (2014), Maraghechi et al. (2014) and Zhang et al. (2017), and/or SF/MK addition in the system causing more potassium ions to be "entrapped" through pozzolanic C-S-H formation (Zheng 2016). This would however need to be confirmed through, for example, comparative microprobe analyses on the "solid phases" of those mixtures.

For MK-bearing pastes, Figure 3.18 (d to f) shows that increasing the $Na_2O_{eq}$ content of cement in the system (i.e. *alkali boosting* effect) from 0.94 to 1.25% $Na_2O$eq almost always results in a reduction of $[K^+]$ in the pore solution, even at lower MK and GG contents. This also suggests some sort of "activation-like phenomenon" of GG and/or MK by the NaOH addition, as mentioned earlier, leading to lower $[K^+]$ in the pore solution. An exception to the above trend is the "outlier" mixture 30GG-15MK-1.25%, for which more investigations would be required.

An example of the "GG*Alk" interaction in lowering $[OH^-]$ in the pore solution is presented in Table **3.14**. The data suggest that for the "boosted" paste (C2 + NaOH) incorporating SF, the impact of increasing GG content from 10 to 30% on the $[OH^-]$ in the pore solution is almost negligible (-5%), while it results in a 33% increase in $[OH^-]$ for C1 pastes and 27% for C2 pastes. A similar observation can be made in MK-bearing pastes for which the coefficient for the "GG*Alk" interaction is -15 (Table 3.7); one can note in Table **3.14** that the contribution of GG to the alkalinity of the pore solution is also modulated by the $Na_2O$eq content of the cement. Those latter observations raise the question about the impact and even the appropriateness of the NaOH addition in the evaluation of the efficiency of high-alkali SCM in preventing ASR. The data in this study show that, in the case of GG, the contribution of GG to the alkalinity of the pore solution is indeed not significant when NaOH is added to the cement in SF-bearing pastes and negative in MK-bearing pastes.

**Table 3.14: $[OH^-]$ at 182 days for pastes made with 5% of SF or MK and various contents of GG and different "cement" alkali contents.**

| | | $[OH^-]$ (mmoles/L) | | | | Increase of $[OH^-]$ caused by increasing "GG" from 10 to 30% | |
|---|---|---|---|---|---|---|---|
| | | 5 %SF | | 5% MK | | 5% SF | 5% MK |
| | GG content → | 10% | 30% | 10% | 30% | | |
| Cement of various $Na_2O_{eq}$ | C1 (0.63%) | 347 | 460 | 345 | 434 | 33% | 26% |
| | C2 (0.94%) | 416 | 527 | 595 | 521 | 27% | -12% |
| | C2+NaOH (1.25) | 617 | 586 | 641 | 560 | -5% | -13% |

Although the magnitude of the effect of the $Na_2O$eq content of cement varies for every paste system analysed in this study, the use of a cement with higher $Na_2O$eq (including the systems with NaOH addition) almost always results in a higher $[OH^-]$ in the pore solution. However, although such a trend can be seen at each GG content, it does not necessarily result in an overall increasing trend with increasing GG contents from 10 to 30%, as illustrated in Figure 3.19. This suggests that the total alkali content of a cementitious mixture (dry composition)

does not necessarily provide a good indication of the predicted [$OH^-$] of a pore solution in the context of ternary mixtures incorporating the high-alkali GG and SF/MK.

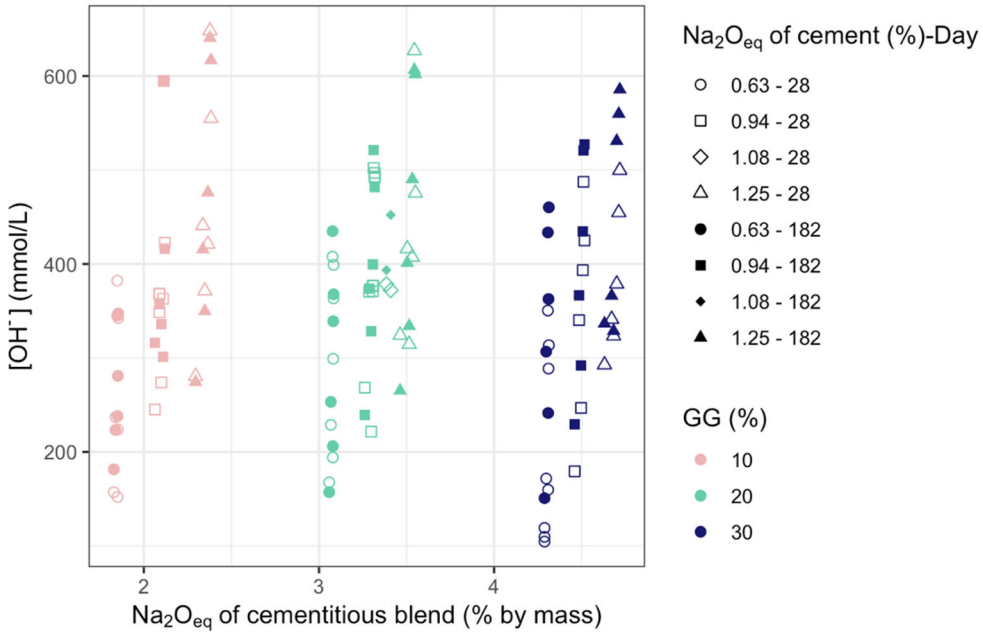


**Figure 3.19: [$OH^-$] of the pore solution and its relation to the $Na_2O_{eq}$ content of the cementitious mixture at 28 and 182 days for all mixtures selected in this study (SF 5% to 10%; MK 5% to 15%; GG 10 to 30%).**

As discussed in section 2.4.1 and illustrated in Figure 3.7 and 2.8, the composition of the pore solution of the ternary systems analysed in this study varies significantly between 28 and 182 days. In the case of [$Na^+$], this is highlighted by "Day" coefficients of 30 (Table 3.6) and 25 (Table 3.7) for SF- and MK-bearing pastes, respectively. The coefficient for the interaction "GG*Day" is 12 and 9 for SF- and MK-bearing pastes, respectively, which suggest that GG released a small portion of its sodium between 28 and 182 days. The [$K^+$] in the pore solution generally reduces over time, as illustrated in Figure 3.8, and confirmed by the negatives "Day" coefficients of -6 (Table 3.6) and -13 (Table 3.7) for SF- and MK bearing pastes, respectively.

Regarding the effect of time on [$OH^-$], "Day" coefficients of 23 (Table 3.6) and 10 (Table 3.7) obtained for SF- and MK-bearing systems, respectively, indicate that the alkalinity generally increases over time, and this trend is more pronounced in SF-bearing pastes (Figure 3.9a to c) than in MK-bearing pastes (Figure 3.9d to f). Also, a positive value for the interaction "GG*Day" of 14 (Table 3.6) and 10 (Table 3.7) for SF- and MK-bearing systems, respectively, suggests that GG modestly contributed in raising [$OH^-$] between 28 and 182 days.

## 3.5 Conclusion

Previous research has shown that SCMs such as high-alkali fly ash and high-alkali ground glass have the potential of reducing expansion in concrete incorporating reactive aggregates, however generally not to an acceptable level when used in binary systems at 20 to 30% cement replacement levels.

This study was aimed at evaluating the potential effect, on the pore solution composition of paste specimens made with cements of different alkali contents, and incorporating different proportions of a high-alkali ground glass (10 to 30%) in combination with silica fume (5 to 10%) or metakaolin (5 to 15%). The paste compositions were selected using a *factorial* $3^3$ approach. The pore solutions extracted after 28 and 182 days of curing at 38°C, were analysed for Na and K content and data were processed using a *Response Surface Methodology* (RSM) approach. The following conclusions can be drawn from this research:

1. The high sodium content of GG is not reflected in the composition of the pore solution, since $[Na^+]$ is only weakly correlated to the GG content of ternary pastes incorporating SF/MK, especially for cements with higher alkali content;
2. $[K^+]$ in the pore solution is reduced by increasing the SF, MK and GG contents in the paste systems; however, by mass, FS and MK are more efficient than GG for that matter;
3. Estimated $[OH^-]$ by electroneutrality of the pore solution, is strongly and inversely related to the SF and MK contents in the ternary paste systems studied;
4. Estimated $[OH^-]$ by electroneutrality of the pore solution, is negligibly affected by GG and there is no evidence that GG would result in a pore solution of a higher pH that would promote expansion due to ASR;
5. The reduction of $[K^+]$ in the pore solution of the ternary mixtures was found to go beyond that of cement dilution, especially in systems using a high-alkali cement with NaOH addition and high SCM contents;
6. NaOH addition (i.e. high-alkali C2 cement + NaOH) increases the $[Na^+]$ in the pore solution for most mixes but reduces the contribution of GG to the $[Na^+]$ in the pore solution and increases the beneficial contribution of SF/MK in reducing the $[Na^+]$ in the pore solution;
7. The quantitative result of the experimental program using factorial and RSM approaches allowed to evaluate the main trends of this multivariate experiment, but also to identify more subtle interactions between various parameters in the systems that would not be so clearly pointed out with a more basic data treatment with tables and plots presenting experimental data; $[Na^+]$ in the pore solution of the GG-bearing ternary paste systems is strongly and inversely related to their SF and MK content.

## 3.6 Acknowledgement

The authors would like to thank the Centre de Recherche des Infrastructure en Béton (CRIB) for the space, equipment and technical support provided. Also, the authors are grateful to the Chaire de recherche de la SAQ and the Centre de Recherche en Sciences Naturelles et en Génie (CRSNG) for their financial support.

## 3.7 References


ASTM (2014). Standard guide for reducing the risk of deleterious alkali–aggregate reaction in concrete (ASTM C 1778-14). ASTM International, West Conshohocken, PA, USA.

Carsana, M., M. Frassoni and L. Bertolini (2014). "Comparison of ground waste glass with other supplementary cementitious materials." Cement and Concrete Composites 45 (Supplement C): 39-45.

CSA (2014). Standard Practice for laboratory testing to demonstrate the effectiveness of supplementary cementing materials and lithium-based admixtures to prevent alkali–silica reaction in concrete (CSA A23.2-28A). In CSA A23.2-14 – Test methods and standard practices for concrete. CSA Group, Mississauga, Ontario, Canada, pp. 452–457.

Cementitious materials compendium A 3000-18. CSA Group, Mississauga, Ontario, Canada, 257p..

Duchesne, J. and M.-A. Bérubé (2001). "Long-term effectiveness of supplementary cementing materials against alkali–silica reaction." Cement and Concrete Research 31(7): 1057-1063.

Duchesne, J. and M. A. Bérubé (1995). "Effect of supplementary cementing materials on the composition of cement hydration products." Advanced Cement Based Materials 2(2): 43-52.

Fily-Paré, I., B. Fournier, J. Duchesne and A. Tagnit-Hamou (2017). Effect of glass powder on the pore solution of cement pastes. 10th ACI/RILEM International conference on cementitious materials and alternative binders for sustainable concrete, Montréal, Canada.

Fournier, B., Nkinamubanzi, P.C., Chevrier, R., Ferro, A. 2008: Evaluation of the effectiveness of high-calcium fly ashes in reducing expansion due to alkali-silica reaction in concrete. Electric Power Research Institute (EPRI), Palo Alto (USA), 1014271.

Idir, R., M. Cyr and A. Tagnit-Hamou (2010). "Use of fine glass as ASR inhibitor in glass aggregate mortars." Construction and Building Materials 24(7): 1309-1312.

Kamali, M. and A. Ghahremaninezhad (2016). "An investigation into the hydration and microstructure of cement pastes modified with glass powders." Construction and Building Materials 112: 915-924.

Lawson, J. (2014). Design and Analysis of Experiments with R, Taylor & Francis.

Lawson, J. and C. Willden (2016). "Mixture experiment in R using mixexp." Journal of Statistical Software 72.

Lenth, R. V. (2009). "Response-Surface Methods in R, Using rsm." Journal of Statistical software 32(7): 1-17.

Liu, S., S. Wang, W. Tang, N. Hu and J. Wei (2015). "Inhibitory effect of waste glass powder on ASR expansion induced by waste glass aggregate." Materials 8(10): 6849-6862.

Maraghechi, H. (2014). "Development and assessment of alkali activated recycled glass-based concretes for civil infrastructure.", Ph. D. Thesis, Pennsylvania State University.

Maraghechi, H., M. Maraghechi, F. Rajabipour and C. G. Pantano (2014). "Pozzolanic reactivity of recycled glass powder at elevated temperatures: Reaction stoichiometry, reaction products and effect of alkali activation." Cement and Concrete Composites 53(0): 105-114.

Mejdi, M., W. Wilson, M. Saillio, T. Chaussadent, L. Divet and A. Tagnit-Hamou (2019). "Investigating the pozzolanic reaction of post-consumption glass powder and the role of portlandite in the formation of sodium-rich C-S-H." Cement and Concrete Research 123.

Montgomery, D. C. (2012). Design and Analysis of Experiments, 8th Edition, John Wiley & Sons, Incorporated.

Montgomery, D. C. and G. C. Runger (2010). Applied Statistics and Probability for Engineers, 5th edition.

Myers, R. H., D. C. Montgomery and C. M. Anderson-Cook (2011). Response Surface Methodology: Process and Product Optimization Using Designed Experiments, Wiley.

Omran, A., D. Harbec, A. Tagnit-Hamou and R. Gagne (2017). "Production of roller-compacted concrete using glass powder: Field study." Construction and Building Materials 133: 450-458.

Omran, A. and A. Tagnit-Hamou (2016). "Performance of glass-powder concrete in field applications." Construction and Building Materials 109: 84-95.

Omran, A. F., E. D.-Morin, D. Harbec and A. Tagnit-Hamou (2017). "Long-term performance of glass-powder concrete in large-scale field applications." Construction and Building Materials 135: 43-58.

Rajabipour, F., H. Maraghechi and G. Fischer (2010). "Investigating the alkali-silica reaction of recycled glass aggregates in concrete materials." Journal of Materials in Civil Engineering 22(12): 1201-1208.

Shayan, A. and A. Xu (2006). "Performance of glass powder as a pozzolanic material in concrete: A field trial on concrete slabs." Cement and Concrete Research 36(3): 457-468.

Shehata, M. H. (2001). The effects of fly ash and silica fume on alkali-silica reaction in concrete. Ph.D Thesis, University of Toronto.

Shehata, M. H. and M. D. A. Thomas (2000). "The effect of fly ash composition on the expansion of concrete due to alkali–silica reaction." Cement and Concrete Research 30(7): 1063-1072.

Shehata, M. H. and M. D. A. Thomas (2002). "Use of ternary blends containing silica fume and fly ash to suppress expansion due to alkali–silica reaction in concrete." Cement and Concrete Research 32(3): 341-349.

Shehata, M. H., M. D. A. Thomas and R. F. Bleszynski (1999). "The effects of fly ash composition on the chemistry of pore solution in hydrated cement pastes." Cement and Concrete Research 29(12): 1915-1920.

Shevchenko, V. (2012). "ASR effect in glasses used as additives to Portland cement." Glass Physics and Chemistry 38(5): 466-471.

Team, R. C. (2013). R: A Language and Environment for Statistical Computing, R Foundation for Statistical Computing.

Thomas, M., B. Fournier, K. Folliard, J. Ideker and M. Shehata (2006). "Test methods for evaluating preventive measures for controlling expansion due to alkali–silica reaction in concrete." Cement and Concrete Research 36(10): 1842-1856.

Vollpracht, A., B. Lothenbach, R. Snellings and J. Haufe (2015). "The pore solution of blended cements: a review." Materials and Structures 49(8): 3341-3367.

Zhang, S., A. Keulen, K. Arbi and G. Ye (2017). "Waste glass as partial mineral precursor in alkali-activated slag/fly ash system." Cement and Concrete Research 102: 29-40.

Zheng, K. (2016). "Pozzolanic reaction of glass powder and its role in controlling alkali–silica reaction." Cement and Concrete Composites 67: 30-38.

# Annex A - Replicates

**Table 3.15 : [$Na^+$] and [$K^+$] of pore solution of replicated pastes samples extracted separately.**

| SF | | | | | | | MK | | | | | | |
|---|---|---|---|---|---|---|---|---|---|---|---|---|---|
| GG | SF | Alk | Age | Paste ID | [$Na^+$] (mmol/l) | [$K^+$] | GG | MK | Alk | Age | Paste ID | [$Na^+$] (mmol/l) | [$K^+$] |
| 10 | 7.5 | 1.25 | 28 | I | 254 | 168 | 10 | 10 | 0.94 | 28 | I | 182 | 186 |
| 10 | 7.5 | 1.25 | 28 | II | 226 | - | 10 | 10 | 0.94 | 28 | II | 177 | 171 |
| 20 | 5 | 0.63 | 28 | I | 285 | 78 | 10 | 10 | 0.94 | 28 | III | 191 | 177 |
| 20 | 5 | 0.63 | 28 | II | 302 | 96 | 10 | 15 | 0.94 | 28 | I | 103 | 143 |
| 20 | 5 | 0.94 | 28 | I | 313 | 180 | 10 | 15 | 0.94 | 28 | II | 108 | - |
| 20 | 5 | 0.94 | 28 | II | 311 | 185 | 10 | 15 | 0.94 | 28 | III | 98 | - |
| 20 | 5 | 0.94 | 28 | III | 310 | 182 | 20 | 5 | 0.63 | 28 | I | 315 | 92 |
| 20 | 5 | 1.25 | 28 | I | 306 | 169 | 20 | 5 | 0.63 | 28 | II | - | 92 |
| 20 | 5 | 1.25 | 28 | II | 315 | - | 20 | 5 | 0.63 | 28 | III | - | 104 |
| 20 | 7.5 | 0.94 | 28 | I | 208 | 163 | 30 | 5 | 1.25 | 28 | I | 333 | 122 |
| 20 | 7.5 | 0.94 | 28 | II | 212 | 165 | 30 | 5 | 1.25 | 28 | II | 324 | - |
| 20 | 7.5 | 0.94 | 28 | III | 205 | 172 | 30 | 5 | 1.25 | 28 | III | 324 | - |
| 20 | 10 | 1.25 | 28 | I | 209 | 105 | 30 | 10 | 0.63 | 28 | I | 137 | 35 |
| 20 | 10 | 1.25 | 28 | II | 207 | - | 30 | 10 | 0.63 | 28 | II | - | 38 |
| 20 | 10 | 1.25 | 28 | III | 200 | - | 30 | 10 | 0.63 | 28 | III | - | 38 |
| 30 | 7.5 | 0.63 | 28 | I | 231 | 58 | 30 | 10 | 0.94 | 28 | I | 222 | 118 |
| 30 | 7.5 | 0.63 | 28 | II | 238 | - | 30 | 10 | 0.94 | 28 | II | - | 121 |
| | | | | | | | 30 | 10 | 0.94 | 28 | III | - | 113 |
| | | | | | | | 30 | 15 | 0.63 | 28 | I | 69 | 40 |
| | | | | | | | 30 | 15 | 0.63 | 28 | II | 82 | 37 |
| | | | | | | | 30 | 15 | 0.63 | 28 | III | 64 | 41 |
| | | | | | | | 30 | 15 | 0.94 | 28 | I | 96 | 84 |
| | | | | | | | 30 | 15 | 0.94 | 28 | II | 89 | - |
| | | | | | | | 30 | 15 | 0.94 | 28 | III | 90 | - |

# Annex B – Regression model validation plot

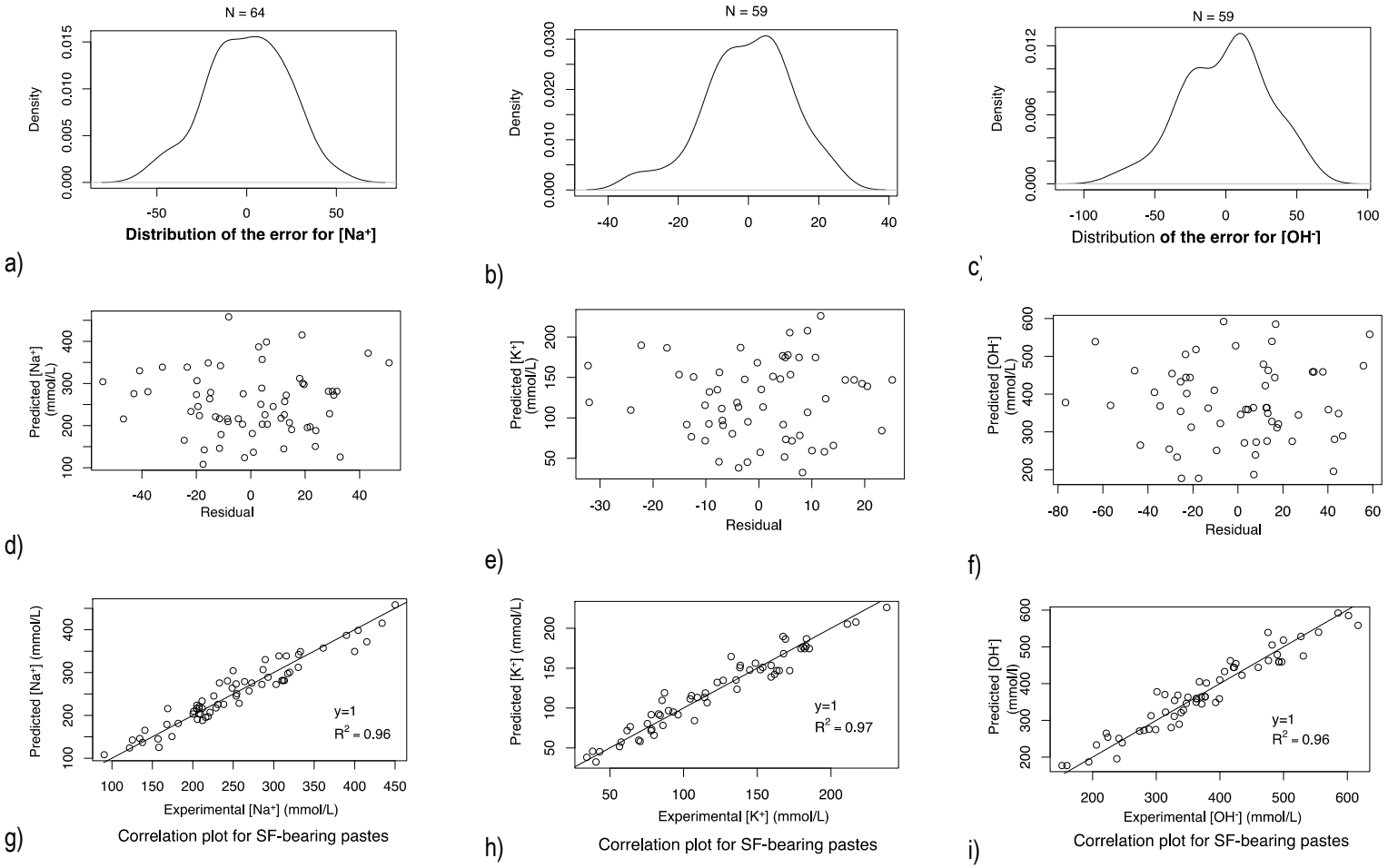


**Figure 3.20: Regression model validation plots for the pore solution composition of SF-bearing pastes for [$Na^+$] (a, d and g); [$K^+$] (b, e and h); and [$OH^-$] (c, f and i).**

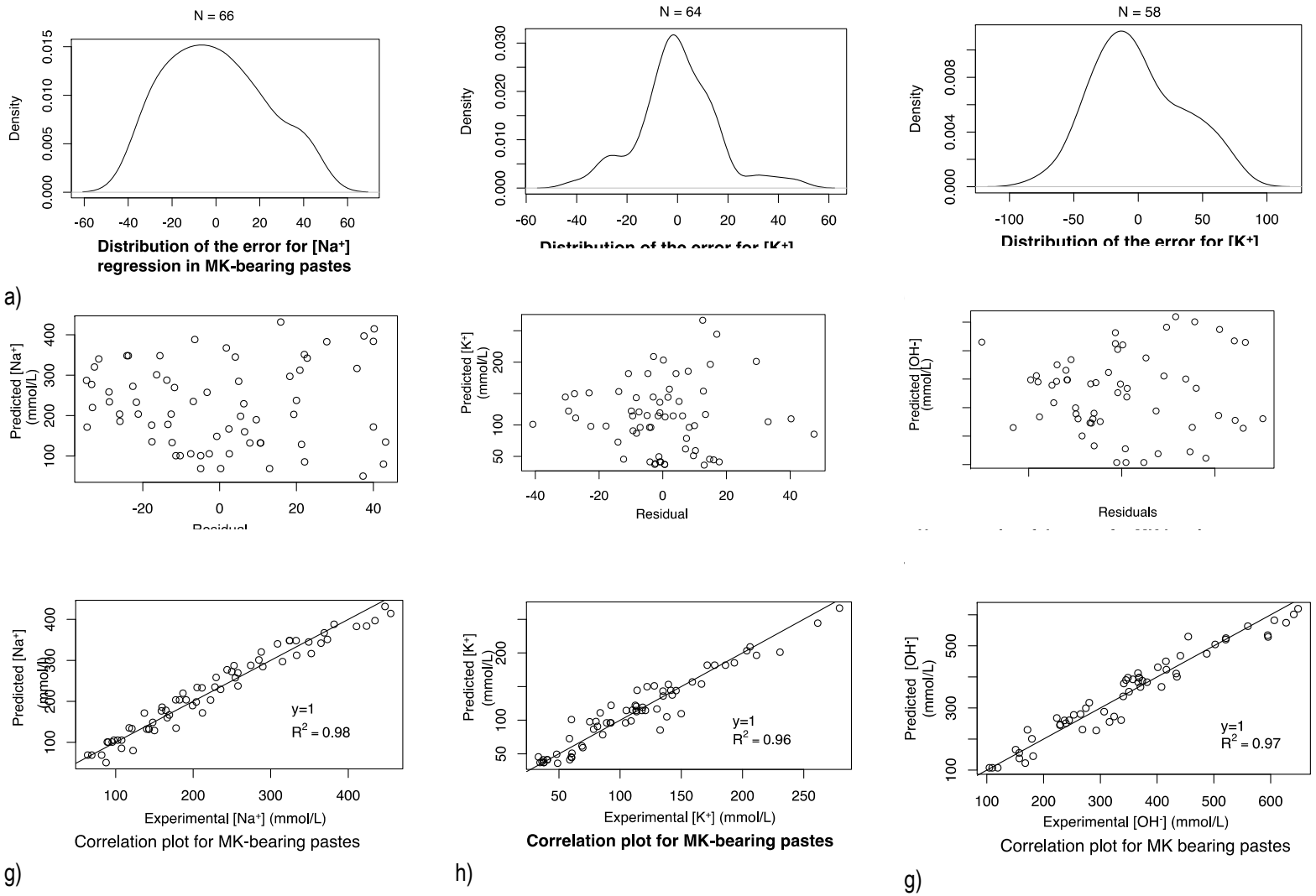


**Figure 3.21: Regression model validation plots for the pore solution composition of MK-bearing pastes for [$Na^+$] (a, d and g); [$K^+$] (b, e and h) and [$OH^-$] (c, f and i).**

# Annex C -Data

**Table 3.16 : Experimental results for [$Na^+$] and corresponding fitted values of the proposed regression model with confidence interval of 95% at 28 and 182 days for mixtures of various levels of GG, SF and $Na_2O_{eq}$ contents of cement.**

| GG | SF | Cement | | 28-day data (Mmol/L) | | | | | 182-day data (Mmol/L) | | | | |
|---|---|---|---|---|---|---|---|---|---|---|---|---|---|
| | | Type | Alk | Experimental data | | Data from the Model | | | Experimental data | | Data from the Model | | |
| (%) | (%) | | $Na_2O_{eq}$ | [$Na^+$] | SD | [$Na^+$] | Min | Max | [$Na^+$] | SD | [$Na^+$] | Min | Max |
| 10 | 5 | C1 | 0.63 | 229 | 7 * | 217 | 191 | 244 | 254 | 7 * | 251 | 223 | 278 |
| 10 | 5 | C2 | 0.94 | 211 | 6 * | 233 | 211 | 256 | 233 | 7 * | 276 | 252 | 300 |
| 10 | 5 | C2 | 1.25 | 317 | 9 * | 298 | 272 | 323 | 400 | 12 * | 349 | 322 | 376 |
| 10 | 7.5 | C1 | 0.63 | 141 | 4 * | 165 | 143 | 187 | 206 | 6 * | 191 | 168 | 213 |
| 10 | 7.5 | C2 | 0.94 | 182 | 5 * | 181 | 164 | 199 | 169 | 5 * | 216 | 198 | 234 |
| 10 | 7.5 | C2 | 1.25 | 240 | 20 | 245 | 225 | 265 | 293 | 9 * | 289 | 267 | 311 |
| 10 | 10 | C1 | 0.63 | 91 | 3 * | 108 | 82 | 134 | 158 | 5 * | 125 | 99 | 152 |
| 10 | 10 | C2 | 0.94 | 122 | 4 * | 124 | 102 | 146 | 174 | 5 * | 151 | 127 | 174 |
| 10 | 10 | C2 | 1.25 | 212 | 6 * | 188 | 165 | 212 | 205 | 6 * | 224 | 197 | 250 |
| 20 | 5 | C1 | 0.63 | 294 | 12 | 272 | 254 | 291 | 289 | 9 * | 330 | 309 | 352 |
| 20 | 5 | C2 | 0.94 | 312 | 2 | 282 | 266 | 297 | 333 | 10 * | 349 | 330 | 368 |
| 20 | 5 | C2 | 1.25 | 311 | 6 | 339 | 321 | 357 | 434 | 13 * | 415 | 394 | 437 |
| 20 | 7.5 | C1 | 0.63 | 221 | 7 * | 207 | 191 | 223 | 270 | 8 * | 257 | 239 | 275 |
| 20 | 7.5 | C2 | 0.94 | 208 | 3 | 216 | 203 | 230 | 273 | 8 * | 276 | 261 | 290 |
| 20 | 7.5 | C2 | 1.25 | 254 | 7 * | 274 | 259 | 288 | 331 | 10 * | 342 | 324 | 360 |
| 20 | 10 | C1 | 0.63 | 138 | 4 * | 137 | 117 | 157 | 168 | 5 * | 179 | 157 | 200 |
| 20 | 10 | C2 | 0.94 | 135 | 4 * | 146 | 128 | 164 | 219 | 6 * | 197 | 178 | 216 |
| 20 | 10 | C2 | 1.25 | 206 | 5 | 203 | 185 | 221 | 249 | 7 * | 264 | 242 | 285 |
| 30 | 5 | C1 | 0.63 | 250 | 7 * | 304 | 280 | 328 | 390 | 11 * | 387 | 361 | 413 |
| 30 | 5 | C2 | 0.94 | 287 | 8 * | 307 | 285 | 328 | 404 | 12 * | 398 | 375 | 422 |
| 30 | 5 | C2 | 1.25 | 361 | 11 * | 357 | 331 | 383 | 450 | 13 * | 458 | 431 | 485 |
| 30 | 7.5 | C1 | 0.63 | 235 | 5 | 226 | 206 | 246 | 320 | 9 * | 301 | 279 | 323 |
| 30 | 7.5 | C2 | 0.94 | 257 | 8 * | 228 | 211 | 246 | 330 | 10 * | 312 | 294 | 330 |
| 30 | 7.5 | C2 | 1.25 | 264 | 8 * | 279 | 257 | 301 | 415 | 12 * | 372 | 349 | 394 |
| 30 | 10 | C1 | 0.63 | 125 | 4 * | 142 | 117 | 168 | 201 | 6 * | 209 | 182 | 236 |
| 30 | 10 | C2 | 0.94 | 157 | 5 * | 145 | 122 | 168 | 208 | 6 * | 221 | 197 | 245 |
| 30 | 10 | C2 | 1.25 | 216 | 6 * | 195 | 170 | 221 | 243 | 7 * | 281 | 253 | 308 |

* Based on the average coefficient of variation of the replicates, standard deviation of single measurement is estimated with a coefficient of variation of 3%.

**Table 3.17 : Experimental results for $[K^+]$ and corresponding fitted values of the proposed regression model with confidence interval of 95% at 28 and 182 days for mixtures of various levels of GG, SF and $Na_2Oeq$ contents of cement.**

| GG | SF | Cement | | 28-day data (Mmol/L) | | | | | 182-day data (Mmol/L) | | | | |
|---|---|---|---|---|---|---|---|---|---|---|---|---|---|
| | | Type | Alk | Experimental data | | Data from the Model | | | Experimental data | | Data from the Model | | |
| (%) | (%) | | $Na_2O_{eq}$ | $[K^+]$ | SD | $[K^+]$ | Min | Max | $[K^+]$ | SD | $[K^+]$ | Min | Max |
| 10 | 5 | C1 | 0.63 | 28 | 5 * | 113 | 100 | 127 | 93 | 4 * | 95 | 81 | 109 |
| 10 | 5 | C2 | 0.94 | 28 | 10 * | 205 | 194 | 216 | 183 | 9 * | 187 | 175 | 198 |
| 10 | 5 | C2 | 1.25 | 28 | 11 * | 226 | 212 | 240 | 217 | 10 * | 208 | 194 | 222 |
| 10 | 7.5 | C1 | 0.63 | 28 | 4 * | 93 | 82 | 103 | 75 | 4 * | 80 | 70 | 91 |
| 10 | 7.5 | C2 | 0.94 | 28 | 9 * | 177 | 168 | 185 | 132 | 6 * | 165 | 156 | 174 |
| 10 | 7.5 | C2 | 1.25 | 28 | 8 * | 190 | 179 | 200 | 183 | 9 * | 178 | 167 | 188 |
| 10 | 10 | C1 | 0.63 | 28 | 3 * | 72 | 58 | 85 | 80 | 4 * | 66 | 52 | 79 |
| 10 | 10 | C2 | 0.94 | 28 | 7 * | 148 | 138 | 159 | 162 | 8 * | 142 | 132 | 153 |
| 10 | 10 | C2 | 1.25 | 28 | 7 * | 153 | 140 | 167 | 145 | 7 * | 148 | 134 | 161 |
| 20 | 5 | C1 | 0.63 | 28 | 13 | 92 | 81 | 102 | 78 | 4 * | 73 | 61 | 85 |
| 20 | 5 | C2 | 0.94 | 28 | 3 | 175 | 166 | 184 | 149 | 7 * | 156 | 146 | 167 |
| 20 | 5 | C2 | 1.25 | 28 | 8 * | 187 | 175 | 198 | 168 | 8 * | 168 | 156 | 180 |
| 20 | 7.5 | C1 | 0.63 | 28 | 4 * | 72 | 63 | 80 | 70 | 3 * | 60 | 51 | 68 |
| 20 | 7.5 | C2 | 0.94 | 28 | 5 | 147 | 139 | 154 | 127 | 6 * | 135 | 126 | 143 |
| 20 | 7.5 | C2 | 1.25 | 28 | 7 * | 151 | 142 | 160 | 159 | 7 * | 139 | 130 | 148 |
| 20 | 10 | C1 | 0.63 | 28 | 3 * | 52 | 39 | 64 | 38 | 2 * | 46 | 33 | 58 |
| 20 | 10 | C2 | 0.94 | 28 | 4 * | 119 | 109 | 129 | 109 | 5 * | 113 | 103 | 124 |
| 20 | 10 | C2 | 1.25 | 28 | 5 * | 115 | 103 | 128 | 85 | 4 * | 110 | 97 | 122 |
| 30 | 5 | C1 | 0.63 | 28 | 3 * | 77 | 64 | 89 | 70 | 3 * | 58 | 45 | 71 |
| 30 | 5 | C2 | 0.94 | 28 | 6 * | 151 | 141 | 160 | 123 | 6 * | 132 | 121 | 143 |
| 30 | 5 | C2 | 1.25 | 28 | 6 * | 154 | 140 | 167 | 136 | 6 * | 135 | 122 | 148 |
| 30 | 7.5 | C1 | 0.63 | 28 | 3 * | 57 | 47 | 68 | 43 | 2 * | 45 | 35 | 56 |
| 30 | 7.5 | C2 | 0.94 | 28 | 6 * | 124 | 115 | 132 | 104 | 5 * | 111 | 103 | 120 |
| 30 | 7.5 | C2 | 1.25 | 28 | 5 * | 119 | 108 | 130 | 116 | 5 * | 107 | 96 | 117 |
| 30 | 10 | C1 | 0.63 | 28 | 2 * | 38 | 24 | 52 | 41 | 2 * | 32 | 18 | 46 |
| 30 | 10 | C2 | 0.94 | 28 | 4 * | 97 | 85 | 108 | 84 | 4 * | 91 | 79 | 102 |
| 30 | 10 | C2 | 1.25 | 28 | 5 * | 84 | 70 | 98 | 86 | 4 * | 78 | 64 | 92 |

* Standard deviation of single measurement is estimated based on the average coefficient of variation of the replicates (5%).

**Table 3.18 : [$OH^-$], estimated by electroneutrality and corresponding fitted values of the proposed regression model with confidence interval of 95% at 28 and 182 days for mixtures of various levels of GG, SF and $Na_2O_{eq}$ contents of cement.**

| GG | SF | Cement | | 28-day data (Mmol/L) | | | | | 182-day data (Mmol/L) | | | | |
|---|---|---|---|---|---|---|---|---|---|---|---|---|---|
| | | Type | Alk | Experimental data | | Data from the Model | | | Experimental data | | Data from the Model | | |
| (%) | (%) | | $Na_2O_{eq}$ | [$OH^-$] | SD | [$OH^-$] | Min | Max | [$OH^-$] | SD | [$OH^-$] | Min | Max |
| 10 | 5 | C1 | 0.63 | 343 | 9 * | 328 | 293 | 363 | 347 | 9 * | 346 | 311 | 381 |
| 10 | 5 | C2 | 0.94 | 423 | 11 * | 444 | 414 | 473 | 416 | 10 * | 462 | 432 | 492 |
| 10 | 5 | C2 | 1.25 | 555 | 14 * | 540 | 504 | 576 | 617 | 15 * | 558 | 523 | 594 |
| 10 | 7.5 | C1 | 0.63 | 224 | 6 * | 254 | 226 | 283 | 281 | 7 * | 273 | 245 | 301 |
| 10 | 7.5 | C2 | 0.94 | 363 | 9 * | 359 | 335 | 384 | 301 | 8 * | 378 | 353 | 403 |
| 10 | 7.5 | C2 | 1.25 | 421 | 10 * | 444 | 416 | 473 | 476 | 12 * | 463 | 435 | 491 |
| 10 | 10 | C1 | 0.63 | 152 | 4 * | 177 | 142 | 212 | 238 | 6 * | 196 | 161 | 230 |
| 10 | 10 | C2 | 0.94 | 274 | 7 * | 271 | 242 | 300 | 336 | 8 * | 289 | 260 | 318 |
| 10 | 10 | C2 | 1.25 | 371 | 9 * | 345 | 310 | 380 | 350 | 9 * | 363 | 328 | 398 |
| 20 | 5 | C1 | 0.63 | 381 | 25 | 359 | 334 | 384 | 368 | 9 * | 405 | 378 | 432 |
| 20 | 5 | C2 | 0.94 | 494 | 2 | 459 | 439 | 479 | 482 | 12 * | 505 | 482 | 528 |
| 20 | 5 | C2 | 1.25 | 476 | 12 * | 539 | 512 | 566 | 602 | 15 * | 585 | 557 | 613 |
| 20 | 7.5 | C1 | 0.63 | 299 | 7 * | 275 | 255 | 295 | 339 | 8 * | 321 | 300 | 342 |
| 20 | 7.5 | C2 | 0.94 | 375 | 3 | 364 | 346 | 382 | 400 | 10 * | 410 | 390 | 430 |
| 20 | 7.5 | C2 | 1.25 | 407 | 10 * | 433 | 412 | 454 | 490 | 12 * | 479 | 457 | 500 |
| 20 | 10 | C1 | 0.63 | 194 | 5 * | 187 | 159 | 215 | 206 | 5 * | 233 | 205 | 261 |
| 20 | 10 | C2 | 0.94 | 222 | 6 * | 265 | 243 | 287 | 328 | 8 * | 311 | 287 | 335 |
| 20 | 10 | C2 | 1.25 | 315 | 8 * | 323 | 295 | 350 | 334 | 8 * | 369 | 340 | 397 |
| 30 | 5 | C1 | 0.63 | 314 | 8 * | 370 | 336 | 483 | 460 | 11 * | 444 | 409 | 478 |
| 30 | 5 | C2 | 0.94 | 425 | 11 * | 454 | 426 | 553 | 527 | 13 * | 528 | 499 | 557 |
| 30 | 5 | C2 | 1.25 | 500 | 12 * | 518 | 483 | 304 | 586 | 15 * | 592 | 557 | 627 |
| 30 | 7.5 | C1 | 0.63 | 289 | 7 * | 276 | 248 | 373 | 363 | 9 * | 349 | 321 | 377 |
| 30 | 7.5 | C2 | 0.94 | 393 | 10 * | 349 | 325 | 430 | 435 | 11 * | 422 | 398 | 447 |
| 30 | 7.5 | C2 | 1.25 | 379 | 9 * | 401 | 373 | 213 | 531 | 13 * | 475 | 447 | 503 |
| 30 | 10 | C1 | 0.63 | 160 | 4 * | 177 | 141 | 269 | 241 | 6 * | 251 | 216 | 286 |
| 30 | 10 | C2 | 0.94 | 247 | 6 * | 239 | 209 | 316 | 292 | 7 * | 313 | 283 | 343 |
| 30 | 10 | C2 | 1.25 | 324 | 8 * | 281 | 245 | 381 | 329 | 8 * | 354 | 319 | 390 |

* Standard deviation of single measurement is estimated based on the average coefficient of variation of the replicates (2%).

**Table 3.19 : Experimental results for [$Na^+$] and corresponding fitted values of the proposed regression model with confidence interval of 95% at 28 and 182 days for mixtures of various levels of GG, MK and $Na_2O$eq contents of cement.**

| GG | MK | Cement | | 28-day data (Mmol/L) | | | | | 182-day data (Mmol/L) | | | | |
|---|---|---|---|---|---|---|---|---|---|---|---|---|---|
| | | Type | Alk | Experimental data | | Data from the Model | | | Experimental data | | Data from the Model | | |
| (%) | (%) | | $Na_2O_{eq}$ | [$Na^+$] | SD | [$Na^+$] | Min | Max | [$Na^+$] | SD | [$Na^+$] | Min | Max |
| 10 | 5 | C1 | 0.63 | 254 | 9 * | 258 | 235 | 281 | 253 | 9 * | 287 | 264 | 311 |
| 10 | 5 | C2 | 0.94 | 333 | 11 * | 312 | 293 | 332 | 365 | 12 * | 342 | 322 | 362 |
| 10 | 5 | C2 | 1.25 | 369 | 12 * | 367 | 344 | 390 | 434 | 15 * | 397 | 374 | 420 |
| 10 | 10 | C1 | 0.63 | 148 | 5 * | 149 | 130 | 167 | 165 | 6 * | 178 | 158 | 199 |
| 10 | 10 | C2 | 0.94 | 184 | 7 | 203 | 190 | 217 | 211 | 7 * | 233 | 217 | 249 |
| 10 | 10 | C2 | 1.25 | 230 | 8 * | 258 | 240 | 277 | 274 | 9 * | 288 | 268 | 308 |
| 10 | 15 | C1 | 0.63 | 88 | 3 * | 50 | 31 | 70 | 123 | 4 * | 80 | 58 | 102 |
| 10 | 15 | C2 | 0.94 | 103 | 5 | 105 | 90 | 120 | 178 | 6 * | 135 | 117 | 153 |
| 10 | 15 | C2 | 1.25 | 167 | 6 * | 160 | 140 | 180 | 199 | 7 * | 190 | 168 | 212 |
| 20 | 5 | C1 | 0.63 | 315 | 11 * | 297 | 280 | 314 | 349 | 12 * | 345 | 328 | 362 |
| 20 | 5 | C2 | 0.94 | 309 | 10 * | 340 | 325 | 356 | 382 | 13 * | 388 | 373 | 403 |
| 20 | 5 | C2 | 1.25 | 424 | 14 * | 384 | 367 | 401 | 447 | 15 * | 431 | 415 | 448 |
| 20 | 10 | C1 | 0.63 | 160 | 5 * | 186 | 172 | 200 | 205 | 7 * | 234 | 220 | 248 |
| 20 | 10 | C2 | 0.94 | 235 | 8 * | 229 | 218 | 241 | 244 | 8 * | 277 | 265 | 289 |
| 20 | 10 | C2 | 1.25 | 250 | 8 * | 272 | 259 | 286 | 288 | 10 * | 320 | 306 | 334 |
| 20 | 15 | C1 | 0.63 | 108 | 4 * | 85 | 69 | 102 | 121 | 4 * | 133 | 116 | 150 |
| 20 | 15 | C2 | 0.94 | 150 | 5 * | 129 | 114 | 144 | 159 | 5 * | 177 | 161 | 192 |
| 20 | 15 | C2 | 1.25 | 212 | 7 * | 172 | 155 | 189 | 187 | 6 * | 220 | 203 | 237 |
| 30 | 5 | C1 | 0.63 | 290 | 10 * | 285 | 264 | 306 | 373 | 13 * | 351 | 330 | 372 |
| 30 | 5 | C2 | 0.94 | 352 | 12 * | 317 | 300 | 333 | 411 | 14 * | 383 | 365 | 400 |
| 30 | 5 | C2 | 1.25 | 327 | 5 | 348 | 330 | 366 | 455 | 15 * | 414 | 395 | 434 |
| 30 | 10 | C1 | 0.63 | 137 | 5 * | 172 | 154 | 190 | 258 | 9 * | 238 | 218 | 257 |
| 30 | 10 | C2 | 0.94 | 222 | 8 * | 203 | 190 | 216 | 258 | 9 * | 269 | 253 | 286 |
| 30 | 10 | C2 | 1.25 | 228 | 8 * | 235 | 219 | 251 | 285 | 10 * | 301 | 282 | 320 |
| 30 | 15 | C1 | 0.63 | 72 | 9 | 69 | 51 | 87 | 118 | 4 * | 135 | 114 | 156 |
| 30 | 15 | C2 | 0.94 | 92 | 3 | 101 | 87 | 115 | 169 | 6 * | 167 | 148 | 185 |
| 30 | 15 | C2 | 1.25 | 142 | 2 | 132 | 115 | 150 | 204 | 7 * | 198 | 177 | 220 |
| 10 | 5 | C1 | 0.63 | 254 | 9 * | 258 | 235 | 281 | 253 | 9 * | 287 | 264 | 311 |

* Standard deviation of single measurement is estimated based on the average coefficient of variation of the replicates (3%).

**Table 3.20 : Experimental results for [$K^+$] and corresponding fitted values of the proposed regression model with confidence interval of 95% at 28 and 182 days for mixtures of various levels of GG, MK and $Na_2O$eq contents of cement.**

| GG | MK | Cement | | 28-day data (Mmol/L) | | | | | 182-day data (Mmol/L) | | | | |
|---|---|---|---|---|---|---|---|---|---|---|---|---|---|
| | | Type | Alk | Experimental data | | Data from the Model | | | Experimental data | | Data from the Model | | |
| (%) | (%) | | $Na_2O$eq | [$K^+$] | SD | [$K^+$] | Min | Max | [$K^+$] | SD | [$K^+$] | Min | Max |
| 10 | 5 | C1 | 0.63 | 128 | 6 * | 151 | 132 | 170 | 93 | 4 * | 122 | 101 | 143 |
| 10 | 5 | C2 | 0.94 | 261 | 12 * | 244 | 228 | 261 | 231 | 11 * | 201 | 184 | 219 |
| 10 | 5 | C2 | 1.25 | 279 | 13 * | 267 | 246 | 287 | 206 | 10 * | 209 | 189 | 229 |
| 10 | 10 | C1 | 0.63 | 89 | 4 * | 96 | 80 | 112 | 59 | 3 * | 73 | 56 | 89 |
| 10 | 10 | C2 | 0.94 | 178 | 7 | 182 | 170 | 194 | 146 | 7 * | 144 | 131 | 157 |
| 10 | 10 | C2 | 1.25 | 211 | 10 * | 197 | 180 | 213 | 141 | 7 * | 144 | 128 | 161 |
| 10 | 15 | C1 | 0.63 | 70 | 3 * | 59 | 40 | 79 | 59 | 3 * | 41 | 21 | 61 |
| 10 | 15 | C2 | 0.94 | 143 | 7 * | 137 | 122 | 152 | 138 | 7 * | 105 | 89 | 121 |
| 10 | 15 | C2 | 1.25 | 114 | 5 * | 144 | 125 | 164 | 75 | 4 * | 98 | 78 | 118 |
| 20 | 5 | C1 | 0.63 | 96 | 7 | 96 | 82 | 110 | 86 | 4 * | 78 | 62 | 95 |
| 20 | 5 | C2 | 0.94 | 193 | 9 * | 185 | 172 | 199 | 139 | 7 * | 153 | 139 | 168 |
| 20 | 5 | C2 | 1.25 | 204 | 10 * | 203 | 186 | 221 | 159 | 8 * | 157 | 140 | 174 |
| 20 | 10 | C1 | 0.63 | 69 | 3 * | 62 | 51 | 73 | 48 | 2 * | 49 | 37 | 62 |
| 20 | 10 | C2 | 0.94 | 135 | 6 * | 143 | 133 | 154 | 130 | 6 * | 117 | 106 | 128 |
| 20 | 10 | C2 | 1.25 | 166 | 8 * | 154 | 141 | 166 | 113 | 5 * | 113 | 100 | 125 |
| 20 | 15 | C1 | 0.63 | 60 | 3 * | 45 | 30 | 61 | 36 | 2 * | 39 | 21 | 56 |
| 20 | 15 | C2 | 0.94 | 118 | 6 * | 119 | 105 | 134 | 80 | 4 * | 98 | 83 | 113 |
| 20 | 15 | C2 | 1.25 | 112 | 5 * | 122 | 105 | 140 | 78 | 4 * | 87 | 70 | 103 |
| 30 | 5 | C1 | 0.63 | 61 | 3 * | 51 | 34 | 68 | 60 | 3 * | 44 | 24 | 64 |
| 30 | 5 | C2 | 0.94 | 135 | 6 * | 136 | 121 | 151 | 110 | 5 * | 115 | 99 | 131 |
| 30 | 5 | C2 | 1.25 | 122 | 6 * | 150 | 130 | 170 | 105 | 5 * | 115 | 94 | 135 |
| 30 | 10 | C1 | 0.63 | 37 | 2 | 37 | 25 | 50 | 49 | 2 * | 36 | 20 | 52 |
| 30 | 10 | C2 | 0.94 | 117 | 4 | 114 | 103 | 126 | 109 | 5 * | 99 | 86 | 112 |
| 30 | 10 | C2 | 1.25 | 113 | 5 * | 121 | 105 | 137 | 82 | 4 * | 91 | 74 | 108 |
| 30 | 15 | C1 | 0.63 | 39 | 2 | 41 | 26 | 57 | 33 | 2 * | 46 | 25 | 66 |
| 30 | 15 | C2 | 0.94 | 84 | 4 * | 111 | 96 | 126 | 60 | 3 * | 101 | 84 | 118 |
| 30 | 15 | C2 | 1.25 | 150 | 7 * | 110 | 89 | 130 | 133 | 6 * | 85 | 64 | 106 |

* Standard deviation of single measurement is estimated based on the average coefficient of variation of the replicates (5%).

**Table 3.21 : Experimental results for [$OH^-$] and corresponding fitted values of the proposed regression model with confidence interval of 95% at 28 and 182 days for mixtures of various level of GG, MK and $Na_2O$eq content of cement.**

| GG | MK | Cement | | 28-day data (Mmol/L) | | | | | 182-day data (Mmol/L) | | | | |
|---|---|---|---|---|---|---|---|---|---|---|---|---|---|
| | | Type | Alk | Experimental data | | Data from the Model | | | Experimental data | | Data from the Model | | |
| (%) | (%) | | $Na_2O_{eq}$ | [$OH^-$] | SD | [$OH^-$] | Min | Max | [$OH^-$] | SD | [$OH^-$] | Min | Max |
| 10 | 5 | C1 | 0.63 | 382 | 15 * | 383 | 344 | 422 | 345 | 14 * | 390 | 352 | 429 |
| 10 | 5 | C2 | 0.94 | 595 | 24 * | 534 | 507 | 562 | 595 | 24 * | 529 | 499 | 559 |
| 10 | 5 | C2 | 1.25 | 648 | 26 * | 619 | 580 | 658 | 641 | 25 * | 601 | 562 | 641 |
| 10 | 10 | C1 | 0.63 | 237 | 9 * | 260 | 227 | 294 | 223 | 9 * | 268 | 234 | 301 |
| 10 | 10 | C2 | 0.94 | 362 | 11 | 398 | 373 | 422 | 357 | 14 * | 392 | 365 | 419 |
| 10 | 10 | C2 | 1.25 | 441 | 17 * | 468 | 435 | 502 | 416 | 16 * | 450 | 417 | 484 |
| 10 | 15 | C1 | 0.63 | 157 | 6 * | 138 | 99 | 176 | 182 | 7 * | 145 | 105 | 184 |
| 10 | 15 | C2 | 0.94 | 245 | 10 * | 261 | 233 | 288 | 316 | 13 * | 255 | 225 | 285 |
| 10 | 15 | C2 | 1.25 | 280 | 11 * | 317 | 278 | 356 | 274 | 11 * | 299 | 260 | 339 |
| 20 | 5 | C1 | 0.63 | 408 | 16 * | 368 | 336 | 399 | 435 | 17 * | 401 | 369 | 432 |
| 20 | 5 | C2 | 0.94 | 502 | 20 * | 504 | 481 | 528 | 521 | 21 * | 525 | 501 | 549 |
| 20 | 5 | C2 | 1.25 | 627 | 25 * | 575 | 543 | 606 | 606 | 24 * | 582 | 551 | 614 |
| 20 | 10 | C1 | 0.63 | 229 | 9 * | 245 | 223 | 268 | 253 | 10 * | 278 | 254 | 302 |
| 20 | 10 | C2 | 0.94 | 370 | 15 * | 368 | 348 | 387 | 374 | 15 * | 388 | 367 | 408 |
| 20 | 10 | C2 | 1.25 | 416 | 16 * | 423 | 399 | 448 | 401 | 16 * | 431 | 407 | 456 |
| 20 | 15 | C1 | 0.63 | 168 | 7 * | 123 | 95 | 150 | 157 | 6 * | 155 | 124 | 186 |
| 20 | 15 | C2 | 0.94 | 268 | 11 * | 231 | 208 | 254 | 239 | 9 * | 251 | 227 | 275 |
| 20 | 15 | C2 | 1.25 | 324 | 13 * | 272 | 241 | 304 | 265 | 11 * | 280 | 248 | 312 |
| 30 | 5 | C1 | 0.63 | 350 | 14 * | 353 | 315 | 391 | 434 | 17 * | 411 | 371 | 451 |
| 30 | 5 | C2 | 0.94 | 487 | 19 * | 474 | 444 | 505 | 521 | 21 * | 520 | 490 | 550 |
| 30 | 5 | C2 | 1.25 | 455 | 18 * | 530 | 490 | 569 | 560 | 22 * | 563 | 524 | 603 |
| 30 | 10 | C1 | 0.63 | 172 | 7 * | 230 | 201 | 259 | 307 | 12 * | 288 | 255 | 322 |
| 30 | 10 | C2 | 0.94 | 340 | 13 * | 338 | 311 | 364 | 367 | 15 * | 383 | 356 | 411 |
| 30 | 10 | C2 | 1.25 | 341 | 14 * | 379 | 345 | 413 | 366 | 15 * | 412 | 378 | 446 |
| 30 | 15 | C1 | 0.63 | 111 | 7 | 107 | 75 | 139 | 151 | 6 * | 166 | 127 | 204 |
| 30 | 15 | C2 | 0.94 | 179 | 7 * | 201 | 172 | 230 | 229 | 9 * | 247 | 216 | 277 |
| 30 | 15 | C2 | 1.25 | 293 | 12 * | 228 | 188 | 267 | 337 | 13 * | 261 | 222 | 300 |

* Standard deviation of single measurement is estimated based on the average coefficient of variation of the replicates (4%).

# Chapter 4. Database and Response Surface Methodology to Portrait the Alkalinity of Ternary Paste Mixtures Incorporating Ground Glass (GG) and Fly Ash (FA) or Blast Furnace Slag (BFS)


## Résumé

Dans le contexte du développement durable dans le secteur de la construction, les sources de matériaux cimentaires alternatifs sont de plus en plus évaluées pour leurs effets bénéfiques sur les propriétés du béton, notamment la durabilité. L'objectif des travaux décrits dans cette étude est de documenter l'évolution du contenu en alcalis de la solution interstitielle de matrices cimentaires ternaires incorporant le verre broyé (VB), un ajout cimentaire à haute teneur en alcalis. Pour ce faire, un plan expérimental factoriel à trois niveaux a été conçu. Des mélanges de pâtes ternaires ont ainsi été fabriqués avec des ciments à différents contenus en $Na_2Oeq$, du verre broyé (VB) (10 à 20%) et l'un ou l'autre des ajouts cimentaires suivants : cendre volante de classe F (CV; 15 à 30%) ou laitier de hauts fourneaux de grade 80 (LHF; 20 à 40%) en remplacement du ciment, par masse. Les pâtes avaient un rapport eau : liant de 0,50 et étaient conservées pendant 28 et 182 jours dans des contenants scellés à 38°C. La solution interstitielle de ces spécimens a ensuite été extraite sous pression et leur [Na+], [$K^+$] et [$OH^-$] mesurées (calculées pour [$OH^-$]) par spectrophotométrie d'absorption atomique. Les données ont ensuite été traitées selon une approche de méthodologie de réponse de surface.

Les résultats d'analyses suggèrent que la [$OH^-$] dans la solution interstitielle est légèrement ou négligemment augmentée par un contenu plus élevé en VB et que la réduction de [$OH^-$] est fortement corrélée au contenu en FA et BFS dans les systèmes ternaires. La contribution du VB à la [$Na^+$] dans la solution interstitielle est plus importante pour le ciment à faible teneur en alcalis et est très limitée pour un ciment à haute teneur en alcalis avec NaOH ajouté pour atteindre 1,25% de $Na_2Oeq$. La [$K^+$] dans la solution interstitielle est abaissée quand plus de 20% de CV est combinée avec jusqu'à 20% VB. Les synergies les plus fortes observées sont entre le contenu en CV/LHF et la teneur en alcalis du ciment plutôt qu'entre les dosages en VB et CV/LHF.

## Abstract

In view of sustainable development in the construction sector, sources of alternative Supplementary Cementitious Materials (SCMs) are increasingly being evaluated for their beneficial effects on concrete properties, notably durability. The objective of the present work is to document the overall availability of alkalis in the pore solution of ternary cementitious matrices incorporating Ground Glass (GG), a high-alkali alternative SCM. In order to do so, a three-level factorial experimental plan was designed. More precisely ternary paste mixtures were made with cements of various $Na_2Oeq$ contents, Ground Glass (GG; 10 to 20%) and either Class F Fly Ash (FA; 15 to 30%) or Grade 80 Blast Furnace Slag (BFS; 20 to 40%) as cement replacement, by mass. Pastes had a water/binder of 0.50 and were stored for 28 and 182 days in sealed containers at 38°C. The pore solution from those specimens was then extracted under pressure and their $[Na^+]$, $[K^+]$ and $[OH^-]$ measured (calculated for $[OH^-]$) by atomic absorption spectrophotometry. The data were then processed with a *Response Surface Methodology* (RSM) approach.

The results of the analyses suggest that $[OH^-]$ in the pore solution is faintly or negligibly enhanced by higher contents of GG and that the reduction in $[OH^-]$ is strongly correlated to FA and BFS contents in the ternary systems. The contribution of GG to the $[Na^+]$ in the pore solution is more significant for low-alkali cement and is very limited for a high-alkali cement with NaOH added to reach 1.25% of $Na_2Oeq$. The $[K^+]$ in the pore solution is lowered when more than 20% FA is combined with up to 20% GG. The strongest synergies observed are between FA/BFS and the alkali content of the cement rather than between GG and FA/BFS.

## 4.1 Introduction

According to the global cement technology roadmap crafted by the *World Business Council for Sustainable Development* (WBCSD), the carbon footprint of the cement industry is expected to stabilize at about 2300Mt of $CO_2$/year even if the demand is expected to increase by 12-23% by 2050 compared to 2014 (WBCSD, 2018). This feat is expected to be possible in part by improving thermal efficiency of the kiln (3%) and by the increased use of alternative fuels (12%). However, reduction in GHG emissions due to clinker production can hardly be pushed any further since they are chemically inherent. Indeed, clinker requires calcium oxide (CaO), which is obtained by heating calcium carbonate ($CaCO_3$) to ≈1450°C until gaseous $CO_2$ is extracted and liquid/solid CaO remains. Hence, a reduction of the clinker-to-cement ratio is unavoidable to maintain the sustainability objectives of WBCSD, which has and will continue to imply the use of Supplementary Cementitious Materials (SCMs) to achieve that goal. More precisely, SCMs are a family of materials for which the environmental benefits over Ordinary Portland Cement (OPC) are specific to the region of the world in which they are used and sourced. Indeed, transportation and manufacturing/processing must be considered for many SCMs; however, the carbon footprint related to the production of a ton of such materials remains lower than that of OPC.

In Québec, ground glass (GG) is worth of attention as a SCM since it is readily available on the local market. Actually, due to low profitability, the center which was recycling 70-80% of the glass collected in the province stopped its activities in 2012 ( Bussière, 2013, Charles, 2013). Outlet for post-consumed glass is still an issue and several research projects are studying the feasibility of its incorporation, as an SCM, into concrete. This strategy is thought to have a positive effect on the environmental footprint of concrete since it involves less clinker and allows the re-utilization of post consumed material.

Although this strategy is attractive on the short term, the long-term durability of concrete incorporating GG is not without concerns. Because post-consumed glass has a high content in sodium (>13%), questions are being raised regarding its potential contribution to the phenomenon of Alkali-Silica Reaction (ASR) in concrete. ASR is, indeed, known to reduce the service life of concrete structures, which can involve high financial and environmental costs. What is interesting about glass is that its high sodic content can possibly fuel ASR, but, when finely ground, its high amorphous silica content can result in pozzolanic reactions which are known to mitigate ASR when used in proper amounts. The above dual expectations of ground glass (GG), which are tremendously intriguing, namely regarding the availability/release of alkalis from GG into the concrete pore solution, is the object of the present work.

When first documented, ASR expansion was found to be linearly related to the $Na_2O_{eq}$ content of concrete incorporating OPC with alkali contents ranging from 0.02 to 1.14% of $Na_2Oeq$ (Stanton, 1940). Later research showed that cement alkalis tend to rise the pH of the pore solution. Hydroxyl ions then attack siliceous phases of some fine/coarse aggregates and corrode/dissolve the silica, thus making it available to react with other ionic species in solution ($Ca^{2+}$, $Na^{+}$ and $K^{+}$) to produce the swelling gel specific to ASR (Diamond, 1989, Fournier and Bérubé, 2000). From the aggregate's perspective, ASR is often referred to a question of pH because an alkaline environment is essential to the attack of the reactive phases. Understandably, for the decades where the majority of the concrete used only OPC as a cementitious material, the strategy to lower the $Na_2Oeq$ of the cement in order to avoid ASR was appropriate. Indeed, Diamond (1989) highlighted the direct correlation between the $Na_2O_{eq}$ content of an OPC and the $[OH^-]$ of the pore solution (Figure 4.1).

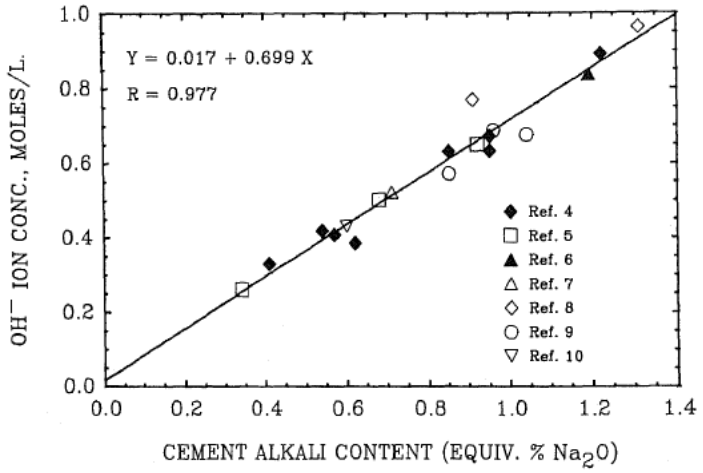


**Figure 4.1 : Relation between equilibrium $OH^-$ ion concentrations of pore solution and alkali content of cement. For pastes and mortars with w/c of 0.50 (Diamond, 1989).**

The connection between the composition of the pore solution and the reactivity of aggregates is also used to accelerate expansion due to ASR in several test methods where NaOH is either added to the concrete mixture or used as an immersion solution for mortar specimens (ASTM C 1260, CSA23.2-14A, CSA23.2-25A). Indeed, for most reactive aggregates, an increase in alkalinity and temperature in laboratory testing allows to accelerate ASR that takes up to decades to develop under outdoor/natural conditions. Those standards based on empirical data obtained from OPC mixtures were vital for characterizing proper combinations of aggregates and OPC and to evaluate the beneficial effect of many SCMs in preventing ASR.

The relationship between the $Na_2O_{eq}$ content of a cementitious blend incorporating SCMs and the alkalinity of the resulting pore solution can somehow differ from that established for OPC and illustrated in Figure 4.1. Indeed, the beneficial effect of SCMs in reducing the deleterious impact of ASR in concrete has been associated to

different factors, including their capacity to reduce the concentration of alkalis (or $OH^-$) available for reaction, the latter being related at least in part to their composition and their proportion in the binder. Thomas (2011) further stated that the ability of SCMs to reduce the pore solution alkalinity is linked to their effect on the composition and alkali-binding capacity of the hydrates (especially C–S–H); also, it was shown that SCMs with increased amounts of alkalis and calcium have to be used at higher replacement levels to be effective in reducing pore solution alkalinity.

Shehata (2001) analysed the pore solution of binary or ternary pastes specimens incorporating Fly Ashes (FAs) with a wide variety of chemical composition and/or Silica Fume (SF). The author observed that the relationship between $[OH^-]$ and the chemical composition of the cementitious blend is not proportional to the $Na_2Oeq$, like it was the case for OPC. Instead, it follows a second order function related to $(10Na_2O_{eq}+0.34CaO)/SiO_2$ of the cementitious blend, as presented in Figure 4.2. Other research pointed out other relations, such as Thomas (2011)

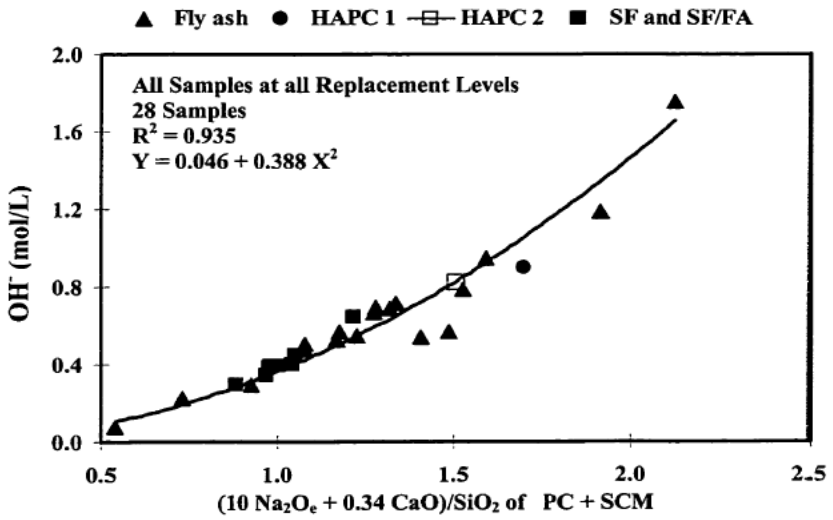


**Figure 4.2 : Effect of alkalis, calcium and silica content of the cementitious system (HAPC1 + FA or HAPC 2 + SF + FA) on pore solution alkalinity of control paste samples containing SCMs after two years (Shehata, 2001). (HAPC: high-alkali Portland cement; FA fly ash, SF : silica fume).**

Fernández et al. (2018) analysed the pore solution extracted under pressure at different ages from ternary pastes containing 1) two types of OPC ($Na_2Oeq$ of 0.40 or 0.69); 2) Blast Furnace Slag (BSF) and 3) Limestone Filler (LF) or FA. The authors observed that the ternary mixtures with higher alkalinity always have lower or at least similar alkali content in their pore solution, as presented in Figure 4.3 and Table 4.1.

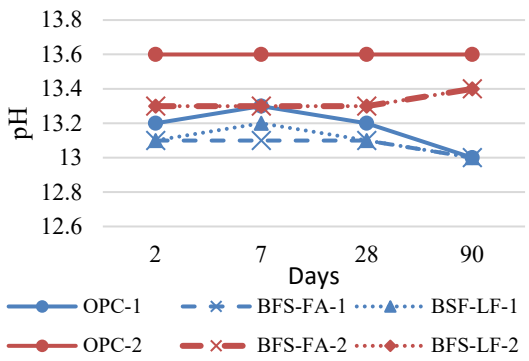


**Figure 4.3 : pH of the pore solution of paste specimens from cementitious blends containing 30% of BFS and 6% of LF or 26% of BFS and 10% of FA (Fernández et al., 2018).**

**Table 4.1 : Alkaline oxide composition of the cementitious blends presented in Figure 4.3 (Fernández et al., 2018).**

| Materials | $Na_2O$ (%) | $K_2O$ (%) | $Na_2Oeq$ (%) |
|---|---|---|---|
| OPC1 | 0.18 | 0.34 | 0.40 |
| BFS-FA-1 | 0.30 | 0.80 | 0.63 |
| BFS-LF-1 | 0.28 | 0.52 | 0.62 |
| OPC2 | 0.08 | 0.92 | 0.69 |
| BFS-FA-2 | 0.24 | 1.17 | 1.01 |
| BFS-LF-2 | 0.21 | 0.89 | 0.8 |

After microstructural analysis of the paste specimens, the authors also suggested that in many mixtures, less common phases, such as monocarboaluminate, hemicarboaluminate and hydrotalcites, are formed to the detriment of $Al_2O_3$–$Fe_2O_3$-mono (AFM.) The hydrates formed in those ternary mixtures suggest that the chemistry of those concretes is different or happens in different proportions compared to OPC, which also supports the idea that the behavior of ternary blends should not be extrapolated from that of OPC or binary mixtures. The following phenomena were proposed to explain why cementitious mixtures (e.g. OPC + SCM) richer in alkalis than OPC alone lead to lower alkali contents in their pore solution: 1) the reactivity of the SCMs is sometimes lower than that of OPC and alkalis remain in unreacted phases, 2) in presence of SCMs, the released $Na^+$ and $K^+$ ions can be adsorbed on the surface of low C/S C-S-H, or even incorporated in C-(N)-S-H, C-(N)-A-S-H or in some cases N-A-S-H (Hong and Glasser, 1999, Hong and Glasser, 2002, Warner et al., 2012, Kupwade-Patil and Allouche, 2013). Other authors proposed that the adsorption of monovalent alkali ions ($Na^+$, $K^+$) by C-S-H is enhanced in the context of pore solution of high pH. For instance, Labbez et al. (2011) worked with C-S-H suspensions and, using the radioactive tracer technique and electrophoresis to measure the electrokinetic potential of C-S-H particles, the authors found that for Ca/Si of 0.7 and 1.6, C-S-H in contact with solutions of higher $Na^+$ concentration tend to adsorb more of this ion on their surface. Although the strength and the durability of bonding allowing $Na^+$ to be removed from the pore solution remains unknown, the interesting point suggested by this study is that the potential of C-S-H to uptake cations is also related to the composition of the contact solution. The importance of the composition of the pore solution had also been highlighted by Ke-rui et al. (2004) who worked with synthetic C-S-H that were immersed in solutions of various $[Ca^{2+}]/[Na^+]$ (prepared with $Ca(OH)_2$ and NaOH). The C-S-H were washed in distilled water and vacuum filtrated several times in order to remove soluble alkalis; the $\zeta$ potential of the C-S-H was then measured with a micro-electrophoresisa and the $Na^+$ concentration of C-S-H determined with a flame spectrophotometer. The authors

found that the ζ potential of the C-S-H was greater after a two-hour immersion in a $Na^+$ rich solution, which indirectly suggests that $Ca^{2+}$ ions where replaced by $Na^+$ on the surface of the C-S-H because the resulting charge imbalances increased the ζ potential. On the other hand, the ζ potential decreased when C-S-H where immersed in a $Ca^{2+}$ rich solution, thus indicating that the negatively charged surface of the C-S-H was better balanced because of the presence of additional $Ca^{2+}$ ions. The analysis of the sodium content of the C-S-H with a flame spectrophotometer directly corroborated the fact that the C-S-H adjust their composition relatively to the composition of the contact solution. In the light of this study, suggesting that the composition of the pore solution is related to the effectiveness of C-S-H to incorporate/adsorb alkalis, and considering that the composition of the pore solution is the key to limit the reactivity of reactive aggregates, a good understanding of the behavior of pore solution is essential to the safe use into concrete of a high-alkali pozzolanic material such as GG.

The synergy between GG and other SCMs is the purpose of recent papers that highlight the beneficial effect of alkali release from GG when used in BFS or FA-based alkali activated systems (Maraghechi, 2014, Maraghechi et al., 2017, Zhang et al., 2017, Zhang and Yue, 2018). For instance, Zhang and Yue (2018) used *Response Surface Methodology* (RSM) which suggested that replacing 14.57% of the (Alkali Activated) Slag (AAS) by GG using a 8.31% $Na_2O_{eq}$ activator lead to an increase by 9.8% of the 28-day compressive strength compared to an AAS system without GG. Maraghechi et al. (2017) also studied alkali activated BFS and FA systems incorporating 20 to 50% of GG with an alkali activator with pH values ranging from 13.7 to 14.6. From the investigation of the expansive behavior, the microstructure and the compressive strength of such concretes, the authors mentioned : "*Dissolution of GG in alkali activated slag–GG and fly ash–GG increases the silica content of the reaction products, specifically C–A–S–H and N–A–S–H and that the gradual release of sodium from GG, as an internal source of alkalis, may also serve to maintain the pH of the pore solution high which can help further hydration of slag and fly ash at longer ages*." This last point is interesting because in the context of alkali-activated materials, the dissolution of GG and the inherent release of silica and sodium do not produce ASR gel, although the chemical species required for ASR are available in solution. Those studies on alkali activated concretes suggest that the composition of the hydrates is related to the species in solution, which was also observed in non-activated materials (Ke-rui et al., 2004, Labbez et al., 2011). The latter studies uncovered fundamentals questions about the "sharpness/blurriness" of the line separating the alkali-activated reaction products and alkali-rich pozzolanic reaction products.

The ASR reaction products is another known hydration product composed of silica, calcium, monovalent alkalis ($K^+$ and $Na^+$) and that require an alkali/silica-rich pore solution to form; actually, the most consensual way to be sure of the presence of ASR products, to the detriment of others incorporating the same chemical species, is to follow the expansive behavior of concrete specimens. Indeed, in the study of Maraghechi et al. (2017) on alkali-activated concretes incorporating GG and FA or BFS, the hydrates observed where C-(N)-A-S-H and N-A-S-H when FA or BFS are used in combination with GG. The authors suggested that GG and FA/BFS influence each other's reaction product and GG does not seem to result in "deleterious" ASR products in mortar bar specimens. In Figure 4.4, the expansion of alkali-activated mortar bars incorporating 20% GG remains below the acceptance limit of 0.10% when tested according to ASTM C1260 with a non-reactive limestone. Another relevant observation by the authors is that there is a gel rim around glass particles and that the composition of the rim is closer to N-A-S-H than that of ASR gel (Figure 4.5). This suggests that the nature of the hydrates induced by the incorporation of GG is related to the presence of FA and also to the composition of the pore solution.

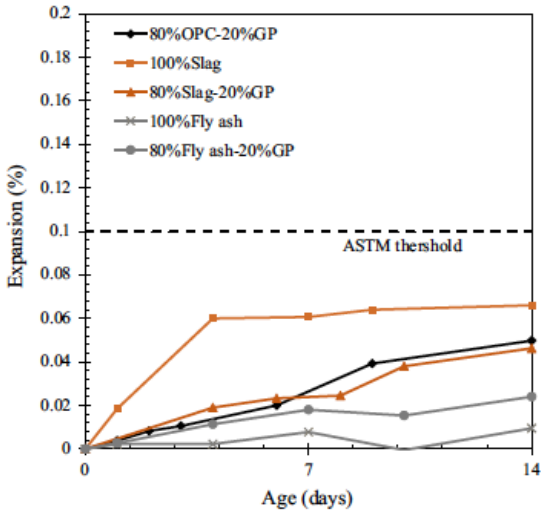


**Figure 4.4 : Accelerated mortar bar (ASTM C1260) expansion of selected mortars containing 0 to 20% Glass Powder (GP)(Maraghechi, et al., 2017).**

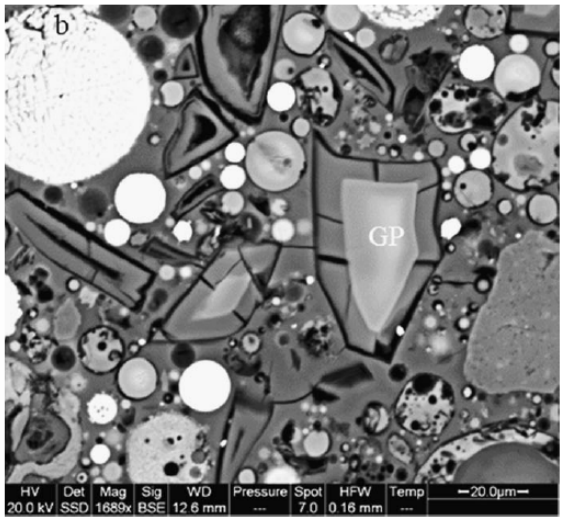


**Figure 4.5 : SEM micrograph of paste composed of 80 % fly ash – 20 % GP mortars, steam cured at 60°C for 56 days (Maraghechi et al., 2017).**

There is no guarantee that the interaction observed in alkali-activated context also occurs in non-activated concrete. Actually, there is a knowledge gap since nothing indicates that GG and FA/BFS react independently from one another in non-activated or "boosted" systems such as in CPT or AMBT. Actually, it would be a trivial hypothesis to suppose that they do interact since the ternary cementitious components share their reaction time and location as well as their reactants (same chemical species in solution). This understanding gap suggests that the ASR in ternary concretes depends on phenomena that are not fully understood, which uphold the predictability of their expansive behavior. Consequently, it seems to be fully appropriate to push further the knowledge on the pore solution chemistry of such concretes, with the intent of adding the informative assets to the understanding of the behavior of such systems when incorporating alkali-silica reactive aggregates.

## 4.2 Objective and Scope of Work

The incorporation of GG in concrete mixtures tested in accordance with CSA Standard Practice A23.2-28A showed the potential of using GG to reduce expansion due to ASR when it was sometimes expected that its high alkali content would rather promote it. When tested under AMBT conditions or used with alkali activators, other studies found that, when used conjointly with BFS or FA, the mortar bar expansion is reduced below the acceptance limit.

The main goal of this study is to assess the pore solution chemistry of ternary mixtures incorporating GG and a third SCM such as FA or BFS and to understand how synergy (if any?) could affect the availability of the alkalis from GG. a common practice when testing the effectiveness of SCMs to prevent ASR in the laboratory.

In order to do so, ternary paste systems were made with various percentages of GG and FA/BFS, as replacement by mass of OPC (different levels of $Na_2O_{eq}$). Pore solutions were then obtained (pressure extraction) from those pastes after 28 and 182 days of storage (cured at 38°C). Solutions were analyzed for their content in $Na^+$ and $K^+$ and the data were processed using a *Response Surface Methodology* (RSM) approach.

## 4.3 Materials and Methods

### 4.3.1 Materials Characteristics

Paste samples were made using post-consumed GG from a recycling facility located in Quebec Province (Canada), type F FA from Alberta (Canada), grade 80 BFS from Ontario (Canada) and two Canadian type GU portland cements (0.63% and 0.94% $Na_2Oeq$). Pastes with 1.08% and 1.25% "cement" alkali contents were made by adding NaOH to portland cement C2 mixture. The chemical composition of each material used in this study is presented in Table 4.2, while their particle size distribution is illustrated in Figure 4.6.

**Table 4.2 : Chemical composition of cementitious materials.**

| | Portland cements | | SCMs | | |
|---|---|---|---|---|---|
| Oxides | C1 | C2 | GG | FA | BFS |
| $SiO_2$ | 19.58 | 18.7 | 70.53 | 56.72 | 37.74 |
| CaO | 62.09 | 60.8 | 10.77 | 9.29 | 36.20 |
| $Al_2O_3$ | 4.58 | 5.0 | 2.06 | 24.07 | 9.45 |
| $Fe_2O_3$ | 2.85 | 3.7 | 0.35 | 3.14 | 0.36 |
| $Na_2O$ | 0.22 | 0.25 | 12.49 | 2.50 | 0.26 |
| $K_2O$ | 0.62 | 1.05 | 0.66 | 0.64 | 0.36 |
| $Na_2O_{eq}$ | 0.63 | 0.94 | 12.92 | 0.55 | 0.50 |
| $SO_3$ | 4.02 | 3.8 | 0.11 | - | 2.45 |
| MgO | 2.91 | 2.7 | 1.14 | 1,05 | 9.96 |
| $TiO_2$ | 0.23 | - | 0.07 | 0,65 | 0.94 |
| $P_2O_5$ | 0.10 | - | 0.03 | 0,09 | 0.08 |
| MnO | | | 0.02 | 0.04 | 0.72 |
| L.O.I | 2.45 | 1.9 | 1.71 | 1.05 | 1.84 |

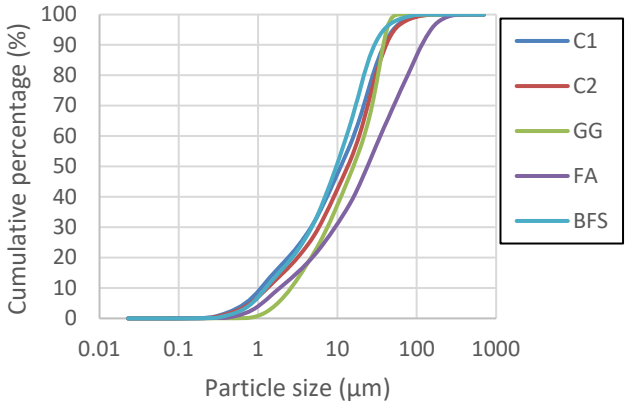


**Figure 4.6: Particle size distribution of cementitious materials.**

### 4.3.2 Design of Experiment

#### 4.3.2.1 Experimental Plan

The experimental design consisted in a complete factorial plan with three levels for each of the three main variables, as indicated below:

1) GG – 10, 15 and 20% (cement replacement, by mass)
2) FA – 15, 22.5 and 30% or BFS – 20, 30 and 40% (cement replacement, by mass)
3) Alk – 0.63, 0.94, and 1.25% (i.e. 0.94% + NaOH), which corresponds to the $Na_2Oeq$, by cement mass.

An additional “check point” (1.08% $Na_2Oeq$) was added to the experimental plan and is illustrated in black with the rest of the proposed mixtures presented in Figure 4.7 for FA. The design strategy is identical for FA and BFS.

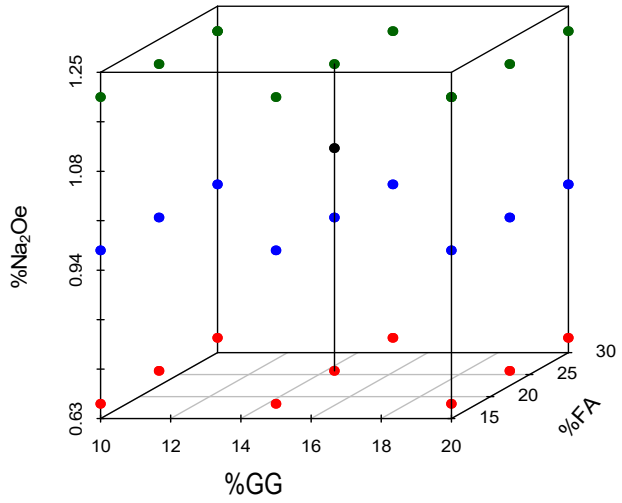


**Figure 4.7 : Mixture design for the experimental plan of FA and “check point” with an alkali content of 1.08%, $Na_2Oeq$.**

For the interpretation of the results of the RSM numerical processing, the variables were coded between -1 and 1, which “rescales” or “balances” their effect on the response according to their typical range of use. Table 4.3 and Table 4.4 present the coding system of the variables for both plans. The triplicates of the centre point and the 28-day extraction results are used to calculate a typical coefficient of variation and to estimate the standard deviation of single measurements; these results are presented in Annex A.

**Table 4.3 : Coded and corresponding uncoded values.**

| | Uncoded parameters | | | |
|---|---|---|---|---|
| coded | GG | FA | BFS | Cement $Na_2Oeq$ |
| -1 | 10 | 15 | 20 | 0.63 |
| 0 | 15 | 22.5 | 30 | 0.94 |
| 1 | 20 | 30 | 40 | 1.25 |

**Table 4.4: Model of the coded values of the experimental plan.**

| GG = -1 | | GG = 0 | | GG = 1 | |
|---|---|---|---|---|---|
| FA or BFS | Cement $Na_2Oeq$ | FA or BFS | Cement $Na_2Oeq$ | FA or BFS | Cement $Na_2Oeq$ |
| -1 | -1 | -1 | -1 | -1 | -1 |
| -1 | 0 | -1 | 0 | -1 | 0 |
| -1 | 1 | -1 | 1 | -1 | 1 |
| 0 | -1 | 0 | -1 | 0 | -1 |
| 0 | 0 | 0 | 0 | 0 | 0 |
| 0 | 1 | 0 | 1 | 0 | 1 |
| 1 | -1 | 1 | -1 | 1 | -1 |
| 1 | 0 | 1 | 0 | 1 | 0 |
| 1 | 1 | 1 | 1 | 1 | 1 |

#### 4.3.2.2 Time Repeated Measurements

Measurements of the pore solution composition were made on pastes at 28 and 182 days. *Time* is thus considered the fourth parameter for numerical processing.

#### 4.3.2.3 Mixture Experiment

The cement content, as the fifth variable "Cem" ($x_5$), is related to the GG and FA/BFS content, but is inherent to mixture experiment using RSM, as mentioned by Myers et al. (2011) and Lawson (2014). The (dependent) "Cem" variable is coded similarly to the other variables using Equation 1 (Table 4.5).

$$x_5 = \frac{Cem\% - {Max_{Cem} + Min_{Cem}}/{2}}{{Max_{Cem} - Min_{Cem}}/{2}} \qquad \text{Equation 1}$$

**Table 4.5: Coded values and corresponding cement contents for the FA and BFS systems.**

| Cement content (%) | 40 | 45 | 50 | 55 | 57.5 | 60 | 62.5 | 65 | 67.5 | 70 | 75 |
|---|---|---|---|---|---|---|---|---|---|---|---|
| FA | | | -1 | -0.75 | -0.5 | -0.25 | 0.00 | 0.25 | 0.50 | 0.75 | 1.00 |
| BFS | -1 | -0.67 | -0.33 | 0 | | -0.33 | | 0.67 | | 1 | |

### 4.3.3 Manufacturing of Paste Specimens

The following procedure was modified from ASTM C305 to produce pastes with fixed water-to-binder ratio of 0.50 and without using chemical additives. Water and FA or BFS were first mixed together in the bowl of the mixer at slow speed (140 $\pm$ 5 r/min) for 15 sec. GG and cement were then added to the mixer and the standard procedure was followed as is : 1) components are left waiting 30 seconds in the bowl to allow the absorption of water; 2) mixing at slow speed (140 $\pm$ 5 r/min) for 30 sec; 3) mixer is stopped 15 sec to allow to scrape down the paste stuck to the side of the bowl and 4) mixing 60 sec at medium speed (285 $\pm$ 5 r/min). The pastes were then poured in a plastic bottle, 30 mm by 55 mm in size (12ml), sealed and gently agitated for 24h at 23 ± 2°C. The bottles were finally stored in a sealed plastic bag at 38°C for 28 or 182 days before pore solution extraction.

### 4.3.4 Pore Solution Extraction Process

The paste specimens were stored at 23 ± 2°C for a period of 24h prior to extraction to ensure uniform temperature throughout the extraction process. As a precaution against water loss and carbonation, the paste specimens were left in their plastic container until their placement in the extraction cell. The pore solution was extracted using a pressure of 320 MPa (200kN) and collected with a syringe. The latter was then sealed with proper plastic cap and wax tape to prevent possible carbonation or evaporation of the solution.

### 4.3.5 Chemical Analysis

Solutions were analyzed for their sodium and potassium concentrations with a PerkinElmer AAnalyst 100 atomic absorption spectrophotometer (AAS) at wavelengths of respectively 589 and 766.5 nm using an air-acetylene flame. To avoid interferences, cesium chloride was added to the solutions at a concentration of 1.5g/L. Full solubility of the species was assured by the dilution of the extracted solutions in 5% V/V nitric acid. [$OH^-$] were estimated by electroneutrality and calculated according to Equation 2.

$$[OH^-] \approx [Na^+] + [K^+] \qquad \text{Equation 2}$$

### 4.3.6 Numerical Treatment

#### 4.3.6.1 Equation of The Surface Response

Computations were made with R freeware from R Core R.C. Team (2013) and packages used were those proposed by Lenth (2009), Lawson (2014) and Lawson and Willden (2016). The general equation of the RSM is presented in Equation 3, where $b_i$ are the coefficients corresponding to the $x_i$ variables. Equation 4 is the matrix equation proposed by Myers et al. (2011) to solve the value of the coefficient [b] for a given set of observations [y], under the context of the variable expressed in [X].

$$y = b_0 + b_1x_1 + \cdots + b_5x_5 + b_6x_1x_2 + \cdots + b_{15}x_4x_5 + b_{16}{x_1}^2 + + \cdots b_{20}{x_5}^2 \qquad \text{Equation 3}$$

$$[b] = ([X'] \times [X])^{-1} \times [X'] \times [y] \qquad \text{Equation 4}$$

**For example, the two first lines of Matrix [X] mixture 10GG-15FA-0.63A at 28 and 182 days and the two first line of [y] for observations of [$K^+$] are 108 and 77 mmol/L, respectively (Table 4.6). After construction of [X] and [y], Equation 4 is used to find [b], which is then used to complete Equation 3, the latter being the equation of the surface response.**

**Table 4.6 : Example of the first two lines of the matrix [X] and [y] for a first order model neglecting the interactions.**

| Uncoded parameters [X] | | | | | Coded parameters [X] | | | | | [y] |
|---|---|---|---|---|---|---|---|---|---|---|
| GG | FA | Alk | Day | Cem | $x_1$ | $x_2$ | $x_3$ | $x_4$ | $x_5$ | [$K^+$] |
| 10 | 15 | 0.63 | 28 | 75 | -1 | -1 | -1 | -1 | 1 | 108 |
| 10 | 15 | 0.63 | 182 | 75 | -1 | -1 | -1 | 1 | 1 | 77 |

In this study, [b] is calculated with the coded parameters to discuss the coefficient of the variables and compare their weight on the response. It is worth mentioning that [b], calculated with the uncoded parameter (often referred to as [$\beta$]), is used to provide the "natural equation" which will be used to present the ternary diagram discussed later, to predict new data and to validate the model with the "check points".

#### 4.3.6.2 Variables Selection

The most accurate regression model is obtained through a backward stepwise iterative process starting with all variables and interactions and removing the least significant effect at each steps using $R^2_{adj}$ as the decision criterion, as proposed by Montgomery and Runger (2010). Least significant variables were judged according to their t-values and were discarded as long as the removal did not reduce the overall $R^2_{adj}$ of the regression model. To avoid converging through a model overly sensitive to single data points, the PRESS (*Prediction Error Sum Square*) statistic was also computed during the iteration process. Since the PRESS number is an indicator of how well the model is likely to perform when predicting new data according to Montgomery and Runger (2010), the PRESS number should increase when the model improves in accuracy. The predictive capability of the model was also computed using *Sum Square Total* (SST) (Equation 5), as proposed by Myers et al. (2011).

$$R^2_{prediction} = 1 - PRESS/SST \qquad \text{Equation 5}$$

#### 4.3.6.3 Model Validation

In the first place, $R^2$ above 0.90 was used to validate the overall quality of the model. In order to verify that the good $R^2$ value was not artificially enhanced by a group of variables especially well represented to the detriment of others, the heterogeneity of the error as well as the normality were then graphically assessed (see Annex B). Since $R^2$ could also be artificially inflated by multicollinearity, the *Variance Inflator Factor* (VIF) was also computed and since Montgomery and Runger (2010) suggested that a VIF below 10 indicates a model with no multicollinearity issue, variables with a VIF over or near 10 were eliminated and the computations were redone from the variable selection step. $F_0$ was computed and compared to a p-value to discard the hypothesis that the mean of all samples represents the observations better than the regression model. P-value over 0.05 for $F_0$ discards the latter hypothesis, as proposed by Montgomery (2012). The last regression model validation consists in plotting the fitted values against the experimental data and verify the correlation between the two. In this study, the correlations between the regression and the experimental data were found to be over 0.95 and are presented in the Annex B.

#### 4.3.6.4 Confidence Interval for the Regression Model

The confidence interval (C.I.) relative to the regression model is given by Equation 6 for data within the range of the dataset, while Equation 7 stands for data outside the range of the dataset, as proposed by (ULaval 2010).

$$\text{C.I.} = \widehat{Y_0} \pm t_{\frac{a}{2}:n-k-1}\sqrt{MSE\left(x_0'(X'X)\right)^{-1}x_0} \quad \text{Equation 6}$$

$$\text{C.I.} = \widehat{Y_0} \pm t_{\frac{a}{2}:n-k-1}\sqrt{MSE\left(1 + x_0'(X'X)\right)^{-1}x_0} \quad \text{Equation 7}$$

where MSE is the *Mean Square Error* (MSE), $t_{\frac{a}{2}:n-k-1}$ is the percentage point on a Student distribution for a confidence interval of $\alpha$, n observations and k degrees of freedom.

## 4.4 Results of the testing program

### 4.4.1 Chemical Analyses of The Pore Solutions

Annex C provides the detailed results of the chemical analyses of the pore solutions extracted from the ternary paste systems incorporating GG, FA/BFS and portland cements (C1 or C2), with and without NaOH, after 28 and 182 days of storage at 38°C. Standard deviation (SD) values are calculated for the 28-day replicates presented in Annex A and a constant coefficient of variation was assumed to estimate the SD of the 182-day analyses. Figure 4.8 presents the results of the analysis of the sodium concentration of paste systems incorporating GG, cements of different $Na_2Oeq$ contents and FA (Figure 4.8 a to c) and BFS (Figure 4.8 d to f). A general trend of increasing $[Na^+]$ is observed for all mixtures between 28 and 182 days. Also, FA-bearing pastes with higher FA contents generally tend to display lower $[Na^+]$. In addition, pastes made with the lower alkali cement C1 exhibit lower $[Na^+]$ compared to the companion mixtures made with cement C2 or C2+NaOH. Another observation is that pastes incorporating more GG had higher $[Na^+]$ for a given cement and a given FA content.

Similar observations stand for BFS-bearing pastes; $[Na^+]$ tends to increase between 28 and 182 days; pastes with 40% of BFS have lower $[Na^+]$ than those incorporating 20% BFS, and it especially true for pastes made with cement C2 + NaOH; pastes made with cement of higher alkali content show higher $[Na^+]$ and inversely; finally, pastes incorporating more GG tend to have higher $[Na^+]$ for a given cement and a given percentage of BFS.

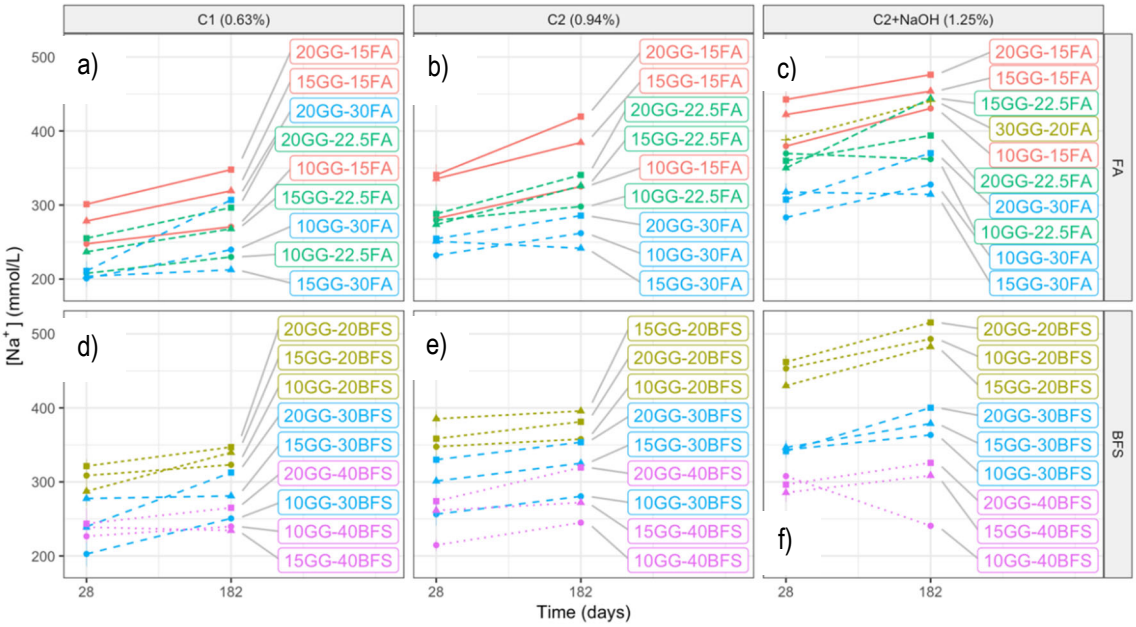


**Figure 4.8: Evolution of [$Na^+$] between 28 and 182 days for pastes with various contents of GG, FA or BFS and cement alkalis.**

Figure 4.9 presents the results of the analysis of the potassium concentration of paste systems incorporating GG, cements of different alkali contents and FA (Figure 4.9 a to c) and BFS (Figure 4.9 d to f). The general trend for most mixtures is that [$K^+$] tends to decrease between 28 and 182 days. Pastes made with cement C1 show [$K^+$] notably lower than those made with cement C2, which is expected since the $K_2O$ contents of the above cements are respectively 0.62% and 1.02%. Also, for FA-bearing pastes, the [$K^+$] of pastes made with cement C2 are similar to those made with C2+ NaOH, since the alkali addition was from NaOH.

In the case of BFS-bearing pastes, [$K^+$] are different at 182 days for pastes with and without NaOH. In many cases, the reduction of [$K^+$] between 28 and 182 days is less pronounced for mixtures made with cement C2 compared to the same mixture with NaOH addition. Also, pastes with higher content of FA or BFS have lower [$K^+$]. The effect of GG on [$K^+$] is opposite to that on [$Na^+$], which means that pastes with more GG have lower [$K^+$] for a given content of cement and a given content of FA or BFS. It is interesting to remember that the $K_2O$ content of GG, cements C1 and C2 are respectively 0.66%, 0.62% and 1.02%.

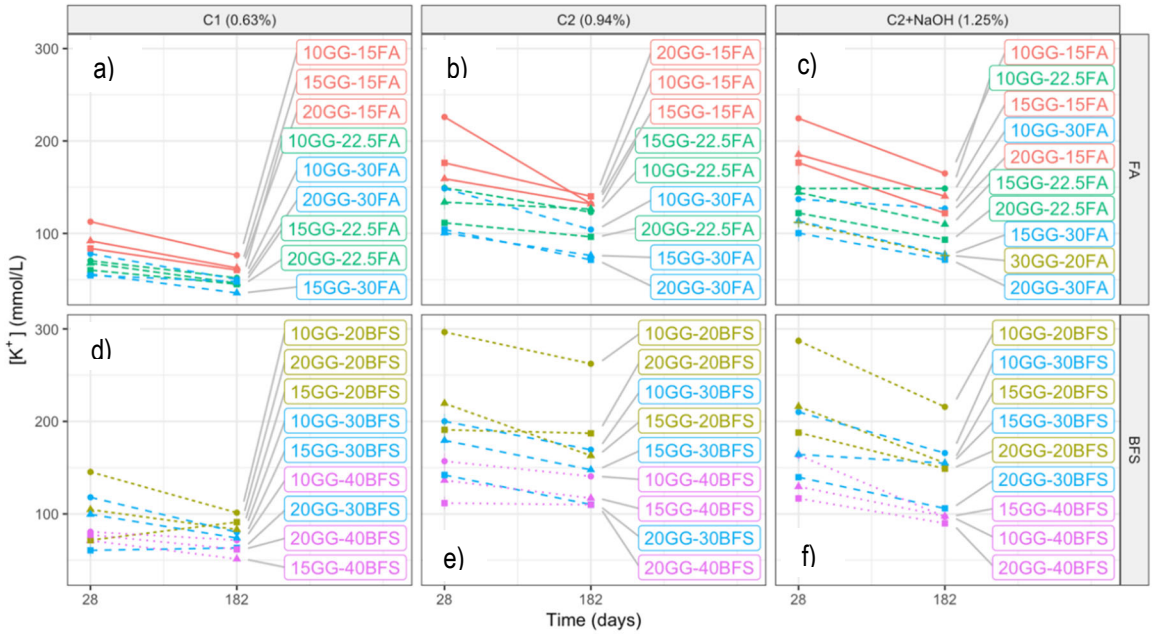


**Figure 4.9 : Evolution of [$K^+$] between 28 and 182 days for pastes with various contents of GG, FA or BFS and cement alkalis.**

Figure 4.10 presents the [$OH^-$] at 182 days, estimated from Equation 2, of the paste mixtures analyzed in this study. One of the main trends is that higher [$OH^-$] are almost always associated with cement of higher alkali contents. Also, higher contents of FA or BFS tend to lower [$OH^-$]. The effect of the GG content on the alkalinity of the pore solution however seems to be inconsistent; a somewhat "pessimum" GG content is observed at 15% for pastes incorporating 30%FA, 20%BFS and 40%BFS, while an arguably subtle "optimum" also appears at 15%GG for 22.5%FA and 30%BFS and for the mixture incorporating 40% of BFS made with cement C2 and a NaOH addition.

For all FA-bearing mixtures made with the low-alkali cement C1, the incorporation of GG increases the alkalinity by approximately 20 to 50 mmol/L. For FA- bearing pastes made with cement C2, the addition of GG tends to increase [$OH^-$] by about 100 mmol/L when only 15% of FA is used, while GG has almost no effect on the [$OH^-$] when at least 22.5% of FA are used. The addition of GG seems to lower the alkalinity when C2 + NaOH is used with FA.

For BFS-bearing pastes, the use of GG tends to lower the alkalinity by approximately 50mmol/L when 20%BFS are used, while its impact is near negligible for most pastes incorporating 30% and 40%BFS. Also, the addition of GG lowers the alkalinity of the pore solution of pastes made with cement C2 (with and without NaOH) and 20-30%BFS.

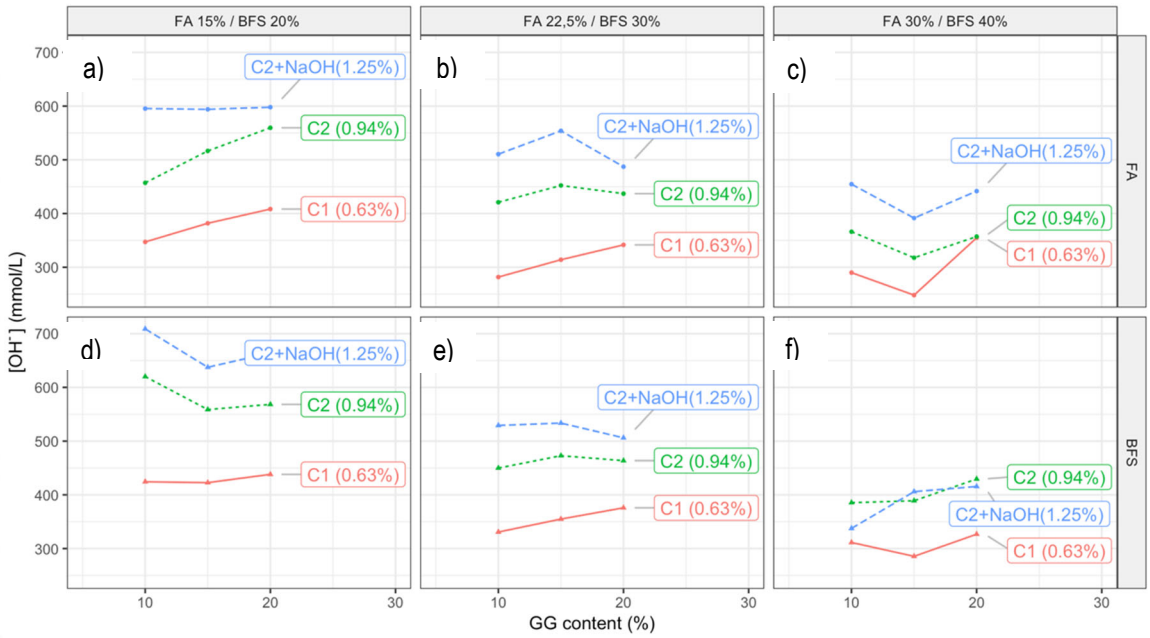


**Figure 4.10 : [$OH^-$] at 182 days of the pore solution of pastes made with cements of various $Na_2Oeq$ contents and different GG contents.**

Figure 4.11 presents the [$OH^-$] at 28 days, estimated from Equation 2, of the paste mixtures analyzed in this study. The results suggest that the use of cement of higher $Na_2Oeq$ contents tend to significantly increase [$OH^-$] at that early age. Also, higher percentages of FA/BFS are associated to lower alkalinity while the addition of GG has no or little effect on the 28-day alkalinity in FA-bearing pastes. For BFS-bearing pastes, the result of the addition of GG is between alkali-reducer and neutral on the 28-day alkalinity.

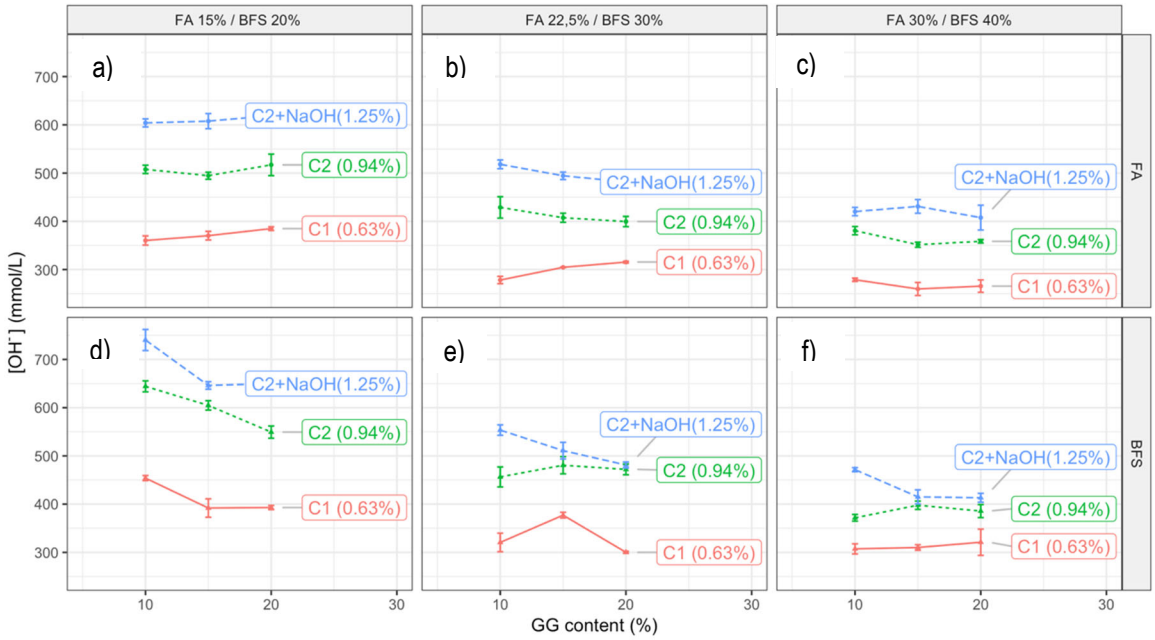


**Figure 4.11 : [$OH^-$] at 28 days of the pore solution of pastes made with cements of various $Na_2Oeq$ contents and different GG contents.**

## 4.4.2 Numerical Treatment

Table 4.7 and Table 4.8 present the regression models proposed to represent the data. The coefficients and other model information correspond to the coded variables in order to compare the effects on the same scale, while the intercept of a coded regression model corresponds to the average value of the data set. The coefficients of the variables are proportional to their effect and a negative coefficient indicates that the variable contributes at reducing the concentration. For example, in Table 4.7, the coefficients -44 for FA and 21 for GG in the model proposed for [$Na^+$] indicate that the addition of FA tends to lower [$Na^+$] (negative coefficient), while the use of GG tends to enhance [$Na^+$] (positive coefficient); the impact on [$Na^+$] is roughly twice as much for FA compared to GG (i.e. 44 compared to 21 in absolute values). In Table 4.7 and Table 4.8, the effects are also labelled as “Main”, “Low” or “Optimum/Pessimum”. Those labels indicate in what extent the variable influences the response and their types are discussed below.

Equations 8 to 10 are proposed to predict new data for paste systems incorporating FA, while equations 11 to 13 are proposed for pastes made with BFS. “GG”, “FA”, “BFS” and “Cem” represent respectively the content of GG, FA, BFS (i.e. between 0.1 and 0.4) and cement (0.4 to 0.75) in the systems; “Alk” represents the $Na_2O_{eq}$ (i.e. between 0.63 and 1.25) of the cement and “Day” is the age (in days) of the paste sample.

**Table 4.7 Regression model of FA and significance of the information provided by the various coefficients.**

| | | $Na^+$ | | | $K^+$ | | | $OH^-$ | | |
|---|---|---|---|---|---|---|---|---|---|---|
| Type of effect | Relative uncoded variable | Coeff | t-value | Prob. | Coeff | t-value | Prob. | Coeff | t-value | Prob. |
| | (Intercept) | 303 | 74 | 0 | 121 | 42 | 0 | 420 | 84 | 0 |
| "Main" | GG | 21 | 9 | 0 | -16 | -10 | 0 | 7 | 2 | 4 |
| | FA | -44 | -21 | 0 | -25 | -14 | 0 | -72 | -27 | 0 |
| | Alk | 60 | 28 | 0 | 35 | 20 | 0 | 97 | 37 | 0 |
| | Day | 19 | 9 | 0 | -15 | -10 | 0 | 4 | 2 | 9 |
| "Low" | GG*FA | -9 | -3 | 0 | -8 | -3 | 0 | -19 | -4 | 0 |
| | GG*Alk | -4 | -2 | 9 | -6 | -3 | 0 | -10 | -3 | 0 |
| | GG*Day | 5 | 2 | 2 | - | - | - | 8 | 3 | 1 |
| | GG*Cem | - | - | - | - | - | - | -5 | -11 | 34 |
| | FA*Alk | -11 | -4 | 0 | -10 | -6 | 0 | -22 | -7 | 0 |
| | FA*Day | - | - | - | 5 | 3 | 1 | - | - | - |
| | FA*Cem | - | - | - | -22 | -5 | 0 | -27 | -4 | 0 |
| | Alk*Day | - | - | - | -3 | -2 | 12 | - | - | - |
| Optimum/Pessimum | $GG^2$ | -4 | -1 | 0 | - | - | - | - | - | |
| | $Alk^2$ | 17 | 4 | 0 | -31 | -12 | 0 | -15 | -3 | 0 |
| Model information | | $R^2$=0.94, N=108 $R^2_{Prediction}$ = 0.92 | | | $R^2$=0.93, N=108 $R^2_{Prediction}$ = 0.92 | | | $R^2$=0.95, N=108 $R^2_{Prediction}$ = 0.95 | | |
| Model significance | | p. for $F_0$<2.2e-16, Cor.=0.97 | | | p. for $F_0$<2.2e-16, Cor.=0.95 | | | p. for $F_0$<2.2e-16, Cor.=0.98 | | |

Equation 8

$$[\mathrm{Na}^+] = 88 + 1444\mathrm{GG} - 237\mathrm{FA} + 18\mathrm{Alk} - 2443\mathrm{GG} * \mathrm{FA} - 259\mathrm{GG} * \mathrm{Alk} + 2\mathrm{GG} * \mathrm{Week} - 488\mathrm{FA} * \mathrm{Alk} - 1782\mathrm{GG}^2 + 173\mathrm{Alk}^2$$

Equation 9

$$[\mathrm{K}^+] = -141 - 4\mathrm{GG} + 1255\mathrm{FA} + 889\mathrm{Alk} - 2196\mathrm{GG} * \mathrm{FA} - 369\mathrm{GG} * \mathrm{Alk} - 442\ \mathrm{FA} * \mathrm{Alk} + 1\mathrm{FA} * \mathrm{Day} - 2340\mathrm{FA} * \mathrm{Cem} - 324\mathrm{Alk}^2$$

Equation 10

$$[\mathrm{OH}^-] = -1 + 1018\mathrm{GG} + 1846\mathrm{FA} + 899\mathrm{Alk} + 5181\mathrm{GG} * \mathrm{FA} - 678\mathrm{GG} * \mathrm{Alk} + 2\mathrm{GG} * \mathrm{Day} - 930\mathrm{FA} * \mathrm{Alk} - 2882\mathrm{FA} * \mathrm{Cem} - 1951\mathrm{Alk}^2$$

**Table 4.8 : Regression model of BFS and significance of the information provided by the various coefficients.**

| | | $Na^+$ | | | $K^+$ | | | $OH^-$ | | |
|---|---|---|---|---|---|---|---|---|---|---|
| Type of effect | Relative uncoded variable | Coeff | t-value | Prob. | Coeff | t-value | Prob. | Coeff | t-value | Prob. |
| | (Intercept) | 301 | 62 | 0 | 163 | 48 | 0 | 463 | 87 | 0 |
| Main | GG | 18 | 6 | 0 | -25 | -12 | 0 | -7 | -2 | 5 |
| | BFS | -61 | -20 | 0 | -36 | -20 | 0 | -95 | -30 | 0 |
| | Alk | 51 | 20 | 0 | 37 | 18 | 0 | 88 | 24 | 0 |
| | Day | 13 | 5 | 0 | -14 | -8 | 0 | - | - | - |
| Low | GG*BFS | -6 | -2 | 13 | 10 | 4 | 0 | - | - | - |
| | GG*Alk | -4 | -1 | 22 | -7 | -3 | 0 | -11 | -3 | 1 |
| | GG*Day | 6 | 2 | 4 | 6 | 3 | 0 | 12 | 3 | 0 |
| | GG*Cem | - | - | | - | - | 0 | - | - | - |
| | BFS *Alk | -22 | -7 | 0 | -14 | -7 | 0 | -37 | -10 | 0 |
| | BFS *Day | -5 | -2 | 11 | | | | - | - | - |
| | BFS *Cem | -31 | -5 | 0 | -11 | -2 | 2 | -46 | -7 | 0 |
| | Alk*Day | - | - | - | | | | -6 | -2 | 8 |
| Optimum/Pessimum | $Alk^2$ | 10 | 2 | 3 | -6 | -3 | 0 | -37 | -7 | 0 |
| Model information | | $R^2$=0.91, N=108 $R^2_{Prediction}$ =0.89 | | | $R^2$=0.94, N=108 $R^2_{Prediction}$=0.93 | | | $R^2$=0.95, N=108 $R^2_{Prediction}$=0.94 | | |
| Model significance | | p. for $F_0$=2.2e-16, Cor.=0.96 | | | p. for $F_0$= 2.2e-16, Cor.=0.97 | | | p. for $F_0$= 2.2e-16, Cor.=0.95% | | |

Equation 11

$$[\mathrm{Na}^+] = 341 + 159\mathrm{GG} + 829\mathrm{BFS} + 225\mathrm{Alk} - 1193\mathrm{GG} * \mathrm{BFS} - 251\mathrm{GG} * \mathrm{Alk} - 2\mathrm{GG} * \mathrm{Day} - 725\mathrm{BFS} * \mathrm{Alk} - 1\mathrm{BFS} * \mathrm{Week} - 2053\mathrm{BFS} * \mathrm{Cem} + 103\mathrm{Alk}^2$$

Equation 12

$$[\mathrm{K}^+] = -181 - 1071\mathrm{GG} - 45\mathrm{BFS} + 1266\mathrm{Alk} + 2029\mathrm{GG} * \mathrm{BFS} - 449\mathrm{GG} * \mathrm{Alk} + 2\mathrm{GG} * \mathrm{Day} - 464\mathrm{BFS} * \mathrm{Alk} - 737\mathrm{BFS} * \mathrm{Cem} - 485\mathrm{Alk}^2$$

Equation 13

$$[\mathrm{OH}^-] = 157 - 695\mathrm{GG} + 937\mathrm{BFS} + 1498\mathrm{Alk} - 698\mathrm{GG} * \mathrm{Alk} + 2\mathrm{GG} * \mathrm{Day} - 1187\mathrm{BFS} * \mathrm{Alk} - 3074\mathrm{BFS} * \mathrm{Cem} + -381\mathrm{Alk}^2$$

### 4.4.3 Model Accuracy

Three of the paste mixtures were made and the pore solution extracted and analyzed in tri- or duplicates at 28 and 182 days. The results from the 11 paste samples obtained from separated extractions were excluded from the dataset used to build the regression model and the 33 observations (i.e.: $[Na^+]$, $[K^+]$ and $[OH^-]$ for 11 solutions) were rather used to assess the accuracy of the regression models. The results of the model predictions versus the experimental data are presented in Table 4.9. Equations 8 to 13 were used to compute the predicted values presented in Table 4.9.

**Table 4.9 : Predicted values compared to experimental "check points" excluded from the dataset used to build the models.**

| Mixture | Age | $[Na^+]$ (mmol/L) | | | $[K^+]$ (mmol/L) | | | $[OH^-]$ (mmol/L) | | |
|---|---|---|---|---|---|---|---|---|---|---|
| | | Predict. | Exp. | Diff. | Predict. | Exp. | Diff. | Predict. | Exp. | Diff. |
| 15GG-22.5FA-1.08Alk* | 28 | 315 | 295 | 6% | 146 | 160 | -14% | 456 | 456 | 0% |
| | | | 314 | 0% | | 140 | 4% | | 454 | 0% |
| | | | 317 | -1% | | 140 | 4% | | 458 | 0% |
| | 182 | 114 | 109 | 5% | 114 | 109 | 4% | 465 | 452 | -3% |
| 15GG-30BFS-1.08Alk* | 28 | 314 | 315 | 0% | 187 | 166 | 11% | 500 | 511 | 3% |
| | | | 324 | -3% | | 186 | 1% | | 472 | 5% |
| | | | 300 | 3% | | 178 | 5% | | 491 | 2% |
| | 182 | 339 | 355 | -5% | 153 | 136 | 11% | 490 | 491 | 0% |
| 30GG-20FA-1.25Alk** | 28 | 394 | 385 | 2% | 91 | 116 | -27% | 505 | 502 | 1% |
| | | | 390 | 1% | | 107 | -18% | | 498 | 1% |
| | 182 | 468 | 440 | 6% | 53 | 76 | 4% | 562 | 516 | -8% |

Points located *inside and **outside of the experimental region

## 4.5 Discussion

### 4.5.1 Interpretation of the Effects of The Variables

In Table 4.7 and Table 4.8, "Main" corresponds to the average effects of the principal variables of the model. For example, in the $Na^+$ numerical model presented in Table 4.7, "GG" and "FA" have coefficients of 21 and -44, which suggest that the effect of "FA" is about double of that of "GG" and in the opposite direction since the signs are opposed.

Table 4.10 presents the experimental $[Na^+]$ at 28 days as well as the average effects at 28 and 182 days, which are in accordance with the latter statements since the average effect of FA is a reduction of 85 mmol/L and the

average effect of GG is an increase of 39mmol/L. In a ternary diagram, the "main" effect appears as parallel lines with no curvatures.

In the absence of synergy between the variables, the model is simple enough so that the average effect alone can accurately predict the behavior. When a synergy or an interaction is happening between the variables, the average effect alone lacks accuracy in explaining the results. Indeed, a closer look at

Table 4.10 suggests that the "reducing effect" of FA on [$Na^+$] is more important when 20% GG is used (instead of 10%), which is in accordance with the "-9" interaction coefficient for GG*FA in Table 4.7. This same GG*FA interaction of -9 can also be interpreted as that "sodium enhancing" effect of GG on [$Na^+$] is less important when 30% FA is used. Such lower interaction effects are labeled as "low" in Table 4.7. In a ternary diagram, "low" effects induce curvature to the contour lines while they might "tighten" / "loosen" the contour lines in certain areas of the graph.

**Table 4.10 : [$Na^+$] in mmol/L of the pore solution at 28 days of pastes made with the three "cement" alkali contents and various contents of GG and FA.**

| | C1 (0.63% $Na_2Oeq$) | | | C2 (0.94% $Na_2Oeq$) | | | C2 +NaOH (1.25% $Na_2Oeq$) | | |
|---|---|---|---|---|---|---|---|---|---|
| %GG→ % FA↓ | 10 | 20 | Diff. GG | 10 | 20 | Diff. GG | 10 | 20 | Diff. GG |
| 15 | 248 | 301 | +53 | 282 | 341 | +59 | 380 | 443 | +63 |
| 30 | 201 | 211 | +10 | 232 | 254 | +22 | 283 | 307 | +24 |
| Diff. FA | -47 | -90 | | -50 | -87 | | -97 | -136 | |

Average effect of FA: -85 Average effect of GG: +39

The "Optimum/Pessimum" effect indicates a parabolic shape where a Maximum (negative coefficient) or Minimum (positive coefficient) appears. A coefficient of a negative sign was detected in [$K^+$] and [$OH^-$] regression model for the "$Alk^2$" parameter, thus suggesting a "maximum" concentration related to a specific $Na_2O_{eq}$ content. A positive coefficient for the "$Alk^2$" parameter for the [$Na^+$] regression model suggests that there is a specific $Na_2Oeq$ content for which the [$Na^+$] is a "minimum". It worth mentioning that although "Optimum" and "Pessimum" were detected by the model, they were not always observed within the range of observations of the experimental program.

### 4.5.2 Graphical Layout of The Results

The shape of the surface response on ternary diagrams and the related equation were considered the best tools to discuss the trends revealed by the multivariate experimental plan. The ternary diagrams presented in this section are constructed with decreasing proportions of the analysed components (GG, FA/BFS and cement) moving from the tip towards the opposite side of the triangle; the corresponding gradations appear on the side located clockwise. For example, the GG parameter ranges from 0.35 (35%) at the top to 0.10 (10%) at the bottom of the diagram (e.g. Figure 4.12); the "working range" for GG in this study ranges between 10% and 20% and is indicated with dashed lines in the graphs, which also are the borders of the "experimental region".

The ternary graphs include contour lines representing the computed $[Na^+]$, $[K^+]$ and $[OH^-]$ that compose the surface responses resulting from data processing. Indications on the accuracy of the computed data against the experimental data, as well as the confidence interval of the surface responses, can be found in Annex C of this paper (i.e. *Data from the model*, i.e. $[Na^+]$, $[K^+]$ or $[OH^-]$ and min / max values).

In the following sections, the contour lines will be discussed by comparing the orientation of the contour lines against an axis relative to a component. For instance, contour lines parallel or near parallel to an axis suggest that the proportion of this specific component has no/little influence on the response; on the other hand, when contour lines are perpendicular or near perpendicular to an axis, it can be interpreted that the component has the strongest impact on the response.

### 4.5.3 Impact of Mixture Design on $[Na^+]$ in the Pore Solution of Pastes

Figure 4.12 a) presents $[Na^+]$ at 182 days of pastes made with the C2 cement, 10% to 20% GG and 15 to 30% FA. The contour lines being near parallel to the Cem axis (orange line) suggest that the cement content of the mixture design has little impact on $[Na^+]$. An "intermediate" orientation (curvature) of the contour lines between the GG axis (red line) and the FA axis (blue line) suggests that both GG and FA have a significant influence on $[Na^+]$. Indeed, in Table 4.7 the coefficient of -44 for FA means that increasing the FA content tends to lower $[Na^+]$, while the coefficient of 21 for GG means that increasing GG tends to increase $[Na^+]$; as mentioned before, the impact on $[Na^+]$ of FA is inversed and roughly twice that of GG.

For example, following the horizontal dashed line in Figure 4.12 from right to left indicates that increasing the FA content from 15% to 30% in a 20% GG system results in a reduction in $[Na^+]$ from 400 mmol/L to ≈290mmol/L. On the other hand, following the diagonal dashed line, standing for the pastes incorporating 30% FA, shows that increasing GG from 10% to 20% increases $[Na^+]$ from ≈260 mmol/L to ≈290 mmol/L.

Figure 4.13 presents the effect of FA and GG on [$Na^+$] for given contents of FA, GG and "cement" $Na_2Oeq$. In this context, incremental amounts of 15% or 1%FA are associated to [$Na^+$] reduction of 90 or 6 mmol/L, while incremental amounts of 10% or 1% GG are associated to [$Na^+$] increase of 50 or 5 mmol/L. Consequently, a FA:GG ratio of 6:5 results in a neutral effect on [$Na^+$]; however, [$Na^+$] is expected to decrease for a ratio above that value (more FA) and to increase for a ratio below that value (more GG).

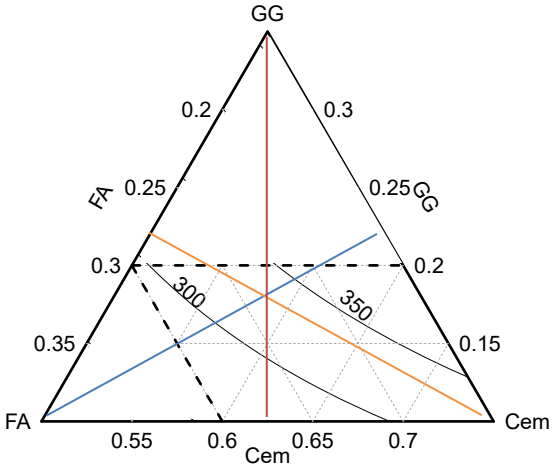


**Figure 4.12: Ternary diagram of the surface response for the [$Na^+$] of pastes aged 182 days made with cement C2 (0.94% $Na_2Oeq$) and containing various percentages of GG and FA.**

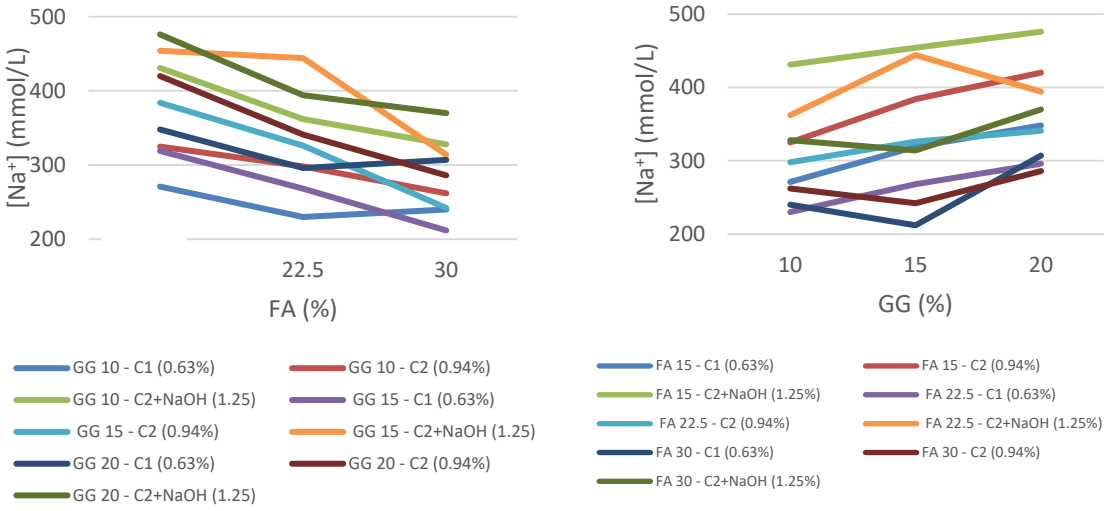


**Figure 4.13 : Average [$Na^+$] at 182 days of pastes containing various contents of GG and FA and made with cements C1 (0.63% $Na_2Oeq$), C2 (0.94% $Na_2Oeq$) and C2 + NaOH (1.25% $Na_2Oeq$).**

Figure 4.14 presents the effect of BFS and GG on [$Na^+$] for given contents of BFS, GG and "cement" $Na_2Oeq$. For mixtures incorporating BFS, trends are similar but the average [$Na^+$] reduction associated to an incremental amount of 20% or 1% BFS are respectively 67 or 3mmol/L, while the average [$Na^+$] increase associated to an incremental amount of 10% or 1% GG are respectively 19 or 2mmol/L. A rough threshold ratio for neutrality of the two SCMs would thus be 3:2 for BFS:GG, while [$Na^+$] is expected to decrease for a ratio above that value (more BFS) and to increase slightly for a ratio below that value (more GG).

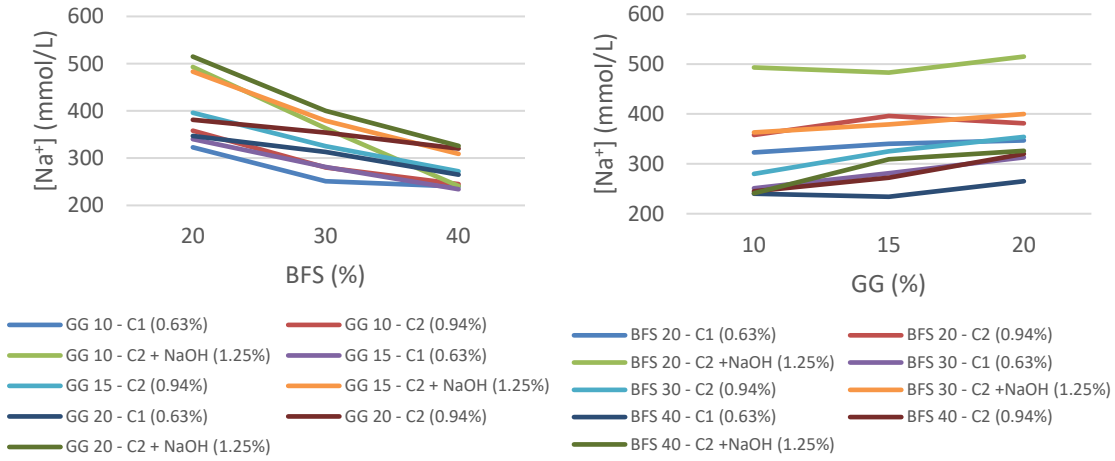


**Figure 4.14 : Average [$Na^+$] at 182 days of pastes containing various contents of GG and BFS and made with cements C1 (0.63% $Na_2Oeq$), C2 (0.94% $Na_2Oeq$) and C2 + NaOH (1.25% $Na_2Oeq$).**

### 4.5.4 Effect of the Mixture Proportion on [$K^+$] in the Pore Solution of Pastes

In Table 4.7, the coefficient for "GG" and "FA" regarding the [$K^+$] are respectively -16 and -25, which indicate that they have a somewhat similar influence in reducing [$K^+$] in the pore solutions analysed. The coefficients "GG*FA" and "FA*Cem" are respectively -8 and -22, which suggest that interactions modulate the effect of GG and FA. Figure 4.15 presents the surface response of [$K^+$] at 28 days (a to c) and 182 days (d to f) for pastes made with various amounts of GG/FA and cements C1, C2 or C2 + NaOH. On the left side of the "experimental region", i.e. for lower cement and higher FA contents, "near horizontal" contour lines indicate that the "GG" parameter has a high impact on [$K^+$]; this trend seems to be somewhat better defined at 182 days. Indeed, on the left side of the ternary diagrams (with at least 25%FA), higher dosages of GG are associated with lower [$K^+$]. However, on the right side of the diagram, i.e. for higher cement or lower FA contents, the contour lines are near vertical; this indicates that the GG content has no effect on [$K^+$] in such conditions. In other words, if 15% to 25% of FA are used, FA rather than GG will reduce [$K^+$] in the pore solution.

When comparing the effect of the "cement" alkali content in Figure 4.15 it can be noticed that for mixtures with higher $Na_2Oeq$ contents, contour lines tend to be near vertical in a greater portion of the diagram; this suggests that cements with higher contents of $Na_2Oeq$ allow FA to take over GG in reducing $[K^+]$ (especially at 28 days). It is worth noting that the $K_2O$ contents of C1, C2, GG and FA are respectively 0.62%, 1.02%, 0.66% and 0.65%. In the case of pastes made with C1, GG and FA do not contribute in diluting the alkalis of cement; hence, the observed reduction in $[K^+]$ can be explained by the slower reactivity of those materials, different release potential between the above materials, and/or by the fact that the pozzolanic materials tend to generate C-S-H with lower Ca/Si ratio, which are often thought to have the capability of incorporating more alkali ions in their structure or on their surface. However, microstructural analyses of paste specimens would be required to confidently associate the trend observed to any specific phenomenon. In the case of pastes made with C2, increased cement replacements do contribute at diluting the total potassium content in the systems; however, if $[K^+]$ was essentially controlled by dilution-related phenomena, the contour lines would be perpendicular to the "Cem" axis, which is not the case. Also, one can note that the addition of NaOH influences $[K^+]$ to a certain extent since the ternary diagrams presenting pastes made with cement C2 (Figure 4.15b & e) and C2 + NaOH (Figure 4.15c and f) are somewhat different.

Figure 4.16 presents the surface response of $[K^+]$ at 28 days (a to c) and 182 days (d to f) for pastes made with various cements and amounts of GG/BFS. The main trend is illustrated by contours lines that are nearly perpendicular to the "Cem" axis in most parts of the ternary diagrams, which suggests that lower $[K^+]$ are associated to lower cement contents in the system (dilution effect). For mixtures made without NaOH addition (cements C1 and C2), the orientation of the contour lines tends to be more aligned, at least in certain portions of the diagrams at 182 days, with GG and BFS axes when the contents of the two are increasing; this suggests that sufficient amounts of either of GG or BFS are required to observe a reduction effect on $[K^+]$. For GG-BFS ternary cement pastes made with C2 + NaOH Figure 4.16c and f), neither GG nor BFS seem to be more effective than the other in reducing $[K^+]$. They are probably still contributing in reducing $[K^+]$, and they might work with similar reach, since absolute values of $[K^+]$ in the pore solution are lower when NaOH is added to the mixture compared to the same combinations of GG and BFS without NaOH addition (when sufficient amounts are used).

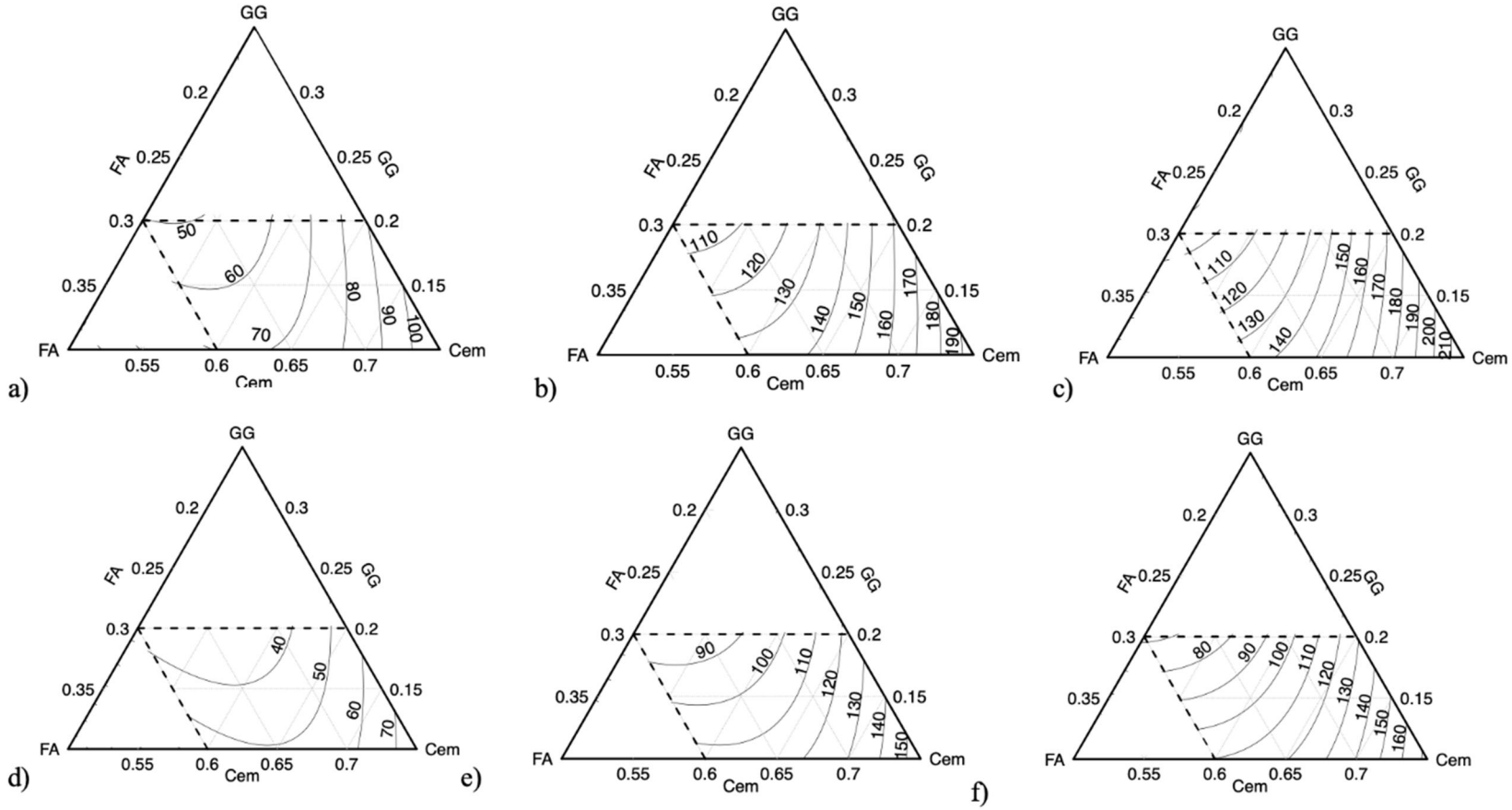


**Figure 4.15 : Ternary diagrams of the surface response for the [$K^+$] in the pore solution of ternary mixtures incorporating various amounts of GG/FA and made with the following cements : C1 (0.63% $Na_2Oeq$) cement aged a) 28 days and d) 182 days; C2 (0.94% $Na_2Oeq$) aged b) 28 days and e) 182 days and C2 + NaOH (1.25% $Na_2Oeq$) aged c) 28 days and f) 182 days**

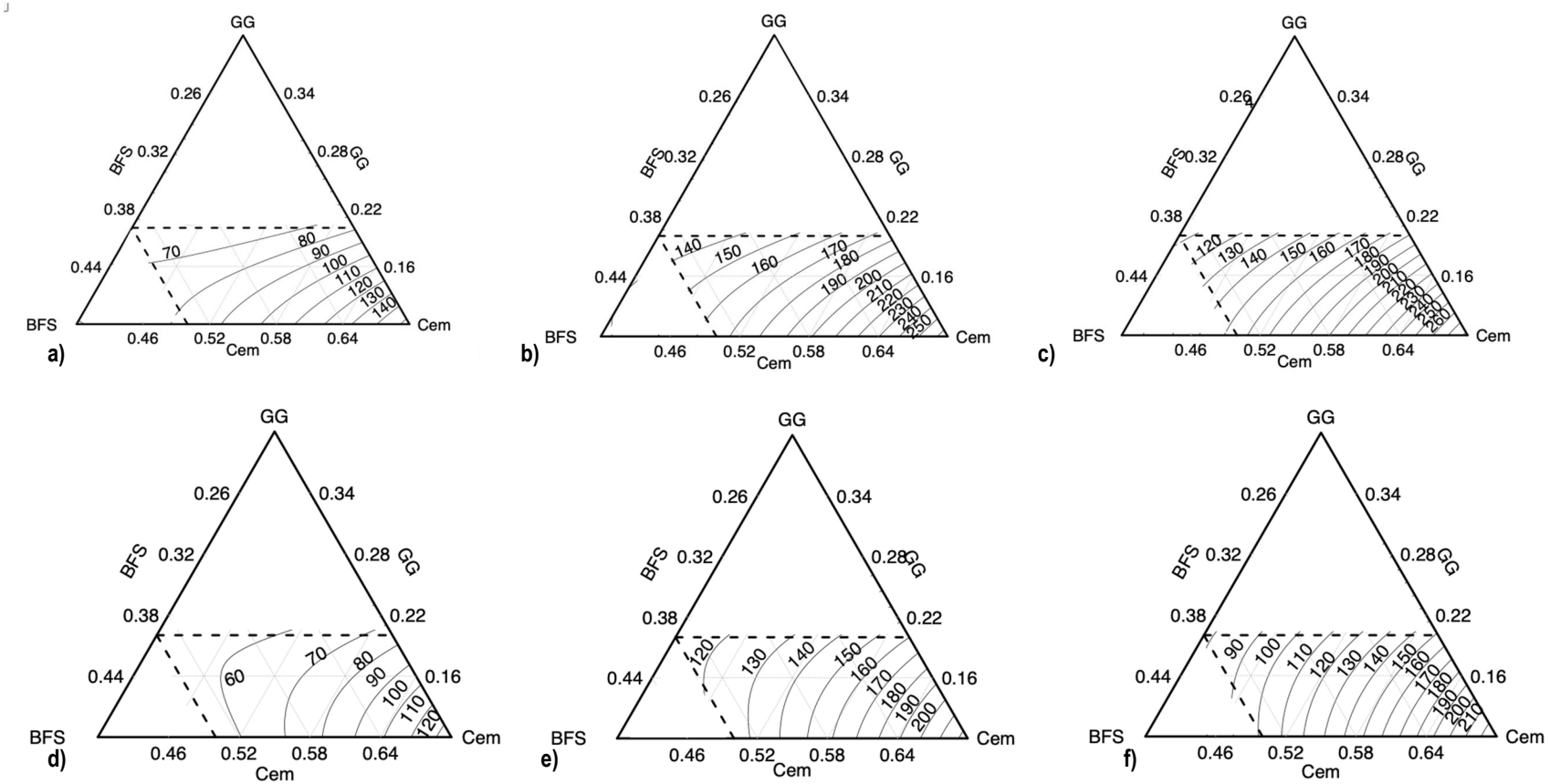


**Figure 4.16 : Ternary diagrams of the surface response for the [$K^+$] in the pore solution of ternary mixtures incorporating various amounts of GG/BFS and made with the following cements : C1 (0.63% $Na_2Oeq$) cement aged a) 28 days and d) 182 days; C2 (0.94% $Na_2Oeq$) aged b) 28 days and e) 182 days; and C2 +NaOH (1.25% $Na_2Oeq$) aged c) 28 days and g) 182 days.**

### 4.5.5 Effect of the Mixture Proportion on [$OH^-$] in the Pore Solution Of Pastes

A coefficient of -72 is associated to the "FA" variable regarding the [$OH^-$] in Table 4.7, while a coefficient of only 7 is associated to "GG". This suggests that for a given FA content, higher contents of GG are associated to very modest increments of [$OH^-$]. In Figure 4.17, this observation is illustrated by contour lines that are more or less perpendicular to the FA axis. The somewhat stronger tilt between Figure 4.17 a) and b) indicates that for pastes made with cement C1 (0.63% $Na_2Oeq$), GG will eventually and modestly release its alkalis, thus contributing at increasing [$OH^-$] in the pore solution; however, the latter trend does not seem to stand as much for mixtures made with cement C2 (0.94% $Na_2Oeq$) and C2 + NaOH (1.25% $Na_2Oeq$).

Table 4.11 presents more detailed effects of FA and GG on the [$OH^-$] in the pore solution of such systems. There is a constant trend suggesting that when only 15%FA are used, increasing GG from 10 to 20% increases [$OH^-$] and the increment is generally more important at 182 days (except for the C2 + NaOH mix). On the other hand, when 30% FA are used, this same trend is generally reversed (5 out of 6 cases), which suggest a synergetic effect between the two SCMs for reducing [$OH^-$]. The fact that increasing the FA content from 15 to 30% generally results in higher reductions in [$OH^-$] when 20% of GG is used also supports the idea of a synergy between FA and GG.

**Table 4.11: [$OH^-$] in mmol/L of the pore solution at 28 and 182 days of pastes incorporating the three cements and various contents of GG and FA.**

| Time | | C1 (0.63% $Na_2Oeq$) | | | C2 (0.94% $Na_2Oeq$) | | | C2 + NaOH (1.25% $Na_2Oeq$) | | |
|---|---|---|---|---|---|---|---|---|---|---|
| | %GG→ ↓% FA | 10 | 20 | Diff. GG | 10 | 20 | Diff. GG | 10 | 20 | Diff. GG |
| 28 days | 15 | 360 | 385 | +25 | 508 | 517 | +9 | 604 | 619 | +15 |
| | 30 | 279 | 266 | -13 | 381 | 359 | -22 | 420 | 408 | -12 |
| | Diff. FA | -81 | -119 | | -127 | -158 | | -184 | -211 | |
| 182 days | 15 | 347 | 408 | +61 | 457 | 560 | +103 | 595 | 598 | +3 |
| | 30 | 290 | 355 | +65 | 366 | 357 | -9 | 455 | 442 | -13 |
| | Diff. FA | -57 | -53 | | -91 | -203 | | -140 | -156 | |

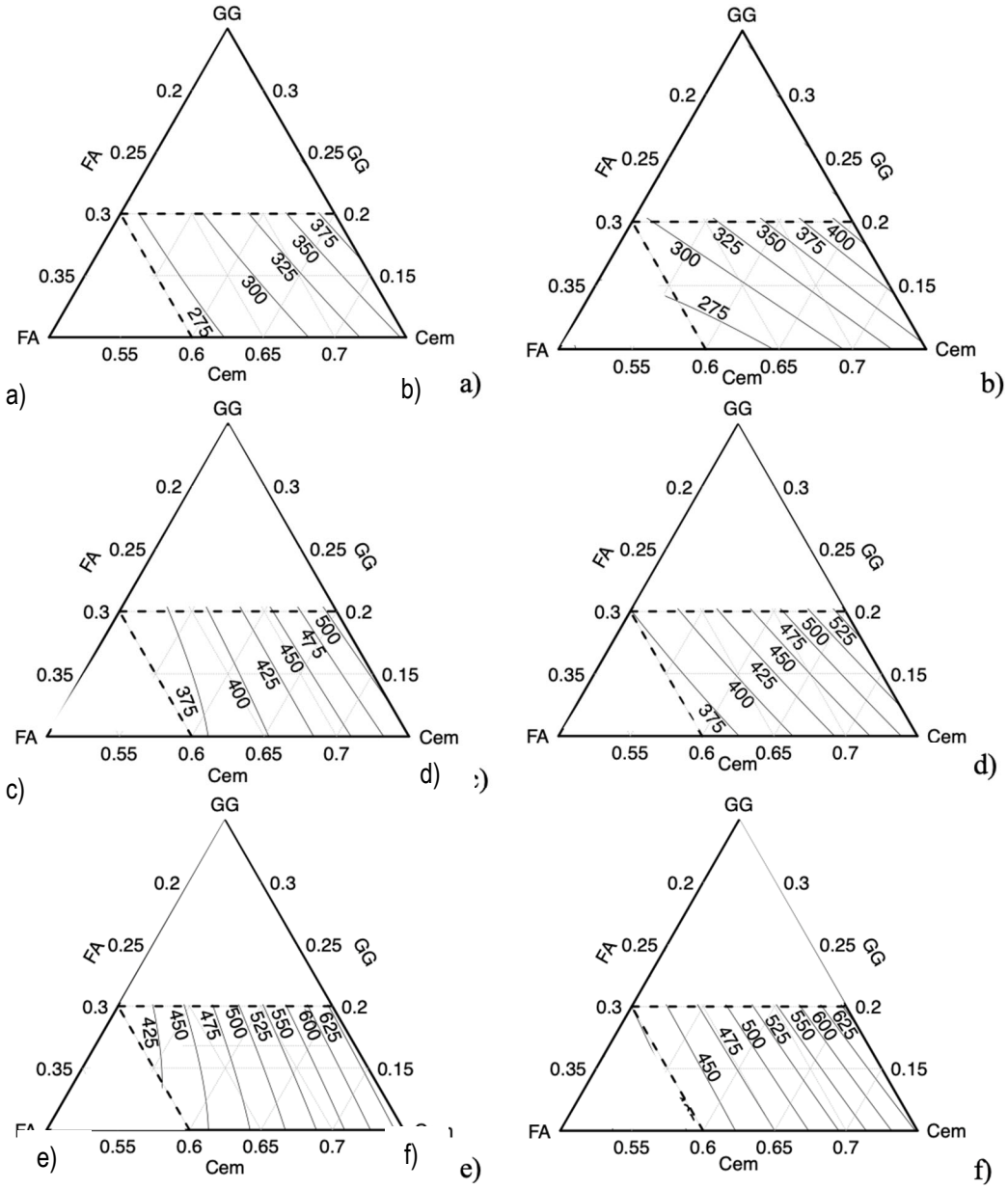


**Figure 4.17 : Ternary diagrams of the surface response for the [$OH^-$] in the pore solution of ternary mixtures incorporating various amounts of GG/FA and made with the following cements : C1 (0.63% $Na_2Oeq$) cement aged a) 28 days and b) 182 days; C2 (0.94% $Na_2Oeq$) aged c) 28 days and d) 182 days ; and C2 + NaOH (1.25% $Na_2Oeq$) aged e) 28 days and f) 182 days.**

Figure 4.18 shows that the trends mentioned before for FA are similar with BFS. Indeed, contour lines nearly perpendicular to the "BFS" axis indicate that this parameter is the most significant element related to [$OH^-$]. Similarly, increased GG contents are associated to modest increases in [$OH^-$] in the pore solution and this is especially the case for cement with lower $Na_2Oeq$ contents.

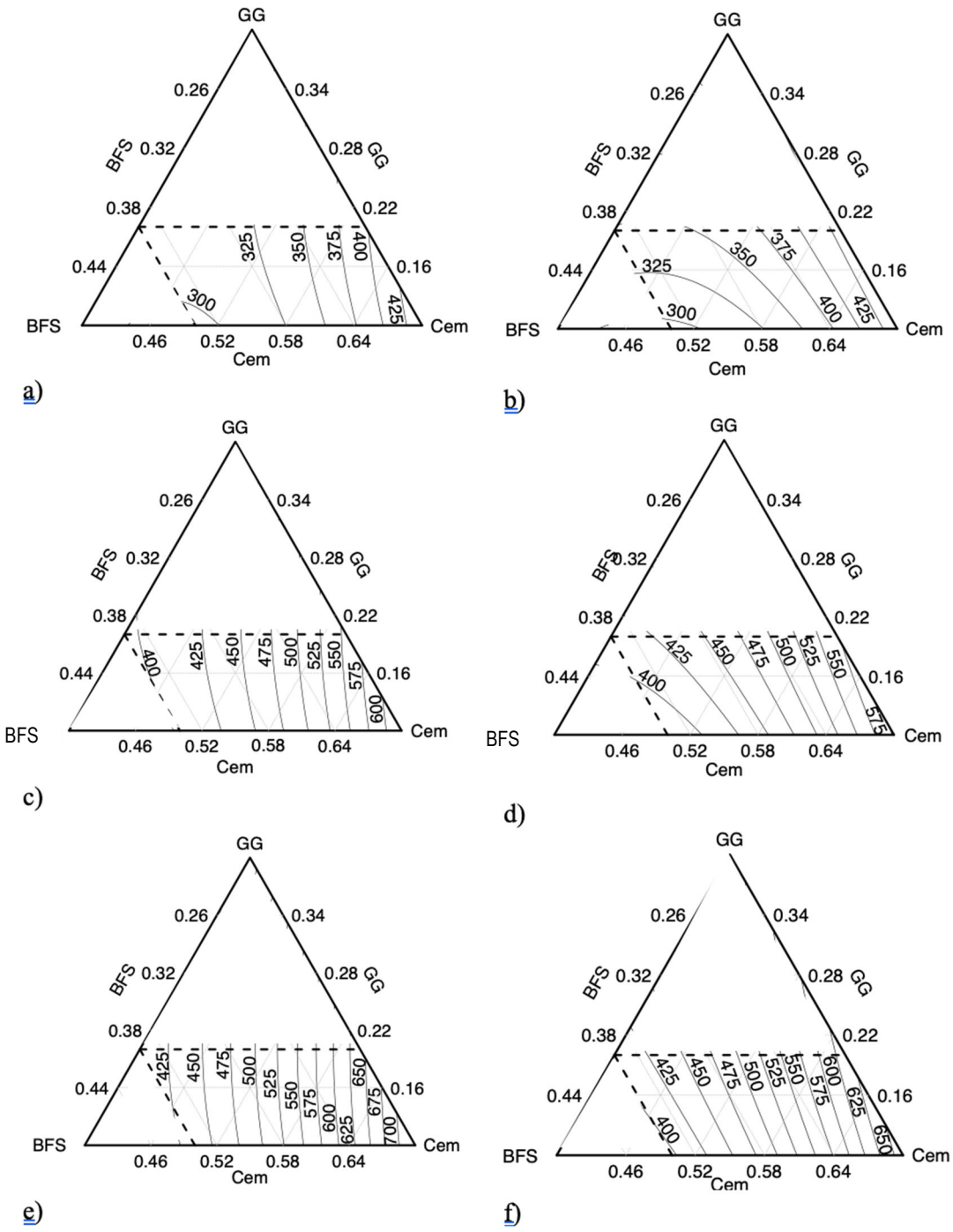


**Figure 4.18 : Ternary diagrams of the surface response for the [$OH^-$] in the pore solution of ternary mixtures incorporating various amounts of GG/BFS and made with the following cements : C1 (0.63% $Na_2Oeq$) cement aged a) 28 days and b) 182 days; C2 (0.94% $Na_2Oeq$) aged c) 28 days and d) 182 days ; and C2 +NaOH (1.25% $Na_2Oeq$) aged e) 28 days and f) 182 days.**

Table 4.12 presents more detailed effects of the GG and BFS variables on the [$OH^-$] in the pore solution. The data suggest that the effect of GG greatly varies depending on the BFS and $Na_2Oeq$ contents. This table also

suggest a synergetic effect between GG and BFS since the impact of GG is different for different levels of BFS and vice versa; however, this synergy is not constant. In general, when 20% BFS are used, increasing GG from 10 to 20% decreases [$OH^-$] in the pore solution (5 out of 6 cases), while the opposite is observed at the 40% BFS content (5 out of 6 cases); however, the magnitude of those variations varies significantly. On the other hand, contrary to the FA/GG systems, the impact of increasing BFS contents from 20 to 40% on reducing [$OH^-$] is always more significant when 10% of GG is used. A synergetic effect between GG and BFS in reducing [$OH^-$] in the pore solution thus appear unclear.

**Table 4.12 : [$OH^-$] in mmol/L of the pore solution at 28 and 182 days of pastes made with the three cements and various contents of GG and BFS.**

| Time | | C1 (0.63% $Na_2Oeq$) | | | C2 (0.94% $Na_2Oeq$) | | | C2 + NaOH (1.25% $Na_2Oeq$) | | |
|---|---|---|---|---|---|---|---|---|---|---|
| | %GG→ ↓% BFS | 10 | 20 | Diff. GG | 10 | 20 | Diff. GG | 10 | 20 | Diff. GG |
| 28 days | 20 | 454 | 393 | -61 | 644 | 549 | -95 | 740 | 650 | -90 |
| | 40 | 307 | 321 | +14 | 372 | 386 | +14 | 471 | 413 | -58 |
| | Diff. BFS | -147 | -72 | | -272 | -163 | | -269 | -237 | |
| 182 days | 20 | 424 | 438 | +14 | 620 | 568 | -52 | 709 | 664 | -45 |
| | 40 | 311 | 327 | +16 | 386 | 430 | +44 | 338 | 416 | +78 |
| | Diff. BFS | -113 | -111 | | -234 | -138 | | -371 | -248 | |

### 4.5.6 The "Alk" Parameter or the $Na_2O_{eq}$ Content Of Cement

The coefficient of the "Alk" parameter was computed at values of 60, 35 and 97 for [$Na^+$], [$K^+$] and [$OH^-$], respectively, in FA/GG-bearing pastes (Table 4.7) and at values of 51, 37 and 88 for [$Na^+$], [$K^+$] and [$OH^-$], respectively, in BFS/GG-bearing pastes (Table 4.8). This is indicating that cements with higher $Na_2O_{eq}$ content promote higher concentrations of those three species in solution. Computational analysis also suggests that increasing the $Na_2Oeq$ between 0.94% and 1.25% has an effect that can be counteracted by increasing BFS contents in the system from 20% to 40% because "BFS" > "Alk" in absolute value. This is however not the case when increasing FA content from 15% to 30% (since "FA"< "Alk" in absolute value). It is worth noting that, in FA and BFS-bearing systems, the effect on [$Na^+$] of increasing the GG content from 10% to 20% is approximately only one third of that of increasing the $Na_2O_{eq}$ content from 0.94% to 1.25%. In other words, the release associated to the use of 10%GG is comparable to an increase in the $Na_2O_{eq}$ content of the cement by 0.10%.

"FA*Alk" and "BFS*Alk" interactions were detected for the [$OH^-$] response with coefficients of respectively -22 (Table 4.7) and -37 (Table 4.8); this indicates that the raise in alkalinity induced by an increase in "cement" alkali content is lower when higher dosages of FA/BFS are used compared to pastes with low dosage of FA/BFS.

Similarly, “GG*Alk” was detected in FA and BFS-bearing pastes with coefficients of respectively -10 (Table 4.7) and -11 (Table 4.8); this indicates that the increase in [$OH^-$] in the pore solution associated to an increase in ”cement’ alkali content is relatively less important in pastes with high dosages of GG than in paste with low GG contents.

### 4.5.7 The “Day” Parameter

For FA/GG-bearing pastes, the coefficient of the “Day” parameter is positive for [$Na^+$] (+19) and negative for [$K^+$] (-15) and both coefficients are of similar order of magnitude (Table 4.7). Not surprisingly, those two effects somehow compensate each other and the alkalinity of the pore solution over time is estimated to be stable as expressed by a coefficient of only 4 for [$OH^-$]. In the case of BFS/GG-bearing pastes, the time effect is similar since the “Day” coefficient for [$Na^+$] is 13, and -14 for [$K^+$], while no time effect was detected for [$OH^-$].

Over the time, computations showed that the [$Na^+$] in pore solutions tend to increase more with higher GG contents since the coefficients for the “GG*Day” interactions are 5 (FA systems; Table 4.7) and 6 (BFS systems; Table 4.8); this suggests that GG released only a slight amount of $Na^+$ between 28 and 182 days in those systems.

For the [$OH^-$] response, the “GG*Day” interactions, with coefficients of 8 (FA systems; Table 4.7) and 12 (BFS systems; Table 4.8), indicated that GG contributed in raising the alkalinity in the pore solution between 28 and 182 days.

## 4.6 Conclusion

Previous research has shown that the composition of the pore solution is the key to limit the alkali-silica reactivity of concrete aggregates. Since it was found that high-alkali GG shows a somewhat limited effectiveness in reducing expansion in binary concretes due to ASR, this study was conducted to better understand the potential effect, on the pore solution composition, of paste specimens made with cements of different alkali contents and different proportions of a high-alkali GG (10 to 20%) blended with fly ash (FA) (15 to 30%) or blastfurnace slag (BFS) (20 to 40%). The paste compositions were selected according to a specific experimental plan and the pore solution of those pastes was extracted after 28 and 182 days of storage in hermetic plastic containers at 38°C. Pore solutions were then analyzed for Na and K content and data were processed using a *Response Surface Methodology* (RSM) approach.

The following conclusions can be drawn from this research work :

### 4.6.1 Effect of GG Combined with FA/BFS on the [$Na^+$] in the Pore Solution

Generally speaking, GG releases a small amount of sodium into the pore solution. When combined with GG, FA and BFS did not have the same impact on the pore solution composition and the differences are the following :

1) In ternary paste mixtures incorporating GG and FA, GG released small amounts of $Na^+$ ions into the pore solution. The Na release was proportionally more important with a cement of low-alkali content (0.63% $Na_2O$eq). For pastes made with a high-alkali cement with alkalis boosted to 1.25% $Na_2O$eq, by cement mass, no significant contribution of GG to the [$Na^+$] in the pore solution was measured;
2) In ternary paste mixtures incorporating GG and BFS, GG released small amounts of $Na^+$ ions into the pore solution. High alkali (cement) content coupled to high BFS content tend to show low [$Na^+$] for various GG contents. According to experimental data and associated computations, the average $Na^+$ contribution to the pore solution by 10%GG can be counteracted by, in average, 12% FA and 15% BFS.

### 4.6.2 Effect of GG Combined with FA/BFS on the [$K^+$] in the Pore Solution

Overall, GG tends to lower [$K^+$]. More precisely for each SCMs, [$K^+$] is modulated according to the following :

1) In ternary paste mixtures incorporating 10 to 20% GG and FA, GG lowered [$K^+$] in the pore solution when 25% of FA or more was used. For FA contents ranging between 15% and 25%, GG showed little effect on [$K^+$] in the pore solution.
2) In ternary paste mixtures incorporating GG and BFS, the lowering effect of GG and BFS on [$K^+$] in the pore solution was found to be similar.

3) In ternary paste mixtures incorporating GG and BFS, lower [$K^+$] are associated to cementitious blends with lower cement contents (i.e. higher SCMs contents).

### 4.6.3 Effect of GG Combined with FA/BFS on the [$OH^-$] in the Pore Solution

The overall effect of GG on [$OH^-$] is often negligible; however, the following elements are worth noticing :

1) In ternary paste mixtures incorporating GG and FA, the presence of GG results in a small rise in the alkalinity when a low-alkali cement is used, but has almost no effect when a cement with added alkalis (NaOH) is used. In such systems, the FA content is, by far, the parameter with the largest influence on [$OH^-$] in the pore solution, i.e. more than other parameters such as the GG content, the “cement” alkali content and the cement content.

2) In ternary paste mixes incorporating GG and BFS, the presence of GG has no significant impact on the alkalinity of the pore solution at 28 days while, at 182 days, it results in a small increase in alkalinity when the low-alkali cement is used. Experimental data and computations suggest that in such systems, the BFS content is the most impactful parameter on the [$OH^-$] in the pore solution, i.e. i.e. more than other parameters such as the GG content, the “cement” alkali content and the cement content.

## 4.7 Acknowledgement

The authors would like to thank the Centre de Recherche des Infrastructure en Béton (CRIB) for the space, equipment and technical support provided. Also, the authors are grateful to the Chaire de recherche de la SAQ and the Centre de Recherche en Sciences Naturelles et en Génie (CRSNG) for their financial support.

## 4.8 References


(WBCSD), W. B. C. f. S. D. (2018). "Technology Roadmap: Low-Carbon Transition in the Cement Industry." Retrieved january 4, 2019, 2018, from https://www.wbcsd.org/Sector-Projects/Cement-Sustainability-Initiative/Resources/Technology-Roadmap-Low-Carbon-Transition-in-the-Cement-Industry.

ASTM C 1260-14. Standard Test Method for Potential Alkali Reactivity of Aggregates. ASTM International, West Conshohocken, PA, USA.

Bussière, I. (2013). Usine de recyclage fermée une montagne de verre prend la poussière. . Québec, Le Soleil. **2020**.

Charles (2013). Dur coup pour le recyclage du verre. LaPresse. Montréal.

CSA A23.2-14A. Potential expansivity of aggregates (procedure for length change due to alkali-aggregate reaction in concrete prisms at 38 °C). In CSA A23.2-19 – Test methods and standard practices for concrete. CSA Group, Mississauga, Ontario, Canada.

CSA A23.2-25A. Test method for detection of alkali-silica reactive aggregate by accelerated expansion of mortar bars. In CSA A23.2-19 – Test methods and standard practices for concrete. CSA Group, Mississauga, Ontario, Canada.

Diamond, S. (1989). ASR-Another Look at Mechanisms. 8th Eight International Conference on Alkali–Aggregate Reaction in Concrete, Kyoto, Japan.

Fernández, Á., J. L. García Calvo and M. C. Alonso (2018). "Ordinary Portland Cement composition for the optimization of the synergies of supplementary cementitious materials of ternary binders in hydration processes." Cement and Concrete Composites **89**: 238-250

Fournier, B. and M.-A. Bérubé (2000). "Alkali-aggregate reaction in concrete: a review of basic concepts and engineering implications." Canadian Journal of Civil Engineering **27**(2): 167-191.

Hong, S.-Y. and F. Glasser (1999). "Alkali binding in cement pastes: Part I. The CSH phase." Cement and Concrete Research **29**(12): 1893-1903.

Hong, S.-Y. and F. P. Glasser (2002). "Alkali sorption by C-S-H and C-A-S-H gels: Part II. Role of alumina." Cement and Concrete Research **32**(7): 1101-1111.

Ke-rui, Y., Z. Cai-wen, L. Zhi-gang, G. Zhi and N. Cong (2004). A study on alkali-fixation ability of CSH gel. 12th International Conference on Alkali-Aggregate Reaction in Concrete, Beijing, China. **120:** 2.

Kupwade-Patil, K. and E. N. Allouche (2013). "Impact of alkali silica reaction on fly ash-based geopolymer concrete." Journal of Materials in Civil Engineering **25**(1): 131-139.

Labbez, C., I. Pochard, B. Jönsson and A. Nonat (2011). "C-S-H/solution interface: Experimental and Monte Carlo studies." Cement and Concrete Research **41**(2): 161-168.

Lawson, J. (2014). Design and Analysis of Experiments with R, Taylor & Francis.

Lawson, J. and C. Willden (2016). "Mixture experiment in R using mixexp." Journal of Statistical Software **72**.

Lenth, R. V. (2009). "Response-Surface Methods in R, Using rsm." Journal of Statistical software **32**(7): 1-17.

Maraghechi, H. (2014). "Development and assessment of alkali activated recycled glass-based concretes for civil infrastructure." Ph. D. Thesis, Pennsylvania State University.

Maraghechi, H., S. Salwocki and F. Rajabipour (2017). "Utilisation of alkali activated glass powder in binary mixtures with Portland cement, slag, fly ash and hydrated lime." Materials and Structures **50**(1): 16.

Montgomery, D. C. (2012). Design and Analysis of Experiments, 8th Edition, John Wiley & Sons.

Montgomery, D. C. and G. C. Runger (2010). Applied Statistics and Probability for Engineers, 5th edition.

Myers, R. H., D. C. Montgomery and C. M. Anderson-Cook (2011). Response Surface Methodology: Process and Product Optimization Using Designed Experiments, Wiley.

Shehata, M. H. (2001). The effects of fly ash and silica fume on alkali-silica reaction in concrete. PhD Thesis, University of Toronto.

Stanton, T. E. (1940). "Expansion of Concrete through Reaction between Cement and Aggregate." Proceedings of the Americain Society of Civil Engineer **66**(10): 1871-1811.

Team, R. C. (2013). R: A Language and Environment for Statistical Computing, R Foundation for Statistical Computing.

Thomas, M. (2011). "The effect of supplementary cementing materials on alkali-silica reaction: A review." Cement and Concrete Research **41**(12): 1224-1231.

U.Laval, D. d. m. e. d. s. d. (2010). "aide-mémoire-stt." Retrieved june, 2018, from https://www.mat.ulaval.ca/fileadmin/mat/documents/CDA/aide-mémoire-mat.pdf.

Warner, S., J. Ideker and K. Schumacher (2012). Alkali-silica reactivity and the role of alumina. International Conference on Alkali Reaction. Austin, Texas.

Zhang, L. and Y. Yue (2018). "Influence of waste glass powder usage on the properties of alkali-activated slag mortars based on response surface methodology." Construction and Building Materials **181**: 527-534.

Zhang, S., A. Keulen, K. Arbi and G. Ye (2017). "Waste glass as partial mineral precursor in alkali-activated slag/fly ash system." Cement and Concrete Research **102**: 29-40.

# Annex A - Replicates

**Table 4.13 : Results of the analysis of replicates from separate pore solution extractions.**

| | | | GG 10% | | GG 15% | | GG 20% | |
|---|---|---|---|---|---|---|---|---|
| FA | Alk | ID | $[K^+]$ | $[Na^+]$ | $[K^+]$ | $[Na^+]$ | $[K^+]$ | $[Na^+]$ |
| | | | (mmol/l) | | (mmol/l) | | (mmol/l) | |
| 15.0 | 0.63 | I | 269 | 108 | 266 | 87 | 297 | 81 |
| 15.0 | 0.63 | II | 244 | 114 | 280 | 93 | 303 | 82 |
| 15.0 | 0.63 | III | 229 | 116 | 289 | 95 | 304 | 88 |
| 15.0 | 0.94 | I | 270 | 223 | 328 | 156 | 324 | 164 |
| 15.0 | 0.94 | II | 296 | 227 | 345 | 164 | 329 | 173 |
| 15.0 | 0.94 | III | 279 | 228 | 333 | 157 | 369 | 192 |
| 15.0 | 1.25 | I | 363 | 225 | 430 | 201 | 438 | 163 |
| 15.0 | 1.25 | II | 386 | 224 | 411 | 168 | 430 | 165 |
| 15.0 | 1.25 | III | 390 | 224 | 426 | 188 | 460 | 201 |
| 22.5 | 0.63 | I | 193 | 71 | 233 | 73 | 260 | 59 |
| 22.5 | 0.63 | II | 221 | 69 | 240 | 65 | 252 | 60 |
| 22.5 | 0.63 | III | 209 | 72 | 238 | 66 | 254 | 62 |
| 22.5 | 0.94 | I | 314 | 159 | 270 | 119 | 263 | 117 |
| 22.5 | 0.94 | II | 267 | 138 | 278 | 140 | 294 | 109 |
| 22.5 | 0.94 | III | 258 | 150 | 273 | 143 | 307 | 109 |
| 22.5 | 1.08 | I | - | - | 296 | 160 | - | - |
| 22.5 | 1.08 | II | - | - | 315 | 140 | - | - |
| 22.5 | 1.08 | III | - | - | 318 | 140 | - | - |
| 22.5 | 1.25 | I | 377 | 149 | 344 | 144 | 340 | 122 |
| 22.5 | 1.25 | II | 377 | 152 | 343 | 143 | 376 | 128 |
| 22.5 | 1.25 | III | 356 | 145 | 363 | 147 | 363 | 117 |
| 30.0 | 0.63 | I | 197 | 75 | 177 | 56 | 185 | 55 |
| 30.0 | 0.63 | II | 207 | 77 | 215 | 55 | 225 | 54 |
| 30.0 | 0.63 | III | 198 | 82 | 219 | 58 | 223 | 55 |
| 30.0 | 0.94 | I | 217 | 147 | 256 | 105 | 243 | 116 |
| 30.0 | 0.94 | II | 241 | 150 | 254 | 99 | 255 | 97 |
| 30.0 | 0.94 | III | 238 | 149 | 243 | 98 | 265 | 100 |
| 30.0 | 1.25 | I | 269 | 136 | 301 | 118 | 292 | 102 |
| 30.0 | 1.25 | II | 299 | 136 | 311 | 103 | 287 | 84 |
| 30.0 | 1.25 | III | 281 | 139 | 340 | 119 | 343 | 115 |
| 20 | 1.25 | I | | | | | 386* | 116* |
| 20 | 1.25 | II | | | | | 390* | 108* |
| 20 | 1.25 | III | | | | | 409* | - |

*30%GG

**Table 4.14 : Results of the analysis of replicates from separate pore solution extractions.**

| | | | GG 10% | | GG 15% | | GG 20% | |
|---|---|---|---|---|---|---|---|---|
| BFS | Alk | ID | $[K^+]$ | $[Na^+]$ | $[K^+]$ | $[Na^+]$ | $[K^+]$ | $[Na^+]$ |
| | | | (mmol/L) | | (mmol/L) | | (mmol/L) | |
| 20.0 | 0.63 | I | 138 | 308 | 105 | 268 | 92 | 304 |
| 20.0 | 0.63 | II | 146 | 306 | 104 | 307 | 61 | 336 |
| 20.0 | 0.63 | III | 152 | 312 | | | 61 | 323 |
| 20.0 | 0.94 | I | 286 | 349 | 224 | 365 | 177 | 349 |
| 20.0 | 0.94 | II | 298 | 368 | 222 | 400 | 207 | 362 |
| 20.0 | 0.94 | III | 306 | 325 | 212 | 391 | 189 | 365 |
| 20.0 | 1.25 | I | 297 | 487 | 205 | 427 | 184 | 476 |
| 20.0 | 1.25 | II | 285 | 426 | 221 | 426 | 188 | 459 |
| 20.0 | 1.25 | III | 280 | 447 | 222 | 437 | 192 | 451 |
| 30.0 | 0.63 | I | 119 | 228 | 95 | 280 | 74 | 231 |
| 30.0 | 0.63 | II | 111 | 172 | 103 | 265 | 54 | 243 |
| 30.0 | 0.63 | III | 123 | 209 | 101 | 288 | 54 | 244 |
| 30.0 | 0.94 | I | 185 | 231 | 201 | 315 | 134 | 316 |
| 30.0 | 0.94 | II | 202 | 284 | 167 | 291 | 142 | 339 |
| 30.0 | 0.94 | III | 213 | 254 | 171 | 297 | 151 | 334 |
| 30.0 | 1.08 | I | - | - | 166 | 315 | - | - |
| 30.0 | 1.08 | II | - | - | 186 | 324 | - | - |
| 30.0 | 1.08 | III | - | - | 178 | 300 | - | - |
| 30.0 | 1.25 | I | 210 | 323 | 150 | 328 | 137 | 332 |
| 30.0 | 1.25 | II | 211 | 359 | 176 | 359 | 141 | 346 |
| 30.0 | 1.25 | III | 209 | 348 | 167 | 353 | 142 | 346 |
| 40.0 | 0.63 | I | 78 | 210 | 69 | 232 | 78 | 220 |
| 40.0 | 0.63 | II | 81 | 229 | 76 | 245 | 65 | 226 |
| 40.0 | 0.63 | III | 83 | 241 | 70 | 239 | 90 | 285 |
| 40.0 | 0.94 | I | 140 | 227 | 138 | 254 | 97 | 262 |
| 40.0 | 0.94 | II | 163 | 200 | 137 | 278 | 121 | 271 |
| 40.0 | 0.94 | III | 168 | 217 | 134 | 252 | 117 | 288 |
| 40.0 | 1.25 | I | 161 | 312 | 124 | 262 | 106* | 291* |
| 40.0 | 1.25 | II | 169 | 309 | 128 | 297 | 122 | 299 |
| 40.0 | 1.25 | III | 161 | 303 | 136 | 297 | 127 | 309 |
| 40 | 1.25 | I | | | | | 112* | 286* |

*Different batches

# Annex B – Regression Model Validation Plot

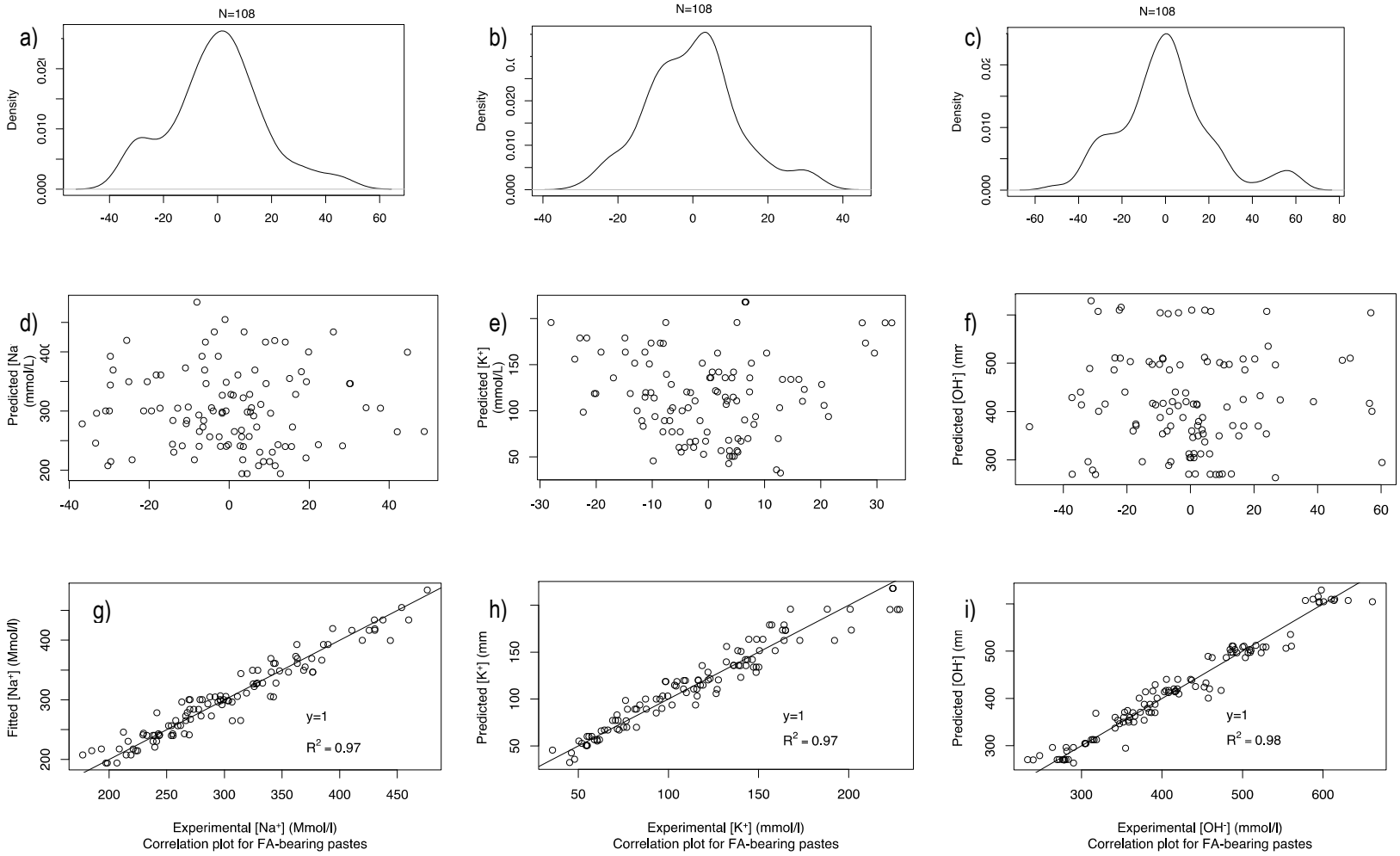


**Figure 4.19 : Regression model validation plots for FA-bearing pastes for [$Na^+$] (a, d, g); [$K^+$] (b, e, h); [$OH^-$] (c, f, i).**

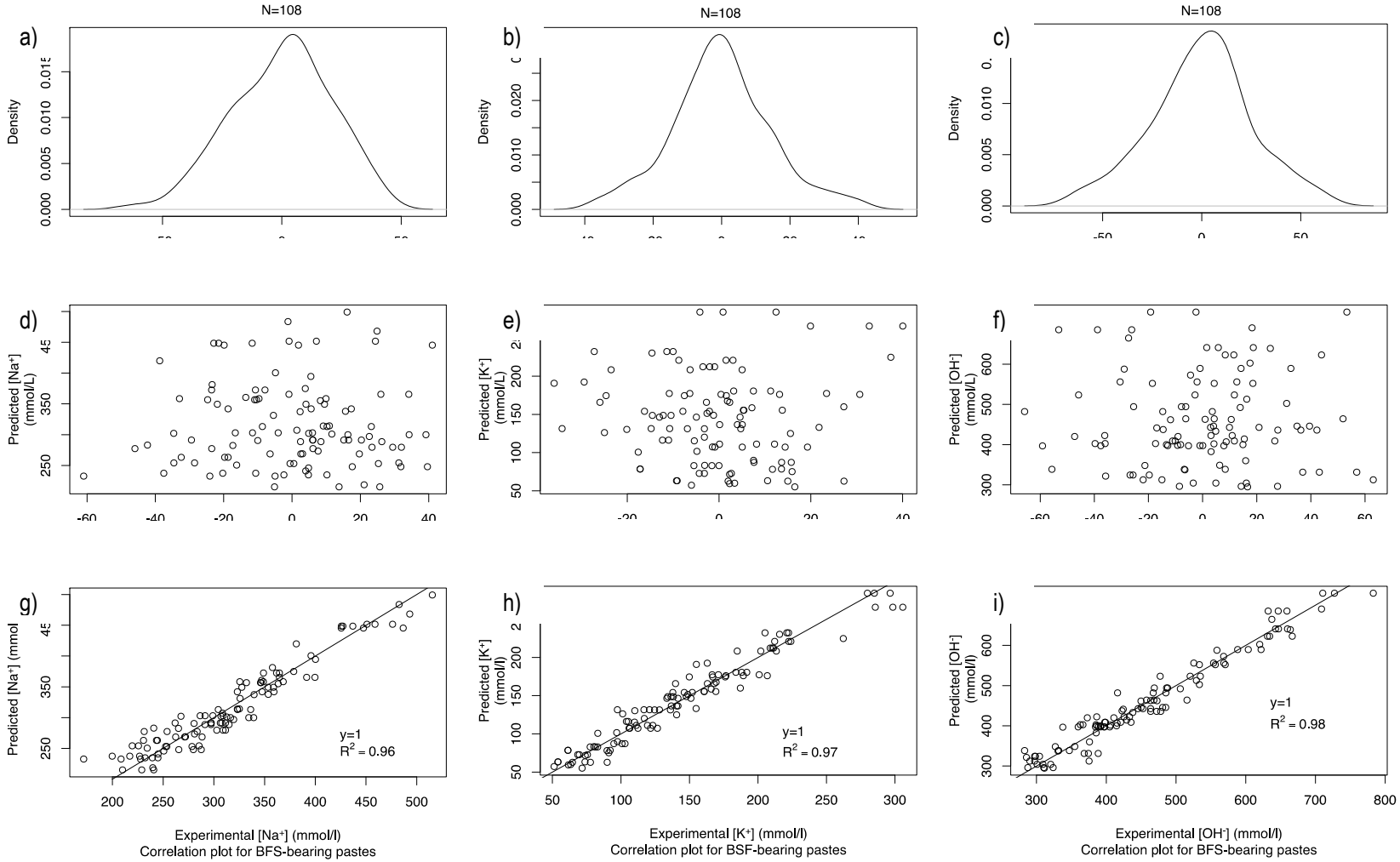


**Figure 4.20 : Regression model validation plots for BFS-bearing pastes for [$Na^+$] (a, d, g); [$K^+$] (b, e, h); [$OH^-$] (c, f, i).**

# Annex C -Data

**Table 4.15 : Experimental results for [$Na^+$] and corresponding fitted value of the proposed regression model with confidence interval of 95% at 28 and 182 days, for mixtures of various levels of GG, FA and $Na_2O$eq content of cement.**

| GG | FA | Cement | | 28-day data (Mmol/L) | | | | | 182-day data (Mmol/L) | | | | |
|---|---|---|---|---|---|---|---|---|---|---|---|---|---|
| | | Type | Alk | Experimental data | | Data from the Model | | | Experimental data | | Data from the Model | | |
| (%) | (%) | | $Na_2O$eq | [$Na^+$] | SD | [$Na^+$] | Min | Max | [$Na^+$] | SD | [$Na^+$] | Min | Max |
| 10 | 15 | C1 | 0.63 | 248 | 20 | 241 | 228 | 254 | 271 | 22 * | 268 | 252 | 284 |
| 10 | 15 | C2 | 0.94 | 282 | 13 | 300 | 289 | 311 | 325 | 15 * | 327 | 313 | 341 |
| 10 | 15 | C2 | 1.25 | 380 | 15 | 393 | 379 | 406 | 431 | 17 * | 419 | 403 | 435 |
| 10 | 22.5 | C1 | 0.63 | 208 | 14 | 218 | 208 | 228 | 230 | 15 * | 244 | 231 | 258 |
| 10 | 22.5 | C2 | 0.94 | 280 | 30 | 265 | 257 | 274 | 298 | 32 * | 292 | 279 | 304 |
| 10 | 22.5 | C2 | 1.25 | 370 | 12 | 346 | 336 | 356 | 362 | 12 * | 373 | 359 | 386 |
| 10 | 30 | C1 | 0.63 | 201 | 5 | 194 | 181 | 207 | 240 | 6 * | 220 | 204 | 237 |
| 10 | 30 | C2 | 0.94 | 232 | 13 | 230 | 220 | 241 | 262 | 15 * | 257 | 243 | 271 |
| 10 | 30 | C2 | 1.25 | 283 | 15 | 300 | 287 | 313 | 328 | 17 * | 327 | 311 | 343 |
| 15 | 15 | C1 | 0.63 | 278 | 11 | 273 | 262 | 284 | 319 | 13 * | 311 | 299 | 323 |
| 15 | 15 | C2 | 0.94 | 335 | 8 | 328 | 319 | 337 | 384 | 9 * | 366 | 356 | 377 |
| 15 | 15 | C2 | 1.25 | 422 | 10 | 416 | 406 | 427 | 454 | 11 * | 455 | 443 | 467 |
| 15 | 22.5 | C1 | 0.63 | 237 | 4 | 240 | 232 | 248 | 268 | 5 * | 279 | 269 | 289 |
| 15 | 22.5 | C2 | 0.94 | 274 | 4 | 284 | 276 | 292 | 326 | 5 * | 322 | 312 | 332 |
| 15 | 22.5 | C2 | 1.25 | 350 | 11 | 361 | 353 | 369 | 444 | 14 * | 399 | 389 | 409 |
| 15 | 30 | C1 | 0.63 | 204 | 23 | 208 | 197 | 218 | 212 | 24 * | 246 | 234 | 258 |
| 15 | 30 | C2 | 0.94 | 251 | 7 | 240 | 231 | 249 | 242 | 7 * | 278 | 267 | 289 |
| 15 | 30 | C2 | 1.25 | 317 | 20 | 306 | 295 | 316 | 314 | 20 * | 344 | 332 | 356 |
| 20 | 15 | C1 | 0.63 | 301 | 4 | 298 | 285 | 312 | 348 | 5 * | 349 | 333 | 365 |
| 20 | 15 | C2 | 0.94 | 341 | 24 | 349 | 339 | 360 | 420 | 30 * | 400 | 385 | 414 |
| 20 | 15 | C2 | 1.25 | 443 | 15 | 434 | 421 | 447 | 476 | 16 * | 484 | 468 | 500 |
| 20 | 22.5 | C1 | 0.63 | 255 | 4 | 257 | 246 | 267 | 296 | 5 * | 307 | 293 | 320 |
| 20 | 22.5 | C2 | 0.94 | 288 | 22 | 296 | 288 | 305 | 341 | 26 * | 346 | 334 | 359 |
| 20 | 22.5 | C2 | 1.25 | 360 | 18 | 369 | 359 | 379 | 394 | 20 * | 420 | 406 | 433 |
| 20 | 30 | C1 | 0.63 | 211 | 23 | 215 | 201 | 228 | 307 | 33 * | 265 | 249 | 281 |
| 20 | 30 | C2 | 0.94 | 254 | 11 | 243 | 232 | 254 | 286 | 12 * | 293 | 279 | 307 |
| 20 | 30 | C2 | 1.25 | 307 | 31 | 305 | 292 | 318 | 370 | 37 * | 355 | 339 | 371 |

* Based on the average coefficient of variation of the replicates (Annex A); the standard deviation of single measurement is estimated with a coefficient of variation of 5%.

**Table 4.16 : Experimental results for [$K^+$] and corresponding fitted value of the proposed regression model with confidence interval of 95% at 28 and 182 days for mixtures of various levels of GG, FA and $Na_2O$eq content of cement.**

| GG | FA | Cement | | 28-day data (Mmol/L) | | | | | 182-day data (Mmol/L) | | | | |
|---|---|---|---|---|---|---|---|---|---|---|---|---|---|
| | | Type | Alk | Experimental data | | Data from the Model | | | Experimental data | | Data from the Model | | |
| (%) | (%) | | $Na_2O$eq | [$K^+$] | SD | [$K^+$] | Min | Max | [$K^+$] | SD | [$K^+$] | Min | Max |
| 10 | 15 | C1 | 0.63 | 113 | 4 | 111 | 101 | 120 | 77 | 3 * | 77 | 64 | 89 |
| 10 | 15 | C2 | 0.94 | 226 | 3 | 195 | 188 | 203 | 132 | 2 * | 156 | 146 | 166 |
| 10 | 15 | C2 | 1.25 | 224 | 0 | 218 | 208 | 227 | 165 | 0 * | 173 | 161 | 185 |
| 10 | 22.5 | C1 | 0.63 | 71 | 2 | 77 | 70 | 85 | 52 | 1 * | 53 | 43 | 63 |
| 10 | 22.5 | C2 | 0.94 | 149 | 10 | 152 | 145 | 158 | 123 | 8 * | 122 | 114 | 129 |
| 10 | 22.5 | C2 | 1.25 | 149 | 4 | 164 | 156 | 171 | 149 | 4 | 128 | 119 | 138 |
| 10 | 30 | C1 | 0.63 | 78 | 4 | 70 | 60 | 79 | 50 | 3 * | 55 | 43 | 68 |
| 10 | 30 | C2 | 0.94 | 149 | 1 | 134 | 126 | 142 | 104 | 1 * | 114 | 104 | 124 |
| 10 | 30 | C2 | 1.25 | 137 | 2 | 136 | 126 | 145 | 127 | 2 * | 110 | 98 | 123 |
| 15 | 15 | C1 | 0.63 | 92 | 4 | 100 | 93 | 107 | 63 | 3 * | 66 | 55 | 77 |
| 15 | 15 | C2 | 0.94 | 159 | 4 | 179 | 173 | 185 | 132 | 3 * | 140 | 131 | 148 |
| 15 | 15 | C2 | 1.25 | 186 | 17 | 196 | 188 | 203 | 140 | 13 * | 151 | 140 | 162 |
| 15 | 22.5 | C1 | 0.63 | 68 | 4 | 67 | 61 | 73 | 46 | 3 * | 43 | 34 | 51 |
| 15 | 22.5 | C2 | 0.94 | 134 | 13 | 136 | 130 | 141 | 126 | 12 * | 106 | 99 | 113 |
| 15 | 22.5 | C2 | 1.25 | 144 | 2 | 142 | 136 | 148 | 110 | 2 * | 107 | 98 | 115 |
| 15 | 30 | C1 | 0.63 | 56 | 1 | 60 | 53 | 67 | 36 | 1 * | 46 | 35 | 56 |
| 15 | 30 | C2 | 0.94 | 101 | 4 | 119 | 113 | 125 | 76 | 3 * | 99 | 90 | 107 |
| 15 | 30 | C2 | 1.25 | 113 | 9 | 115 | 108 | 122 | 77 | 6 * | 89 | 78 | 100 |
| 20 | 15 | C1 | 0.63 | 84 | 3 | 89 | 80 | 99 | 60 | 2 * | 55 | 43 | 68 |
| 20 | 15 | C2 | 0.94 | 176 | 14 | 163 | 155 | 170 | 140 | 11 * | 123 | 113 | 133 |
| 20 | 15 | C2 | 1.25 | 177 | 22 | 173 | 164 | 183 | 122 | 15 * | 129 | 116 | 141 |
| 20 | 22.5 | C1 | 0.63 | 60 | 1 | 57 | 49 | 64 | 45 | 1 * | 32 | 22 | 42 |
| 20 | 22.5 | C2 | 0.94 | 111 | 4 | 120 | 113 | 126 | 96 | 3 * | 90 | 82 | 98 |
| 20 | 22.5 | C2 | 1.25 | 122 | 6 | 120 | 113 | 128 | 93 | 5 * | 85 | 75 | 95 |
| 20 | 30 | C1 | 0.63 | 55 | 0 | 50 | 41 | 60 | 48 | 0 * | 36 | 23 | 48 |
| 20 | 30 | C2 | 0.94 | 104 | 10 | 103 | 96 | 111 | 71 | 7 * | 83 | 73 | 93 |
| 20 | 30 | C2 | 1.25 | 100 | 16 | 94 | 84 | 103 | 72 | 11 * | 68 | 56 | 80 |

* Based on the average coefficient of variation of the replicates (Annex A); the standard deviation of single measurement is estimated with a coefficient of variation of 5%.

**Table 4.17 : Experimental results for [$OH^-$] and corresponding fitted value of the proposed regression model with confidence interval of 95% at 28 and 182 days for mixtures of various levels of GG, FA and $Na_2O$eq content of cement.**

| GG | FA | Cement | | 28-day data (Mmol/L) | | | | | 182-day data (Mmol/L) | | | | |
|---|---|---|---|---|---|---|---|---|---|---|---|---|---|
| | | Type | Alk | Experimental data | | Data from the Model | | | Experimental data | | Data from the Model | | |
| (%) | (%) | | $Na_2O$eq | [$OH^-$] | SD | [$OH^-$] | Min | Max | [$OH^-$] | SD | [$OH^-$] | Min | Max |
| 10 | 15 | C1 | 0.63 | 360 | 16 | 354 | 338 | 370 | 347 | 15 * | 346 | 327 | 366 |
| 10 | 15 | C2 | 0.94 | 508 | 15 | 496 | 483 | 510 | 457 | 14 * | 489 | 472 | 506 |
| 10 | 15 | C2 | 1.25 | 604 | 14 | 610 | 594 | 626 | 595 | 14 * | 602 | 583 | 622 |
| 10 | 22.5 | C1 | 0.63 | 278 | 13 | 296 | 283 | 309 | 282 | 13 * | 289 | 271 | 306 |
| 10 | 22.5 | C2 | 0.94 | 429 | 38 | 417 | 405 | 429 | 421 | 37 * | 410 | 393 | 426 |
| 10 | 22.5 | C2 | 1.25 | 518 | 16 | 509 | 496 | 522 | 511 | 16 * | 501 | 484 | 519 |
| 10 | 30 | C1 | 0.63 | 279 | 6 | 271 | 255 | 287 | 290 | 6 * | 263 | 244 | 283 |
| 10 | 30 | C2 | 0.94 | 381 | 15 | 370 | 357 | 383 | 366 | 14 * | 363 | 345 | 380 |
| 10 | 30 | C2 | 1.25 | 420 | 15 | 440 | 424 | 456 | 455 | 16 * | 433 | 413 | 452 |
| 15 | 15 | C1 | 0.63 | 370 | 15 | 371 | 359 | 383 | 382 | 15 * | 379 | 366 | 393 |
| 15 | 15 | C2 | 0.94 | 495 | 13 | 504 | 494 | 513 | 517 | 14 * | 512 | 500 | 524 |
| 15 | 15 | C2 | 1.25 | 608 | 27 | 607 | 595 | 619 | 594 | 26 * | 616 | 602 | 630 |
| 15 | 22.5 | C1 | 0.63 | 305 | 1 | 304 | 294 | 314 | 314 | 1 * | 313 | 301 | 325 |
| 15 | 22.5 | C2 | 0.94 | 407 | 16 | 415 | 406 | 425 | 452 | 18 * | 424 | 412 | 436 |
| 15 | 22.5 | C2 | 1.25 | 494 | 13 | 498 | 488 | 507 | 554 | 15 * | 506 | 494 | 518 |
| 15 | 30 | C1 | 0.63 | 260 | 23 | 270 | 259 | 282 | 248 | 22 * | 279 | 265 | 293 |
| 15 | 30 | C2 | 0.94 | 352 | 9 | 360 | 350 | 370 | 318 | 8 * | 368 | 356 | 381 |
| 15 | 30 | C2 | 1.25 | 431 | 24 | 420 | 409 | 432 | 392 | 22 * | 429 | 415 | 443 |
| 20 | 15 | C1 | 0.63 | 385 | 7 | 388 | 372 | 404 | 408 | 7 * | 412 | 393 | 432 |
| 20 | 15 | C2 | 0.94 | 517 | 39 | 511 | 497 | 524 | 560 | 42 * | 535 | 518 | 552 |
| 20 | 15 | C2 | 1.25 | 619 | 37 | 605 | 589 | 621 | 598 | 36 * | 629 | 610 | 649 |
| 20 | 22.5 | C1 | 0.63 | 315 | 3 | 313 | 299 | 326 | 342 | 3 * | 337 | 320 | 354 |
| 20 | 22.5 | C2 | 0.94 | 400 | 18 | 414 | 402 | 426 | 437 | 20 * | 439 | 423 | 455 |
| 20 | 22.5 | C2 | 1.25 | 482 | 21 | 486 | 473 | 500 | 487 | 21 * | 511 | 494 | 528 |
| 20 | 30 | C1 | 0.63 | 266 | 22 | 270 | 254 | 286 | 355 | 29 * | 295 | 275 | 314 |
| 20 | 30 | C2 | 0.94 | 359 | 6 | 350 | 336 | 363 | 357 | 6 * | 374 | 357 | 392 |
| 20 | 30 | C2 | 1.25 | 408 | 45 | 400 | 384 | 417 | 442 | 49 * | 425 | 406 | 445 |

* Based on the average coefficient of variation of the replicates (Annex A); the standard deviation of single measurement is estimated with a coefficient of variation of 4%.

**Table 4.18 : Experimental results for [$Na^+$] and corresponding fitted value of the proposed regression model with confidence interval of 95% at 28 and 182 days for mixtures of various levels of GG, BFS and $Na_2O$eq content of cement.**

| GG | BFS | Cement | | 28-day data (Mmol/L) | | | | | 182-day data (Mmol/L) | | | | |
|---|---|---|---|---|---|---|---|---|---|---|---|---|---|
| | | Type | Alk | Experimental data | | Data from the Model | | | Experimental data | | Data from the Model | | |
| (%) | (%) | | $Na_2O$eq | [$Na^+$] | SD | [$Na^+$] | Min | Max | [$Na^+$] | SD | [$Na^+$] | Min | Max |
| 10 | 20 | C1 | 0.63 | 309 | 3 | 291 | 275 | 308 | 323 | 3 * | 314 | 293 | 335 |
| 10 | 20 | C2 | 0.94 | 348 | 21 | 358 | 345 | 372 | 358 | 22 * | 381 | 362 | 400 |
| 10 | 20 | C2 | 1.25 | 453 | 31 | 445 | 429 | 461 | 493 | 34 * | 468 | 447 | 489 |
| 10 | 30 | C1 | 0.63 | 203 | 28 | 233 | 220 | 246 | 251 | 35 * | 246 | 229 | 263 |
| 10 | 30 | C2 | 0.94 | 256 | 26 | 277 | 266 | 289 | 280 | 28 * | 291 | 275 | 306 |
| 10 | 30 | C2 | 1.25 | 343 | 18 | 342 | 329 | 355 | 363 | 19 * | 355 | 338 | 372 |
| 10 | 40 | C1 | 0.63 | 227 | 16 | 215 | 199 | 231 | 240 | 17 * | 219 | 198 | 240 |
| 10 | 40 | C2 | 0.94 | 215 | 14 | 237 | 224 | 251 | 245 | 16 * | 241 | 222 | 260 |
| 10 | 40 | C2 | 1.25 | 308 | 4 | 279 | 263 | 296 | 241 | 3 * | 283 | 262 | 304 |
| 15 | 20 | C1 | 0.63 | 287 | 28 | 302 | 290 | 315 | 340 | 33 * | 337 | 321 | 353 |
| 15 | 20 | C2 | 0.94 | 385 | 18 | 365 | 355 | 376 | 396 | 18 * | 401 | 386 | 415 |
| 15 | 20 | C2 | 1.25 | 430 | 6 | 449 | 437 | 461 | 483 | 7 * | 484 | 468 | 500 |
| 15 | 30 | C1 | 0.63 | 278 | 11 | 248 | 238 | 258 | 281 | 11 * | 273 | 262 | 285 |
| 15 | 30 | C2 | 0.94 | 301 | 12 | 289 | 279 | 298 | 325 | 13 * | 314 | 302 | 326 |
| 15 | 30 | C2 | 1.25 | 347 | 17 | 349 | 340 | 359 | 379 | 19 * | 375 | 363 | 387 |
| 15 | 40 | C1 | 0.63 | 239 | 6 | 235 | 223 | 247 | 234 | 6 * | 251 | 234 | 267 |
| 15 | 40 | C2 | 0.94 | 261 | 15 | 253 | 243 | 263 | 272 | 16 * | 269 | 254 | 284 |
| 15 | 40 | C2 | 1.25 | 285 | 20 | 291 | 280 | 303 | 309 | 22 * | 307 | 291 | 323 |
| 20 | 20 | C1 | 0.63 | 321 | 16 | 313 | 297 | 329 | 347 | 17 * | 361 | 339 | 382 |
| 20 | 20 | C2 | 0.94 | 358 | 8 | 372 | 359 | 386 | 381 | 9 * | 420 | 401 | 439 |
| 20 | 20 | C2 | 1.25 | 462 | 13 | 452 | 436 | 468 | 515 | 15 * | 499 | 478 | 520 |
| 20 | 30 | C1 | 0.63 | 239 | 8 | 263 | 250 | 276 | 313 | 10 * | 301 | 284 | 318 |
| 20 | 30 | C2 | 0.94 | 330 | 12 | 300 | 289 | 311 | 354 | 13 * | 338 | 322 | 354 |
| 20 | 30 | C2 | 1.25 | 341 | 8 | 357 | 344 | 370 | 400 | 9 * | 395 | 378 | 412 |
| 20 | 40 | C1 | 0.63 | 244 | 36 | 254 | 238 | 270 | 265 | 39 * | 282 | 261 | 304 |
| 20 | 40 | C2 | 0.94 | 274 | 13 | 269 | 256 | 282 | 320 | 15 * | 297 | 278 | 316 |
| 20 | 40 | C2 | 1.25 | 296 | 10 | 303 | 288 | 318 | 326 | 11 * | 331 | 310 | 352 |

* Based on the average coefficient of variation of the replicates (Annex A); the standard deviation of single measurement is estimated with a coefficient of variation of 5%.

**Table 4.19 : Experimental results for [$K^+$] and corresponding fitted value of the proposed regression model with confidence interval of 95% at 28 and 182 days for mixtures of various levels of GG, BFS and $Na_2O$eq content of cement.**

| GG | BFS | Cement | | 28-day data (Mmol/L) | | | | | 182-day data (Mmol/L) | | | | |
|---|---|---|---|---|---|---|---|---|---|---|---|---|---|
| | | Type | Alk | Experimental data | | Data from the Model | | | Experimental data | | Data from the Model | | |
| (%) | (%) | | $Na_2O$eq | [$K^+$] | SD | [$K^+$] | Min | Max | [$K^+$] | SD | [$K^+$] | Min | Max |
| 10 | 20 | C1 | 0.63 | 145 | 7 | 154 | 143 | 165 | 101 | 5 * | 126 | 112 | 141 |
| 10 | 20 | C2 | 0.94 | 297 | 10 | 266 | 257 | 275 | 262 | 9 * | 225 | 213 | 237 |
| 10 | 20 | C2 | 1.25 | 287 | 9 | 284 | 273 | 295 | 216 | 7 * | 230 | 216 | 245 |
| 10 | 30 | C1 | 0.63 | 118 | 6 | 111 | 102 | 120 | 80 | 4 * | 83 | 70 | 97 |
| 10 | 30 | C2 | 0.94 | 200 | 14 | 208 | 201 | 216 | 169 | 12 * | 168 | 157 | 179 |
| 10 | 30 | C2 | 1.25 | 210 | 1 | 212 | 203 | 222 | 166 | 1 * | 159 | 145 | 172 |
| 10 | 40 | C1 | 0.63 | 81 | 3 | 83 | 72 | 94 | 72 | 3 * | 55 | 40 | 70 |
| 10 | 40 | C2 | 0.94 | 157 | 15 | 166 | 157 | 175 | 141 | 13 * | 125 | 113 | 137 |
| 10 | 40 | C2 | 1.25 | 164 | 5 | 155 | 144 | 167 | 97 | 3 * | 102 | 87 | 116 |
| 15 | 20 | C1 | 0.63 | 105 | 1 | 116 | 108 | 125 | 83 | 1 * | 101 | 89 | 112 |
| 15 | 20 | C2 | 0.94 | 220 | 6 | 221 | 214 | 228 | 163 | 4 * | 192 | 184 | 201 |
| 15 | 20 | C2 | 1.25 | 216 | 10 | 232 | 224 | 241 | 155 | 7 * | 191 | 180 | 202 |
| 15 | 30 | C1 | 0.63 | 100 | 4 | 87 | 80 | 94 | 74 | 3 * | 72 | 61 | 82 |
| 15 | 30 | C2 | 0.94 | 179 | 19 | 177 | 171 | 184 | 148 | 16 * | 149 | 141 | 157 |
| 15 | 30 | C2 | 1.25 | 164 | 13 | 174 | 167 | 182 | 155 | 12 * | 133 | 123 | 143 |
| 15 | 40 | C1 | 0.63 | 71 | 4 | 73 | 65 | 81 | 51 | 3 * | 57 | 46 | 68 |
| 15 | 40 | C2 | 0.94 | 136 | 2 | 149 | 142 | 155 | 117 | 2 * | 120 | 112 | 128 |
| 15 | 40 | C2 | 1.25 | 130 | 6 | 131 | 123 | 139 | 97 | 5 * | 90 | 79 | 101 |
| 20 | 20 | C1 | 0.63 | 72 | 18 | 78 | 67 | 90 | 91 | 23 * | 75 | 60 | 90 |
| 20 | 20 | C2 | 0.94 | 191 | 15 | 176 | 167 | 185 | 187 | 15 * | 160 | 148 | 172 |
| 20 | 20 | C2 | 1.25 | 188 | 4 | 181 | 170 | 192 | 149 | 3 * | 151 | 137 | 166 |
| 20 | 30 | C1 | 0.63 | 61 | 11 | 63 | 54 | 73 | 63 | 11 * | 60 | 47 | 73 |
| 20 | 30 | C2 | 0.94 | 142 | 9 | 147 | 139 | 154 | 110 | 7 * | 130 | 119 | 141 |
| 20 | 30 | C2 | 1.25 | 140 | 3 | 137 | 128 | 146 | 106 | 2 * | 107 | 94 | 121 |
| 20 | 40 | C1 | 0.63 | 77 | 13 | 63 | 52 | 74 | 62 | 10 * | 59 | 45 | 74 |
| 20 | 40 | C2 | 0.94 | 112 | 13 | 132 | 123 | 140 | 110 | 13 * | 115 | 104 | 127 |
| 20 | 40 | C2 | 1.25 | 117 | 9 | 107 | 97 | 118 | 90 | 7 * | 78 | 64 | 93 |

* Based on the average coefficient of variation of the replicates (Annex A); the standard deviation of single measurement is estimated with a coefficient of variation of 6%.

**Table 4.20 : Experimental results for [$OH^-$] and corresponding fitted value of the proposed regression model with confidence interval of 95% at 28 and 182 days for mixtures of various levels of GG, BFS and $Na_2O$eq content of cement.**

| GG | BFS | Cement | | 28-day data (Mmol/L) | | | | | 182-day data (Mmol/L) | | | | |
|---|---|---|---|---|---|---|---|---|---|---|---|---|---|
| | | Type | Alk | Experimental data | | Data from the Model | | | Experimental data | | Data from the Model | | |
| (%) | (%) | | $Na_2O$eq | [$OH^-$] | SD | [$OH^-$] | Min | Max | [$OH^-$] | SD | [$OH^-$] | Min | Max |
| 10 | 20 | C1 | 0.63 | 454 | 9 | 443 | 424 | 461 | 424 | 8 * | 441 | 422 | 461 |
| 10 | 20 | C2 | 0.94 | 644 | 20 | 623 | 608 | 638 | 620 | 19 * | 603 | 585 | 621 |
| 10 | 20 | C2 | 1.25 | 740 | 38 | 730 | 711 | 749 | 709 | 36 * | 691 | 665 | 716 |
| 10 | 30 | C1 | 0.63 | 321 | 33 | 339 | 324 | 353 | 331 | 34 * | 337 | 322 | 353 |
| 10 | 30 | C2 | 0.94 | 456 | 36 | 482 | 469 | 495 | 450 | 35 * | 462 | 446 | 478 |
| 10 | 30 | C2 | 1.25 | 554 | 19 | 552 | 536 | 568 | 529 | 18 * | 513 | 490 | 536 |
| 10 | 40 | C1 | 0.63 | 307 | 18 | 296 | 279 | 313 | 311 | 18 * | 295 | 277 | 312 |
| 10 | 40 | C2 | 0.94 | 372 | 12 | 403 | 390 | 416 | 386 | 12 * | 382 | 366 | 399 |
| 10 | 40 | C2 | 1.25 | 471 | 7 | 436 | 418 | 454 | 338 | 5 * | 397 | 372 | 421 |
| 15 | 20 | C1 | 0.63 | 392 | 27 | 420 | 406 | 435 | 423 | 29 * | 437 | 420 | 455 |
| 15 | 20 | C2 | 0.94 | 605 | 17 | 589 | 578 | 601 | 559 | 16 * | 588 | 574 | 602 |
| 15 | 20 | C2 | 1.25 | 646 | 13 | 685 | 671 | 700 | 638 | 13 * | 665 | 646 | 683 |
| 15 | 30 | C1 | 0.63 | 377 | 10 | 331 | 320 | 343 | 355 | 9 * | 349 | 334 | 364 |
| 15 | 30 | C2 | 0.94 | 481 | 31 | 464 | 453 | 475 | 473 | 30 * | 462 | 449 | 476 |
| 15 | 30 | C2 | 1.25 | 511 | 30 | 523 | 512 | 535 | 534 | 31 * | 503 | 486 | 519 |
| 15 | 40 | C1 | 0.63 | 310 | 10 | 304 | 290 | 318 | 286 | 9 * | 321 | 304 | 339 |
| 15 | 40 | C2 | 0.94 | 398 | 15 | 400 | 388 | 412 | 389 | 15 * | 398 | 384 | 412 |
| 15 | 40 | C2 | 1.25 | 415 | 25 | 422 | 409 | 436 | 406 | 24 * | 402 | 383 | 420 |
| 20 | 20 | C1 | 0.63 | 393 | 7 | 397 | 379 | 416 | 438 | 8 * | 433 | 409 | 458 |
| 20 | 20 | C2 | 0.94 | 549 | 22 | 556 | 543 | 569 | 568 | 23 * | 573 | 555 | 591 |
| 20 | 20 | C2 | 1.25 | 650 | 9 | 641 | 624 | 658 | 664 | 9 * | 639 | 619 | 659 |
| 20 | 30 | C1 | 0.63 | 300 | 4 | 324 | 308 | 340 | 376 | 5 * | 360 | 337 | 383 |
| 20 | 30 | C2 | 0.94 | 472 | 19 | 446 | 433 | 459 | 464 | 19 * | 463 | 445 | 481 |
| 20 | 30 | C2 | 1.25 | 481 | 11 | 494 | 479 | 509 | 506 | 12 * | 492 | 474 | 511 |
| 20 | 40 | C1 | 0.63 | 321 | 47 | 312 | 293 | 331 | 327 | 48 * | 348 | 323 | 373 |
| 20 | 40 | C2 | 0.94 | 386 | 23 | 397 | 382 | 412 | 430 | 26 * | 414 | 395 | 433 |
| 20 | 40 | C2 | 1.25 | 413 | 18 | 409 | 391 | 426 | 416 | 18 * | 407 | 386 | 428 |

* Based on the average coefficient of variation of the replicates (Annex A); the standard deviation of single measurement is estimated with a coefficient of variation of 4%.

# Chapter 5. - Impact of GG (Ground Glass) on the ASR Expansion of Ternary Concrete Prisms Incorporating Silica Fume (SF), Metakaolin (MK), Fly Ash (FA) or Blast Furnace Slag (BFS)

## Résumé

Afin de déterminer la proportion de verre broyé (VB), un matériau pozzolanique à haute teneur en alcalis (environ 13 % de $Na_2Oeq$), qui peut être incorporée dans le béton sans provoquer d'expansion nuisible en raison de la réaction alcalis-silice (RAS), des prismes de béton de compositions binaire et ternaire ont été fabriqués et testés conformément à la pratique normalisée de la CSA A23.2-28A. Ainsi, les spécimens ont été fabriqués avec un granulat hautement réactif (Spratt), divers pourcentages de VB, des ciments de divers contenus en $Na_2Oeq$ et un troisième matériau cimentaire, c'est-à-dire la fumée de silice (FS), le Métakaolin (MK), la Cendre Volante (CV) ou le Laitier de hauts-fourneaux (LHF). Des mesures d'expansion ont été réalisées pendant une période de deux ans au cours de laquelle les spécimens ont été conservés à 38°C et R.H. > 95%. Les résultats ont révélé que la présence du VB n'engendre pas en soi une augmentation de l'expansion des éprouvettes de béton. En effet, le VB peut être considéré comme une mesure préventive contre la RAS mais son potentiel de prévention varie entre 1/8 et 1/2 de celui des autres ajouts cimentaires utilisés dans cette étude. Les résultats ont également suggéré que l'utilisation de NaOH, tel que prescrit dans la pratique normalisée de la CSA A23.2-28A, pour fins d'accélération, peut en fait induire un biais positif qui entraîne une diminution des expansions dans les mélanges ternaires incorporant du VB par rapport au même mélange sans ajout de NaOH. Des doses minimales de FS/MK/CV/LHF sont suggérées en combinaison avec le VB afin de prévenir l'expansion associable à la RAS dans les systèmes ternaires de béton incorporant un granulat fortement réactif.

## Abstract

In order to establish safe proportions of Ground Glass (GG) that could be incorporated into concrete without causing detrimental expansion, binary and ternary concrete prisms were made with highly reactive aggregate (Spratt limestone), various contents of GG, cement of various $Na_2O$eq contents and a third cementitious material (SCM), i.e. (Silica Fume (SF), Metakaolin (MK), Fly Ash (FA) or Blast Furnace Slag (BFS)). Expansion measurements of test prisms taken for a period up to two years (38°C, 100% R.H.) revealed that GG is not in itself promoting expansion of concrete prisms. Indeed, GG is considered as a preventing measure but it preventing power ranges between 1/8 and ½ of the other SCM investigated in this study. Results obtained in this study also suggested that the use of NaOH can induce a positive bias that lowers the expansion of given ternary mixtures incorporating GG compared to the same mixture without NaOH. Minimum dosages of SF/MK/FA/BFS are proposed to use in complement of GG in order to prevent expansion due to ASR in concrete incorporating highly-reactive aggregates.

## 5.1 Introduction

The durability of concrete incorporating Ground Glass (GG) was for long and is still considered by some a source of concerns because of the high alkali content of GG, which was thought to fuel or aggravate expansion in concrete due to Alkali-Silica Reaction (ASR). In the latest version of the Canadian standards CSA-A3000-18, GG was introduced as a new Supplementary Cementitious Material (SCM). More specifically, $G_L$ corresponds to GG with a low-alkali content ($\leq$ 4% $Na_2Oeq$) that can be used with no restrictions regarding the type of aggregates it can be combined with; on the other hand, $G_H$ is a GG with alkali contents ranging from 4% to 13% that shall not be used with alkali-silica or alkali-carbonate reactive aggregates. Most of the glass treated by recycling facilities would be classified as $G_H$ since ordinary and soda-lime glass have a high sodium content.

### 5.1.1 GG and Glass Aggregates Assessed by Accelerated Mortar Bar Testing

The ASR behavior of cementitious systems incorporating GG is most frequently assessed with the Accelerated Mortar Bar Test (AMBT) ASTM C1260 / ASTM C1567, or hybrid methods between the above. These testing methods present the advantage of providing results in a short period of time considering the 1N NaOH solution at 80°C in which the mortar bars are soaked that increases the reaction rate of most potentially reactive aggregates; however, when it comes to test high alkali SCMs, such methods have their limitations. For instance, there is no guarantee that using a 1N NaOH soak solution is not masking or interfering with possible alkali release that may occur when GG is incorporated into concrete. Actually, Standard Practice CSA A23.2-28A-2019, which covers the evaluation of the effectiveness of SCMs against ASR in Canadian Standards, specifies that : "*When evaluating the effectiveness of a fly ash with total alkali content greater than 4.5%..., CSA A23.2-14A* (i.e. Concrete prism test - CPT) *shall be used*". Although GG is not specifically mentioned in the above statement, since it had not been introduced in the 2019 edition of Canadian concrete standards (A23.1/A23.2), a similar recommendation would have applied to GG because of its high alkali content.

Although largely opened to questions, the results of several studies where AMBT was used with GG or crushed glass are summarized in Table 5.1 to Table 5.3. Table 5.1 focuses on studies on mortar bars incorporating natural reactive aggregates. Although quite variable, the results suggest that the use of GG is generally efficient in reducing expansion compared to the control specimens without GG. In the case of highly to extremely-reactive aggregates, the amount of GG required to reduce expansion below the 14-day 0.10% limit of Standard Test Method ASTM C 1567 or Standard Practice CSA A23.2-28A ranged from 30% (Lafrenière, 2017) to 50% (Shi et al., 2004), while 20 to even 40% seemed insufficient in many cases (Pereira-de-Olivera et al., 2012, Zidol, 2009, Shi et al., 2004, Zheng, 2016). On the other hand, some studies showed that 20 to 30% of GG as cement replacement (by mass) seemed to be sufficient in reducing AMBT expansions below the above limit for several highly/moderately-reactive aggregates (Serpa et al., 2013, Afshinnia and Rangaragu, 2015a, Zheng, 2016,

Lafrenière, 2017, Chen and Poon, 2017), but not always (Schwarz et al., 2008, Lafrenière, 2017). Lower proportions of GG (5 -10%) were found to display limited effectiveness in controlling ASR expansion (Schwarz et al., 2008, Afshinnia and Rangaragu, 2015b, Serpa et al., 2013, Chen and Poon, 2017). Data in Table 5.1 also highlight the fact that finely-ground GG is more efficient than coarser ones in reducing expansion due to ASR. For instance, in the study of Zheng (2016), GG with $D_{50}$ of 200 and 20μm lead to 14-day expansions of respectively 0.20 and 0.12% for mortars incorporating the highly-reactive Jobe sand from Texas.

Table 5.2 presents the results of AMBT incorporating crushed glass as reactive aggregates (either borosilicate or the same glass as that used to manufacture GG) and GG as a SCM. When the reactive aggregate is crushed glass, the expansion potential can generally be prevented (i.e. expansion < 0.10% at 14 days) for 20 to 30% mass replacements of the cement by GG, provided the latter is ground below 100μm; on the other hand, although efficient in reducing expansion compared to the control, replacing cement by 10% GG was found insufficient to meet the 14-day 0.10% expansion limit (Maraghechi et al., 2012, Liu et al., 2015, Lu et al., 2017, Matos and Sousa-Coutinho, 2012, Kamali and Ghahremaninezhad, 2015, Chen and Poon, 2017, Afshinnia and Rangaragu, 2015b). The potential of coarse GG to limit ASR expansion appears limited; for instance, glass powder with particles coarser than 200μm used at 20% of cement replacement could not efficiently prevent ASR expansion (Lu et al., 2017). Actually, the results of studies reported in both Table 5.2 (reactive glass aggregates) and Table 5.1 (natural reactive aggregates) suggest that 20 to 30% GG used as cement replacement is effective in reducing mortar bar expansions below the 0.10% limit, while 10% is always inefficient in doing so.

Table 5.3 presents the results of studies where mortar bars incorporating glass, either as aggregates or SCM, were made in combination with fly ash (FA), metakaolin (MK), or blastfurnace slag (BFS). The results suggest that a combination FA-GG is beneficial in reducing expansion in mortar bars incorporating a reactive siliceous sand (Schwarz et al., 2008); moreover, the use of 2.5 to 10% of FA or MK was effective in controlling expansion in mortar bars where 50% of the sand was replaced by crushed glass (Lam et al., 2007). Cota et al. (2015) showed that the use of 7.5 or 15% MK can prevent expansion in mortar bars incorporating 7.5% of crushed glass as replacement of a non-reactive sand. Afshinnia and Rangaragu (2015a) and Maraghechi et al. (2017) also showed the beneficial effect in reducing mortar bar expansion of combining GG with BFS, MK or FA.
Several studies were conducted where mortar bar mixtures were made with non-reactive aggregates (i.e. inducing expansions below the acceptance limit) and GG as a SCM to partially replace portland cement. The results of those studies showed that the use of 5 to 30% of GG (as cement replacement) did not induce expansion beyond the 0.10% expansion level in such mortar bars (Shao et al., 2000, Karamberi et al., 2006, Parghi and Shahria Alam, 2016, Shi et al., 2004, Maraghechi et al., 2017).

### 5.1.2 GG and Glass Aggregate Assessed in Concrete Prism Testing

As highlighted in Table 5.4, a number of studies assessed expansion in concrete prisms incorporating reactive and non-reactive aggregates, along with crushed/ ground glass particles ranging from 10μm to 19mm. Shayan and Xu (2006) did not observe any significant expansion in concrete specimens made with a non-reactive coarse aggregate, a low alkali cement (0.46% $Na_2Oeq$) and glass used either as a SCM (20 & 30% cement replacement) and/or as 40 to 75% replacement of the fine aggregate (0.6 to 2.25 mm particle size). Dhir et al. (2009) found that the use of 10 and 30% GG was efficient in reducing the expansion in concrete prisms incorporating an aggregate that was exhibiting borderline expansion in the CPT. On the other hand, Zidol (2009) and Lafrenière (2017) found that the use of 20 or 30% GG was insufficient in reducing expansion in concrete prisms incorporating the highly-reactive Spratt and moderately-reactive Sudbury aggregates below the two-year 0.040% limit proposed in CSA Standard Practice A23.2-28A. Johnston (1974) obtained low expansion when using coarse glass aggregate in concrete mixtures with a low-alkali cement and a low cement content; however, all other concrete prisms using coarse glass aggregates along with a high-alkali cement and low to high cement dosages largely failed to meet the non-expansive criterion. Dhir et al. (2009) and Taha and Nounu (2008) also found that the use of glass sand as replacement of fine aggregate can result in significant concrete prism expansions.

**Table 5.1 Expansion of mortar bars according to ASTM C1260 with natural reactive aggregates used in combination with GG with an $Na_2O_{eq}$ content ranging between 11.30 and 13.80% (mortar bars immersed in 1 N NaOH at 80°C for 14 days); expansion < 0.10%: innocuous; expansion > 0.20%: deleterious (Fily-Paré et al. 2020).**

| Mix design | Expansion (%) | | Aggregate | Cement and alkali addition | % of cement replacement | Size of glass particles | Source |
|---|---|---|---|---|---|---|---|
| | Specimens with GG | Control | | | | | |
| Highly reactive aggregate and 50% of GG | 0.08* | ≈ 0.50 | Highly reactive (Spratt limestone) | 0.63% of $Na_2Oeq$ NaOH added to 0.90% $Na_2Oeq$ | 50% | $D_{50}$ ≈ 50µm | Shi et al. 2004 |
| Highly/Extremely reactive aggregate and 10 to 40% of GG | <0.20 and >0.10 | 0.38 | Natural sand | 0.84% of $Na_2Oeq$ | 40% | 45 to 75 µm | Pereira-de-Oliveira et al. 2012 |
| | 0.41**, 0.30** and 0.30** | 0.72 | Highly reactive (Spratt limestone) | 0.73% of $Na_2Oeq$ | 20, 30 and 40% | $D_{50}$ ≈ 10µm | Zidol 2009** |
| | 0.42* ,0.22* and 0.11* | 0.5 | Highly reactive (Spratt limestone) | 0.63% of $Na_2Oeq$ NaOH added to 0.90% $Na_2Oeq$ | 10, 20, 30% | $D_{50}$ ≈ 50µm | Shi et al. 2004 |
| | 0.20*** and 0.12*** | 0.64 | Extremely reactive (Jobe sand) | 1.22% of $Na_2Oeq$ | 30% | $D_{50}$ ≈ 200µm and $D_{50}$ ≈ 20µm | Zheng 2016*** |
| Extremely/Highly reactive aggregate and 20 to 30% of GG | 0.07 and 0.07 | 0.20 | Reactive sand | 0.86% of $Na_2Oeq$ | 20 and 30% | <125µm | Serpa et al. 2013 |
| | 0.09 and 0.06 | 0.27 | Reactive Argillite | 0.88% $Na_2Oeq$ | 20 and 30% | $D_{50}$ ≈ 70µm | Afshinnia and Rangaraju 2015c |
| | 0.08*** and 0.05*** | 0.29 | Reactive (Wright sand) | 1.22% of $Na_2Oeq$ | 30% | $D_{50}$ ≈ 200µm and $D_{50}$ ≈ 20µm | Zheng 2016*** |
| | 0.120 and 0.066<br>0.119 and 0.052 | 0.272<br>0.276 | Reactive limestone<br>Reactive gravel | 1.00% of $Na_2Oeq$ | 20, 30% | Blaine fineness of 440 $m^2/kg$ | Lafrenière 2017 |
| | 0.04 | 0.26 | Not mentioned | 0.46% of $Na_2Oeq$ | 20% | $D_{50}$ ≈ 10µm | Chen and Poon 2017 |
| Extremely/Highly reactive and 5 to 20% of GG | 0.20, 0.17 and 0.13 | 0.22 | Reactive siliceous sand | 0.73% of $Na_2Oeq$ | 5, 10, and 20% | $D_{50}$ ≈ 20µm | Schwarz et al. 2008 |
| | 0.18 | 0.27 | Reactive Argillite | 0.88% of $Na_2Oeq$ | 10% | $D_{50}$ ≈ 70µm | Afshinnia and Rangaraju 2015c |
| | 0.13 and 0.13 | 0.20 | Alkali reactive sand | 0.86% of $Na_2Oeq$ | 5 and 20% of aggregate | 4.75 to 150µm | Serpa et al. 2013 |
| | 0.12 | 0.26 | Not mentioned | 0.46% of $Na_2Oeq$ | 10 % | $D_{50}$ ≈ 10µm | Chen and Poon 2017 |

* Specimens with and without NaOH addition showed similar expansion

** CSA 23.2-25A

*** ASTM C227, 38°C, immersed in 0.6 N NaOH for 6 months and expansion limit of 0.10% at 6 months

**Table 5.2 : Expansion of mortar bars tested according to ASTM C1260 or ASTM C1567 and using 100% crushed glass aggregate as reactive aggregate and GG as pozzolanic material for ASR prevention (mortar bars immersed in 1N NaOH at 80°C for 14 days); expansion < 0.10%: innocuous, expansion > 0.20%: deleterious.**

| | Expansion (%) | | Cement and alkali addition | Glass replacement | Size of glass particle | Source |
|---|---|---|---|---|---|---|
| | Specimen | Control | | | | |
| Heated glass | *0.02** and *0.05*** | 0.8 | $Na_2O$eq of 1.81% | 100% of aggregate | 4.75 to 150µm | Maraghechi et al. 2012 |
| 20 to 30% of GG ground to ≤100µm as a cement replacement | <*0.10* | 0.22 | 1.04% of $Na_2O$eq | 30% of cement | 100 to 9µm | Liu et al. 2015 |
| | <*0.10* | | | 20% of cement | 15 and 9µm | |
| | *0.02*, *0.0* and *0.0* | 0.15 | 0.10% of $Na_2O$eq | 20% of cement | Mean diameter of 89, 48 and 28µm | Lu et al. 2017 |
| | *0.04*† | 0.18† | Not mentioned† | 20% of cement † | $D_{50}$ ≈ 10µm† | Matos and Sousa-Coutinho 2012 † |
| | *0.01*†† | ≈0.47††† | Not mentioned | 20% of cement | Median size 8.4µm | Kamali and Ghahremaninezhad 2015 †† |
| | *0.04* | 0.27 | 0.46% Of $Na_2O$eq | 20% of cement | $D_{50}$ ≈ 10µm | Chen and Poon 2017 |
| | 0.11 and 0.19 | 0.97 | 0.88% $Na_2O$eq | 20% of cement | Mean diameter of 17 and 70 µm | Afshinnia and Rangaraju 2015b |
| 10% of GG as a cement replacement | 0.13† | 0.18* | Not mentioned* | 10% of cement * | $D_{50}$ ≈ 10µm* | Matos and Sousa-Coutinho 2012 † |
| | <0.2 and >0.1 | 0.22 | 1.04% of $Na_2O$eq | 10% of cement | 100 to 9µm | Liu et al. 2015 |
| | 0.5 and 0.56 | 0.97 | 0.88% of $Na_2O$eq | 10% of cement | Mean diameter of 17 and 70µm | Afshinnia and Rangaraju 2015b |
| | 0.15†† | ≈0.47†† | Not mentioned | 10% of cement | > 44µm | Kamali and Ghahremaninezhad 2015 †† |
| | 0.12 | 0.26 | 0.46 of $Na_2O$eq | 10% of cement | $D_{50}$ ≈ 10µm | Chen and Poon 2017 |
| Coarse GG | 0.1 | 0.15 | 0.10% of $Na_2O$eq | 20% of cement | Mean diameter of 204µm | Lu et al. 2017 |
| | 0.4*** and 0,4**** | 0.8 | $Na_2O$eq of 1.81% | 100% of aggregate | 4.75 to 150µm | Maraghechi et al. 2012, Rajabipour et al. 2012 |
| Delayed expansion | *0.03* and 0.19††† | - | 0.86% of $Na_2O$eq | 100% of aggregate | 4.75 to 150µm | Serpa et al. 2013 ††† |

Heated 40 min at: *650°C, **680°C, ***560°C,****600°C

†Borosilicate glass as reactive aggregate

†† 80% of crushed glass and 20% of sand with unmentioned reactivity

††† at 28 days

**Table 5.3 : Expansion of mortar bars tested according to ASTM C1260 or ASTM C1567 and incorporating SCM other than GG when glass is used as a cement or aggregate replacement (mortar bars immersed in 1N NaOH at 80°C for 14 days); expansion < 0.10% innocuous; expansion > 0.20%: deleterious.**

| Expansion (%) | | Aggregate | Cement $Na_2O_{eq}$ | Glass replacement | Size of glass particle | Other SCM | Source |
|---|---|---|---|---|---|---|---|
| Specimen | Control | | | | | | |
| >0.1 | 0.22 | Reactive siliceous sand | 0.73% | 5, 10, and 15% of cement | $D_{50} \approx 20\mu m$ | 15, 10 and 5% FA (for total cement replacement of 20%) | Schwarz et al. 2008 |
| <0.05 | 0.25 | Not mentioned | 0.38% | 50% of aggregate | ASTM 1260 aggregate specification | 2.5 to 10% of MK or FA | Lam et al. 2007 |
| <0.10 | 0.02 | River sand | Not mentioned | 100% of aggregate | Sieved at 5, 2.36, 1.18 and 0.6-0mm | 5 to 20% MK and 5 to 20% FA | Lee et al. 2011 |
| 0.05 and 0.00 | 0.009 | Quartz aggregate | $K_2O$ of 0.66, $Na_2O$ or $Na_2O$eq not mentioned | 7.5% of aggregate | 4.75 to 2mm | 7.5 and 15% of MK | Cota et al. 2015 |
| 0.02 and 0.0 | | | | | 850 to 300µm | | |
| <0.10 | 0.02 | River sand and granite | 0.38% | 15, 30 and 45% of sand | 80% > 0.6mm | 33% FA | Kou and Poon 2009 |
| <0.05 | 0.9 | 100% crushed glass | 0.88 | 10% of cement | Mean diameter of 17µm | 30% of BFS | Afshinnia and Rangaraju 2015a |
| | | | | | | 10% MK | |
| | | | | 20% of cement | | 20% of BFS | |
| 0.62, 0.40 and 0.22 | 0.9 | 100% crushed glass | 0.88 | 0 | Mean diameter of 17µm | 10,20 and 30% FA | Afshinnia and Rangaraju 2015a |
| 0.15 | | | | 20 | | 10% FA | |
| 0.04 and 0.02 | - | Non-reactive sand | ** *** | 20% of alkali-activated BFS of FA | $D_{50} \approx 20\mu m$ | 80% BFS or 80% FA | Maraghechi et al. 2017 |

* ASTM and modified ASTM just enough water for cohesion and slump of 0
** $Na_2O$ of 0.3 and $K_2O$ not mentioned
*** $SiO_2/Na_2O$ of 1.6 for BFS and 1.8 for FA

**Table 5.4 Expansion of concrete prisms incorporating reactive aggregates or non-reactive aggregates and glass as cement or aggregate replacement.**

| | Expansion (%) | | | Aggregate | Cement $Na_2O_{eq}$ kg/m$^3$ | Type and % of glass replacement | Size of glass particles | Note | Source |
|---|---|---|---|---|---|---|---|---|---|
| | Specimen | Control | Limit | | | | | | |
| 20 and 30% replacement of cement by GG | < 0.007% | 0.002 | 0.04* | Non-reactive | 0.46% | 20 and 30% of cement | 88% < 10µm, | A. | Shayan and Xu 2006 |
| | < 0.015% | 0.002 | 0.04* | Non-reactive | 0.46% | 20 and 30% of cement<br>40 to 75% of sand | 88% < 10µm<br>0.6 to 2.25mm | A. | Shayan and Xu 2006 |
| | < 0.005% | 0.002 | 0.04* | Non-reactive | 0.46% | 50% of sand | 0.6 to 2.25 mm | A. | Shayan and Xu 2006 |
| | 0.02 | 0.05 | 0.2 | Non-reactive | † | 30% of cement | $D_{50}$ ≈ 10µm | B. | Dhir et al. 2009 |
| | ≤0.05 | 0.05 | 0.2 | Non-reactive | † | 10% of cement | $D_{50}$ ≈ 10µm | B. | Dhir et al. 2009 |
| | <0.03 | 0.03 | 0.2 | Limestone | 0.58% † | 0, 50 and 100% of fine aggregate<br>20% of cement | Sand (<5mm)<br>GG<45µm | C. | Taha and Nounu 2008 |
| | 0.10, 0.09<br>0.10, 0.07 | 0.21<br>0.17 | 0.040 | Spratt limestone<br>Sudbury gravel | 1.00%<br>(NaOH added) | 20 and 30% of cement replacement | Blaine fineness of 440 m$^2$/kg | Exp. at two years | Zidol 2009 |
| | 0.12, 0.09, 0.11 and 0.08 | 0.27 | 0.04 | Highly reactive (Spratt) | 0.73%†† | 20, 30, 20 and 30% of cement replacement | $D_{50}$ ≈ 10µm | D. | Zidol 2009 |
| Low cement concrete | 0.01 and 0.02 | 0.003 and 0.008 | 0.04* | Gravel | 0.58%<br>237 and 355 kg/m$^3$ | 100% gravel | 19 mm; fines removed | E. | Johnston 1974 |

| | Expansion (%) | | | Aggregate | Cement $Na_2O_{eq}$ kg/m$^3$ | Type and % of glass replacement | Size of glass particles | Note | Source |
|---|---|---|---|---|---|---|---|---|---|
| | Specimen | Control | Limit | | | | | | |
| Coarse glass | 0.15 and 0.47 | 0.02 | 0.2 | Reactive limestone | 0.58% † | 50 and 100% of fine aggregate | Sand (<5mm) | C. | Taha and Nounu 2008 |
| | 0.06 and 0.05 | 0.05 | 0.2 | Limestone | † | 50 and 100% of fine aggregate | Sand $D_{50}$ ≈1mm | B. | Dhir et al. 2009 |
| | >0.30 | 0.016 | 0.04* | Gravel | 0.58% 474 kg/m$^3$ | 100% gravel | 19 mm; fines removed | E. | Johnston 1974 |
| | 0.15, 0.27 and 0.28 | 0.012, 0.018 and 0.027 | 0.04* | Gravel | 1.23% 237, 355 and 474 kg/m$^3$ | 100% gravel | 19 mm; fines removed | E. | Johnston 1974 |
| | 0.15, >0.30 and >0.30 | 0.012, 0.018 and 0.027 | 0.04* | Gravel | 1.23% 237, 355 and 474 kg/m$^3$ | 100% gravel | 19 mm | E. | Johnston 1974 |
| | 0.07, 0.2 and >0.3 | 0.012 ** | 0.04* | Gravel | 1.23% 415 kg/m$^3$ | 20, 60, 100% | 19 mm | E. | Johnston 1974 |

A. Prisms of 75 x 75 x 285mm in size, stored at 38°C,100% RH and test duration over 2 years
B. BS 812 part 123:1999; prisms of 100 x 100 x 300 mm in size, stored at 38°C for 52 weeks, “at high humidity”; Expansive limit is 0.2% and non-expansive threshold is 0.05%
C. BS 812 part 123:1999; prisms of 75 x 75 x 279 mm in size, stored at 38°C for 52 weeks, “at high humidity”, Expansive limit is 0.2% and non-expansive threshold is 0.05%
D. CSA 23.2-14A, interrupted at 26 seem, 38°C. GG was ground by crushing 20kg of glass for 150 and 225 minutes
E. Prisms of 102 x 102 x 305 mm in size, conditioned in a fog room at 21°C for 52 weeks

† $K_2SO_4$ added to obtain $Na_2O_{eq}$ of 1.00%

†† NaOH added to obtain $Na_2O_{eq}$ of 1.25%; measurements at ≈180 days

*Expansion limit of 0.04% assumed

**Data for 415 kg/m$^3$ Extrapolated between 355 and 474 kg/m$^3$

## 5.2 Scope and Objective

Previous research has highlighted the limited effectiveness of a high-alkali GG available on the Quebec market in preventing deleterious expansion in binary concrete (20 and 30% cement replacement) and mortar (20% cement replacement) specimens made with highly- and moderately reactive aggregates (Zidol, 2009, Lafrenière, 2017, Fily-Paré et al., 2020). In that context, the objective of this work was to evaluate, using the CPT, the beneficial effect regarding ASR prevention of ternary cementitious systems incorporating GG. To do so, 10 to 30% of GG was used in concretes incorporating the highly-reactive Spratt limestone and 5 to 10% silica fume (SF), 5 to 15% metakaolin (MK), 15 to 30% fly ash (FA) or 20 to 40% ground granulated blast furnace slag (BFS) as replacement, by mass, of a high-alkali ordinary portland cement (OPC). Unboosted (i.e. high alkali cement only; 0.94% $Na_2Oeq$) and boosted concrete mixtures (high-alkali cement with NaOH addition – 1.08 and 1.25% $Na_2Oeq$) were made to try isolating potential (deleterious) alkali contribution by the high-alkali GG to the expansive behavior of the test specimens.

Concrete prisms were made and stored in accordance with Standard Practice CSA 23.2-28A, which has been slightly modified to limit alkali leaching from the test prisms (100 x 100 x 300mm instead of 75 x 75 x 300mm). The length and mass changes of the above specimens were regularly monitored over two years under laboratory test conditions (storage at 38°C, R.H. > 95%).

## 5.3 Materials and Methods

### 5.3.1 Cementitious Materials

Concrete specimens were made using the following cementitious materials: GG from a local recycling facility in the province of Québec (Canada); SF from a ferro-silicon plant also located in the province of Québec (Canada); MK from Georgia (USA); class F FA from Alberta (Canada); grade 80 BFS from Ontario (Canada) and GU type OPC, also from Québec (Canada). The chemical composition and the specific gravity of the above materials are presented in Table 5.5. The $D_{50}$ of GG is approximately 30 microns.

**Table 5.5 : Chemical composition of binders and fine aggregate.**

| Oxide | $SiO_2$ | CaO | $Al_2O_3$ | $Fe_2O_3$ | $SO_3$ | MgO | L.O.I. | $Na_2O$ | $K_2O$ | $Na_2Oeq$ | S.G. |
|---|---|---|---|---|---|---|---|---|---|---|---|
| **Cement** | 18.7 | 60.8 | 5.00 | 3.70 | 3.80 | 2.70 | 1.90 | 0.25 | 1.05 | 0.94 | 3.15 |
| **BFS** | 37.74 | 36.20 | 10.75 | 0.50 | - | 1.05 | 1.80 | 2.50 | 0.64 | 2,92 | 2.92 |
| **FA** | 56.72 | 9.29 | 24.07 | 3.14 | - | 12.62 | 0.80 | 0.41 | 0.49 | 0.73 | 2.54 |
| **GG** | 70.53 | 10.77 | 2.06 | 0.35 | 0.11 | 1.14 | 1.71 | 12.49 | 0.66 | 12.92 | 2.35 |
| **SF** | 94.27 | 0.54 | 0.30 | 0.10 | 0.02 | 0.28 | 3.2 | 0.12 | 0.65 | 1.43 | 2.24 |
| **MK** | 51.6 | 0.02 | 43.97 | 0.49 | 0.00 | 0.04 | 1.84 | 0.27 | 0.25 | 0.43 | 2.20 |
| **Fine agg.** | 0.46 | 63.63 | 0.10 | 0.09 | - | 0.31 | 35.37 | 0.00 | 0.05 | 0.03 | 2.70 |

### 5.3.2 Aggregates

The non-reactive fine aggregate used for concrete was a manufactured high purity limestone sand for which the chemical composition is given in Table 5.5. The density of the fine aggregate is 2.70 and its absorption capacity is 0.57%. The coarse aggregate is the highly-reactive Spratt limestone from Ontario (Canada), which shows a density of 2.70 and an absorption capacity of 0.43%.

### 5.3.3 Design of Experiment (DOE) and Mix Design

A *Face Centered Central Composite Design* (FCCD) was used to build the four experimental plans implemented in this study. Concrete mixtures incorporating 5-10% SF or 5-15% MK ranged in their GG content between 10 and 30% (Figure 5.1), while mixtures incorporating 15-30% FA or 20-40% BFS ranged in their GG content between 10 and 20% (Figure 5.2). The same high-alkali (0.94% $Na_2Oeq$) portland cement was used in all mixtures; however, selected concrete mixtures were also made in which NaOH was added to raise the “cement” alkali content to 1.08% and 1.25%, $Na_2Oeq$.

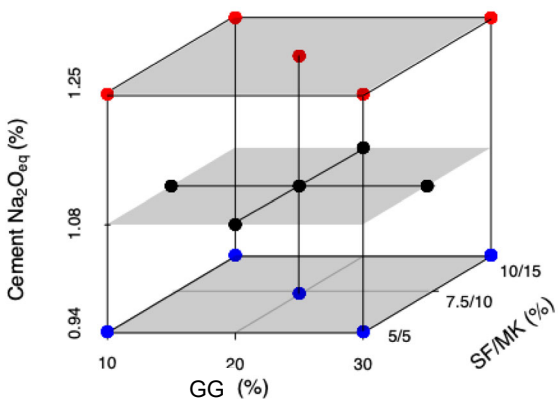


**Figure 5.1 : Experimental plan indicating the percentages of GG and either SF or MK used as cement replacement and the $Na_2Oeq$ of the cement for mixtures selected in this study.**

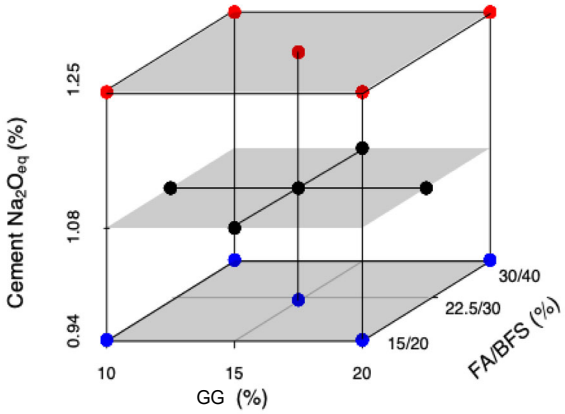


**Figure 5.2 : Experimental plan indicating the percentages of GG and either FA or BFS used as cement replacement and the $Na_2Oeq$ of the cement for mixtures selected in this study.**

In addition to the four FCCD experimental plans, ternary mixtures incorporating 30%GG, 20%FA / 30%BFS and with a "cement" $Na_2O_{eq}$ content of 1.25% were manufactured and monitored for expansion. Finally, binary concrete mixtures incorporating 10, 20 and 30% GG in combination with "cement" $Na_2Oeq$ contents of 0.94, 1.08 and 1.25% were also added to the experimental plans.

All concrete mixtures were made with 420 kg/m$^3$ of cementitious materials, 1054 kg/m$^3$ of coarse reactive aggregate and between 677 and 732 kg/m$^3$ of non-reactive fine aggregate. Fine aggregate mass variations were implemented to accommodate the volume changes associated to the differences in density of the SCM. Consequently, the 60:40 mass proportion for coarse aggregate-to-fine aggregate proposed by in Standard Practice CSA 23.2-28A is ultimately 60±1: 40±1 to maintain a constant amount of reactive coarse aggregate in each mixture. A water-to-binder ratio of 0.42 was selected for all mixtures, while a polycarboxylate superplasticizer was used when appropriate to reach slumps between 100 and 150mm, as required by the Standard Practice CSA 23.2-28A.

### 5.3.4 Methods

Concrete specimens were made in accordance with CSA 23.2-28A, except for two modifications that were adopted to minimize alkali leaching of the specimens (Lindgård et al., 2013). First, the section of the concrete specimens was increased from 75x75x300 $mm^3$ to 100x100x300 $mm^3$. Second, temperature cycling and their inherent condensation and runoffs promoting alkali leaching were suppressed by performing length-change measurements without pre-cooling of the test specimens. A polycarboxylate based superplasticizer was used to meet the 100 mm to 150 mm slump requirements of CSA 23.2-28A in the case of ternary blends incorporating SF and MK. This was also done to ensure proper workability especially when NaOH was added to increase the alkali content of the system.

A total of four large prisms were made from each ternary concrete mixture; in the case of control (100% OPC) and binary (cement + GG) mixtures, six and two prisms were made, respectively.

The first measurement was taken on concrete specimens 48h after casting since prisms were left 24h in their moulds in a moist chamber and then 24h at 38°C and 100% RH to reach temperature equilibrium. Because of their larger section, two prisms were stored per 25-L plastic pails. Some basic information on the chemical "stability" of the GG could be obtained from dissolution work of GG specimens of different composition and in different alkaline solutions (NaOH/KOH, different concentrations, in the presence or not of $Ca(OH)_2$).All specimens were regularly monitored for mass and length variations over a period of two years.

## 5.4 Results of Expansion Testing

### 5.4.1 Control and Binary Concrete Mixtures (GG only)

Figure 5.3 presents the expansion results, as a function of time, of the control mixtures incorporating the highly-reactive Spratt aggregate as well as the binary mixtures incorporating 10 to 30% GG. The large control prisms (i.e. 100 x 100 mm2) reached average expansions of about 0.140% at one year while the "standard-size" test prisms (75 x 75 mm2) showed an average expansion of 0,160% at that age (not illustrated in Figure 5.3).However, both sets of test specimens reached similar expansion s of 0.177% and 0.173% at two years for the 75 x 75 mm2 and 100 x 100 mm2 specimens, respectively. For that reason, it was decided to maintain the use of a two-year 0.040% expansion for evaluating the effectiveness of binary and ternary cementitious incorporating the Spratt aggregate in this study, i.e. on the basis of expansion data obtained on large-section (100 x 100 mm2) concrete specimens. Those are the expansion results that will be presented and discussed in more details in the following sections.

The incorporation of GG always resulted in lower expansions compared to the controls; however, in binary systems, 10 to 30% GG replacement levels were insufficient to meet the 0.040% expansion limit of the Canadian standard. For concrete mixtures incorporating 10%GG, increasing expansion is observed with increasing "cement" alkali content in the mixture, i.e. from 0.94 to 1.25% $Na_2Oeq$; however, the opposite trend is observed for mixtures incorporating 30%GG, where non-boosted test prisms reached higher expansions than those with NaOH addition. A mixed behavior was observed in the case of the 20% GG set of concrete mixtures.

Figure 5.3 also illustrates the expansion results of two ternary mixtures incorporating 30%GG / 30% BFS and 30%GG / 20%FA. The results suggest that expansion in ternary mixtures can be reduced significantly compared to that in binary mixtures incorporating only GG.

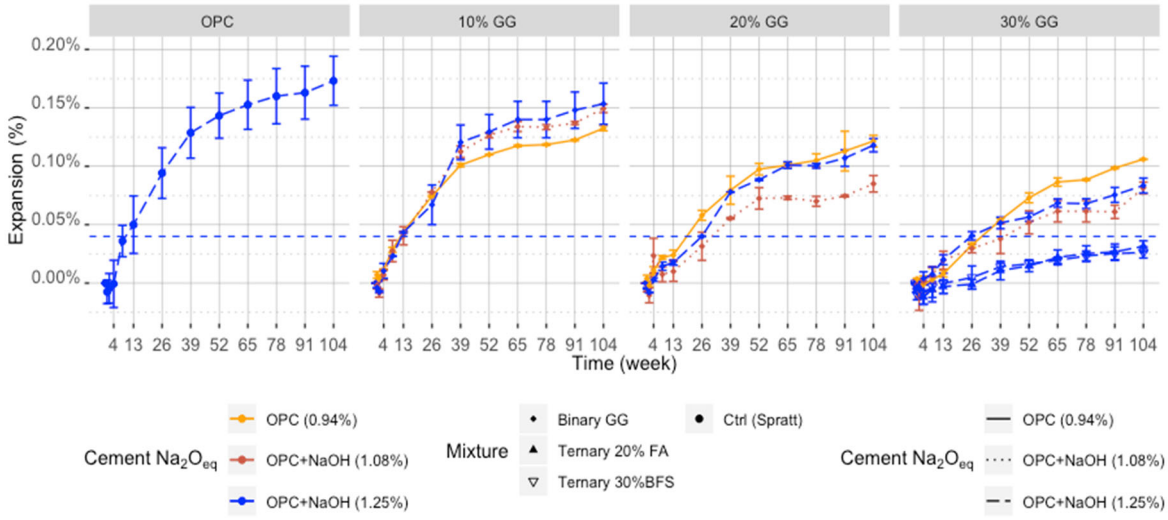


**Figure 5.3: Expansion results of the control and binary mixtures (with and without NaOH addition) incorporating the highly-reactive Spratt limestone and various amounts of GG. Two ternary mixtures incorporating 30%GG and 20%FA / 30%BFS are added, and the error bars relate to Standard Deviation (SD).**

### 5.4.2 Ternary Concrete Mixtures Incorporating SF / MK

Figure 5.4 presents the expansion results of the ternary mixtures incorporating GG and SF / MK. All 10 mixtures incorporating 5% SF or MK (i.e. with 10 to 30% GG) and 8 out of 10 mixtures incorporating 10% GG failed to meet the two-year 0.040% expansion limit of CSA Standard Practice A23.2-28A Only the use of 10 or 15% MK with lower concrete alkali contents resulted in two-year expansions well below 0.040% for mixtures with 10 % of GG. Concrete mixtures that clustered around the 0.040% limit are mostly those incorporating intermediate amounts of SCMs, such as 20% GG and 5 to 10% of SF/MK, while most mixtures comfortably below the 0.040% limit incorporate higher levels of SCMs. In most cases, deleterious expansion in concrete prisms incorporating the highly-reactive Spratt aggregate can be prevented when 20 or 30% of the high alkali GG is combined with 10-15%MK, regardless of the "cement" alkali content. Similar observations can be drawn for mixtures incorporating 20-30% GG and 7.5-10% SF, although the SF systems seem to be more sensitive to the "cement" alkali content (or alkali addition). Actually, higher expansions are sometimes obtained with lower-to-intermediate "cement" alkali contents. This is the case for instance of the 30%GG-10%SF-0.94Alk, which resulted in a two-year average expansion of 0.065% compared to 0.023% for mixture 30GG-10SF-1.25Alk. This will be discussed further in the paper.

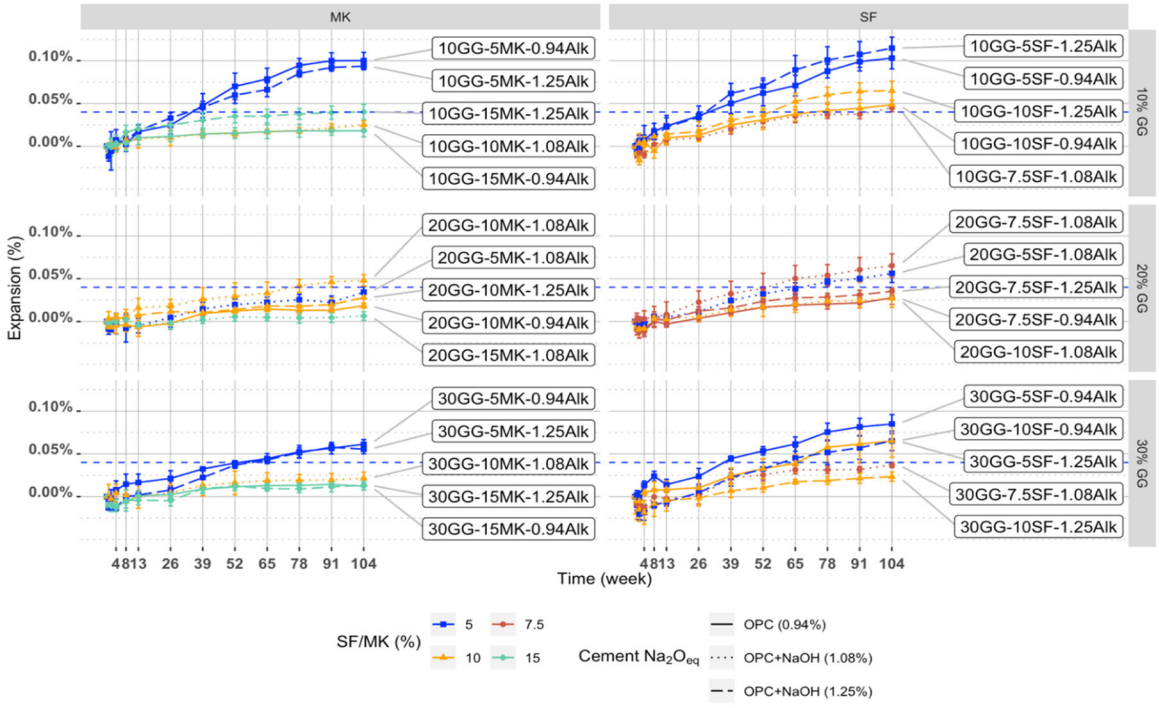


**Figure 5.4 : Expansion results of ternary mixtures (with and without NaOH addition) incorporating the highly-reactive Spratt limestone and various amounts of GG, SF or MK. Each result indicated in this figure corresponds to the average expansion obtained on four test prisms and the error bars relate to standard deviation. The dotted line corresponds to the 0.040% acceptance limit of CSA Standard Practice A23.2-28A.**

### 5.4.3 Ternary Concrete Mixtures Incorporating FA / BFS

Figure 5.5 presents the expansion results of the ternary mixtures incorporating GG and FA / BFS. Similarly, to SF and MK, lower amounts of FA or BFS lead to concrete prism expansions that are above the two-year 0.040% limit. Actually, 9 out of 10 mixtures with the lowest dosages (20% BFS or 15% FA – with 10 to 20% GG) resulted in expansions above 0.040%. In this study, 12 out of 15 mixtures combining BFS and GG resulted in average expansions higher than the 0.040% limit. The mixtures incorporating BFS that displayed average concrete prism expansions < 0.040% are: 10GG-40BFS-1.25Alk (0.033%), 15GG-30BFS-1.08Alk (0.035%), and 20GG-40BFS-1.25Alk (0.036%), which are still relatively close to the limit.

A large proportion of mixtures incorporating GG and FA resulted in concrete prism expansions clustered around the 0,040% limit, ranging between 0.03% and 0.05%, the lowest expansion being obtained for mixtures 10GG-22.5FA-1.08Alk (0.033%), 15GG-30FA-1.08Alk (0.029%) and 20GG-30FA-1.25Alk (0.013%).

Increasing the "cement" alkali content in the BFS-mixtures sometimes resulted in lower concrete prism expansions. The latter phenomenon is more pronounced when 20%GG is used compared to 10%GG. Similar trends were observed for mixtures incorporating FA where this observation stands for all GG contents.

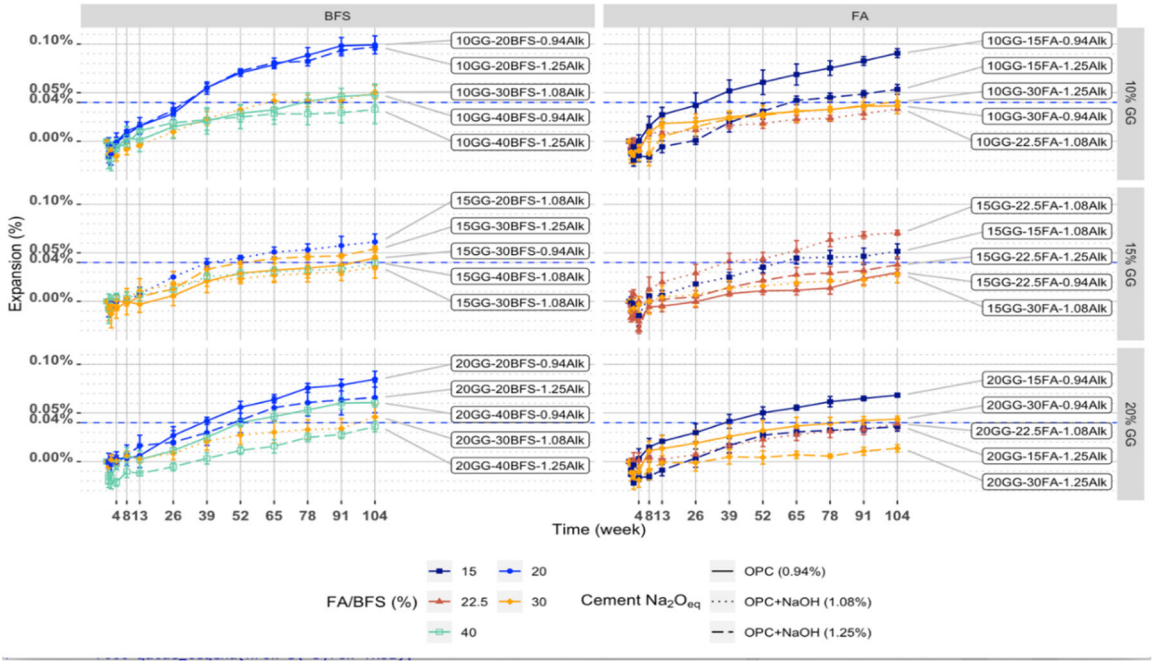


**Figure 5.5 : Expansion results of ternary mixtures (with and without NaOH addition) incorporating the highly-reactive Spratt limestone and various amounts of GG, FA or BFS. Each result indicated in this figure corresponds to the average expansion obtained on four test prisms and the error bars relate to standard deviation. Dotted line is related to the 0.040% acceptance limit of Standard Practice CSA23.2-28A.**

## 5.5 Discussion

### 5.5.1 ASR Preventing Effect of GG

Table 5.6 presents the average two-year expansion values, for given GG contents, of control and binary concrete prisms incorporating the highly-reactive Spratt limestone and cements of various $Na_2O$eq contents. Binary mixtures incorporating 10 to 30% GG generally display expansions well beyond the CSA 0.040% limit, thus suggesting that such dosages of GG cannot prevent expansion in concrete incorporating the highly-reactive Spratt aggregate. The above results are in accordance with those obtained with ASTM C1260 presented in Table 5.1 (Shi et al., 2004, Zidol, 2009, Pereira-de-Oliveira et al., 2012, Zheng, 2016), and also with CPT results (Lafrenière, 2017, Zidol, 2009). The CPT results presented in Figure 5.4 and in Table 5.6 confirmed that 10-30% cement replacement by high-alkali GG do contribute at reducing expansion under the acceptance threshold but do not promote expansion beyond that of the control mixture.

**Table 5.6 : Two-year expansions of binary concrete prisms made with cements of $Na_2O_{eq}$ contents of 0.94, 1.08% (0.94% +NaOH) and 1.25% (0.94%+NaOH).**

| | Cements of $Na_2O_{eq}$ contents of | | | Average |
|---|---|---|---|---|
| GG | 0.94% | 1.08% | 1.25% | |
| (%) | (%) | (%) | (%) | (%) |
| 0* | | | 0.170 | 0.170 |
| 10 | 0.132 | 0.149 | 0.153 | 0.145 |
| 20 | 0.122 | 0.085 | 0.118 | 0.108 |
| 30 | 0.106 | 0.081 | 0.083 | 0.090 |

Table 5.7 presents the average expansion reduction associated with10% GG increments. It is suggested that the impact of GG in reducing concrete prism expansion is not linearly proportional to the replacement level in the system. For instance, an increase of 10 to 20% in GG content is associated to a 0.037% reduction of expansion, which is almost twice that of an increase from 20 to 30% GG content (0.018%).

**Table 5.7: Average two-year expansions of binary concrete systems incorporating the highly-reactive Spratt limestone and various $Na_2O_{eq}$ contents, grouped by GG contents.**

| GG content (%) | Average % of expansion reduction for 10% of GG | Confidence interval (95%) | |
|---|---|---|---|
| | | Min | Max |
| 10 to 20 | -0.037 | -0.016 | -0.057 |
| 20 to 30 | -0.018 | -0.003 | -0.038 |

Table 5.8 presents the average expansion of concrete prisms of different "cement" alkali contents ($Na_2O_{eq}$) for the ternary mixtures grouped by SCM type and percentage of cement replacement. GG increments are always associated with expansion reduction. As suggested in Table 5.8 by the expansion reduction for 10% cement replacement with SCM, GG only shows about 1/2 of the mitigation power of FA and BFS by mass and about 1/5 or 1/8 of the mitigation power of SF and MK by mass, respectively.

**Table 5.8 : Average expansions of the pool of ternary concrete prisms incorporating the highly-reactive Spratt limestone and various amounts of SCMs, along with the average impact of SCM increase with 95% confidence interval and impact for 10% mass replacement.**

| Materials | | (%) | Avg. Exp. (%) | (%) | Avg. Exp. (%) | Diff. (%) | Confidence interval (95%) Min. (%) | Max (%) | Expansion reduction for 10% of targeted SCM (%) |
|---|---|---|---|---|---|---|---|---|---|
| SF/MK | GG | 10 | 0.065 | 30 | 0.044 | -0.021 | -0.008 | -0.035 | -0.011 |
| | SF | 5 | 0.085 | 10 | 0.046 | -0.039 | -0.024 | -0.054 | -0.078 |
| | MK | 5 | 0.069 | 15 | 0.018 | -0.051 | -0.038 | -0.064 | -0.051 |
| FA/BFS | GG | 10 | 0.059 | 20 | 0.049 | -0.010 | -0.001 | -0.020 | -0.010 |
| | FA | 15 | 0.060 | 30 | 0.033 | -0.027 | -0.017 | -0.038 | -0.018 |
| | BFS | 20 | 0.082 | 40 | 0.043 | -0.038 | -0.028 | -0.048 | -0.019 |

Figure 5.6 and Figure 5.7 respectively present the concrete prism expansions at the "two-year time limit" for control concretes, binary concretes (i.e. with GG only) and ternary mixtures incorporating SF/MK and FA/BFS, classified by GG content. The two-year expansions of ternary mixtures incorporating 5-10%SF and 5-15%MK vary from 0.120 to 0.027% and from 0.100% to 0.007%, respectively. In the case of the ternary mixtures with 15-30%FA and 20-40%BFS, the two-year expansions range from 0.091 to 0.014% and from 0.099 to 0.026%, respectively.

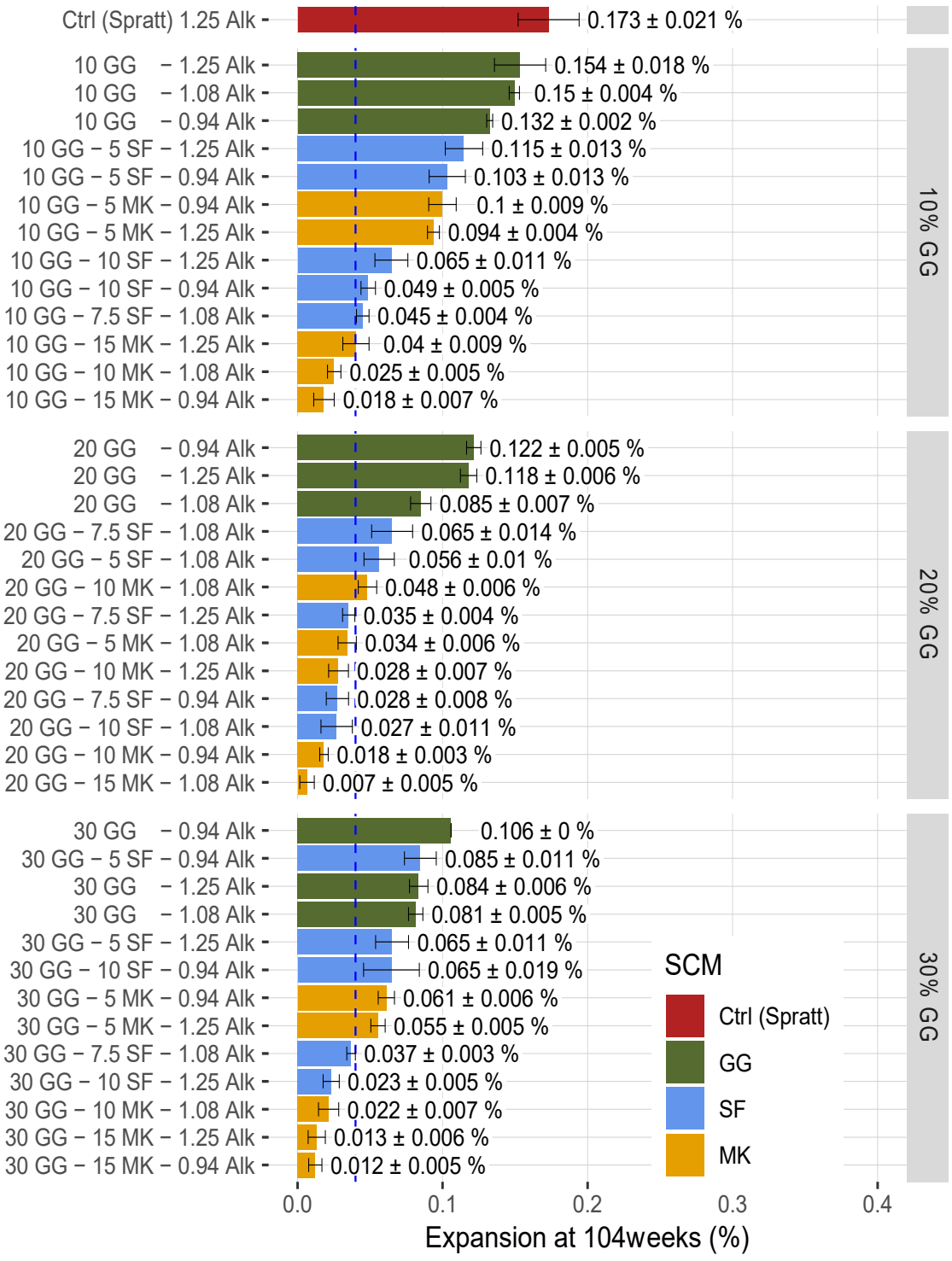


**Figure 5.6 : Two-year expansions of concrete prisms incorporating the highly-reactive Spratt limestone, various amounts of GG, various amounts of SF or MK and made with the selected high-alkali cement (with and without NaOH addition). The dotted line is the 0.040% limit of CSA Standard Practice A23.2-28A and the error bar corresponds to the standard variations.**

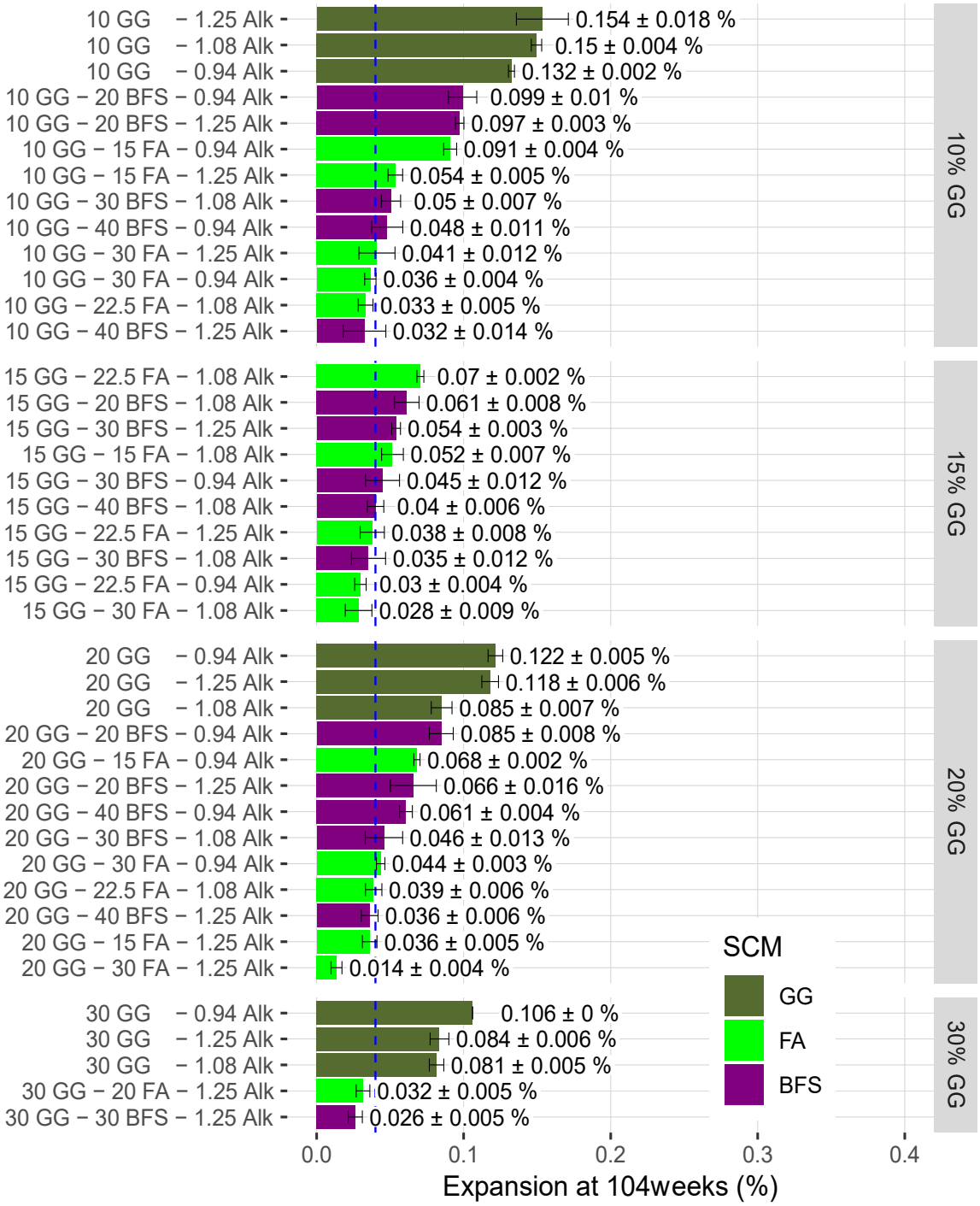


**Figure 5.7: Two-year expansions of concrete prisms incorporating the highly-reactive Spratt limestone, various amounts of GG, various amounts of FA or BFS and made with the selected high-alkali cement (with and without NaOH addition). The dotted line is the 0.040% limit of CSA Standard Practice A23.2-28A and the error bar corresponds to the standard variations.**

### 5.5.2 Linear Trends Related to GG, SF/MK/FA/BFS and $Na_2O_{eq}$ Content of Cement

The goal of the experimental plan used in this investigation was to determine whether somewhat linear trends exist between the contents in GG, other SCMs, the $Na_2Oeq$ in the cement, and the expansive behavior of the ternary systems investigated. The linear models presented in Table 5.9 were attempted to picture the two-year expansions in the SF, MK, FA and BFS ternary concrete mixtures, but were found to display relatively poor $R^2$. A closer look at the data reveals that there are indeed some interactions between the parameter GG, SF/MK/FA/BFS and cement $Na_2O_{eq}$ content, but the effect is too inconsistent to be translated into a linear trend; which makes each mixture somewhat "unique".

**Table 5.9: Multiple regression output from the fit of the model of expansion data for mixtures incorporating various amounts of GG, SF/MK/FA/BFS and $Na_2Oeq$ contents of cements.**

| | | SF | MK | FA | BFS |
|---|---|---|---|---|---|
| First order | Intercept | -0.024 | 0.13 | 0.25 | 0.092 |
| | GG | 0.005 | 0.000 | -0.000 | 0.000 |
| | SCM | -0.006 | -0.013 | -0.007 | -0.002 |
| | $Na_2Oeq$ | 0.176 | 0.000 | -0.013 | 0.096 |
| Interaction | GG*SCM | 0.000 | 0.000 | 0.000 | 0.000 |
| | GG*$Na_2Oeq$ | -0.007 | -0.002 | -0.001 | 0.005 |
| | SCM*$Na_2Oeq$ | -0.005 | 0.005 | 0.004 | 0.002 |
| | $R^2$ | 0.53 | 0.69 | 0.58 | 0.65 |

It was shown in Figure 5.3 that the two-year expansions in binary concrete mixtures incorporating 10 to 30% GG were always beyond the 0.040% acceptance limit of CSA A23.2-28A. Based on the results presented in Figure 5.4 and Figure 5.5 and on the basis of the materials and results obtained in this study, Table 5.10 provides minimum contents in SF/MK/FA/BFS that would allow to meet the above acceptance limit in ternary blends incorporating GG and the highly-reactive Spratt aggregate.. Those will be further discussed in the following sections.

**Table 5.10: Minimum replacement levels to meet the two-year expansion limit of 0.040% for ternary concretes incorporating highly-reactive Spratt limestone, 10 to 30% GG and various proportions of SF, MK, FA or BFS. Information is given for mixtures without and with added alkalis (i.e. cement alkali content of 0.94 and 1.25%, $Na_2O$eq; the latter corresponds to 0.94% + NaOH addition to reach 1.25% $Na_2O$eq).**

| SCM → | % SF | | % MK | | % FA | | % BFS | |
|---|---|---|---|---|---|---|---|---|
| %GG↓ | 0.94 $Na_2O$eq | 1.25 $Na_2O$eq | 0.94 $Na_2O$eq | 1.25 $Na_2O$eq | 0.94 $Na_2O$eq | 1.25 $Na_2O$eq | 0.94 $Na_2O$eq | 1.25 $Na_2O$eq |
| 10 | >10 | >10 | 10 | 15 | 30 | 30 | 50 | 40 |
| 20 | 7.5 | 7.5 | 10 | 10 | >30 | ≈22.5 | 50 | 40 |
| 30 | >10 | 7.5 | 10 | 10 | n.a. | 20 | n.a. | 30 |

### 5.5.3 Ternary Mixtures Incorporating GG and Silica Fume (SF)

Table 5.11 presents the two-year expansion results for eight mixtures of the SF experimental plan. With the exception of mixture 30GG-10SF-0.94Alk (unusually high expansion), the data of this group display a "logical" pattern characterized by expansion reductions when 1) SF content increases for a given GG content, and 2) GG content increases for a given SF content. In the case of ternary mixtures with added alkalis, increasing the SF content from 5 to 10% results in similar expansion reduction (i.e. about -0.040-0.050%) than increasing the GG content from 10 to 30% (Table 5.11). This relationship is however not so clear for the unboosted ternary mixtures (i.e. cement 0.94% $Na_2O$eq).

The data in Table 5.8 indicate that 7.5 to 10% SF are required to prevent deleterious expansion (i.e. expansion < 0.040%) in ternary concrete mixtures incorporating 10-30%GG; the requirements are not that different whether the concrete mixtures are made with/without added alkalis. This behavior is actually similar to that of a high-alkali fly ash; Fournier et al. (2008) indeed showed that combining 5% SF with 25% of a high-alkali FA (16.8% CaO and 10.5% $Na_2O$eq) was insufficient to prevent expansion in concrete prisms made with the Spratt aggregate (0.067% expansion at two years).

Fournier et al (2004, 2016) Bleszynski (2002) showed that between 10 to 15% SF are required to prevent deleterious expansion in binary concretes (i.e. SF only) incorporating the highly reactive Spratt aggregate. The above suggest that the further addition of 10 to 30% high-alkali GG in ternary concretes does not require to increase (or allow to decrease significantly) the SF content (compared to concrete with SF only) to prevent deleterious expansion; this indicates that GG plays a neutral or perhaps modest beneficial (preventive) effect in the high-alkali GG/SF ternary systems investigated. Comparatively, Shehata and Thomas (2002) and Fournier et al. (2008) reported a synergetic effect in combining 5% SF with 15 to 20% low-alkali class F fly ash or 30% class C fly ash to prevent deleterious expansion in concrete prisms incorporating the Spratt aggregate (two-year expansion < 0.040%).

**Table 5.11: Expansion results of individual mixtures incorporating SF and the impact of GG addition for fixed contents of SF and $Na_2O$eq of cement.**

| | 0.94 $Na_2O$eq | | | 1.25 $Na_2O$eq | | |
|---|---|---|---|---|---|---|
| | 10% GG | 30% GG | Diff 10-30 GG | 10% GG | 30% GG | Diff 10-30 GG |
| 5% SF | 0.103% | 0.085% | -0.018% | 0.115% | 0.065% | -0.050% |
| 10% SF | 0.049% | 0.065% | 0.016% | 0.065% | 0.023% | -0.042% |
| Diff 5-10 SF | -0.054% | -0.020% | - | -0.050% | -0.042% | - |

### 5.5.4 Ternary Mixtures Incorporating GG and Metakaolin (MK)

Table 5.12 presents the two-year expansions for eight mixtures of the MK experimental plan. The data show that large expansion reductions (-0.027 to -0.082%), although variable, are generally obtained when increasing GG or MK contents in those ternary systems. Similar to SF, expansion reductions are indeed obtained when 1) MK content increases for a given GG content, and 2) GG content increases for a given MK content. One can see that increasing the MK content from 5 to 15% in mixtures incorporating 10 or 30% GG results in concrete prism expansions ≤ 0.040%. Data in Table 5.10 and Table 5.12 indicate that adding about 10% MK is effective in preventing expansion in either boosted/unboosted mixtures incorporating 10 to 30% GG. Based on two-year CPT data, Ramlochan et al. (2002) suggested that between 10 to 15% MK are required to prevent deleterious expansion in concrete incorporating the highly-reactive Spratt aggregate. This indicates that the GG is playing a somewhat neutral or modestly synergetic role to prevent ASR in ternary systems incorporating the highly-reactive Spratt limestone and MK.

**Table 5.12 : Expansion results of individual mixtures incorporating MK and the impact of GG addition for fixed contents of MK and $Na_2O$eq of cement.**

| | 0.94 $Na_2O$eq | | | 1.25 $Na_2O$eq | | |
|---|---|---|---|---|---|---|
| | 10% GG | 30% GG | Diff 10-30 GG | 10% GG | 30% GG | Diff 10-30 GG |
| **5% MK** | 0.100% | 0.061% | -0.039% | 0.094% | 0.055% | -0.038% |
| **15% MK** | 0.018% | 0.012% | -0.006% | 0.040% | 0.013% | -0.027% |
| **Diff 5-15 MK** | -0.082% | -0.049% | - | -0.053% | -0.042% | - |

### 5.5.5 Ternary Mixtures Incorporating GG and Fly Ash (FA)

Table 5.13 presents the two-year expansion results for eight mixtures of the FA experimental plan. The most important expansion reduction resulting from an increase of FA content from 15 to 30% (-0.054%) is obtained for the mixture incorporating 10%GG and no NaOH addition. In most other cases, expansion reductions range from -0.013 to -0.027%; however, it is only in the case of mixture 20GG-30FA-1.25Alk that this reduction results in an expansion comfortably below the 0.040% limit. One can note that most mixtures incorporating GG, FA and added alkalis (1.25% $Na_2O$eq) display lower expansions than those of companion mixtures without NaOH addition; this suggest that the alkali addition in such systems results in a beneficial effect on pozzolanic activity that goes beyond that of ASR acceleration (which is normally the objective of adding alkalis, in addition to compensating for alkali leaching from the test prisms). Moreover, data in Table 5.10 indicate that the minimum amount of FA to prevent expansion in concrete prisms incorporating 10 to 30% GG ranges from 30 to 20% (boosted mixtures) and $\geq$30% in the case of unboosted mixtures (0.94% cement alkali). Based on two-year CPT data, Shehata and Thomas (2002) and Fournier et al. (2004) reported that about 20 to 25% low-calcium FA (similar in efficiency to that used in this study) is required to prevent deleterious expansion in binary (i.e. FA only) concretes incorporating the highly-reactive Spratt aggregate. This suggests that combining FA with high-alkali GG contributes at reducing ASR expansion but in a rather less efficient way than MK and even SF considering the high proportions of FA required to reduce expansion under the acceptance limit.

**Table 5.13: Expansion results of individual mixtures incorporating FA and the impact of GG addition for fixed contents of FA and $Na_2O$eq of cement.**

| | 0.94 $Na_2O$eq | | | 1.25 $Na_2O$eq | | |
|---|---|---|---|---|---|---|
| | 10% GG | 20% GG | Diff 10-20 GG | 10% GG | 20% GG | Diff 10-20 GG |
| **15% FA** | 0.091% | 0.068% | -0.023% | 0.053% | 0.036% | -0.017% |
| **30% FA** | 0.036% | 0.041% | 0.004% | 0.041% | 0.014% | -0.027% |
| **Diff 15-30 FA** | -0.054% | -0.013% | - | -0.013% | -0.022% | - |

### 5.5.6 Ternary Mixtures Incorporating GG and BFS

Table 5.14 presents the two-year expansion results for eight mixtures of the BFS experimental plan. Increasing the BFS content from 20 to 40% results in expansion reductions that are two times more important in 10%GG mixtures (-0.051 & -0.064%) than in 20%GG mixtures (-0.024% & -0.030%). Also, NaOH additions (i.e. mixtures 0.94 vs 1.25%) always lead to reduced expansions compared to companion specimens without NaOH addition. Despite that, the two-year expansions in all ternary blends of Table 5.14 remain greater or close to the 0.040% limit, which indicates a rather limited effectiveness of those systems in controlling expansion with the highly-reactive Spratt aggregate.

Table 5.10 shows that the minimum amount of BFS to prevent expansion in concrete prisms incorporating 10 to 30% GG ranges from 40 to 30% (boosted mixtures) and 50% in the case of unboosted mixtures (0.94% cement alkali). Field and laboratory data indicated that between 40 and 50% BFS are necessary to prevent expansion in binary concretes (i.e. BFS only) made with the Spratt limestone (Thomas and Innis 1998, Fournier et al. 2018). This indicates no synergetic effect of combining slag with GG to prevent expansion with the above aggregate as it requires 50 to 70% total SCM for doing so.

**Table 5.14: Expansion results of individual mixtures incorporating BFS and the impact of GG addition for fixed contents of BFS and $Na_2O_{eq}$ of cement.**

| | 0.94 $Na_2Oeq$ | | | 1.25 $Na_2Oeq$ | | |
|---|---|---|---|---|---|---|
| | 10% GG | 20% GG | Diff 10-20 GG | 10% GG | 20% GG | Diff 10-20 GG |
| **20% BFS** | 0.099% | 0.085% | -0.015% | 0.097% | 0.066% | -0.031% |
| **40% BFS** | 0.048% | 0.061% | 0.013% | 0.033% | 0.036% | 0.003% |
| **Diff 20-40 BFS** | -0.051% | -0.024% | - | -0.064% | -0.030% | - |

## 5.6 Conclusion

Previous work suggested the potential of GG at reducing expansion due to ASR when tested under the AMBT conditions. The results obtained in the present study also support the above conclusion but for specimens tested under CPT conditions. In this work, four experimental plans were conducted to assess the expansion of ternary mixtures incorporating GG, in combination with either SF, MK, FA or BFS, and high-alkali cement with and without NaOH addition (i.e. $Na_2O_{eq}$ content ranging between 0.94% and 1.25%). The results of the experimental plans lead to no single reliable linear model that managed to describe the behavior of the above ternary mixtures, which makes those systems somewhat “unique” in their potential for preventing ASR expansion.

Nonetheless, GG like all other SCMs tested in this study show a potential in reducing expansion due to ASR, but its relative potential, by mass, ranges roughly between 1/8 and ½ of that of the other SCMs.

Furthermore, mixtures with and without NaOH show very different behavior. Indeed, NaOH addition enhances the preventing potential of GG in many cases (Fily-Paré et al. 2020).. However, the downside of such synergy is that the above testing (boosting with NaOH) condition is likely introducing a positive bias in the potential of GG to prevent expansion in binary or ternary mixtures incorporating reactive aggregates.

The results obtained in this study also suggest that like other pozzolans, GG exhibits a potential for preventing expansion in concrete due to ASR; however, when coupled with other SCMs, there seems to be limited synergetic effects in further preventing ASR expansion. Indeed, the more SCM is used, the less impactful are SCM increments, which underlines the complexity of the exercise of predicting the behavior of ternary mixtures incorporating such an high-alkali SCM (GG). However, mixtures with higher level of cement replacement exhibited the lowest expansions.

CSA Standard Practice A23.2-27A, which is a *prescriptive approach* framing the use of alkali reactive aggregates and preventive measures such as SCMs, recommends that SCM combinations and alternative SCMs, such as the high-alkali GG used in this study, be evaluated through expansion testing under accelerated laboratory conditions in accordance with Standard Practice A23.2-28A. Consequently, the minimum replacement levels proposed in Table 5.10 for ternary concretes incorporating GG should be taken with care as they are based on combinations of specific SCMs and testing conducted with only one (highly) reactive aggregate ( Spratt limestone). Further recommendations on the use of GG regarding ASR prevention would require further validation with a wider range of reactive aggregates, especially marginally to moderately-reactive aggregate. The somewhat large dosages in ternary cementitious systems proposed in Table 5.10 certainly raise the question about the relevance of using ana high-alkali SCM such as GG, even in ternary systems, to prevent ASR expansion in concrete incorporating a highly-reactive aggregate.

## 5.7 Acknowledgments

The authors greatly thank the financial support of the Chaire de recherche de la SAQ, the Centre de Recherche sur les Infrastructures en Béton (CRIB) and Université Laval for the work presented in this paper.

## 5.8 References


Afshinnia, K. and P. R. Rangaraju (2015a). "Efficiency of ternary blends containing fine glass powder in mitigatingalkali–silica reaction." Construction and Building Materials **100**(15): 234–245.

Afshinnia, K. and P. R. Rangaraju (2015b). "Influence of fineness of ground recycled glass on mitigation of alkali–silica reaction in mortars." Construction and Building Materials **81**: 257-267.

Afshinnia, K. and P. R. Rangaraju (2015c). "Mitigating alkali-silica reaction in concrete: Effectiveness of ground glass powder from recycled glass." Transportation Research Record **2508**: 65-72.

ASTM C-1260 (2014). Standard Test Method for Potential Alkali Reactivity of Aggregates (Mortar-Bar Method). ASTM International, West Conshohocken, PA, USA.

ASTM C1567 (2021). Standard Test Method for Determining the Potential Alkali-Silica Reactivity of Combinations of Cementitious Materials and Aggregate (Accelerated Mortar-Bar Method). ASTM International, West Conshohocken, PA, USA.

Bleszynski, R. (2002). "The performance and durability of concrete with ternary blendsof silica fume and blastfurnace slag". PhD thesis, University of Toronto.

Fournier, B., P.C. Nkinamubanzi, R. Chevrier, R. (2004). "Comparative field and laboratory investigations on the use of supplementary cementing materials to control alkali-silica reaction in concrete". 12th International conference on Alkali-Aggregate Reaction (AAR) in Concrete, Beijing (China), October 2004, Tang and Deng Editors, International Academic Publishers, Beijing World Publishing Corp., 1: 528-537.

Chen, Z. and C. S. Poon (2017). "Comparing the use of sewage sludge ash and glass powder in cement mortars." Environmental Technology **38**(11): 1390-1398.

Cota, F. P., C. C. D. Melo, T. H. Panzera, A. G. Araújo, P. H. R. Borges and F. Scarpa (2015). "Mechanical properties and ASR evaluation of concrete tiles with waste glass aggregate." Sustainable Cities and Society **16**: 49-56.

CSA A3000 (2018). Cementitious materials compendium. CSA Group, Mississauga, Ontario, Canada, 257p.

CSA A23.2-14A (2019). Potential expansivity of aggregates (procedure for length change due to alkali-aggregate reaction in concrete prisms at 38 °C). In CSA A23.2-14 – Test methods and standard practices for concrete. CSA Group, Mississauga, Ontario, Canada.

CSA A23.2-28A (2014). Standard Practice for laboratory testing to demonstrate the effectiveness of supplementary cementing materials and lithium-based admixtures to prevent alkali-silica reaction in concrete. In CSA A23.2-14 – Test methods and standard practices for concrete. CSA Group, Mississauga, Ontario, Canada.

Dhir, R. K., T. Dyer and M. Tang (2009). "Alkali-silica reaction in concrete containing glass." Materials and structures **42**(10): 1451-1462.

Fily-Paré, I., B. Fournier, J. Duchesne and A. Tagnit-Hamou (2020). "Impact of NaOH addition on the ASR expansion of ternary concrete incorporating Ground Glass (GG)". 16th International Conference on Alkali Aggregate Reaction in Concrete. Lisboa, Portugal.

Fournier, B., A. Bilodeau, N. Bouzoubaa, P.C. Nkinamubanzi (2018). “Field and Laboratory Investigations on the Use of Fly Ash and Li-Based Admixtures to Prevent ASR in Concrete”. Sixth International Conference on the Durability of Concrete Structures, 18-20 July 2018, University of Leeds, Leeds.

Fournier, B., R. Chevrier, A. Bilodeau, P.C. Nkinamubanzi, and N. Bouzoubaa (2016). "Comparative field and laboratory investigations on the use of supplementary cementing materials (SCMs) to control alkali-silica reaction in concrete”. 15th International Conference on alkali-aggregate reaction (AAR) in concrete, July 2016, Sao Paulo (Brazil), 10p.

Johnston, C. (1974). "Waste glass as coarse aggregate for concrete." ASTM Journal of Testing and Evaluation **2**(5).

Kamali, M. and A. Ghahremaninezhad (2015). "Effect of glass powders on the mechanical and durability properties of cementitious materials." Construction and Building Materials **98**: 407-416.

Kou, S. C. and C. S. Poon (2009). "Properties of self-compacting concrete prepared with recycled glass aggregate." Cement and Concrete Composites **31**(2): 107-113.

Karamberi, A., E. Chaniotakis, D. Papageorgiou and A. Moutsatsou (2006). ″Influence of glass cullet in cement pastes.″ China Particuology **4**(5): 234-237.

Lafrenière, C. (2017). "Évaluation du comportement en durabilité de nouvelles matrices cimentaires pour l'obtention de bétons respectueux de l'environnement". Master thesis, Université Laval, https://corpus.ulaval.ca/jspui/handle/20.500.11794/27591.

Lam, C. S., C. S. Poon and D. Chan (2007). "Enhancing the performance of pre-cast concrete blocks by incorporating waste glass – ASR consideration." Cement and Concrete Composites **29**(8): 616-625.

Lee, G., T.-C. Ling, Y.-L. Wong and C.-S. Poon (2011). "Effects of crushed glass cullet sizes, casting methods and pozzolanic materials on ASR of concrete blocks." Construction and Building Materials **25**(5): 2611-2618.

Lindgård, J., M. D. A. Thomas, E. J. Sellevold, B. Pedersen, Ö. Andiç-Çakır, H. Justnes and T. F. Rønning (2013). "Alkali–silica reaction (ASR)—performance testing: Influence of specimen pre-treatment, exposure conditions and prism size on alkali leaching and prism expansion." Cement and Concrete Research **53**(0): 68-90.

Liu, S., S. Wang, W. Tang, N. Hu and J. Wei (2015). "Inhibitory effect of waste glass powder on ASR expansion induced by waste glass aggregate." Materials **8**(10): 6849-6862.

Lu, J.-X., B.-J. Zhan, Z.-H. Duan and C. S. Poon (2017). "Using glass powder to improve the durability of architectural mortar prepared with glass aggregates." Materials & Design **135**: 102-111.

Maraghechi, H., S. Salwocki and F. Rajabipour (2017). "Utilisation of alkali activated glass powder in binary mixtures with Portland cement, slag, fly ash and hydrated lime." Materials and Structures **50**(1): 16.

Maraghechi, H., S.-M.-H. Shafaatian, G. Fischer and F. Rajabipour (2012). "The role of residual cracks on alkali silica reactivity of recycled glass aggregates." Cement and Concrete Composites **34**(1): 41-47.

Matos, A. M. and J. Sousa-Coutinho (2012). "Durability of mortar using waste glass powder as cement replacement." Construction and Building Materials **36**(0): 205-215.

Parghi, A. and M. Shahria Alam (2016). "Physical and mechanical properties of cementitious composites containing recycled glass powder (RGP) and styrene butadiene rubber (SBR)." Construction and Building Materials **104**: 34-43.

Pereira-de-Oliveira, L. A., J. P. Castro-Gomes and P. Santos (2012). "The potential pozzolanic activity of glass and red-clay ceramic waste as cement mortars components." Construction and Building Materials **31**: 197-203.

Ramlochan, T., M.D.A. Thomas, K.A. Gruber (2000). "The effect of metakaolin on alkali-silica reaction in concrete". Cement and Concrete Research 30 (3) (2000) 339–344.

Schwarz, N., H. Cam and N. Neithalath (2008). "Influence of a fine glass powder on the durability characteristics of concrete and its comparison to fly ash." Cement and Concrete Composites **30**(6): 486-496.

Serpa, D., A. Santos Silva, J. de Brito, J. Pontes and D. Soares (2013). "ASR of mortars containing glass." Construction and Building Materials **47**(0): 489-495.

Shao, Y., T. Lefort, S. Moras and D. Rodriguez (2000). *"Studies on concrete containing ground waste glass."* Cement and Concrete Research **30**(1): 91-100.

Shayan, A. and A. Xu (2006). "Performance of glass powder as a pozzolanic material in concrete: A field trial on concrete slabs." Cement and Concrete Research **36**(3): 457-468.

Shehata, M.H., M.D.A. Thomas (2002). "Use of ternary blends containing silica fume and fly ash to suppress expansion due to alkali-silica reaction in concrete". Cement and Concrete Research 32 (3): 341–349.
Shi, C., Y. Wu, Y. Shaob and C. Riefler (2004). "Alkali-Aggregate Reaction Expansion of Mortar Bars Containing Ground Glass Powder". age. Pekin. **20:** 10.

Taha, B. and G. Nounu (2008). "Using lithium nitrate and pozzolanic glass powder in concrete as ASR suppressors." Cement and Concrete Composites **30**(6): 497-505.

Thomas, M.D.A. and F.A. Innis (1998). "Effect of slag on expansion due to alkali- aggregate reaction in concrete". ACI Materials Journal 95(6).

Zheng, K. (2016). "Pozzolanic reaction of glass powder and its role in controlling alkali–silica reaction." Cement and Concrete Composites **67**: 30-38.

Zidol, A. (2009). Optimisation de la finesse de la poudre de verre dans les systèmes cimentaires binaires, Université de Sherbrooke, http://savoirs.usherbrooke.ca/handle/11143/1564.

# Chapter 6. - Impact of NaOH addition on the ASR Expansion of Ternary Concrete Incorporating Ground Glass (GG)

## Résumé

L'ajout de NaOH est une pratique courante dans la plupart des méthodes d'essais pour la réaction alcalis-silice (RAS). S'il engendre des conditions sévères pour les granulats et accélère leur réactivité, son interaction potentielle avec les ajouts cimentaires (AC) est un sujet de préoccupation. Dans cette étude, des prismes ont été fabriqués à partir de béton de composition ternaire incorporant un granulat grossier très réactif, avec et sans ajout de NaOH, du verre broyé (VB) et l'un des AC suivants : Cendre Volante (CV), Laitier de hauts-fourneaux (LHF), Fumée de silice (FS) et Métakaolin (MK). Les spécimens ont été conservés pendant deux ans à 38°C et H.R. > 95%, période au cours de laquelle leur changement de longueur a été suivi régulièrement. L'expansion des mélanges étudiés est fortement influencée par l'ajout de NaOH. Dans la plupart des cas, l'ajout de NaOH entraîne une diminution de l'expansion, mais cette réduction n'a souvent pas modifié l'issue du test (passe/passe pas).

## Abstract

NaOH addition is a current practice in most ASR test methods. If it provides severe conditions for the aggregates and accelerates their reactivity, its potential interaction with Supplementary Cementitious materials (SCM) is a matter of concern. In this study, test prisms were manufactured from ternary concretes incorporating a highly-reactive coarse aggregate, with and without NaOH addition, Ground Glass and one of the following SCM : Fly Ash (FA), Blast Furnace Slag (BFS), Silica Fume (SF) and Metakaolin (MK). The specimens were stored for two years at 38°C and R.H. 95%, period over which their length change was monitored regularly. The expansion of given mixtures is significantly influenced by NaOH addition. In most cases, NaOH addition results in reduced expansion, but the latter reduction often did not change the Pass/Fail outcome of the test.

## 6.1 Introduction

Over the last few decades, global authorities worked thoroughly to inform and influence major greenhouse gas (GHG) emitters including the cement industry, which contributes to anthropogenic GHG emissions to a significant level (3.8-5%) [1]. As an example, the World Business Council for Sustainable Development (WBCSD) published reference material [1,2] suggesting that the use of Supplementary Cementitious Materials (SCMs) decreases energy consumption per kilo of cementitious material produced [3] and leads to lower fuel consumption and gas emission per cubic meter of concrete.

Between 1990 and 2017, North American cement producers reduced their $CO_2$ emissions per ton of cementitious materials from 905 to 746 kg [4]. The above reductions in GHG emissions largely correlate with greater use of SCM and limestone fillers; indeed, the clinker-to-cement ratio went from 90% to 82% during that period.

Emerging SCMs, such as Ground Glass (GG), calcined clays or Rice Husk Ash (RHA), are expected to gain in popularity and compensate for the declining or somewhat limited availability of more "conventional" SCMs, such as Blast Furnace Slag (BFS), Silica Fume (SF) or Fly Ash (FA). For instance, FA scarcity is related to the declining use of thermal power as an energy supply in the USA (about 50% in 2005 and less than 38% in 2012) [5]. The availability of BFS is limited since its production is already fully consumed in concrete [6] and the use of SF is often limited by its cost [7]. The next generation of SCMs shall target materials with great availability (although some "local/regional materials could be used on a specific-project basis), acceptable cost, and good performance regarding concrete durability.

Post-consumed Ground Glass (GG) is a pozzolanic material that is worth some attention since the material is available worldwide and municipalities are sometimes paying for disposal since there is no profitable market for recycled glass [8]. However, a closer look at its chemical composition can restrain the above enthusiasm because GG is an SCM with a high-alkali content (≈13% $Na_2Oeq$), which might be problematic regarding Alkali-Silica Reaction (ASR). If alkalis from GG are indeed released in the concrete pore solution, this may increase the concentration in hydroxyl ions present for balancing charges, thus enhancing the attack of reactive phases within the concrete aggregates. The chemical environment is then favorable for the production of the swelling ASR gel, which is known to induce cracking into concrete and to jeopardize its durability. On the other hand, GG reacts into concrete through the pozzolanic reaction [9-12], which is known to generally lower the pH of concrete pore solution and prevent ASR [13]. Scientists are still debating about the beneficial or detrimental effect of GG in the presence of reactive aggregates in concrete.

The Accelerated Mortar Bar Test (AMBT) is generally the most popular method used in studies that aim to assess the beneficial effect of GG in preventing ASR. It is often used to characterize GG although the potential release of alkalis from GG is hard to evaluate under AMBT conditions. Table 6.1 presents a collection of studies using the AMBT to evaluate the ASR potential of mixtures incorporating GG. The above studies suggest that at least 50% of GG ought to be used as a low-alkali cement replacement, by mass, to reduce ASR expansion below the 0.10% limit when used with highly-reactive aggregates. For moderately reactive aggregates, 20 to 30% GG is considered enough/necessary to prevent expansion.

Shayan and Xu [14] used the Concrete Prism Test (CPT) with 20 to 30% mass replacement of a low-alkali cement ($Na_2O$eq of 0.46%) by GG with particle size <10μm; after two years of monitoring, the expansion of the test specimens stored at 38°C and 100%RH was below 0.01% when non-reactive aggregates were used. Zidol [15] assessed the expansion of concrete prisms incorporating a highly-reactive aggregate and 20/30% GG as replacement of a cement with $Na_2O$eq content of 0.73%. As per the test requirement, the alkali content corresponding to the cement part in the system was raised to 1.25% with NaOH. After one year of storage at 38°C and 100% RH, the expansions measured were all beyond the 0.040% limit of CSA Standard Practice A23.2-28A.

Since the beneficial effect of GG in preventing ASR expansion seems somewhat limited in a binary context, several authors documented the expansion of ternary mixtures incorporating reactive aggregates, GG and a second SCM, such as BFS, FA, SF, and MK. The results suggest that ternary systems are more efficient in reducing expansion due to ASR, as presented in Table 6.2.

The potential of ternary mixtures incorporating (high-alkali) GG in preventing deleterious expansion due to ASR in concrete is currently not documented by test methods that could be considered more reliable than those involving soaking of the test specimens in a NaOH solution. On the other hand, using concrete prism testing for evaluating the beneficial effect of SCMs to prevent ASR involves raising the alkali content corresponding to the cement part in the system to 1.25% $Na_2O$eq, as per CSA Standard Practice A23.2-28A and ASTM C 1778. There is currently limited information about the impact that such an alkali addition may have on the expansion process in concretes incorporating an alkali-rich ground glass and whether this practice is appropriate or not.

Such a questioning appears important in view of the dual effect of alkali addition/contribution in concretes incorporating SCMs, i.e. 1) accelerating the “kinetics” of ASR to obtain faster results through laboratory testing; and 2) activating a “beneficial” reaction of SCMs for binder production [16]. Other authors view that alkali addition is actually beneficial to the point that GG could be considered as an activator capable of stretching the activation window of FA, GGBS and Metakaolin (MK) [17-20].

**Table 6.1: Expansion of mortar bars according to ASTM C1260 when natural reactive aggregates are used in combination with GG with an $Na_2O_{eq}$ content ranging between 11.30 and 13.80% (mortar bars immersed 1N NaOH at 80°C for 14 days); expansion < 0.10%: innocuous; expansion > 0.20%: deleterious.**

| | Expansion (%) | | Aggregate | Cement and alkali addition | % of cement replacement | Size of glass particles | Source |
|---|---|---|---|---|---|---|---|
| | Specimens with GG | Control | | | | | |
| Highly reactive aggregate and 50% of GG | 0.08* | ≈0.50 | Highly reactive (Spratt limestone) | 0.63% of $Na_2O$eq NaOH added to 0.90% $Na_2O$eq | 50% | $D_{50}$ ≈ 50µm | [21] |
| Highly reactive aggregate and 10 to 40% of GG | <0.20 and >0.10 | 0.38 | Natural sand | 0.84% of $Na_2O$eq | 40% | 45 to 75 µm | [22] |
| | 0.41**, 0.30** and 0.30** | 0.72 | Highly reactive (Spratt limestone) | 0.73% of $Na_2O$eq | 20, 30 and 40% | $D_{50}$ ≈ 10µm | [15]** |
| | 0.42* ,0.22* and 0.11* | 0.5 | Highly reactive (Spratt limestone) | 0.63% of $Na_2O_{eq}$ NaOH added to 0.90% $Na_2O$eq | 10, 20, 30% | $D_{50}$ ≈ 50µm | [21] |
| | 0.20*** and 0.12*** | 0.64 | Highly reactive (Jobe sand) | 1.22% of $Na_2O$eq | 30% | $D_{50}$ ≈ 200µm and $D_{50}$ ≈ 20µm | [23]*** |
| Moderately reactive aggregate and 20 to 30% of GG | 0.07 and 0.07 | 0.20 | Reactive sand | 0.86% of $Na_2O$eq | 20% and 30% | <125µm | [24] |
| | 0.09 and 0.06 | 0.27 | Reactive Argillite | 0.88% of $Na_2O$eq | 20% and 30% | $D_{50}$ ≈ 70µm | [25] |
| | 0.08*** and 0.05*** | 0.29 | Reactive (Wright sand) | 1.22% of $Na_2O$eq | 30% | $D_{50}$ ≈ 200µm and $D_{50}$ ≈ 20µm | [23]*** |
| | 0.04 | 0.26 | Not mentioned | 0.46% of $Na_2O$eq | 20% | $D_{50}$ ≈ 10µm | [26] |
| Moderately reactive and 5 to 10% of GG | 0.20, 0.17 and 0.13 | 0.22 | Reactive siliceous sand | 0.73% of $Na_2O$eq | 5, 10, and 20% | $D_{50}$ ≈ 20µm | [27] |
| | 0.18 | 0.27 | Reactive Argillite | 0.88% of $Na_2O$eq | 10% | $D_{50}$ ≈ 70µm | [25] |
| | 0.13 and 0.13 | 0.20 | Alkali reactive sand | 0.86% of $Na_2O$eq | 5 and 20% of aggregate | 4.75 to 150µm | [24] |
| | 0.12 | 0.26 | Not mentioned | 0.46% of $Na_2O$eq | 10 % | $D_{50}$ ≈ 10µm | [26] |

* Specimens with and without NaOH addition showed similar expansion

** CSA 23.2-25A,

*** ASTM C227, 38°C, immersed in 0.6 N NaOH for 6 months and expansion limit of 0.10% at 6 months

**Table 6.2: Expansion of mortar bars (testing in accordance with ASTM C 1260 conditions) incorporating GG and another SCM as cement or aggregates replacement.**

| Expansion (%) | | Aggregate | Cement and alkali addition | Type and % of glass replacement | Size of glass particles | Other SCM | Source |
|---|---|---|---|---|---|---|---|
| GG | | | | | | | |
| <0.1 | 0.22 | Reactive siliceous sand | 0.73% of $Na_2Oeq$ | 5, 10, and 15% of cement | $D_{50}$ ≈20µm | 15, 10 and 5% FA (for total cement replacement of 20%) | [27] |
| < 0.05 | 0.25 | Not mentioned | 0.38% of $Na_2Oeq$ | 50% of aggregate | ASTM 1260 aggregate gradation | 2.5 to 10% of MK or FA | [28] |
| <0.02* | 0.02 | River sand | Not mentioned | 100% of aggregate | Sieved at 5, 2.36, 1.18 and 0.6-0mm | 5 - 20% MK | [29]* |
| 0.05 and 0.00 | 0.009 | Quartz aggregate | $K_2O$ of 0.66, $Na_2O$ or $Na_2Oeq$ not mentioned | 7.5% of aggregate | 4.75 to 2 mm | 7.5 and 15% of MK | [30] |
| 0.02 and 0,00 | | | | | 850 to 300µm | | |
| < 0.04 | 0.02 | River sand and granite | 0.38% of $Na_2Oeq$ | 15, 30 and 45% of sand | 80% > 0.6 mm | 33% FA | [31] |
| < 0.05 | 0.9 | 100% crushed glass aggregate | 0.9 of $Na_2Oeq$ | 10% of cement | Average size of 17µm | 30% of BFS | [32] |
| | | | | | | 10% MK | |
| | | | | 20% of cement | | 20% of BFS | |
| 0.04 and 0.02 | - | Non-reactive sand | Cement: $Na_2O$ of 0.3 and $K_2O$ not mentioned Activator: $SiO_2/Na_2O$ of 1.6 for BFS and 1.8 for FA | 20% of alkali-activated BFS of FA | $D_{50}$ ≈ 20µm | 80% BFS or 80%FA | [33] |

* ASTM and modified ASTM; just enough water for cohesion and slump of 0

## 6.2 Objective and Scope of Work

This project aimed at determining the effect of adding alkalis (NaOH) on the "severity" of the CPT used for evaluating the effectiveness in preventing ASR of ternary concrete mixtures incorporating a high-alkali GG. In this study, concrete prisms were made in accordance with CSA Standard Practice A23.2-28A (similar to ASTM C 1778) to assess the expansive behaviour of ternary concrete mixtures, with and without the addition of NaOH, and incorporating a highly-reactive aggregate, GG and ground granulated blast-furnace slag (BFS) / fly ash (FA)/ silica fume (SF) / metakaolin (MK). In this experimental work, some testing included special precautions to avoid leaching (such as no temperature cycle and bigger test specimens).

Ultimately, this work is also aimed at determining whether expansion due to ASR can be efficiently prevented in concrete made with a high-alkali GG through the use of other SCMs, such as BFS, FA, SF or MK.

## 6.3 Materials and Methods

### 6.3.1 Materials

Concrete specimens were made using a General Use (GU) portland cement (C1) with an alkali content of 0.94%, $Na_2Oeq$; GG from a recycling facility located in Quebec (Canada); BFS of grade 80 from Ontario (Canada); Type F FA from Alberta (Canada); SF from a ferro-silicon plant located in Quebec (Canada) and MK from Georgia (USA). The chemical composition and the specific gravity of the above materials are given in Table 6.3.

The fine aggregate used in the concrete mixtures consisted of manufactured high purity limestone sand (98% $CaCO_3$) from Newfoundland (Canada); it presents a density of 2.7 and an absorption capacity of 0.57%. The coarse aggregate was the highly-reactive Spratt limestone from Ontario (Canada) that presents a density of 2.7 and an absorption capacity of 0.43%. Both the non-reactive sand and the highly-reactive Spratt limestone have very low alkali contents and are not considered as potential alkali contributors to the concrete pore solution.

**Table 6.3: Chemical composition and specific gravity of the GU cement and SCMs used in this study**

| Oxides | C1 | GG | BFS | FA | SF | MK |
|---|---|---|---|---|---|---|
| $SiO_2$ | 18.7 | 70.53 | 37.74 | 56,72 | 94.27 | 51.6 |
| CaO | 60.8 | 10.77 | 36.20 | 9,29 | 0.54 | 0.02 |
| $Al_2O_3$ | 5.0 | 2.06 | 9.45 | 24,07 | 0.3 | 43.97 |
| $Fe_2O_3$ | 3.7 | 0.35 | 0.36 | 3,14 | 0.1 | 0.49 |
| $Na_2O$ | 0.25 | 12.49 | 0.26 | 2,50 | 0.12 | 0.27 |
| $K_2O$ | 1.05 | 0.66 | 0.36 | 0,64 | 0.65 | 0.25 |
| $Na_2Oeq$ | 0.94 | 12.92 | 0.50 | 0.55 | 1.43 | 0.43 |
| $SO_3$ | 3.8 | 0.11 | 2.45 | - | 0.02 | - |
| MgO | 2.7 | 1.14 | 9.96 | 1,05 | 0.28 | 0.04 |
| $TiO_2$ | - | 0.07 | 0.94 | 0,65 | 0.01 | 1.4 |
| $P_2O_5$ | - | 0.03 | 0.08 | 0,09 | 0.12 | 0.09 |
| MnO | - | 0.02 | 0.72 | 0.04 | 0.03 | 0.01 |
| L.O.I | 1.9 | 1.71 | 1.84 | 1.05 | 3.2 | 1.84 |
| Specific gravity | 3.15 | 2.54 | 3.04 | 2.35 | 2.24 | 2.20 |

### 6.3.2 Concrete Mix desi

Table 6.4 presents the concrete mix designs used in this study. A constant W/B of 0.42 was used for all concrete mixtures, while superplasticizer was added when necessary to meet the slump requirement of 100 to 150 mm specified in CSA 23.2-28A and to ensure proper dispersion especially in the case of SF and MK. Considering the wide range in specific gravity of the cementitious materials and the specified binder content of 420 kg/m3, the decision was made to maintain a constant proportion of reactive coarse aggregate throughout the

experiment. The amount of non-reactive fine aggregate in the concrete was thus adapted to accommodate the binder volume variations, while maintaining a coarse-to-fine aggregate ratio of 1.50 ± 0.10 (specified mass ratio of 60:40 in CSA A23.2-28A). NaOH was added in selected mixtures to raise the alkali content corresponding to the cement part of the binder to 1.25% Na2Oeq, as required by CSA Standard Practice A23.2-28A.

For comparison purposes, binary concrete mixtures incorporating GG as the only SCM were made, i.e. using cement replacement levels by GG ranging from 10 to 30%, with and without added alkalis.

### 6.3.3 Manufacture, Storage and Testing of Specimens

All concrete mixtures were made in a pan mixer of 30 liters capacity. As a precaution to reduce the deleterious impact of alkali leaching on expansion, test prisms, 100 x 100 x 300 mm in size (instead of 75 x 75 x 300 mm specified in CSA A23.2-28A), were made from each mixture. Four specimens were manufactured from each ternary concrete mixture, two in the case of binary mixtures. After 24 hours in their moulds, the prisms were demoulded and placed in sealed 25L plastic pails (lined with damp geotextile to maintain a relative humidity > 95%; two prisms per container), which were then stored at 38°C.The length change monitoring of the test prisms was performed at regular intervals up to 104 weeks. Moreover, readings were made without pre-cooling of the test specimens prior to measuring, in order to prevent temperature cycles and the inherent condensation and runoff that result in excessive alkali leaching.

**Table 6.4: Proportioning of concrete mixtures made in this study. Each line in the table corresponds to two concrete mixtures manufactured, i.e. one without (0.94% $Na_2Oeq$) and one with added alkalis (1.25% $Na_2Oeq$).**

| Mixture | NaOH (kg/m³) | | Cement and SCMs (kg/m³) | | | | | | Aggregates (kg/m³) | | Eau (kg/m³) |
|---|---|---|---|---|---|---|---|---|---|---|---|
| | $Na_2Oeq$ | | C1 | GG | BFS | FA | SF | MK | Fine | Coarse | |
| | 0.94 | 1.25 | | | | | | | | | |
| 10GG | - | 0.152 | 378 | 42 | - | - | - | - | 723 | 1054 | 176 |
| 20GG | - | 0.135 | 336 | 84 | - | - | - | - | 714 | | |
| 30GG | - | 0.118 | 294 | 126 | - | - | - | - | 710 | | |
| 10GG-20BFS | - | 0.114 | 294 | 42 | 84 | - | - | - | 720 | | |
| 20GG-20BFS | - | 0.098 | 252 | 84 | 84 | - | - | - | 711 | | |
| 10GG-40BFS | - | 0.081 | 210 | 42 | 168 | - | - | - | 717 | | |
| 20GG-40BFS | - | 0.065 | 168 | 84 | 168 | - | - | - | 709 | | |
| 10GG-15FA | - | 0.122 | 315 | 42 | - | 63 | - | - | 704 | | |
| 20GG-15FA | - | 0.106 | 273 | 84 | - | 63 | - | - | 696 | | |
| 10GG-30FA | - | 0.098 | 252 | 42 | - | 126 | - | - | 686 | | |
| 20GG-30FA | - | 0.081 | 210 | 84 | - | 126 | - | - | 677 | | |
| 10GG-5SF | - | 0.138 | 357 | 42 | - | - | 21 | - | 716 | | |
| 20GG-5SF | - | 0.106 | 273 | 84 | - | - | 21 | - | 698 | | |
| 10GG-10SF | - | 0.130 | 336 | 42 | - | - | 42 | - | 708 | | |
| 30GG-10SF | - | 0.098 | 252 | 126 | - | - | 42 | - | 691 | | |
| 10GG-5MK | - | 0.138 | 357 | 42 | - | - | - | 21 | 715 | | |
| 30GG-5MK | - | 0.106 | 273 | 126 | - | - | - | 21 | 698 | | |
| 10GG-15MK | - | 0.122 | 315 | 42 | - | - | - | 63 | 700 | | |
| 20GG-15MK | - | 0.090 | 231 | 84 | - | - | - | 63 | 682 | | |

## 6.4 Results

Figure 6.1 presents the 104-week expansion of the test prisms cast from binary and ternary concretes, with and without added alkalis, incorporating 10 / 20% GG along with 0 / 20 / 40% BFS or 0 / 15 / 30% FA.

Expansions ranging from 0.11 to 0.15%, i.e., way beyond the 0.040% expansion limit, were obtained in the case of test prisms cast from binary mixtures incorporating 10 and 20% GG. The addition of NaOH enhanced slightly the expansion of the test specimens incorporating 10% GG, while having no significant impact on those incorporating 20% GG. When comparing the results obtained for binary mixtures incorporating GG, it is worth mentioning that 1) a 30% GG content resulted in slightly lower expansions than that of a 20% GG mix (Figure 6.1 vs Figure 6.2); however, values are still above the 0.040% limit, and 2) the NaOH addition slightly reduced concrete prism expansion when 30% GG was used, while it slightly enhanced expansion in the case of the 10% GG mix.

For ternary concrete mixtures incorporating 10%GG, the addition of NaOH had no significant impact when 20% BFS and 30% FA were used; however, significant reductions in expansion were noticed in the case of mixtures incorporating 40% BFS and 15% FA. All prisms cast from (ternary) “boosted” mixtures incorporating 20% GG showed significant expansion reduction compared to “unboosted” ones.

Regarding the 0.040% expansion limit proposed by CSA Standard Practice A23.2-28A, mixtures incorporating BFS required a 40% replacement level to reduce the expansion of the test prisms close to the limit regardless of the GG content; interestingly, the addition of NaOH resulted in expansions lower or equal to the limit in the case of the 40% BFS prisms, while the companion “unboosted” prisms expanded slightly above 0.040% (regardless of the GG content). Five out of the eight mixtures incorporating FA are clustered around the 0.040% limit; the concrete prism expansions corresponding to the two 15% FA mixtures without NaOH addition are well above the limit while that corresponding to mixture 20GG-30FA-1.25% is well below. The results suggest that GG concrete mixtures that are the most affected by NaOH addition incorporate 15% FA and/or 20% GG (BFS & FA); for the above combinations, NaOH addition indeed resulted in significant expansion reductions compared to the same combination without NaOH.Figure 6.2 presents the expansion of test prisms cast from binary and ternary concretes, with and without NaOH addition, incorporating 10 / 30% GG along with 0 / 5 / 10% SF and 0 / 5 / 15% MK.

Alkali addition enhanced the expansion of concrete prisms cast from ternary concrete mixtures incorporating 10% GG combined with 5/10% SF and 15% MK. For ternary mixtures incorporating 30% GG, such an increase in alkali content significantly reduced concrete prism expansion when GG was combined with SF, but it had no significant impact when GG was combined with MK.

The only ternary concrete mixture incorporating 10% GG that clearly resulted in concrete prism expansion below the 0.040% level was the “unboosted” mix incorporating 15% MK. In the case of ternary mixtures incorporating 30% GG, those meeting the expansion requirement incorporated 10% SF, without NaOH addition, and 15% MK, regardless of the NaOH addition.

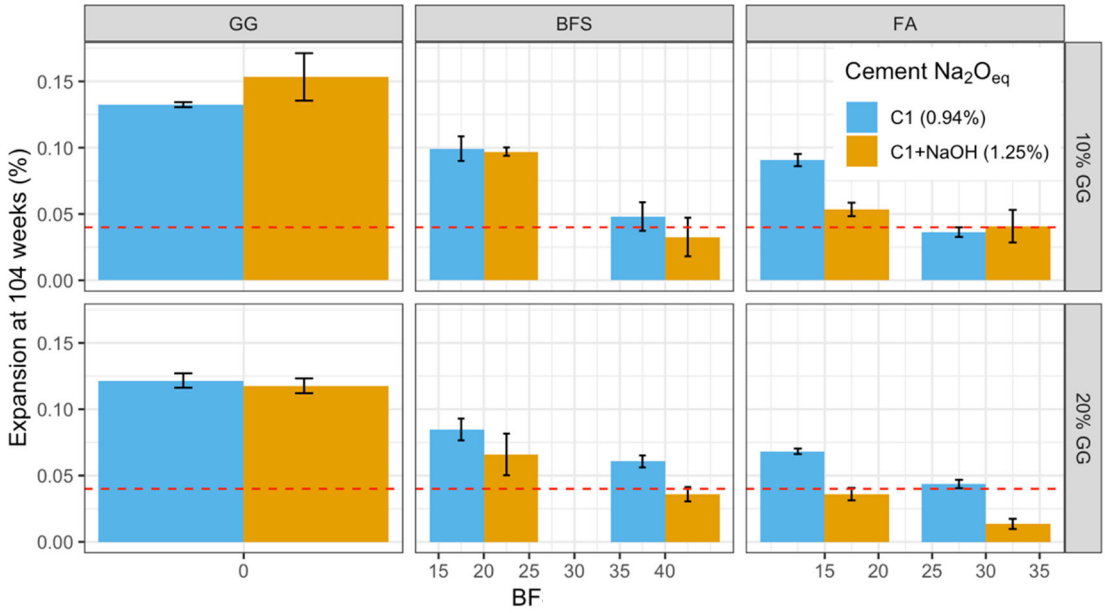


**Figure 6.1: Expansion at 104 weeks of test prisms cast from binary and ternary concrete mixtures incorporating the highly-reactive Spratt limestone, with and without the addition of NaOH, and various amounts of GG and BFS/FA. The error bars correspond to the SD calculated from the two or four test prisms from the same mix, while the red dotted line is the 0.040% expansion limit.**

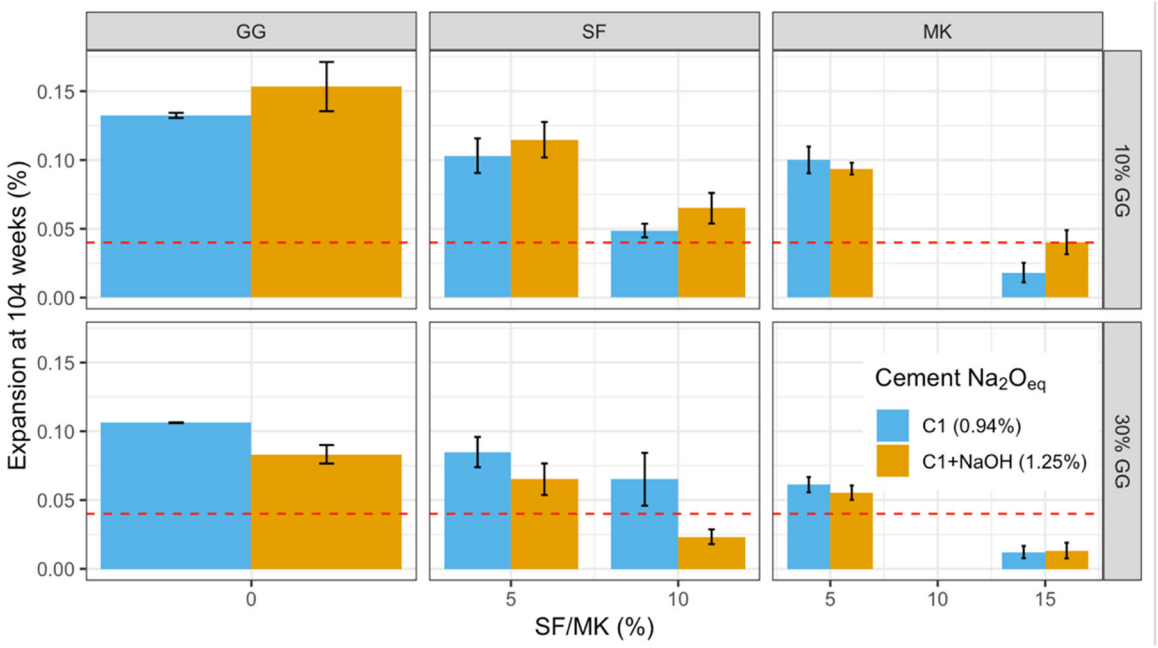


**Figure 6.2: Expansion at 104 weeks of test prisms cast from binary and ternary concrete mixtures incorporating the highly-reactive Spratt limestone, with and without the addition of NaOH, and various amounts of GG and MK/FA. The error bars correspond to the SD calculated from the four test prisms from the same mix, while the red dotted line is the 0.040% expansion limit.**

## 6.5 Discussion

The CPT is generally considered to provide a reliable assessment of the long-term potential alkali-silica reactivity of aggregates, perhaps with the exception of some slowly reactive granitic/gneiss aggregates. In order to do so, the "sensitivity" of the aggregate to deleterious alkali reactions is assessed through accelerated test conditions consisting of a storage at high temperature (38°C) and RH>95%, and NaOH addition (1.25% $Na_2Oeq$, by cement mass; total concrete alkali content of 5.25 kg/m$^3$, $Na_2Oeq$). For the large number/majority of reactive aggregates tested in the CPT, an increase in the concrete alkali content results in higher concrete prism expansion, at least within a certain range of concrete alkali contents. A "threshold" alkali content beyond which "deleterious" expansion is observed can thus be established, provided precautions are taken to avoid/reduce the deleterious effect of alkali leaching on expansion. Such an alkali threshold, which varies from one aggregate to another, can thus be used to establish acceptable concrete compositions as a function of their total alkali content.

For the majority of ternary concrete mixtures tested in this study, which incorporate 10 to 30% of a high-alkali GG, the NaOH addition actually resulted in lower concrete prism expansions compared to unboosted companion mixtures. Considering that precautions were taken to reduce the impact of alkali leaching from test prisms, the above data suggest that NaOH addition did not necessarily play its role of aggregate's reactivity accelerator but rather enhanced the ASR preventive capacity of the binder systems evaluated. It thus appears appropriate to question whether the addition of alkalis is affecting the reliability of the CPT in assessing the long-term effectiveness of the various mixtures investigated (i.e. incorporating the high-alkali GG) in preventing expansion due to ASR.

Table 6.5 presents the 104-week expansions of the various binary and ternary mixtures, with and without NaOH addition, as well as the outcome of the test (i.e. pass or fail), its reliability being based on the p-value of a t-test for the hypothesis that the expansion is truly different (i.e. above or below) than the 0.040% limit. The results in Table 6.5 indicate that 26 out of the 38 mixtures tested, showed a similar outcome (i.e. Pass/Pass or Fail/Fail), regardless of the NaOH addition. Indeed, in most cases, the NaOH addition was found to reduce expansion but did not change the outcome of the test. Twelve mixtures (highlighted in Table 6.5) showed opposite outcomes when considering the effect of NaOH addition. However, for five of those twelve mixtures, the expansion results are either too close to the 0.040% limit or the variability between test specimens is too high to conclude with confidence on the Pass/Fail outcome of the mixture. The lack of confidence on the conclusion of the test is indeed indicated by a p-value below 0.90. Finally, only two SCM combinations (i.e. four mixtures) showed statistically different outcomes for the test specimens, i.e. mixtures 20GG-30FA and 30GG-10SF.

Figure 6.2 illustrates graphically the impact of NaOH addition on the expansion of concrete prisms and the standard deviation between the results obtained for the four prisms of a set. As also observed in Table 6.5, for most mixtures, the addition of NaOH results in lower expansions compared to the companion mixture without NaOH. It is especially the case for mixtures incorporating FA, BFS with an average reduction of 41.6% and 21.4% associated to NaOH addition. Concrete mixtures incorporating MK are mostly non-NaOH sensitive. For SF-bearing mixtures, the addition of NaOH increases the expansion by an average of 18.3% when only 10% GG is used, while it reduces concrete prism expansions by an average of 39.6 % when 30% GG is used.

In the case of binary concrete mixtures, expansion is enhanced (+15.8%) by NaOH addition when 10% GG is used; it has no impact on the expansion when 20% GG (-3.3%) is used and it reduces the expansion when 30% GG is used (-21.6%). The latter suggest a synergetic effect between GG and NaOH addition that is beneficial in reducing the expansion. This effect is also noticeable in ternary mixtures since the average reduction in the expansion values of the test prisms due to NaOH addition is 0.026% for specimens incorporating FA/BFS and 20% GG, while it is 0.015% for the mixtures with the same amount of FA/BFS but with only 10% GG. Similarly, for specimens incorporating SF/MK and 30% GG, the average reduction in concrete prism expansion is 0.017% and for the same mixture with only 10% GG, the average concrete prism expansion enhancement due to NaOH addition is 0.011%.

The average concrete prism expansion changes associated to NaOH addition in the case of ternary mixtures incorporating BFS, FA, SF and MK are respectively -0.015, -0.024, -0.009 and +0.003%; this suggests that the “beneficial” effect of NaOH addition in ternary mixtures incorporating GG is more pronounced when GG is mixed with FA or BFS. Actually, in several mixtures incorporating SF and MK, the NaOH addition leads to an increased expansion of the test specimens. MK-bearing mixtures are somewhat insensitive to NaOH addition and the SCM that is most responsive to NaOH addition when coupled with GG is FA.

**Table 6.5: Expansion of the concrete mixtures, with and without NaOH, as well as the outcome of CPT (i.e. Pass / Fail) based on the two-year 0.040% expansion limit and the reliability of the outcome. The latter considers the standard deviation between the prisms of a set and its significance is expressed as the probability that the expansion is above or below 0.040% (p-value). The yellow lines highlight opposite outcomes between companion mixtures, with and without added alkalis (the significance of the p-value is based on *Ramsey and Schafer [34]*). N is the number of test prisms in a set (i.e. 2 in the case of binary mixtures and 4 in the case of ternary mixtures).**

| | | C1 (0.94%) | | | | C1 +NaOH (1.25%) | | | |
|---|---|---|---|---|---|---|---|---|---|
| Mixture | n | Expansion (%) | Outcome | COV (%) | p-value | Expansion (%) | Outcome | COV (%) | p-value |
| 10GG | 2 | 0.132 | Fail | 1 | 0.9935 | 0.153 | Fail | 12 | 0.9935 |
| 20GG | 2 | 0.122 | Fail | 4 | 0.9789 | 0.118 | Fail | 5 | 0.9772 |
| 10GG-15FA | 4 | 0.091 | Fail | 5 | 0.9998 | 0.053 | Fail | 9 | 0.9903 |
| 10GG-30FA | 4 | 0.036 | Pass | 10 | 0.9102 | 0.041 | Fail | 30 | 0.5420 |
| 20GG-15FA | 4 | 0.068 | Fail | 3 | 0.9999 | 0.036 | Pass | 13 | 0.8798 |
| 20GG-30FA | 4 | 0.044 | Fail | 7 | 0.9307 | 0.014 | Pass | 28 | 0.9994 |
| 10GG-20BFS | 4 | 0.099 | Fail | 9 | 0.9992 | 0.097 | Fail | 3 | 0.9999 |
| 10GG-40BFS | 4 | 0.048 | Fail | 22 | 0.8578 | 0.033 | Pass | 45 | 0.7770 |
| 20GG-20BFS | 4 | 0.085 | Fail | 10 | 0.9987 | 0.066 | Fail | 24 | 0.9678 |
| 20GG-40BFS | 4 | 0.061 | Fail | 7 | 0.9980 | 0.036 | Pass | 15 | 0.8563 |
| 10GG | 2 | 0.132 | Fail | 1 | 0.9935 | 0.153 | Fail | 12 | 0.9935 |
| 30GG | 2 | 0.106 | Fail | 0 | 0.9987 | 0.083 | Fail | 8 | 0.9510 |
| 10GG-5SF | 4 | 0.103 | Fail | 12 | 0.9984 | 0.105 | Fail | 11 | 0.9989 |
| 10GG-10SF | 4 | 0.049 | Fail | 10 | 0.9725 | 0.065 | Fail | 17 | 0.9850 |
| 30GG-5SF | 4 | 0.085 | Fail | 13 | 0.9971 | 0.065 | Fail | 18 | 0.9840 |
| 30GG-10SF | 4 | 0.065 | Fail | 29 | 0.9461 | 0.023 | Pass | 23 | 0.9937 |
| 10GG-5MK | 4 | 0.100 | Fail | 10 | 0.9991 | 0.094 | Fail | 5 | 0.9999 |
| 10GG-15MK | 4 | 0.018 | Pass | 39 | 0.9936 | 0.040 | Fail | 22 | 0.5200 |
| 30GG-5MK | 4 | 0.061 | Fail | 9 | 0.9965 | 0.055 | Fail | 9 | 0.9928 |
| 30GG-15MK | 4 | 0.012 | Pass | 36 | 0.9992 | 0.013 | Pass | 43 | 0.9980 |

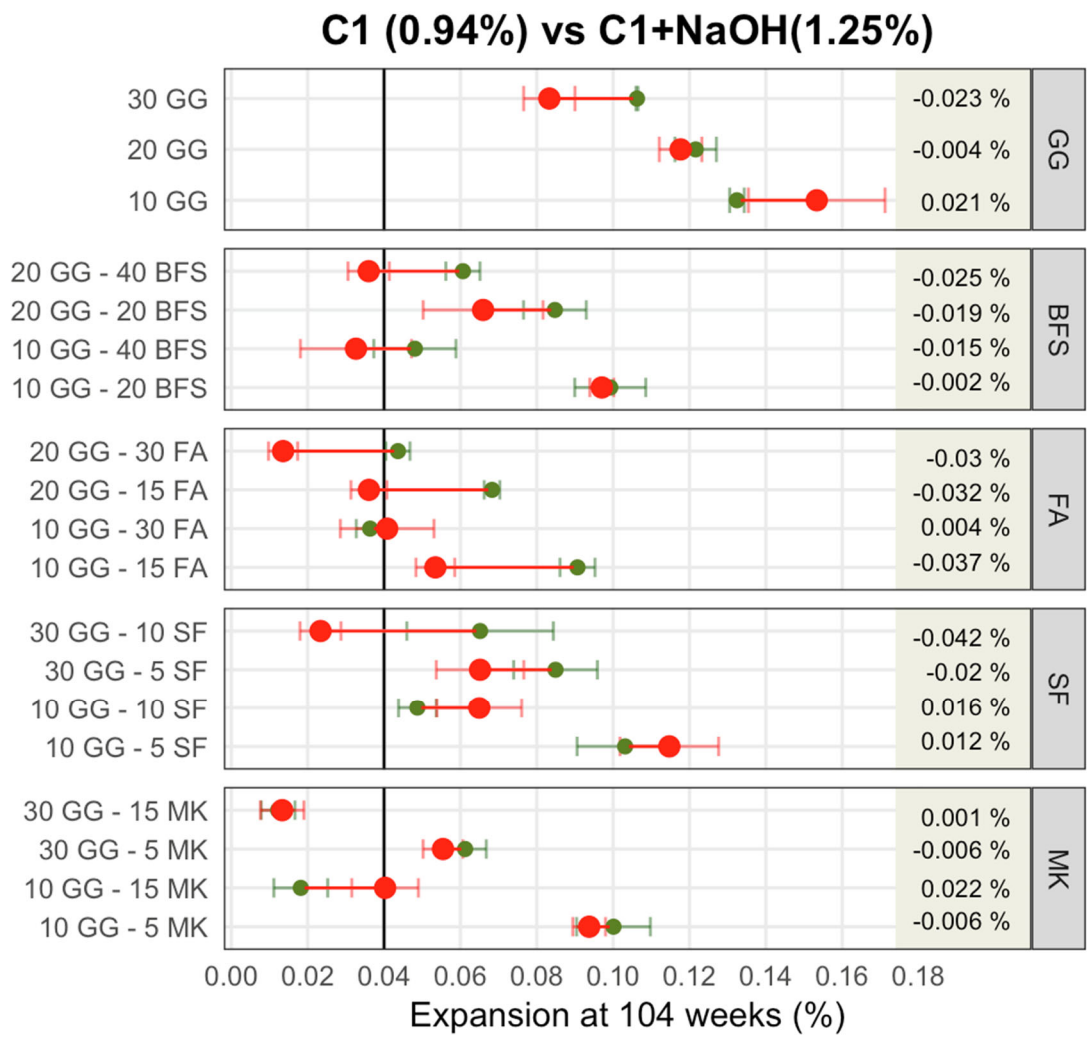


**Figure 6.3: Difference in expansion at 104 weeks between the different concrete mixtures with (red) and without (green) NaOH addition. The error bars represent the standard error.**

## 6.6 Conclusion

In this study, the impact of the NaOH addition in concrete prism testing was assessed by comparing the average expansion of binary/ternary concrete specimens, with and without added alkalis, incorporating 10 to 30% of high-alkali ground glass (GG), a highly-reactive coarse aggregate (Spratt limestone) and various proportions of blast-furnace slag (BFS), fly ash (FA), silica fume (SF) or metakaolin (MK). The concrete prisms were manufactured from the above concrete mixtures and their length-change was monitored up to 104 weeks (stored at 38°C and R.H. > 95%). Special attention was put in reducing the deleterious impact of alkali leaching, i.e. by using larger prisms (100mm instead of 75 mm section, as normally specified in CSA Standard Practice A23.2-28A) and by avoiding the 24-hr pre-cooling period prior to measurements (i.e. prisms were measured “hot”).

The conclusions that can be drawn from this experiment are the following:

1) For most of the tested mixtures, the NaOH addition decreases the expansion compared to the same mixtures without NaOH, but not enough to change the outcome of the test for the mixtures tested (i.e. Pass or Fail).
2) The "severity" of the test is reduced by the addition of NaOH for 13/19 SCM combinations and increased for 6/19. More precisely:
   - For binary mixtures incorporating 10% GG, NaOH addition enhanced the expansion while it has the opposite effect for binary mixtures incorporating 30%GG;
   - NaOH addition leads to lower expansion for all ternary mixtures incorporating 20 or 30% GG coupled with BFS, FA and SF;
   - NaOH addition leads to lower expansion for the large majority of mixtures incorporating BFS and FA, regardless of the GG content;
   - NaOH addition leads to mixed results for SF and MK bearing specimens.
3) None of the binary concrete mixtures incorporating 10 to 30% GG and the highly-reactive Spratt limestone met the 0.040% expansion limit used for concrete prism testing. The only ternary concrete mixtures incorporating 10% GG that resulted in concrete prism expansion below the 0.040% level were the "unboosted" mix incorporating 15% MK and the 30% FA mix (just at the limit). In the case of ternary mixtures incorporating 30% GG, those meeting the expansion requirement incorporated 10% SF, without NaOH addition, and 15% MK, regardless of the NaOH addition.
4) NaOH addition used for concrete prism testing in the laboratory was initially meant to accelerate aggregate's reactivity and combat the deleterious effect of alkali leaching. However, the results obtained in this study strongly suggest that it can also interact to enhance the beneficial effect of SCMs for preventing ASR expansion. Although, in most of the cases presented in this study, the expansion reduction associated to NaOH addition did not change the outcome of the test, it should be considered that NaOH addition may decrease its severity at least in the combinations evaluated through this study. This was especially the case for ternary mixtures with high content of SCM and/or high alkali SCM like in the case of GG.

## 6.7 Acknowledgments

The authors would like to thank the Centre de Recherche des Infrastructure en Béton (CRIB) for the space, equipment and technical support provided. Also, the authors are grateful to the Chaire de recherche de la SAQ and the Centre de Recherche en Sciences Naturelles et en Génie (CRSNG) for their financial support.

## 6.8 References


1. CSI (2009) Cement Industry Energy and $CO_2$ Performance,"Getting the Numbers Right". World Business Council for Sustainable Development

2. IEA/WBCSD (2009) Cement Technology Roadmap 2009. In: Publication I (ed) Carbon emission reduction up to 2050

3. (OECD) OfEC-oaD, (IEA) IEA (2007) Tracking Industrial Energy Efficiency and $CO_2$ Emissions. International Energy Agency 34 (2):1-12

4. (GCCA) GCCA (2017) Get Numbers Right (GNR). https://gccassociation.org/gnr/. 2020

5. IEA I, Energy Agency) (2014) Energy Policies of IEA Countries : The United States.

6. Scrivener K, Martirena F, Bishnoi S, Maity S (2018) Calcined clay limestone cements (LC3). Cement and Concrete Research 114:49-56. doi:10.1016/j.cemconres.2017.08.017

7. Huang W, Kazemi-Kamyab H, Sun W, Scrivener K (2017) Effect of replacement of silica fume with calcined clay on the hydration and microstructural development of eco-UHPFRC. Materials & Design 121:36-46. doi:10.1016/j.matdes.2017.02.052

8. Willona S (2019) 2019 Brings New Changes for Municipal Glass Recycling. https://www.waste360.com/glass/2019-brings-new-changes-municipal-glass-recycling.

9. Idir R, Cyr M, Tagnit-Hamou A (2011) Pozzolanic properties of fine and coarse color-mixed glass cullet. Cement and Concrete Composites 33 (1):19-29

10. Taha B, Nounu G (2008) Using lithium nitrate and pozzolanic glass powder in concrete as ASR suppressors. Cement and Concrete Composites 30 (6):497-505. doi:http://dx.doi.org/10.1016/j.cemconcomp.2007.08.010

11. Shi C, Wu Y, Riefler C, Wang H (2005) Characteristics and pozzolanic reactivity of glass powders. Cement and Concrete Research 35 (5):987-993. doi:http://dx.doi.org/10.1016/j.cemconres.2004.05.015

12. Shi C, Zheng K (2007) A review on the use of waste glasses in the production of cement and concrete. Resources, Conservation and Recycling 52 (2):234-247. doi:http://dx.doi.org/10.1016/j.resconrec.2007.01.013

13. Thomas MDA, Fournier B, Folliard KJ (2013) Alkali-Aggregate Reactivity (AAR) Facts Book. U.S. Dept of Transportation edn.,

14. Shayan A, Xu A (2006) Performance of glass powder as a pozzolanic material in concrete: A field trial on concrete slabs. Cement and Concrete Research 36 (3):457-468. doi:http://dx.doi.org/10.1016/j.cemconres.2005.12.012

15. Zidol A (2009) Optimisation de la finesse de la poudre de verre dans les systèmes cimentaires binaires. Université de Sherbrooke,

16. Li Z, Thomas RJ, Peethamparan S (2019) Alkali-silica reactivity of alkali-activated concrete subjected to ASTM C 1293 and 1567 alkali-silica reactivity tests. Cement and Concrete Research 123. doi:10.1016/j.cemconres.2019.105796

17. Redden R, Neithalath N (2014) Microstructure, strength, and moisture stability of alkali activated glass powder-based binders. Cement and Concrete Composites 45:46-56. doi:http://dx.doi.org/10.1016/j.cemconcomp.2013.09.011

18. Zhang S, Keulen A, Arbi K, Ye G (2017) Waste glass as partial mineral precursor in alkali-activated slag/fly ash system. Cement and Concrete Research 102:29-40. doi:https://doi.org/10.1016/j.cemconres.2017.08.012

19. Maraghechi H, Maraghechi M, Rajabipour F, Pantano CG (2014) Pozzolanic reactivity of recycled glass powder at elevated temperatures: Reaction stoichiometry, reaction products and effect of alkali activation. Cement and Concrete Composites 53 (0):105-114. doi:http://dx.doi.org/10.1016/j.cemconcomp.2014.06.015

20. Zhang L, Yue Y (2018) Influence of waste glass powder usage on the properties of alkali-activated slag mortars based on response surface methodology. Construction and Building Materials 181:527-534. doi:10.1016/j.conbuildmat.2018.06.040

21. Shi C, Wu Y, Shaob Y, C (2004) Alkali-Aggregate Reaction Expansion of Mortar Bars Containing Ground Glass Powder. Paper presented at the age, Pekin,

22. Pereira-de-Oliveira LA, Castro-Gomes JP, Santos P (2012) The potential pozzolanic activity of glass and red-clay ceramic waste as cement mortars components. Construction and Building Materials 31:197-203

23. Zheng K (2016) Pozzolanic reaction of glass powder and its role in controlling alkali–silica reaction. Cement and Concrete Composites 67:30-38. doi:http://dx.doi.org/10.1016/j.cemconcomp.2015.12.008

24. Serpa D, Santos Silva A, de Brito J, Pontes J, Soares D (2013) ASR of mortars containing glass. Construction and Building Materials 47 (0):489-495. doi:http://dx.doi.org/10.1016/j.conbuildmat.2013.05.058

25. Afshinnia K, Rangaraju PR (2015) Mitigating alkali-silica reaction in concrete: Effectiveness of ground glass powder from recycled glass. Transportation Research Record 2508:65-72. doi:10.3141/2508-08

26. Chen Z, Poon CS (2017) Comparing the use of sewage sludge ash and glass powder in cement mortars. Environmental Technology 38 (11):1390-1398. doi:10.1080/09593330.2016.1230652

27. Schwarz N, Cam H, Neithalath N (2008) Influence of a fine glass powder on the durability characteristics of concrete and its comparison to fly ash. Cement and Concrete Composites 30 (6):486-496

28. Lam CS, Poon CS, Chan D (2007) Enhancing the performance of pre-cast concrete blocks by incorporating waste glass – ASR consideration. Cement and Concrete Composites 29 (8):616-625. doi:http://dx.doi.org/10.1016/j.cemconcomp.2007.03.008

29. Lee G, Ling T-C, Wong Y-L, Poon C-S (2011) Effects of crushed glass cullet sizes, casting methods and pozzolanic materials on ASR of concrete blocks. Construction and Building Materials 25 (5):2611-2618. doi:http://dx.doi.org/10.1016/j.conbuildmat.2010.12.008

30. Cota FP, Melo CCD, Panzera TH, Araújo AG, Borges PHR, Scarpa F (2015) Mechanical properties and ASR evaluation of concrete tiles with waste glass aggregate. Sustainable Cities and Society 16:49-56. doi:http://dx.doi.org/10.1016/j.scs.2015.02.005

31. Kou SC, Poon CS (2009) Properties of self-compacting concrete prepared with recycled glass aggregate. Cement and Concrete Composites 31 (2):107-113. doi:http://dx.doi.org/10.1016/j.cemconcomp.2008.12.002

32. Afshinnia K, Rangaraju PR (2015) Efficiency of ternary blends containing fine glass powder in mitigatingalkali–silica reaction. Construction and Building Materials 100 (15):234–245

33. Maraghechi H, Salwocki S, Rajabipour F (2017) Utilisation of alkali activated glass powder in binary mixtures with Portland cement, slag, fly ash and hydrated lime. Materials and Structures 50 (1):16

34. Ramsey F, Schafer D (2002) Inference using t distribution. In: Brooks/Cole CL (ed) The statistical sleuth.

# Chapter 7. - Revisiting the Relationship Between the Alkalinity of Pore solution and the Expansion Due to Alkali-Silica Reaction (ASR) in Ternary Mixtures Incorporating Ground Glass (GG)


## Résumé

Le potentiel d'expansion nuisible dans un béton incorporant du verre broyé (VB) et des granulats réactifs est débattu. D'une part, la teneur en alcalis du VB est significativement plus élevée que celle des ajouts cimentaires conventionnels (AC), ce qui soulève des préoccupations quant à la réactivité alcalis-silice. D'autre part, le VB démontre des propriétés pouzzolaniques qui pourraient contribuer à atténuer la RAS. Cependant, les connaissances sur les facteurs favorisant l'une ou l'autre de ces réactions sont quelque peu limitées.

Dans cette étude, le comportement du VB (10, 20 ou 30 %) en combinaison avec de la fumée de silice (FS) (5, 7,5 ou 12,5%) ou du Métakaolin (MK) (5, 10 ou 15%) est évalué. Les données recueillies comprenaient l'expansion de prismes de béton incorporant un granulat hautement réactif (calcaire Spratt) et la composition de la solution interstitielle déterminée sur des spécimens de pâtes. Les résultats suggèrent que l'augmentation du contenu en FS/MK diminue systématiquement à la fois l'expansion du béton et l'alcalinité de la solution interstitielle, tandis que l'augmentation du contenu en VB a souvent eu un effet irrégulier sur l'expansion et la composition de la solution interstitielle. Les résultats suggèrent que l'utilisation de GG dans les pâtes cimentaires abaisse le $[K^+]$ tout en augmentant $[Na^+]$ et que le résultat net sur $[OH^-]$ est généralement une réduction de l'alcalinité. Les résultats suggèrent une corrélation existante mais faible entre l'alcalinité du mélange cimentaire et l'expansion de tels mélanges cimentaires dosés dans des prismes de béton. En outre, les résultats suggèrent que l'ajout de NaOH, tel que prescrit dans de nombreuses normes pour les essais d'expansion associable à la RAS, n'augmente pas toujours l'ampleur de l'expansion du mélange ternaire incorporant un ajout cimentaire à haute teneur en alcalis comme le VB. En fait, certains résultats suggèrent une expansion réduite pour un mélange donné incorporant du NaOH par rapport à ceux mélangés sans NaOH.

## Abstract

The potential for deleterious expansion in concrete incorporating post consumed finely ground Glass Powder (GG) and reactive aggregates is debated. On the one hand, the alkali content of GG is significantly higher than that of conventional Supplementary Cementitious Materials (SCM), which raises concerns about fueling ASR. On the other hand, GG exhibits pozzolanic properties that could contribute at mitigating ASR. However, knowledge on the factors promoting either reaction is somewhat limited. In this study, behaviour of GG (10, 20 or 30%) in combination with Silica Fume (SF) (5, 7.5 or 12.5%) and Metakaolin (MK) (5, 10 or 15%) is evaluated. Data collected included expansion of concrete prisms incorporating a highly-reactive aggregate (Spratt limestone) and pore solution composition determined on paste specimens. Results suggest that increasing the SF/MK content consistently decreases both expansion and alkalinity while increasing GG content often had unexpected effect on expansion and the composition of the pore solution. The results suggest that the use of GG into cementitious pastes lowers the $[K^+]$ while rising $[Na^+]$ and that the net result on $[OH^-]$ is generally a reduction of alkalinity. Results suggest an existing but weak correlation between the alkalinity of cementitious mixture and the expansion of such cementitious mixtures batched into concrete prisms. Also, results suggest that the NaOH addition, as prescribed in many standards to assess expansion due to ASR, does not always increase severity of the expansion in ternary mixtures incorporating a high alkali SCM such as GG. Actually, some results suggest reduced expansion for a given mixture incorporating NaOH compared to those batched without NaOH.

## 7.1 Introduction

In order to prevent the risk of deleterious expansion in concrete due to alkali-silica reaction (ASR) when reactive aggregates are used, the prescriptive CSA Standard Practice A23.2-27A suggests limiting the total concrete alkali content under certain "threshold" values, and/or to partially replace the cement by a sufficient amount of "efficient" Supplementary Cementitious Materials (SCMs). Those two measures are known to lower the alkalinity of the pore solution; indeed, the incorporation of several types of SCMs into concrete was found to lower the pH of the pore solution by three possible means: 1) the dissolution of the amorphous silica of the SCMs lowers the pH as suggested by Dent-Glasser and Kataoka (1981) who established the solubility curves of various silica gel (Figure 7.1); 2) SCMs generally produce C-S-H of lower C/S, which have demonstrated their potential for uptaking more alkalis in their structure, as demonstrated by the study carried out by Hong and Glasser (1999) on synthetic C-S-H immersed into alkali hydroxide solutions, and 3) SCMs often produce C-A-S-H that tend to uptake alkali ions from the pore solution even more efficiently than C-S-H, as suggested by Hong and Glasser (2002) in their work on synthetic C-A-S-H (Figure 7.2).

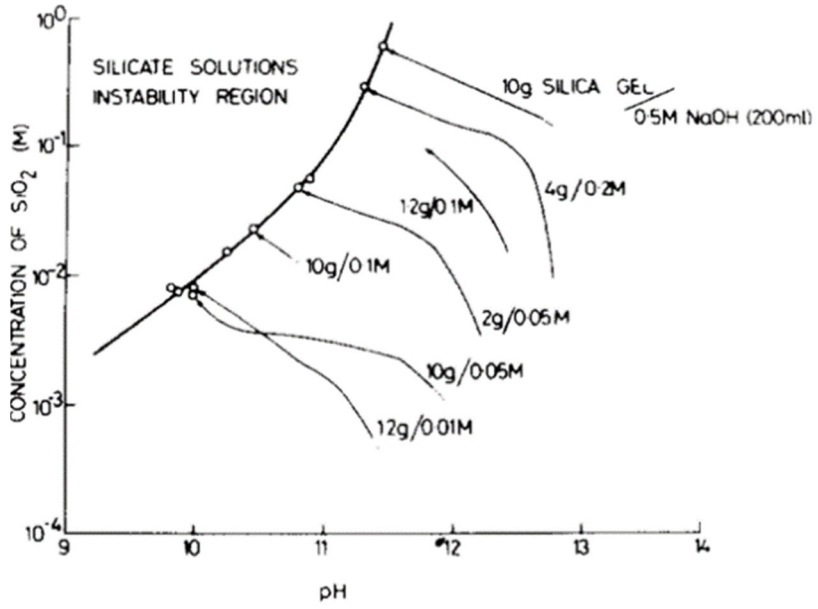


**Figure 7.1 : The final concentration of dissolved silica against pH (Heavy line) and the paths by which individual solutions approach it (light lines) (Dent-Glasser and Kataoka 1981).**

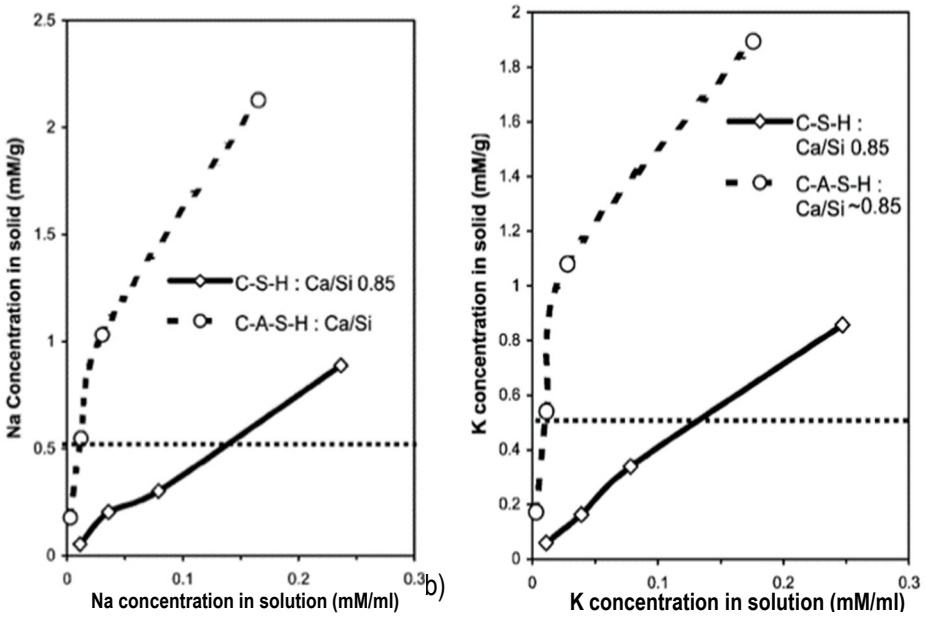


**Figure 7.2. a) Comparison of alkali binding capacity between C-S-H and C-A-S-H gels. Solid lines and dashed lines indicate C-S-H and C-A-S-H gel, respectively (Hong and Glasser 2002).**

Although it is well recognized that most SCMs tend to produce C-A-S-H or C-S-H with low C/S, SCMs do not have homogeneous effects in lowering the alkalinity of the pore solution of concrete and in reducing the expansion of concrete prisms. For instance, in a few studies involving high-alkali Fly Ashes (FA) (8.45 to 10.45% of $Na_2Oeq$ for 15 to 50% cement replacement, by mass), the authors observed that although high-alkali FA generally lower the expansion of concrete prisms by approximately 5 to 75% compared to control, their use is still not sufficient to meet the acceptance limit of 0.040% (Duchesne and Bérubé 1994a, Shehata and Thomas 2000, Fournier et al. 2008), The alkali content of the pore solution of pastes incorporating the above ashes was almost double that of control pastes made without FA (Duchesne and Bérubé 1994b, Shehata 2001).

Fournier et al. (2008) showed that combining 25% of a high-alkali FA (10.45% $Na_2Oeq$) with 5% Silica Fume (SF) reduces the expansion of concrete prisms incorporating the highly-reactive Spratt limestone by as much as 50% compared to the mix incorporating 25% of that FA only. Although, the ternary mixture could not reduce the expansion below the acceptance level, it is interesting to notice that such SCMs combinations might allow "synergy" that somewhat enhances the mitigation potential of high alkali FA. Shehata (2001) also observed a similar synergy between SF and FA with $Na_2O_{eq}$ levels between 1.41% and 4.14%.

High-alkali FA were mentioned above because, in term of their alkali content, they are the closest SCMs to Ground Glass (GG). Indeed, although the composition might vary, post-consumer's glass from recycling facilities, is generally high in its alkali content (can reach above 13%) and $SiO_2$ contents. The pozzolanic

properties of finely ground GG are well recognized but the potential of GG in preventing ASR is somewhat limited, similarly to that of some high alkali FA. Zidol (2009) and Lafrenière (2017) showed that the use of 20 and 30% GG (about 13% $Na_2O$eq) as a replacement by mass of the high-alkali cement reduces the expansion of concrete prisms below that of control mixtures without SCMs, however not enough to meet the two-year 0.040% limit proposed in CSA Standard Practice A23.2-28A. More optimistic results for the use of GG into concrete incorporating reactive aggregates (such as coarse glass) were obtained in a ternary context by Afshinnia and Rangaraju (2015) who used ASTM C1567 to study the expansion of mortar bars incorporating GG, FA, Metakaolin (MK) and Blast Furnace Slag (BFS). Although this test method, involving the immersion of the mortar bars in a 1N NaOH solution, may not be appropriate for testing high alkali SCMs such as GG, some interesting observations were proposed by the authors. They showed that the expansion of mortar bars is above the 14-day 0.10% acceptance limit when 10% to 30% GG is used in a binary context (which is in line with the data obtained by Lafrenière (2017)), but some ternary systems were efficient in reducing expansion below the above limit, e.g. 10%GG with 10% MK and 30% BFS, as well as 20% GG with 20% BFS. Other than that, literature is somewhat limited in providing information on the synergy between GG and other SCMs, from the expansion perspective, but also from a more fundamental or chemical point of view.

## 7.2 Scope and objective

In this study, ternary mixtures incorporating high- and low-alkali portland cements, from 10 to 30% GG and from 5 to 15% of MK or SF were used to manufacture paste samples, as well as concrete prisms incorporating the highly-reactive Spratt limestone. The concrete specimens were stored at 38°C and 100% RH and their length changes periodically monitored for up to 91 weeks (completed to date). The paste samples were stored in closed containers at 38°C and their pore solution extracted under pressure and analyzed by atomic absorption spectroscopy. The objective of this work is to evaluate to what extent the composition of the pore solution can be put in relation with the expansive behaviour of concrete for a wide variety of ternary mixtures incorporating GG and FS or MK.

## 7.3 Materials and Methods

### 7.3.1 Materials

The paste samples were made using GG from a recycling facility in the province of Quebec, Canada, SF from a ferro-silicon plant in the same province, MK from Georgia (USA) and GU (General Use) cement from a Canadian plant. The chemical composition of the cementitious materials is presented at Table 7.1. NaOH was used to "boost" the alkali content of the systems, in order to reach 1.08% or 1.25% of $Na_2O$eq, when required.

**Table 7.1. Chemical composition of binders and fine aggregate**

| Oxide | Cement | GG | SF | MK | Fine agg. |
|---|---|---|---|---|---|
| $SiO_2$ | 18.7 | 70.53 | 94.27 | 51.6 | 0.46 |
| CaO | 60.8 | 10.77 | 0.54 | 0.02 | 63.63 |
| $Al_2O_3$ | 5 | 2.06 | 0.3 | 43.97 | 0.1 |
| $Fe_2O_3$ | 3.7 | 0.35 | 0.1 | 0.49 | 0.09 |
| $Na_2O$ | 0.25 | 12.49 | 0.12 | 0.27 | 0 |
| $K_2O$ | 1.05 | 0.66 | 0.65 | 0.25 | 0.05 |
| $Na_2O_{eq}$ | 0.94 | 12.92 | 1.43 | 0.43 | 0.03 |
| $SO_3$ | 3.8 | 0.11 | 0.02 | 0 | - |
| MgO | 2.7 | 1.14 | 0.28 | 0.04 | 0.31 |
| $TiO_2$ | - | 0.07 | 0.01 | 1.4 | 0.01 |
| $P_2O_5$ | - | 0.03 | 0.12 | 0.09 | 0 |
| MnO | | 0.02 | 0.03 | 0.01 | - |
| L.O.I. | 1.9 | 1.71 | 3.2 | 1.84 | 35.37 |

The concretes were made with the cementitious materials listed in Table 7.1. The fine aggregate is a crushed high purity limestone (98% $CaCO_3$) from Newfoundland (Canada), with a density of 2.7 and an absorption value of 0.57%. The coarse aggregate is the highly-reactive Spratt limestone from Canada; it shows a density of 2.7 and an absorption value of 0.43%.

### 7.3.2 Mix Design

As illustrated in Figure 7.3 for SF-bearing specimens, a *Face Centred Central Composite Design* (FCCD) was used to select the concrete and paste mixtures for this study. The % GG and % SF axes represent the % of cement replaced by those SCMs (by mass), while the % $Na_2O_{eq}$ axis is the alkali content of the cement used for the mixes (1.08 and 1.25% = 0.94% + NaOH). The MK-bearing mixtures follow the same design, but the cement replacement levels are 5%, 10% and 15%.

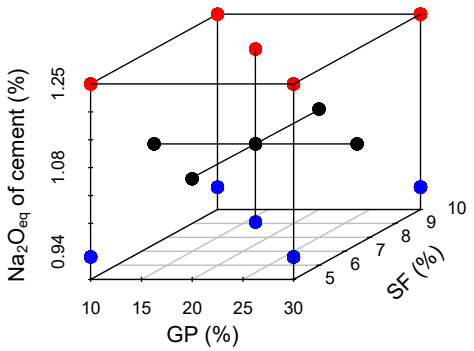


**Figure 7.3. Mixture design for concrete and paste mixtures incorporating various contents of GG, SF and cement of $Na_2Oeq$ contents of 0.94% in blue, 1.08% in black and 1.25% in red.**

### 7.3.3 Methods

Concrete specimens were made with 420 kg/m$^3$ of cementitious materials and a w/b of 0.42, in accordance with CSA Standard Practice A23.2-28A. A constant amount of 1054 kg/m$^3$ of coarse reactive aggregate was adopted for all mixtures, instead of the recommended 60:40 ratio for respectively coarse and fine aggregate. This approach was adopted because the volume occupied by 420 kg/m$^3$ of binders varies from one mixture to another and it was judged more appropriate to accommodate this variation by the dosage of non-reactive fine aggregate only. Test prisms of 100x100x300mm in size, instead of 75x75x300mm, were used in order to minimize the detrimental effect of alkali leaching that could occur during the two-year test period (Lindgård et al. 2013). The prisms were measured "hot", i.e. when still being at 38°C, again as a precaution against further alkali leaching. The length change of the test prisms was monitored at regular intervals up to 91 weeks (testing period completed at this time).

The paste mixtures were made with a w/b of 0.50. The procedure given in ASTM C 305-12 was slightly modified in order to avoid agglomeration of the materials (especially MK). SF or MK were thus first mixed with water at slow speed (140± 5 r/min) for 15 sec and then the GG added and mixed for 15 sec at slow speed. The usual procedure was then followed: the cement is incorporated, and 30 sec are left to allow absorption of water; the paste is then mixed for 30 sec at slow speed, 15 sec are allowed to scrape down the paste stuck on the side of the bowl, and the paste is finally mixed at medium speed (285 ± 5 r/min) for 60 sec. After batching, pastes were poured in cylindrical plastic containers, 30 mm by 55 mm in size, sealed and then gently agitated for the first 24h at 23 ± 2°C. The containers were then stored in a sealed plastic bag at 38°C.

At 28 and 182 days, paste samples were removed from their sealed plastic containers and placed in an extraction cell where the sample are pressed using a maximum pressure of 200 kN. The pore solution thus extracted flows into a plastic tube connected to a syringe which is then sealed with wax paper after extraction. The syringes are stored at 4°C until the solution is analyzed.

The pore solutions were acidified with 5%V/V nitric acid. $[Na^+]$ and $[K^+]$ were analyzed with a PerkinElmer AAnalyst 100 atomic absorption spectrophotometer (AAS) at wavelengths of respectively 589 and 766.5 nm using an air-acetylene flame. Cesium chloride was added to the solutions to a concentration of 1.5 g/L in order to avoid ionization. In this study, the lowest variability between replicates was found when 1) no more than two dilutions were conducted; 2) the dilution factors were approximately 150 for the first dilution; 3) the factor of the second dilution was approximately the same for all replicates; 4) the second dilution targeted the centre of the calibration curve ± 25%; 5) the calibration standards were made in large volume (1 L) from certified solution to ensure a maximal precision; 6) the calibration standards were analyzed every two samples to confirm the accuracy of the calibration curve; and 7) the samples were shaken few seconds prior to analyses in order to avoid concentration gradients. The alkalinity of the paste sample is estimated by electro neutrality using $[OH^-] \approx [Na^+] + [K^+]$.

## 7.4 Results

Figure 7.4 a) presents the average 91-week expansion of four concrete prisms incorporating various amounts of SF, MK or GG with cements of different $Na_2O_{eq}$ contents. An interesting observation is that all prisms incorporating 5%FS/MK (i.e. with 10 to 30% GG - i.e. filled or empty symbols) show expansions above the 0.040% acceptance limit. Interestingly, at that percentage (5%) of FS/MK, the expansion is generally decreased with 30% of GG compared to 10%, although they are still above the 0.040% limit. Increasing the SF content from 5% to 10% result in a 46% expansion reduction, on average, while 30GG-10SF-1.25Alk is the only mixture with an expansion below the 0,040% limit. Interestingly, for mixtures incorporating 30% GG, “boosted” mixtures (1.25% $Na_2Oeq$) show expansion lower than “unboosted” ones (0.94% $Na_2Oeq$). That trend is actually the opposite for mixtures incorporating 10% GG. The mixture incorporating 7.5% SF and 20% GG, however, show inconsistent results regarding the impact of the NaOH on concrete prism expansion. It is interesting to note that the expansion of concrete prisms incorporating 15% MK is ≤ 0.040%. Also, mixtures incorporating MK appear to be only slightly sensitive to NaOH addition in order to increase $Na_2O_{eq}$ content of the concrete mixture. Also, mixtures with 30% GG show expansions that are consistently below those of 10% GG mixtures, despite the large amount of alkalis in the GG. Finally, for intermediate mixtures incorporating 20% GG and 10% MK, the impact of the $Na_2O_{eq}$ content of the cement on expansion is inconsistent as for mixtures incorporating SF.

Figure 7.4 b) presents the 26-week [$OH^-$] of pastes samples corresponding to the same concrete mixtures illustrated in Figure 7.4 a). The most obvious observation is that the alkalinity of the pastes seems to follow a linear trend related to the SF/MK content in the paste. For SF-bearing pastes, the alkalinity of paste containing 10% GG and 5% SF is greatly increased by the NaOH addition (more than 200 mmol/L), while the alkalinity is not as much affected by NaOH addition for the mixture incorporating 10% SF or 30% GG (increase of ≈60 mmol/L or less). Finally, cement pastes with boosted alkalis consistently show increased [$OH^-$] in the pore solution compared to unboosted "companion" pastes. For MK-bearing pastes, small alkalinity increase, averaging ≈40 mmol/L, is associated to the NaOH addition to reach 1.25%. For the mixtures incorporating intermediate values of MK and GG, the impact of NaOH addition is below 25 mmol/L for all mixtures. Observations on MK-bearing pastes are coherent with the hypothesis that the alkalinity is somewhat linearly related to the MK content in the paste. Lastly, the impact of GG content on the alkalinity is not obvious in SF-bearing pastes nor in MK-bearing pastes. Increasing the GG content from 10 to 30% in the ternary pastes, does not result in an increase in the [$OH^-$] of the pore solution, despite the very high alkali content of the GG.

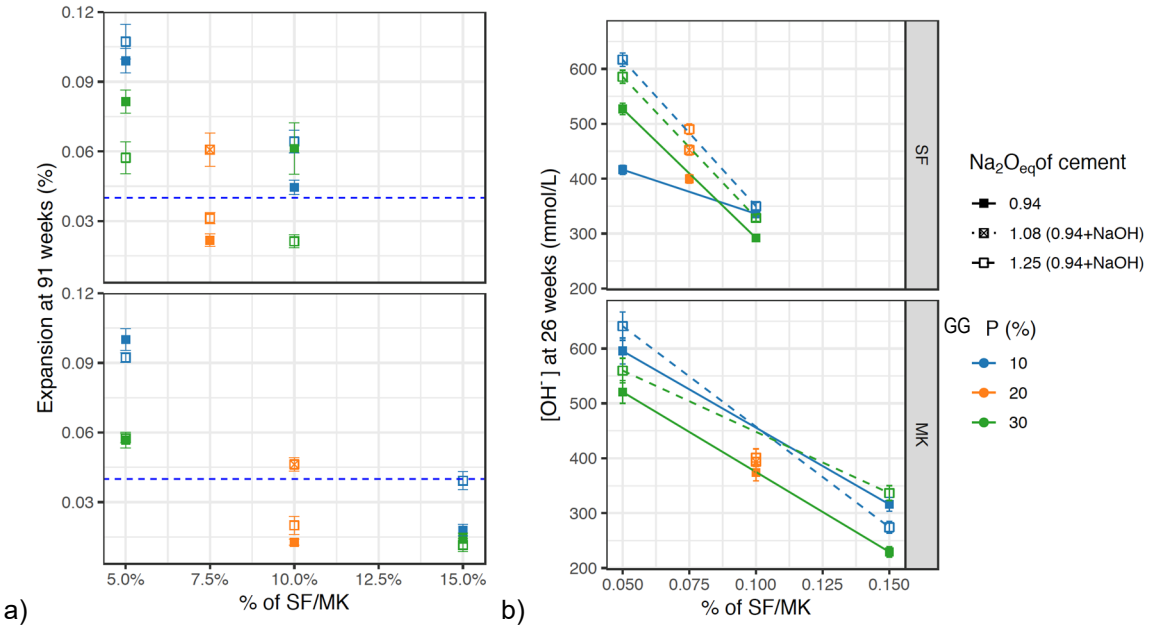


**Figure 7.4. a) Average expansion at 91 weeks and Standard Deviation (SD) of four concrete prisms and the 0.040% threshold in dashed line and b) [$OH^-$] of paste samples made with cement of different $Na_2O_{eq}$ contents and incorporating various percentages of GG, FS/MK. SD of single observations on paste samples is estimated by assuming a 2% and 4% Coefficient of Variation (COV) for SF and MK-bearing pastes respectively, which is the average COV of randomly performed extraction triplicates.**

Figure 7.5 presents the [$Na^+$] and [$K^+$] of the paste mixtures presented in Figure 7.4 b). For SF-bearing pastes, it is interesting to note the decreasing range of [$K^+$] associated to mixtures with decreasing GG, i.e. paste mixtures incorporating 10, 20 and 30% GG. Those pastes have [$K^+$] averaging ≈180 mmol/L, ≈140 mmol/L and ≈110 mmol/L (or ranges of ≈220-150, ≈160-120 and ≈135-85), respectively. Concerning [$Na^+$], an increase in the "cement" $Na_2Oeq$ content from 0.94 to 1.25% results in an increased [$Na^+$] in the pore solution averaging ≈70 mmol/L for all 11 SF-bearing mixtures and ≈ 40 mmol/L when excluding the "outlier" combination 10GG-5SF. However, the SF content has a somewhat stronger influence on the [$Na^+$] in the pore solution since the average [$Na^+$] for pastes with 5%, 7.5% and 10% SF are respectively ≈371 mmol/L, ≈300 mmol/L and ≈ 200 mmol/L.

For MK-bearing pastes, an increased [$Na^+$] in the pore solution is strongly associated to decreased MK contents in the paste, since the average [$Na^+$] for 5%, 10% and 15% MK is respectively ≈ 420 mmol/L, 270 mmol/L and 190 mmol/L; on the other hand, increasing the "cement" alkali content from 0.94 and 1.25% results in an average increase of [$Na^+$] in the pore solution of ≈40 mmol/L. When only 5% MK is used, increasing the GG content from 10% to 30% strongly reduces [$K^+$] and it is worth mentioning that this observation does not stand when 15% MK is used.

It is interesting to note that an increase in the [$K^+$] of the pore solution is generally observed when NaOH is added in SF-bearing pastes while the opposite trend is observed for MK bearing pastes.

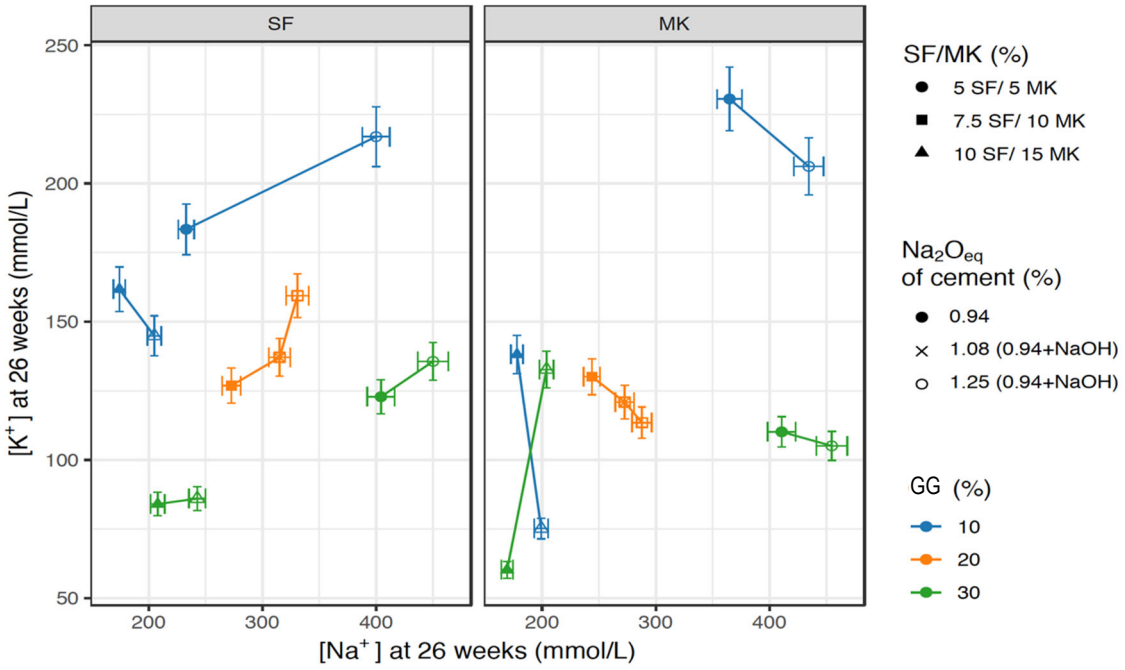


**Figure 7.5. [$Na^+$] and [$K^+$] of paste samples made with cement of different $Na_2O_{eq}$ contents and incorporating various percentages of GG, FS/MK. SD of single observations on paste samples is estimated by assuming a 3% and 5% Coefficient of Variation (COV), which is the average COV for [$Na^+$] and [$K^+$] respectively on triplicates extractions.**

## 7.5 Discussion

Data presented by Duchesne and Bérubé (1994b) (Figure 7.6) and Shehata (2001) (Figure 7.7) have shown that the alkalinity of the pore solution of (binary) pastes incorporating fly ash has largely stabilized within a few months after batching. It is thus reasonable to believe that the composition of the pore solution of paste specimens (w/b of 0.50) made as part of this study had largely stabilized after 26 weeks (at 38˚C) and could be reasonably put in relation with the longer-term expansion behaviour of concrete specimens of similar composition. It is worth considering that the 26-week pore solution composition should be considered as a "window of observation" in the evolution of the ionic concentrations in the ternary paste systems, and also that the presence of a reactive aggregate in concrete reacts with the ionic species in the pore solution in order to produce the expansive gel, thus introducing a significant difference in behaviour compared to the evolution of the pore solution composition in paste systems.

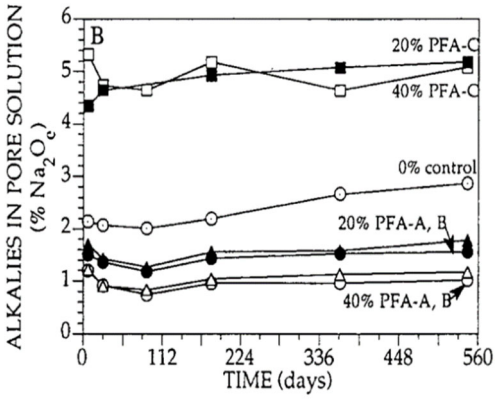


**Figure 7.6. Alkalis in the pore solution of pastes incorporating 20 and 40% of three different Pulverised Fly Ashes (PFA) as a function of time. ($Na_2O_{eq}$ of the cement, PFA A, B and C are respectively 0.74%, 2.34%, 3.07% and 8.55%, (1% $Na_2O_{eq}$ = 0.32N NaOH + KOH)) (Duchesne and Bérubé 1994b).**

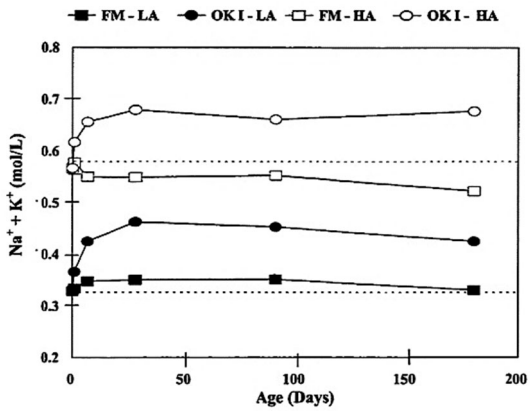


**Figure 7.7. Effect of 13% FA (FM =1.41% $Na_2O$eq; OK1 = 1.65% $Na_2O$eq) on the pore solution alkalinity of systems representing pastes containing low (LA) and high-alkali (HA) cement (LA=0.60% $Na_2O$eq and HA=1.09% $Na_2O$eq (Shehata 2001)).**

Nonetheless, valuable information can be obtained from the analysis of the pore solution extracted from paste specimens (data in Figure 7.8) when related more indirectly to the expansion. For instance, Figure 7.8 gives a plot of the expansion of the concrete prisms at 91weeks against a) $[Na^+]$, b) $[K^+]$ and c) $[Na^+] + [K^+] = [OH^-]$ of the pore solution of paste specimens at 26 weeks. Data are given for the ternary systems where the cement with 0.94% of $Na_2O$eq content was used without or with added NaOH to reach 1.08 or 1.25% $Na_2O$eq. Despite the high sodic content of GG (above 13% $Na_2O$), it is interesting to observe no clear correlation between $[Na^+]$ of the pore solution and the GG content of the mixture. This suggests that either $Na^+$ ions contained in the GG particles remain into the particles, or $Na^+$ ions are released and incorporated into hydrates. In either of the two latter theories, $Na^+$ contained in GG are not available to attack the reactive aggregates. Actually, the highest expansions are observed for mixtures incorporating only 10%GG. Also, no clear correlation was found between the $[K^+]$ and concrete prism expansion; however, as expected, lower $[K^+]$ were measured for pastes incorporating 20 and 30% GG, which is interesting since $K_2O$ content of GG is not negligible with a value of 0.66%. When summing up the two cations, once again, no clear correlation is found between the expansion and the alkalinity of the pore solution (when assuming that $[OH^-] \approx [Na^+] + [K^+]$).

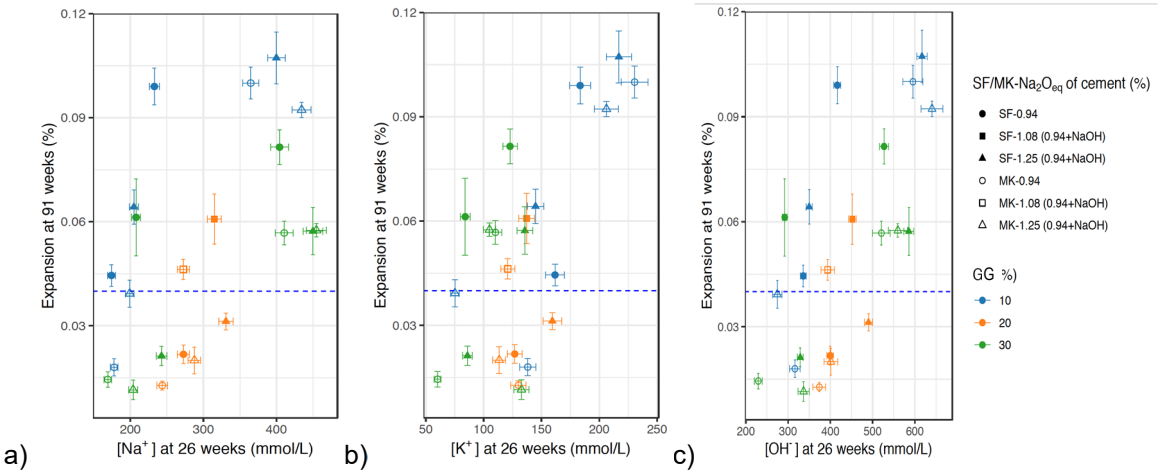


**Figure 7.8. a) [$Na^+$]; b) [$K^+$] and c) [$Na^+$] + [$K^+$] ≈ [$OH^-$] of the pore solution of paste samples at 26 weeks.**

To better highlight the impact of GG on the pore solution chemistry, Table 7.2 allows to compare the results of mixtures with different GG contents but the same SF/MK-Alk content. It is interesting to point out that increasing the GG content from 10% to 30% decreases the expansion by an average of 33%, although the [$OH^-$] in the pore solution of corresponding pastes is decreased by an average of only 3%, the [$Na^+$] is increased by an average of 17% and the [$K^+$] is decreased by an average of 30%. It is interesting to note that, on average, the reduction of expansion associated with increased GG content is more pronounced in mixtures incorporating MK than SF. Actually, reductions in concrete prism expansion were observed in all ternary mixtures combining GG and MK and all but one mixture combining GG with SF. It is worth mentioning that many sets of concrete prisms manufactured in this study displayed low expansion values (e.g. < 0.06%) and that the variability of concrete prism expansion testing could in itself overcome the differences observed between the averages of those small values. It is also worth noting that MK was used in a range between 5% and 15% while the range for SF was between 5% and 10%. An interesting observation concerning the pore solution is that, for FS/MK- $Na_2O$**eq** combination presented in Table 7.2, the increase in GG content is most of the time associated to increases in [$Na^+$] and decreases in [$K^+$] of the pore solution. Similar observations were reported regarding binary cementitious pastes incorporating GG by Fily-Paré et al. (2017).

**Table 7.2. Expansion of concrete specimens aged 91 weeks, [$OH^-$], [$Na^+$] and [$K^+$] of paste samples aged 26 weeks and the relative impact of increasing GG from 10% to 30%.**

| | | Expansion (%) | | [$OH^-$] | | [$Na^+$] | | [$K^+$] | | Impact of GP | | | |
|---|---|---|---|---|---|---|---|---|---|---|---|---|---|
| SF/ MK (%) | Cement $Na_2O_{eq}$ (%) | GP(%)↓→ 10 | 30 | 10 | 30 | 10 | 30 | 10 | 30 | Exp. (%) | [$OH^-$] (%) | [$Na^+$] (%) | [$K^+$] (%) |
| 5SF | 0.94 | 0.10 | 0.08 | 416 | 527 | 233 | 404 | 183 | 123 | -18 | 27 | 74 | -33 |
| 5SF | 1.25 | 0.11 | 0.06 | 617 | 586 | 400 | 450 | 217 | 136 | -47 | -5 | 13 | -37 |
| 10SF | 0.94 | 0.04 | 0.06 | 336 | 292 | 174 | 208 | 162 | 84 | 38 | -13 | 19 | -48 |
| 10SF | 1.25 | 0.06 | 0.02 | 350 | 329 | 205 | 243 | 145 | 86 | -67 | -6 | 18 | -41 |
| 5MK | 0.94 | 0.10 | 0.06 | 595 | 521 | 365 | 411 | 231 | 110 | -43 | -13 | 13 | -52 |
| 5MK | 1.25 | 0.09 | 0.06 | 641 | 560 | 434 | 455 | 206 | 105 | -37 | -13 | 5 | -49 |
| 15MK | 0.94 | 0.02 | 0.01 | 316 | 229 | 178 | 169 | 138 | 60 | -21 | -27 | -5 | -56 |
| 15MK | 1.25 | 0.04 | 0.01 | 274 | 337 | 199 | 204 | 75 | 133 | -71 | 23 | 2 | 77 |
| | | | | | | | | Average | | -33 | -3 | 17 | -30 |
| | | | | | | | | SF | | -23 | 1 | 31 | -40 |
| | | | | | | | | MK | | -43 | -7 | 4 | -20 |

## 7.6 Conclusion

Previous research has shown that higher concentrations of alkali species in the cement lead to higher pH in the pore solution of pastes, mortars or concretes, which in turn leads to the attack of the reactive siliceous phases in aggregates. On the other hand, the dissolution of silica is also a means to lower the pH in the pore solution of cementitious systems, which is the mechanism by which many SCMs are thought to prevent deleterious expansion due to ASR. Pozzolanic reactions lead to C-S-H of lower C/S ratio, which is known to uptake a larger proportion of alkalis from the pore solution, thus contributing at lowering the pH. Other researches also showed that greater uptake of alkalis by C-S-H and C-A-S-H are related to the lower concentration of alkalis in the pore solution. Those last studies surely helped to better understand how materials like SCMs help at mitigating ASR, but limited information exists regarding the combined effects of high-alkali SCMs, especially in ternary systems, on the pore solution chemistry and the expansion of test specimens incorporating reactive aggregates.

The result obtained in this study suggest that the composition of the pore solution alone is a somewhat poor predictor of the expansion potential in ternary systems involving a high-alkali SCM such as glass powder (combined with silica fume/metakaolin in this study) because, although highest expansion are associated to highest [$OH^-$] and vice versa, pore solution composition is not linearly related to expansion in such ternary mixtures. For instance, higher percentages of cement replacement by GG lead to lower expansion compared to specimens with lower GG content (not always controlled below the generally accepted expansion limit of 0.040% at two years), but its effect on the pore solution is not coherent with the latter. Actually, the percentage of SF/MK used as cement replacement remains the most impactful means of controlling expansion below the 0.040% limit

since most mixtures incorporating 15% MK had acceptable expansion levels at 91 weeks. Finally, the results suggest to rethink the common use of NaOH addition in order to accelerate expansion as prescribed by CSA A23.2-28A testing standard since it might not act as expected for most ternary mixtures incorporating GG. Indeed, the mixture in which NaOH was added in order to reach 1.25% show expansion similar and sometimes lower than that of companion mixtures without NaOH. Further work would be required to better understand this behaviour.

## 7.7 References


Afshinnia, K. and P. R. Rangaraju (2015). "Efficiency of ternary blends containing fine glass powder in mitigating alkali–silica reaction." Construction and Building Materials 100(15): 234–245.

Duchesne, J. and M. A. Bérubé (1994a). "The effectiveness of supplementary cementing materials in suppressing expansion due to ASR: Another look at the reaction mechanisms part 1: Concrete expansion and portlandite depletion." Cement and Concrete Research 24(1): 73-82.

Duchesne, J. and M. A. Bérubé (1994b). "The effectiveness of supplementary cementing materials in suppressing expansion due to ASR: Another look at the reaction mechanisms part 2: Pore solution chemistry." Cement and Concrete Research 24(2): 221-230.

Fily-Paré, I., B. Fournier, J. Duchesne and A. Tagnit-Hamou (2017). “Effect of glass powder on the pore solution of cement pastes”. 10th ACI/RILEM International conference on cementitious materials and alternative binders for sustainable concrete, Montréal.

Fournier, B., Nkinamubanzi, P.C., Chevrier, R., Ferro, A. 2008: “Evaluation of the effectiveness of high-calcium fly ashes in reducing expansion due to alkali-silica reaction in concrete”. Electric Power Research Institute (EPRI), Palo Alto (USA), 1014271.

Glasser, L. D. and N. Kataoka (1981). "The chemistry of ‘alkali-aggregate’reaction." Cement and Concrete Research 11(1): 1-9.

Hong, S.-Y. and F. Glasser (1999). "Alkali binding in cement pastes: Part I. The CSH phase." Cement and Concrete Research 29(12): 1893-1903.

Hong, S.-Y. and F. P. Glasser (2002). "Alkali sorption by C-S-H and C-A-S-H gels: Part II. Role of alumina." Cement and Concrete Research 32(7): 1101-1111.

Lafrenière, C. (2017). « Évaluation du comportement en durabilité de nouvelles matrices cimentaires pour l'obtention de bétons respectueux de l'environnement ». Master, Université Laval, https://corpus.ulaval.ca/jspui/handle/20.500.11794/27591.

Lindgård, J., M. D. A. Thomas, E. J. Sellevold, B. Pedersen, Ö. Andiç-Çakır, H. Justnes and T. F. Rønning (2013). "Alkali–silica reaction (ASR)—performance testing: Influence of specimen pre-treatment, exposure conditions and prism size on alkali leaching and prism expansion." Cement and Concrete Research 53(0): 68-90.

Shehata, M. H. (2001). “The effects of fly ash and silica fume on alkali-silica reaction in concrete”. Ph.D Thesis, University of Toronto.

Shehata, M. H. and M. D. A. Thomas (2000). "The effect of fly ash composition on the expansion of concrete due to alkali–silica reaction." Cement and Concrete Research 30(7): 1063-1072.

Zidol, A. (2009). « Optimisation de la finesse de la poudre de verre dans les systèmes cimentaires binaires ». PhD Thesis, Université de Sherbrooke, http://savoirs.usherbrooke.ca/handle/11143/1564.

# Chapter 8. - Relation Between Alkali Silica Reaction (ASR) and Pore Solution Composition of Ternary Blends Incorporating Ground Glass (GG) and Blast Furnace Slag (BFS)

## Résumé

La composition chimique du verre broyé (VB) est soupçonnée d'alimenter simultanément la réaction pozzolanique (contenu de silice amorphe > 70%) et la réaction alcalis-silice (teneur en sodium de 13 %) dans les bétons incorporant un granulat réactif. Afin de mieux comprendre le contexte dans lequel la RAS pourrait potentiellement prendre le relais et provoquer des expansions nuisibles, des éprouvettes de béton de composition ternaire ont été fabriquées avec des ciments incorporant divers contenus en $Na_2O_{eq}$ (0,94% à 0,94% + NaOH pour atteindre 1,25) et divers contenus de VB (10 à 20%) et de laitier de haut fourneau (LHF) (20 à 40 %). Les prismes ont été conditionnés à 38°C et 95 % HR et leur expansion a été suivie pendant une période de deux ans. Des spécimens de pâtes cimentaires avec les mêmes proportions que celles utilisées dans le béton, mais avec un contenu d'alcalis allant de 0,63% à 0,94% + NaOH pour atteindre 1,25% $Na_2Oeq$, ont été fabriquées et leur solution interstitielle extraite après six mois. Les solutions ont ensuite été analysées avec la spectroscopie d'absorption atomique (AAS) pour leurs $[Na^+]$ et $[K^+]$. Les résultats suggèrent que l'expansion des mélanges ternaires incorporant VB et LHF est fortement liée à la $[K^+]$ ($R^2$ à 0,84) et moins à la $[Na^+]$ ou $[OH^-]$ de la solution interstitielle (cette dernière étant estimée par la somme de $[Na^+]$ et $[K^+]$).

## Abstract

The chemical composition of Ground Glass (GG) is suspected to fuel simultaneously the pozzolanic reaction (amorphous silica content >70%) and Alkali Silica Reaction (sodium content >13%) in concrete systems incorporating a reactive aggregate. In order to better understand the context in which ASR could potentially take over and induce harmful expansions, concrete specimens were made from ternary mixtures made with cements incorporating various $Na_2Oeq$ contents (0.94% to 0.94% +NaOH to reach 1.25%) and various contents of GG (10 to 20%) and Blast Furnace Slag (BFS)(20 to 40%). The prisms were stored at 38°C and >95%RH environment and their expansion monitored for up to two years. Paste specimens with the same cementitious mixture proportions, but with alkali contents ranging from 0.63% to 0.94% + NaOH to reach 1.25% $Na_2Oeq$, were made and their pore solution extracted after six months. The solutions were then analysed with Atomic Absorption Spectrophotometry (AAS) for their $[Na^+]$ and $[K^+]$. The results suggest that the expansion of ternary mixtures incorporating GG and BFS is strongly related to the $[K^+]$ ($R^2 > 0.84$) and poorly related to $[Na^+]$ or $[OH^-]$ (estimated by summing $[Na^+]$ and $[K^+]$).

## 8.1 Introduction

The Global Cement and Concrete Association (GCCA) considers that the replacement of primary raw materials in cement and concrete is a longstanding contribution toward circular economy and is making beneficial use of a range of society's waste and by-products (Association 2019). Hence, they promote binary or ternary mixtures to partially (or fully) replace Ordinary Portland Cement (OPC) with supplementary Cementitious Materials (SCM). The popularity of alternative binders is often limited by the fact that their use may require some compromises because they exhibit different properties for fresh and hardened concrete compared to OPC. For instance, the use of Silica Fume (SF) improves compressive strength development of concrete at early age and significantly reduces permeability but its use in concrete is often more expensive than the OPC that it replaces and/or it often requires superplasticizer to ensure proper dispersion and workability (Golafshani and Behnood 2019, Wu et al. 2019). Another example is the case of Fly Ashes (FA), which often improves the rheological properties or long term compressive strength of concrete when used in "conventional" replacement levels (e.g. 15 to 30%) but in exchange of a loss of early-age compressive strength (Lane and Ozyildirim 1999, Vance et al. 2013). Lastly, binary or ternary mixtures incorporating Ground Glass (GG) is also referred as an SCM that can thus reduce the carbon footprint of concrete and improve concrete properties like compressive strength; however, since long term behavior of concrete incorporating coarse glass aggregate had induced premature deterioration due to Alkali Silica Reaction (ASR) (Idir et al. 2010), the use of GG as a cementitious material remains somewhat controversial. For instance, Rodier and Savastano (2018) observed increased compressive strength of 28-day old mortar incorporating up to 20% GG when compared to the control OPC mortar. Du and Tan (2017) observed a compressive strength approximately 10 MPa higher with high replacement level (60%) of OPC by GG% compared to the OPC control (45 MPa) at one year for concrete. Rehman et al. (2018) observed that the 28-day compressive strength of concretes containing GG was enhanced, compared to a 100% OPC control concrete mix and mixtures incorporating 20, 30, and 40% GG had their compressive strength enhanced, unchanged or reduced respectively when coupled with ground steel slag as fine aggregates.

Unfortunately, there is actually a lack of knowledge or confidence regarding the long-term behavior of concrete incorporating GG and alkali-silica reactive aggregates. Indeed, the use for binary GG-cement mixtures may be limited to concrete incorporating non-alkali-silica reactive aggregates. As a matter of fact, few studies suggest that binary mixtures incorporating GG cannot prevent expansion due to ASR in cases where alkali-reactive aggregates are used, as demonstrated by previous testing carried out in accordance with CSA 23.2-28A (Zidol 2009, Lafrenière 2017).

Because, the use of GG is limited in binary blends when reactive aggregates are used, well-chosen and dosed SCM in ternary or even quaternary blends can lead to concrete with "the best of two worlds". An example of ternary mixtures offering the environmental advantages of binary mixtures with little compromise regarding the rest of the concrete properties is documented by Lane and Ozyildirim (1999); the authors indeed proposed to add Silica Fume (SF) to Blast Furnace Slag (BFS) in order to build road with good early compressive strength and local reactive aggregates from Virginia. The ternary mixtures successfully mitigated ASR and showed early strength comparable or better than that of OPC mixtures.

### 8.1.1 The Synergy Between GG and BFS

The combined use of GG and BFS has been relatively popular in the last years since the progressive sodium release of GG is hypothesized to be beneficial when used with "alkali-activable" materials such as BFS. Compressive strength obtained suggested synergetic behavior between the materials. For instance, Zhang et al. (2017) worked on Alkali-Activated (AA) systems incorporating 50% BFS and various proportions of FA and GG and suggested that increasing the GG content up to 30% enhances the 28-day compressive strength of pastes by as much as 35% compared to the 50/50% FA/slag mixture. The best performance was observed at 28-day compressive strengths of 26, 23, 33 and 37 MPa, for respectively the control mixture (50FA-50BFS), 10GG-40FA-50BFS, 20GG-30FA-50BFS, and 30GG-20FA-50BFS. In the study of Maraghechi et al. (2017), an optimum at 30% GG was also observed. The 28-day compressive strength of AA BFS mixtures incorporating 0, 30 and 40% GG, were 68, 80, and 72 MPa, respectively. Zhang and Yue (2018) underlined the synergy between GG and BFS. Their work resulted in an optimum percentage of GG at 14.57%, when testing the 28-day compressive strength of Alkali Activated Slag (AAS) concrete specimens in which slag was replaced by GG and the activator had 8.31% $Na_2O_{eq}$. Indeed, the optimized mixture reached 66.4 MPa at 28 days.

The microstructure of ternary mixtures incorporating GG and BFS was assessed by Maraghechi et al. (2017) using Energy Dispersive x-ray Spectroscopy (EDS) to compare the composition of hydrates of mortar mixtures incorporating 100% BFS and 70% BFS-30%GG or 60% BFS-40%GG. All hydration products were composed of C-A-S-H, with higher silica content for mixtures containing GG. According to the authors, "*[…], by gradual dissolution and release of alkalis from glass, soda-lime glass particles can serve as internal activation source to help maintain high alkalinity in the pore solution. This can beneficially promote hydration of slag particles, which could be another reason for the high long-term strength of alkali-activated slag–GG mortars*". Zhang et al. (2017) suggested that GG prolongs the induction period and facilitates the formation of C-(N)-A-S-H gel, probably to the detriment of N-A-S-H gel that was not observed.

### 8.1.2 Expansion Due to ASR of Mixtures Incorporating GG and BFS

Afshinnia and Rangaraju (2015) assessed the expansive behaviour of mixtures incorporating GG and BFS according to ASTM 1567. This test method is similar to ASTM 1260 except that crushed glass is used as reactive aggregate. Mortar mixtures incorporating 100% OPC and 60% OPC with 40% SCMs (i.e. 10 GG-30 BFS or 20 GG - 20 BFS) were studied. After 14 days, the OPC control showed an expansion of 0.9% while the two GG-BFS mixtures had expansions < 0.05%, which is well below the expansion limit of 0.10%.

## 8.2 Scope of Work

The expansive behaviour of ternary concrete mixtures incorporating GG and BFS, in the presence of reactive aggregates, has not been frequently reported and limited information is available on the chemical composition of the pore solution of such systems. The main objective of this work is to determine if the high sodium content of GG is released into the pore solution and could thus cause ASR. Secondly, this work seeks to contribute to faster prediction of concrete expansion due to ASR by relating the six-month composition of the pore solution to the two-year concrete prism expansion.

In this work, ternary paste mixtures incorporating GG and BFS were made and stored in sealed containers for 182 days at 38°C before extraction and chemical analysis of the pore solution for Na and K contents. In parallel, concrete specimens incorporating OPC, GG and BFS were also manufactured and stored for 104 weeks at 38°C and 100% RH, period over which their length change was monitored regularly. The expansion of the concrete specimens at two years were correlated to the composition of the pore solution of pastes specimens at six months.

## 8.3 Materials and Methods

### 8.3.1 Materials

The paste and prism specimens were manufactured with two GU portland cements from producers located in the province of Quebec (Canada) for which the oxide compositions are presented in Table 8.1. The GG was obtained from a recycling plant treating post consumed glass and located in the province of Quebec (Canada); the BFS is a grade 80 from Ontario (Canada). The fine aggregate consisted of manufactured high purity limestone sand (98% $CaCO_3$) from Newfoundland (Canada); it presents a density of 2.7, an absorption capacity of 0.57% and its chemical composition is presented in Table 8.1. The coarse aggregate was the highly-reactive Spratt limestone from Ontario (Canada) that presents a density of 2.7 and an absorption capacity of 0.43%.

**Table 8.1 : Oxide composition of materials**

| | Portland cement | | SCMs | | Fine Aggregate |
|---|---|---|---|---|---|
| Oxide | C1 | C2 | GG | BFS | |
| $SiO_2$ | 19.58 | 18.7 | 70.53 | 37.74 | 0.46 |
| CaO | 62.09 | 60.8 | 10.77 | 36.20 | 63.63 |
| $Al_2O_3$ | 4.58 | 5.0 | 2.06 | 9.45 | 0.10 |
| $Fe_2O_3$ | 2.85 | 3.7 | 0.35 | 0.36 | 0.09 |
| $Na_2O$ | 0.22 | 0.25 | 12.49 | 0.26 | 0.00 |
| $K_2O$ | 0.62 | 1.05 | 0.66 | 0.36 | 0.05 |
| $Na_2O_{eq}$ | 0.63 | 0.94 | 12.92 | 0.50 | 0.03 |
| $SO_3$ | 4.02 | 3.8 | 0.11 | 2.45 | - |
| MgO | 2.91 | 2.7 | 1.14 | 9.96 | 0.31 |
| $TiO_2$ | - | 0.23 | 0.07 | 0.94 | 0.01 |
| $P_2O_5$ | - | 0.10 | 0.03 | 0.08 | 0.00 |
| MnO | | | 0.02 | 0.72 | - |
| L.O.I | 1.9 | 2.45 | 1.71 | 1.84 | 35.37 |

### 8.3.2 Mix Design

The Design of Experiment (DOE) for the testing of concrete prism followed a *Face Centered Central Composite* design, as illustrated in Figure 8.1. Concrete specimens were manufactured with a total cementitious materials content of 420 kg/m$^3$ and a w/b of 0.42. A polycarboxylate based superplasticizer was used to ensure proper workability especially when NaOH was added to increase the alkali content of the system. In accordance with the DOE approach, the GG and BFS contents in the concrete mixtures ranged from 10 to 30% and 20 to 40%, respectively. All concrete mixtures were made with cement C1 (0.94% $Na_2Oeq$); higher alkali contents (i.e. 1.08 & 1.25% $Na_2Oeq$) were obtained by using adding NaOH to the concrete incorporating the high alkali cement (0.94% $Na_2Oeq$). Paste specimens were manufactured with a w/b of 0.50 and the DOE followed a complete factorial plan of three variables and three levels for each variable, as presented in Figure 8.2. Most mixtures of the concrete and paste DOE are common (same cementitious materials proportioning). They appear in red and blue in Figure 8.1. The mixtures illustrated by a black dot in Figure 8.2 are also common to both DOE. In addition to the DOE, a mixture incorporating 30% GG & 30% BFS, as replacement by mass of the high alkali cement C2 but “boosted” to 1.25% with NaOH, was also made for paste and concrete specimens.

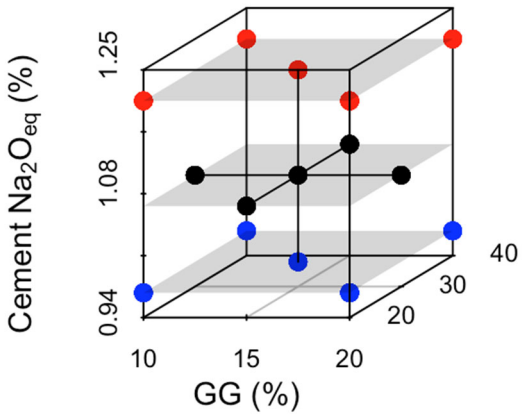


**Figure 8.1: DOE of the face centered central composite design for concrete prism mixtures.**

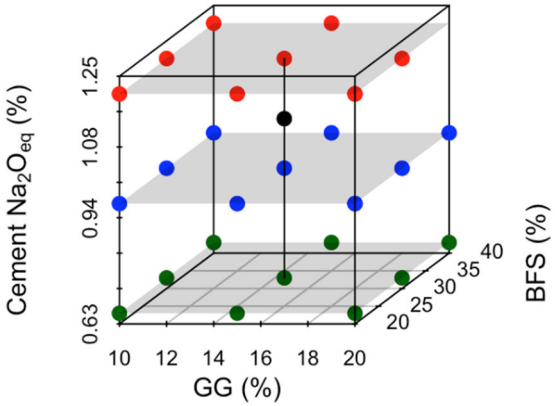


**Figure 8.2: DOE of a complete factorial plan for paste mixtures.**

### 8.3.3 Concrete Prism Test

Concrete specimens contained 420 kg /m$^3$ of cementitious materials and a w/b of 0.42. The recommendations of standard practice CSA A23.2-28A were adapted so that a constant mass of reactive aggregate/m$^3$ was used in every mixture although the paste volume varied according to each GG/BFS combination. The mass of non-reactive fine aggregate was thus set to accommodate the volumetric variations of the pastes across all mixtures of the DOE. To avoid alkali leaching, the section of the concrete specimens was increased from 75 x 75 to 100 x 100 mm, while the length measurements were taken with prisms at 38°C to avoid temperature cycling that are known to contribute to alkali leaching (Lindgård et al. 2013). Length-change measurements were made at regular interval up to 104 weeks.

### 8.3.4 Manufacturing of Cementitious Paste

To produce the paste mixtures, water (with or without NaOH solution) was first poured in the bowl of the mixer and then the GG and BFS added and mixed at slow speed (140 ± 5 r/min) for 15 seconds. Afterwards, cement was added to the mixture, left for 30 seconds to rest and allow the cement to absorb water before being mixed 30 seconds at slow speed. After the above initial mixing of all ingredients of the paste, the mixer was stopped 15 seconds to allow scrapping down any paste sticking to the side of the bowl. Finally, the paste was mixed 60 seconds at medium speed (285 ± 5 r/min), poured in a hermetic plastic container, 30 mm by 55 mm in size, hermetically closed and then lightly agitated for 24h at 23 ± 2°C. The specimens were then stored in sealed plastic bags at 38°C for 182 days.

### 8.3.5 Pore Solution Extraction

The paste specimens were removed from the 38 ± 2°C cabinet 24 hours prior to the extraction, period over which they were stored at 23 ± 2°C. The extraction process was carried out in a laboratory held at 23 ± 2°C. As a precaution against carbonation, paste specimens were not broken before extraction. All solutions were extracted under a pressure of 320 MPa (200kN for a section of 625 $mm^2$). The typical extraction process for a single paste specimen takes about 20 minutes to complete and leads to the collection of about 1.5 ml of pore solution. The solution is collected by a tube connecting the base part of the extraction cell to a syringe that was sealed immediately after extraction with a plastic cap and wax tape to prevent any potential carbonation or evaporation of the solution.

### 8.3.6 Chemical Analysis

$[Na^+]$ and $[K^+]$ were analyzed using a PerkinElmer AAnalyst 100 atomic absorption spectrophotometer (AAS) at wavelengths of 589 and 766.5 nm, respectively, using an air-acetylene flame. To reach the detection range of the apparatus, extracted solutions were diluted twice, with a consistent first dilution ratio of 1:150 and a second dilution ratio ranging from 1:2 to 1:35 for $[K^+]$ and from 1:7 to 1:50 for $[Na^+]$. Dilution and standard calibrations were prepared using nitric acid 5%V/V in which Cesium Chloride was added as a releasing agent to a concentration of 1.5g/L. Solutions were vigorously shaken few seconds prior to the analysis to avoid concentration gradients. It was noticed that solution diluted more than twice, not properly shaken or that targeted different portions of the calibration curves (although always in the central portion of the linear part of the curve) had to be discarded because they showed poor repeatability between replicates and poor coherence between 28- and 182-day analyses of the same mixture.

$[OH^-]$ was calculated by electroneutrality according to Equation 1.

$$[OH^-] \approx [Na^+] + [K^+] \qquad \text{Equation 1}$$

## 8.4 Results

### 8.4.1 Expansion of Concrete Prisms

Figure 8.3 illustrates the expansion over 104 weeks for concrete prisms made with cement C2, with and without addition of NaOH, a GG content between 15% and 30% and a BFS content ranging from 20 to 40%. The results show that, with the highly-reactive Spratt aggregate, ternary mixtures incorporating only 20% of BFS (and 10 to 20% GG) could not meet the 0.040% expansion limit suggested by CSA A23.2-28A for "non-reactive systems". Interestingly, when 20% BFS is used, increasing the GG content from 10 to 20% results in an expansion reduction; also, adding NaOH to raise the alkali content to 1.25% $Na_2O$eq per cement mass (as requested by CSA Standard Practice A23.2-28A) results in expansions lower (20% GG) or equal (10% GG) to that of unboosted mixtures.

In this study, most mixtures incorporating 30BFS were "boosted" to 1.25% or 1.08% $Na_2O$eq and their 104-week expansions are clustered around the 0.040% limit. Concrete prisms incorporating 40% BFS expanded either above (unboosted) or below (boosted) the 104-week 0.040% expansion limit. Unlike mixtures incorporating 20% BFS, the GG addition seemed to enhance the expansion of specimens containing 40% BFS, (i.e. expansion of 20GG-40BFS-0.94 is greater than 10GG-40BFS-0.94).

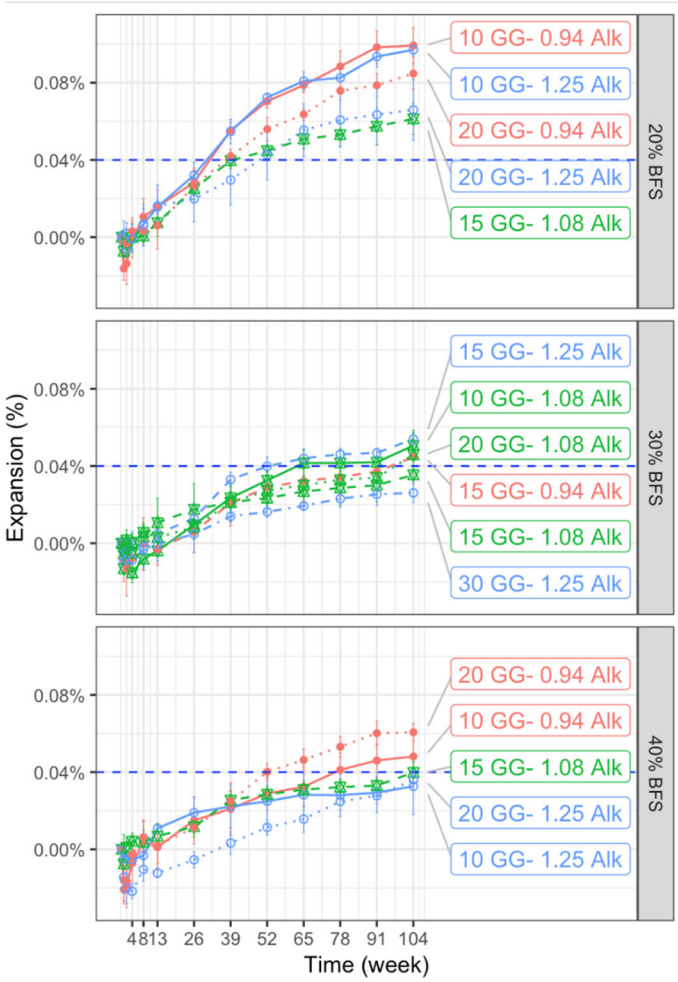


**Figure 8.3: Expansion over two years of boosted and unboosted concrete prisms incorporating various amounts of GG and BFS. Each data point represents the average expansion of four prisms along with the standard variation presented by the error bar.**

### 8.4.2 Pore Solution Composition

Figure 8.4 shows the [$Na^+$] in the pore solution of low- to high-alkali ternary paste specimens after 182 days of storage at 38°C. The [$Na^+$] is generally increasing with increasing $Na_2Oeq$ content in the paste, while higher dosages of BFS resulted in lower [$Na^+$] in the pore solution. Interestingly, higher BFS contents are associated with a relatively lower sensitivity of [$Na^+$] to the increasing $Na_2Oeq$ content in the system.

Also, for the GG parameter and at a given alkali and BFS content in the system, the impact on [$Na^+$] associated with a 5% GG increment ranges between a 4% reduction and a 28% increase. The average impact of 5% GG increment is 8% (≈25 mmol/L) increase of [$Na^+$] in the pore solution; this suggests that GG releases a part of its sodium content to the pore solution. On the other hand, 10% increments of BFS are associated to a [$Na^+$] reduction ranging between 4% and 34%, with an average reduction of 17%.

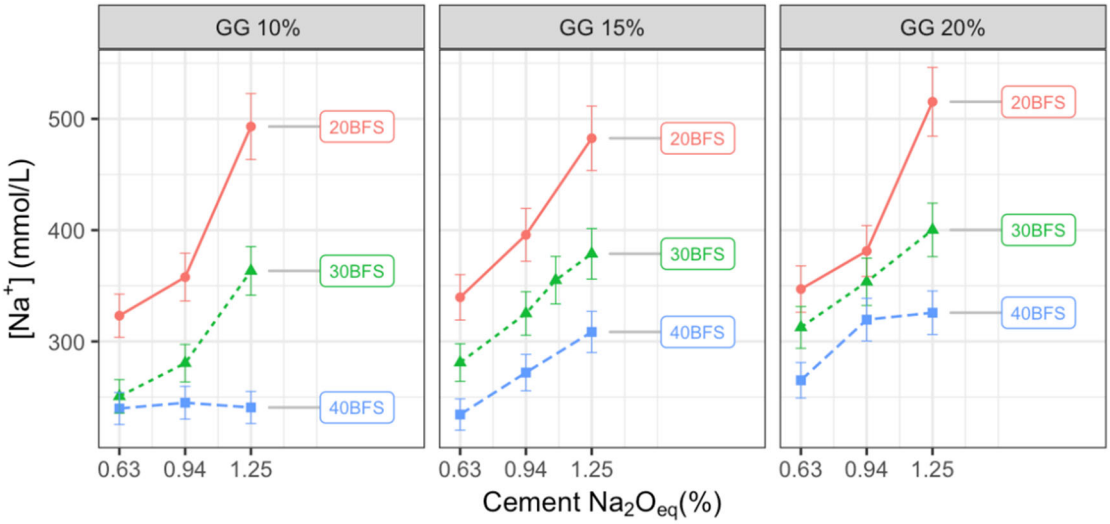


**Figure 8.4 : [$Na^+$] at 182 days in the pore solution of paste specimens incorporating various amounts of GG and BFS, and made with cements of various $Na_2O_{eq}$ contents.**

Figure 8.5 shows the [$K^+$] in the pore solution of low- to high-alkali ternary paste specimens after 182 days of storage at 38°C. The data show that the [$K^+$] is reduced by increasing the BFS content, and that when only 10% GG is used, the impact on the [$K^+$] of cement replacement by BFS is greater.

The average reduction of [$K^+$] associated to an increase in GG content of 10 to 20% is 24% (reductions ranging from 7 to 36%) and the average [$K^+$] reduction associated to BFS increment from 20 to 40% is 39% (ranging from 28 to 55%); this suggests that replacing OPC by both SCMs lowers the potassium content in the pore solution. The constant pessimum value of [$K^+$] observed for the unboosted high-alkali pastes using cement C2 (0.94 $Na_2O_{eq}$) is worth noting and suggests that the addition of NaOH reduces [$K^+$] in the pore solution.

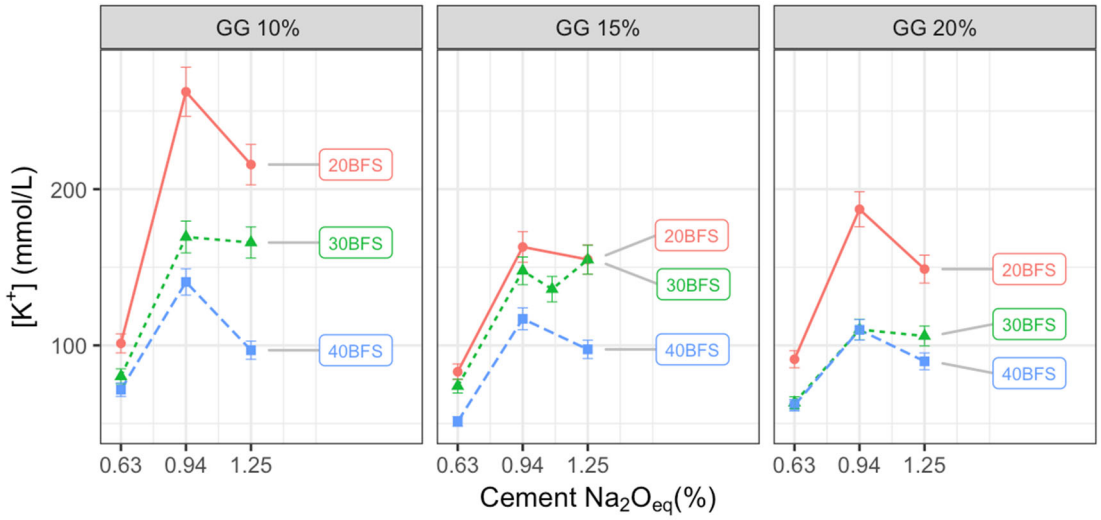


**Figure 8.5: [$K^+$] at 182 days in the pore solution of paste specimens incorporating various amounts of GG and BFS, and made with cements of various $Na_2O_{eq}$ content.**

## 8.5 Discussion

Several studies successfully used data from the chemical analysis of pore solutions extracted from paste specimens at different ages for better understanding and for modelling the beneficial effect of SCMs to control concrete prism expansions due to ASR (Thomas et al. 2013). Regarding the effect of time on the pore solution composition in paste specimens, Vollpracht et al. (2015) showed that the [$K^+$] and [$Na^+$] obtained from pastes (0.50 w/b) incorporating 20 to 40% BFS were reasonably stabilized after about 100 days. Duchesne and Bérubé (1994) and Shehata and Thomas (2002) also showed that only little variations in the [$K^+ + Na^+$] in the pore solution of pastes made with various contents of different FA were obtained after 100 days. It is important to note, however, that changes in the pore solution related to progressive alkali binding by reactive siliceous phases and the secondary reaction products in concrete are not accounted for in the case of paste specimens.

### 8.5.1 Relation Between the Paste and Concrete Specimens

Figure 8.6 presents the relationship between the two-year concrete prism expansions and the [$K^+$] in the pore solution of paste specimens aged 182 days for various mixtures incorporating different levels of GG, BFS, and $Na_2Oeq$ content of cement. Ternary concrete mixtures incorporating 20% BFS showed the highest concrete prism expansions and the highest [$K^+$] in their companion paste specimens. It is expected that mixtures with only 20% of BFS show higher [$K^+$] since there is more cement in those mixtures and cement has a high $K_2O$ content compared to BFS or GG (Table 8.1). However, mixtures incorporating 30% BFS do not necessarily show higher [$K^+$] compared to those with 40% BFS, which suggests that dilution is not the only phenomenon that can reduce [$K^+$] in the pore solution. If the exact mechanism by which [$K^+$] is reduced cannot be isolated, Figure 8.6 suggests that what reduces [$K^+$] also results in expansion reduction. Actually, the relationship is fairly linear with a coefficient of determination $R^2$ of 0.81. According to the regression equation, mixtures with [$K^+$] below about 120 mmol/L at 182 days are likely to show two-year expansions below 0.040%.

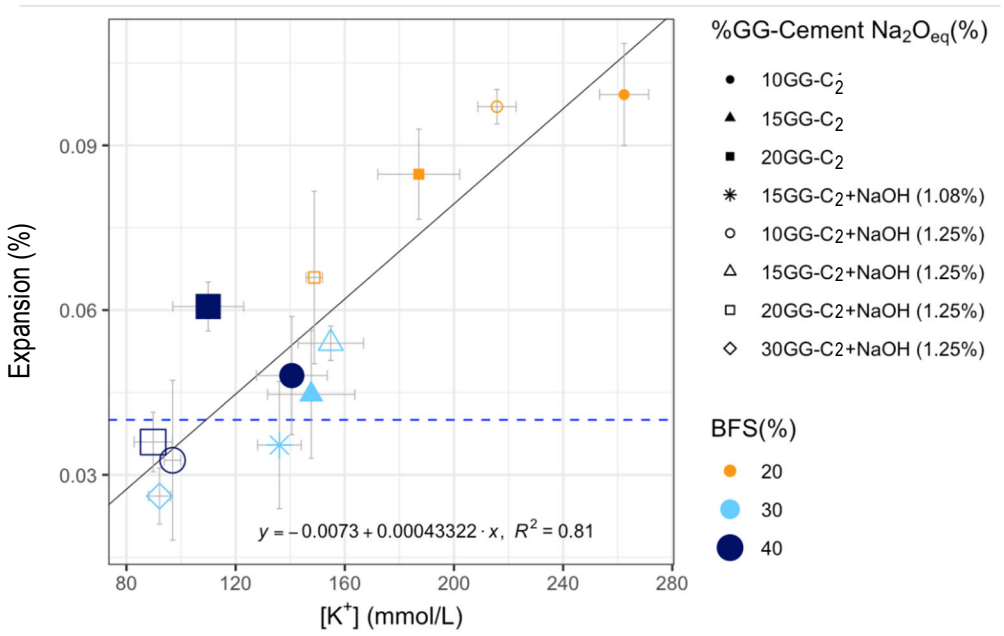


**Figure 8.6: Relationship between the 104-week concrete prism expansions and the [$K^+$] in the pore solution of paste specimens after 182 days of storage at 38°C. The solid line is the equation corresponding to the regression of this linear relation.**

Figure 8.7 presents the relationship between the [$Na^+$] in the pore solution at 182 days and the 104-week concrete prism expansions. Data are clearly more scattered and no linear relationship between these two parameters was detected. The [$Na^+$] in the pore solution can however be grouped as highlighted hereafter: 1) 500 ± 40 mmol/l, 2) 360 ± 50 mmol/L and 3) 245 ± 15 mmol/L.

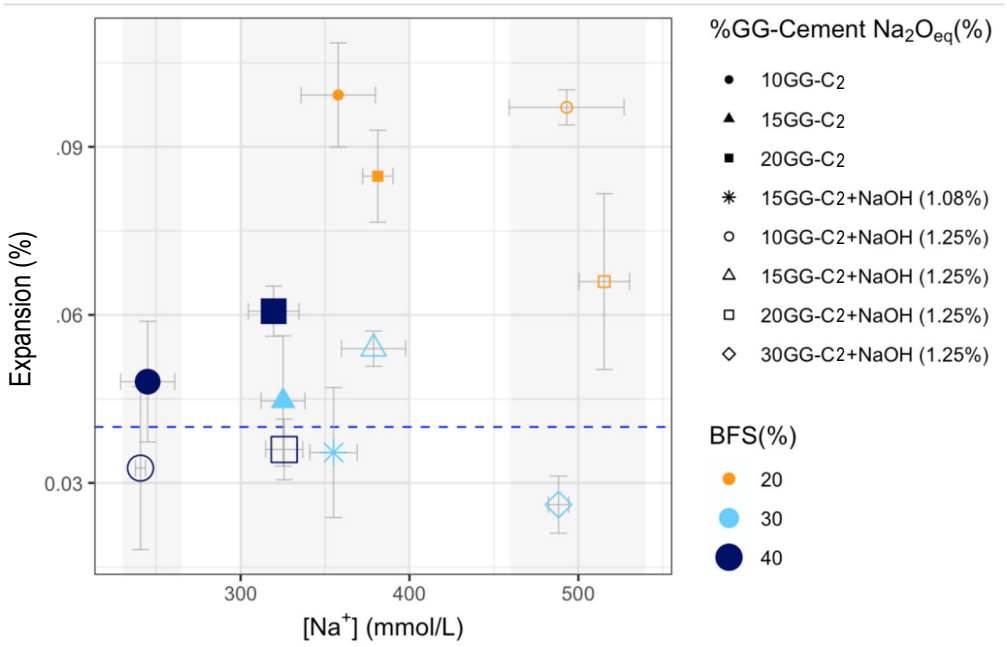


**Figure 8.7: Relationship between the 104-week concrete prism expansions and the [$Na^+$] in the pore solution of paste specimens aged 182 days.**

When the chemical data are used, according to Equation 1, to calculate the [$OH^-$] by electroneutrality, three lines can be "constructed" on Figure 8.8 by using the equation of Figure 8.6 (related to [$K^+$]) and transposing it by the mean value of the group presented in

Figure 8.7 (related to [$Na^+$] (i.e. 500, 350 and 245 mmol/l)). Scattering of the data in Figure 8.7 shows that [$OH^-$] is somewhat poorly correlated to the 104-week expansions of the ternary systems evaluated in this study; however, when [$OH^-$] are grouped according to [$Na^+$], the data are fitting according to the relationship observed for [$K^+$]. This suggests that for ternary mixtures incorporating GG and BFS, high pH (or high [$OH^-$]) is not necessarily the best predictor of the expansion, but better prediction can be achieved through the use of [$K^+$] in the pore solution. This reinforces the importance to differentiate alkali species when predicting concrete prism expansion. Indeed, grouping the latter two anions into $Na_2Oeq$ is a risk of obtaining misleading prediction (or lack of prediction) regarding expansion of concrete specimens.

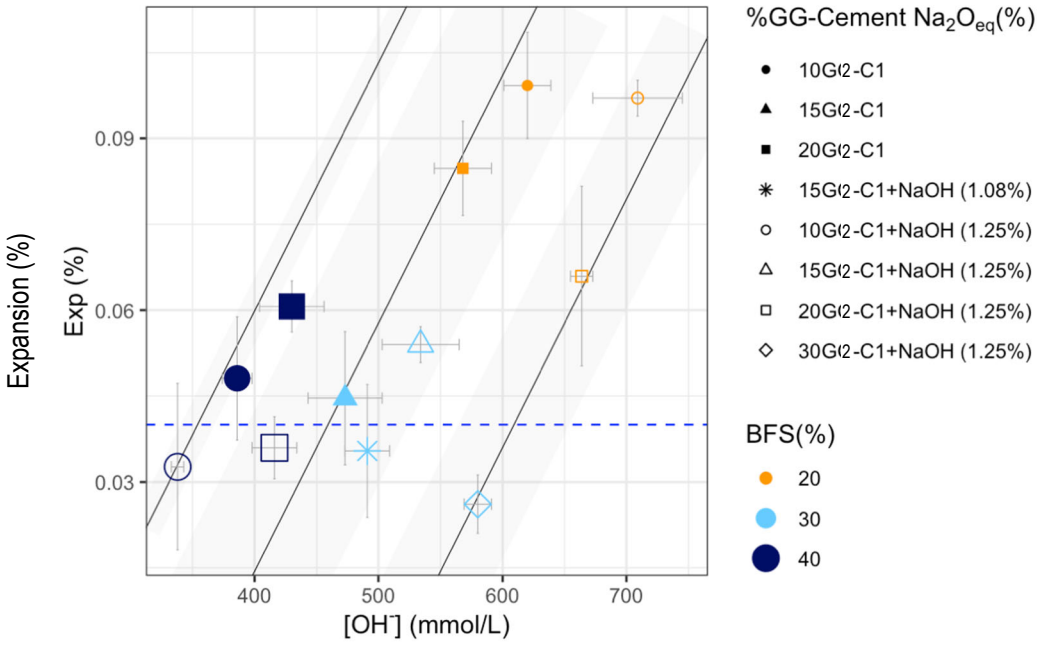


**Figure 8.8: Relationship between the 104-week concrete prism expansions and the [$OH^-$] of the pore solution of paste specimens after 182 days of storage at 38°C. The concentrations are classified in three groups. The boundaries are defined by the equation of Figure 8.6, which is y=-0.0073+0.000443322x, translated and enlarged according to the groups of Advisable Caveat on the Presumed Relationship Between Concrete Expansion and [$K^+$] of the Pore Solution**

The $K_2O$ contents of cement C2, GG, and BFS are 1.05%, 0.66% and 0.36%, respectively. Since the cement is likely the main source of potassium to the pore solution and considering that the [$K^+$] in the pore solution was found to be reasonably correlated to the 104-week concrete prism expansions, it is worth questioning if the low [$K^+$] in the pore solution of pastes, corresponding to low-expansion of ternary concrete systems, can simply be related to a bear cement reduction. For this purpose, Figure 8.9 presents the relationship between the 104-week concrete prism expansions and the cement content in the various ternary mixtures investigated. The data suggest that an expansion reduction is indeed somewhat resulting from a reduction in cement content in the

cementitious system (coefficient of determination $R^2$ of 0.64). However, it appears that the relationship between expansion and cement content is not as strong as that between expansion and [$K^+$]. This supports the hypothesis that the presence of potassium ions in the pore solution is *per se* an early indicator of the amplitude of the expansion of concrete prisms of similar mixture proportioning (for instance incorporating BFS and GG in this study). It is also interesting to note that for a given cement contents, the NaOH addition (as prescribed in CSA standard practice A23.2-28A) results, in most cases, in reduced expansion compared to a companion "unboosted" mixture.

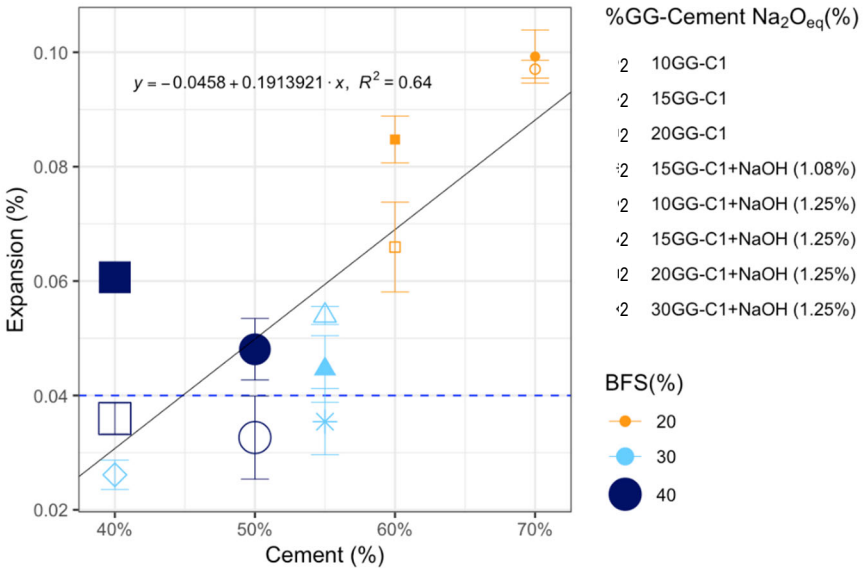


**Figure 8.9: Relationship between concrete prism expansion measured at 104 weeks and the percentage of cement content by GG and BFS.**

## 8.5.2 Influence of NaOH on [$Na^+$], [$K^+$] and Expansion

The impact of NaOH addition is highlighted in Figure 8.10 where the [$Na^+$] and [$K^+$] in the pore solution of different paste mixtures are compared. The effect of NaOH addition on [$K^+$] in the pore solution is always in the same direction. For instance, for mixture 20% BFS, NaOH addition leads to increased [$Na^+$] and decreased [$K^+$]; for mixture 40% BFS, NaOH addition leads to insignificant changes in [$Na^+$], but decreased [$K^+$].

The data reported in Figure 8.3 also suggests that NaOH addition also significantly reduced the expansion of mixtures incorporating 40% BFS, while Figure 8.10 suggests that for this mixture, NaOH addition almost only reduced [$K^+$] (no significant changes of [$Na^+$]). This, again, strengthens the hypothesis that [$K^+$] is the most influential species in solution to predict the 104-week expansions in the ternary systems investigated, and also that higher [$K^+$] in the pore solution of mixtures showing higher concrete prism expansions is not an artefact due

to cement replacement but an indicator of the chemical reaction involved. In accordance with the latter statement, Hou et al. (2004) suggested that ASR reaction products appear faster in cementitious pastes containing Vycor glass,(96% silica and 4% Boron) KOH and $Ca(OH)_2$ compared to those made with NaOH.

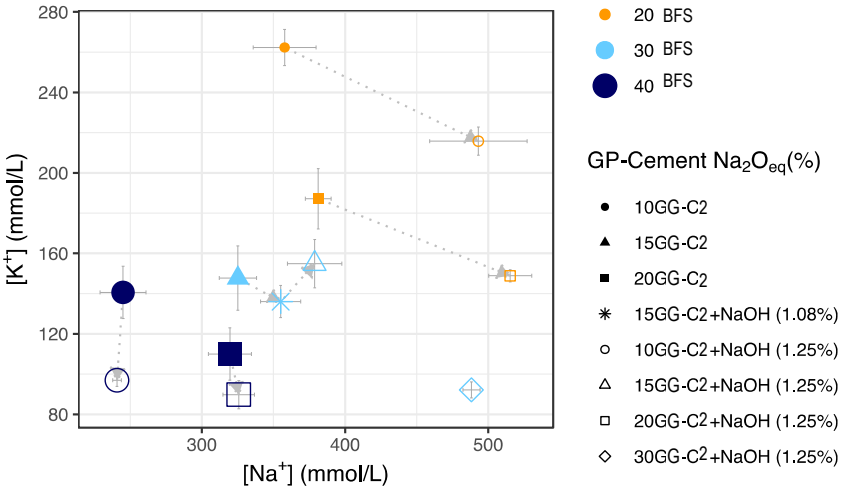


**Figure 8.10: Impact of NaOH addition on the [$Na^+$] and [$K^+$] in the pore solution of paste specimens, as represented by an arrow between C2 (0.94% $Na_2Oeq$) and C2 +NaOH (1.25% $Na_2Oeq$) for a given combination GG/BFS.**

Figure 8.11 presents the expansion of the concrete mixtures (bar chart) and the [$Na^+$] of the corresponding cementitious pastes (dots) grouped by NaOH addition. For most mixtures with NaOH addition, higher [$Na^+$] in the pore solution of paste specimens are related to higher concrete prism expansion; however, this relation does not seem to apply to mixtures without NaOH addition. Actually, mixtures with higher content of GG are not systematically related to higher [$Na^+$] nor higher expansions. This suggests that the sodium content of GG is not fully available into the pore solution and probably did not precipitate into ASR products since higher expansions are not associated to higher GG content.

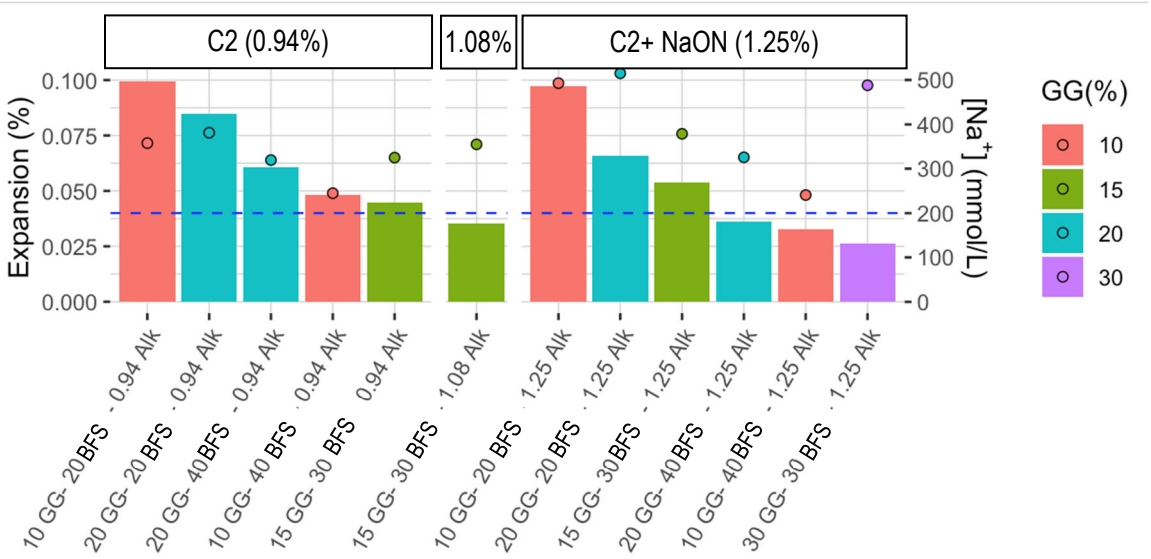


**Figure 8.11: 104-week concrete prism expansions (bar chart) and the [$Na^+$] in the pore solution of paste specimens (dots) after 182 days of storage at 38°C. The dashed line is the 0.04% limit of CSA 23.2-28A.**

## 8.6 Conclusion

In a context in which the expansive behaviour of concrete prisms incorporating ground glass (GG) and reactive coarse aggregates is unpredictable in binary mixtures and even more in ternary mixtures, a better understanding of the factors influencing ASR was required. In this study, 10 to 20% GG were combined to 20 to 40% BFS to replace OPC having various $Na_2O_{eq}$ contents. Concrete prisms, 100 x 100 x 300 mm in size, were stored at 38°C and 100% RH and their length change periodically monitored up to 104 weeks. Paste mixtures of identical cementitious material contents were poured in sealed containers and conditioned at 38°C for 182 days before their pore solution was extracted under pressure and their [$Na^+$] and [$K^+$] analyzed with a flame spectrophotometer.

The result obtained in this study suggest that the expansion at 104 weeks of the mixtures analysed is correlated to the [$K^+$] in the pore solution of paste samples aged 182 days of the same mix designs. The [$K^+$] in the pore solution is lowered by reducing the cement proportion in the mix, but also by adding NaOH to the mixture. Actually, the impact of NaOH addition is indeed similar on [$K^+$] of pore solution of paste samples that it is on the expansion of concrete prisms. A wide range of concrete prism expansions were observed for similar [$Na^+$] of paste samples for various mixtures, suggesting that, in mixtures incorporating GG and BFS, the presence of Na ions in the pore solution is not a good indication of the expansion behavior of a given mixture. Concerning the relationship between the expansion and the [$OH^-$] of the pore solution estimated by electroneutrality, no obvious relationship was observed. Actually, the relationship between [$K^+$] and the expansion supersedes that between [$OH^-$] and the expansion.

## 8.7 References


Afshinnia, K. and P. R. Rangaraju (2015). "Efficiency of ternary blends containing fine glass powder in mitigatingalkali–silica reaction." Construction and Building Materials **100**(15): 234–245.

Association, G. C. a. C. (2019). GCCA Sustainability Guidelines for co-processing fuels and raw materials in cement manufacturing. Sustainability Charter and Guidelines, Global Cement and Concrete Association.

Du, H. and K. H. Tan (2017). "Properties of high volume glass powder concrete." Cement and Concrete Composites **75**: 22-29.

Duchesne, J. and M. A. Bérubé (1994). "The effectiveness of supplementary cementing materials in suppressing expansion due to ASR: Another look at the reaction mechanisms part 2: Pore solution chemistry." Cement and Concrete Research **24**(2): 221-230.

Golafshani, E. M. and A. Behnood (2019). "Estimating the optimal mix design of silica fume concrete using biogeography-based programming." Cement and Concrete Composites **96**: 95-105.

Hou, X., L. J. Struble and R. J. Kirkpatrick (2004). "Formation of ASR gel and the roles of C-S-H and portlandite." Cement and Concrete Research **34**(9): 1683-1696.

Idir, R., M. Cyr and A. Tagnit-Hamou (2010). "Use of fine glass as ASR inhibitor in glass aggregate mortars." Construction and Building Materials **24**(7): 1309-1312.

Lafrenière, C. (2017). "Évaluation du comportement en durabilité de nouvelles matrices cimentaires pour l'obtention de bétons respectueux de l'environnement". Master, Université Laval, https://corpus.ulaval.ca/jspui/handle/20.500.11794/27591.

Lane, D. S. and C. Ozyildirim (1999). "Preventive measures for alkali-silica reactions (binary and ternary systems)." Cement and Concrete Research **29**(8): 1281-1288.

Lindgård, J., M. D. A. Thomas, E. J. Sellevold, B. Pedersen, Ö. Andiç-Çakır, H. Justnes and T. F. Rønning (2013). "Alkali–silica reaction (ASR)—performance testing: Influence of specimen pre-treatment, exposure conditions and prism size on alkali leaching and prism expansion." Cement and Concrete Research **53**(0): 68-90.

Maraghechi, H., S. Salwocki and F. Rajabipour (2017). "Utilisation of alkali activated glass powder in binary mixtures with Portland cement, slag, fly ash and hydrated lime." Materials and Structures **50**(1): 16.

Rehman, S., S. Iqbal and A. Ali (2018). "Combined influence of glass powder and granular steel slag on fresh and mechanical properties of self-compacting concrete." Construction and Building Materials **178**: 153-160.

Rodier, L. and H. Savastano (2018). "Use of glass powder residue for the elaboration of eco-efficient cementitious materials." Journal of Cleaner Production **184**: 333-341.

Shehata, M. H. and M. D. A. Thomas (2002). "Use of ternary blends containing silica fume and fly ash to suppress expansion due to alkali–silica reaction in concrete." Cement and Concrete Research **32**(3): 341-349.

Thomas, M. D. A., B. Fournier and K. J. Folliard (2013). "Alkali-Aggregate Reactivity (AAR) Facts Book 212.

Vance, K., A. Kumar, G. Sant and N. Neithalath (2013). "The rheological properties of ternary binders containing Portland cement, limestone, and metakaolin or fly ash." Cement and Concrete Research **52**: 196-207.

Vollpracht, A., B. Lothenbach, R. Snellings and J. Haufe (2015). "The pore solution of blended cements: a review." Materials and Structures **49**(8): 3341-3367.

Wu, Z., K. H. Khayat and C. Shi (2019). "Changes in rheology and mechanical properties of ultra-high performance concrete with silica fume content." Cement and Concrete Research **123**.

Zhang, L. and Y. Yue (2018). "Influence of waste glass powder usage on the properties of alkali-activated slag mortars based on response surface methodology." Construction and Building Materials **181**: 527-534.

Zhang, S., A. Keulen, K. Arbi and G. Ye (2017). "Waste glass as partial mineral precursor in alkali-activated slag/fly ash system." Cement and Concrete Research **102**: 29-40.

Zidol, A. (2009). "Optimisation de la finesse de la poudre de verre dans les systèmes cimentaires binaires". PhD Thesis, Université de Sherbrooke, http://savoirs.usherbrooke.ca/handle/11143/1564.

# General Conclusion

Previous research has shown that higher concentrations of alkali species in the cement lead to higher pH in the pore solution of pastes, mortars or concretes, which in turn lead to the attack of the reactive siliceous phases in fine/coarse aggregates. On the other hand, the dissolution of silica also results in a reduction in the pH of the pore solution of cementitious systems, which is the mechanism by which many SCMs are taught to reduce/prevent deleterious expansion due to ASR. Pozzolanic reactions indeed lead to C-S-H of lower C/S, which is known to uptake a larger proportion of alkalis from the pore solution, thus contributing at lowering the pH. Other researches also showed that greater uptake of alkalis by C-S-H and C-A-S-H is related to lower concentrations of alkalis in the pore solution. Those last studies surely helped to better understand how materials like SCMs contribute at preventing ASR, but limited information exists regarding the combined effects of high-alkali SCMs, especially in ternary systems, on the pore solution chemistry and the expansion of concrete test specimens incorporating reactive aggregates.

Ground glass (GG) from recycling facilities has long been a somewhat controversial SCM because of its high sodic content that is suspected of fueling expansion due to ASR. If some research works agreed that coarse glass aggregates often act as reactive aggregates, numerous studies claim that finely ground glass behave differently. More specifically, GG has shown to exhibit pozzolanic properties in concrete (higher long-term compressive strengths, lower Ca/Si of C-S-H, etc.). When evaluated through the Concrete Prism Test (CPT), binary mixtures incorporating 10 to 30% GG (as replacement by mass of a high-alkali control cement) and highly-reactive aggregates show expansions lower than the control mixture but expansions that remain higher than the 0.040% limit for acceptance in CSA Standard Practice A23.2-28A. It remains unclear to what extent the high sodic content of GG will be released into the pore solution to initiate and/or maintain ASR, and to what extent the hydrates (such as high Ca/Si C-S-H or C-A-S-H) can uptake high amounts of alkalis and prevent harmful expansion of the test specimens. To have a clearer view of the behaviour of alkalis from GG into concrete, the present research work included the production and testing of concrete and paste specimens.

First, binary and ternary concrete specimens were made, with and without NaOH addition, to reach $Na_2Oeq$ ranging from 0.94% (high alkali ordinary portland cement - OPC) to 1.25% (OPC + NaOH addition). As per CSA Standard Practice A23.2-28A, specimens were stored at 38°C and regularly measured for up to two years. As a precaution against alkali leaching, the cross section of the test specimens was modified from 75mm x 75mm to 100mm x 100mm and measurements were taken with prisms "still hot" (38°C) to avoid condensation runoff that occurs when prisms are cooled to 23°C. Test specimens incorporating either SF or MK had a GG content ranging from 10 to 30%, while SF varied from 5 to 10% and MK from 5 to 15%. The specimens incorporating either FA or BFS had GG contents between 10 and 20%, while FA content ranged between 15 and 30% and BFS content between 20 and 40%. The proportion of the SCMs was chosen according to a *Face Centered Central Composite Design* (FCCD) experimental plan.

The second type of specimens used in this study consisted of ternary cementitious pastes that were stored at 38°C for a period up to six months. The pore solution of those specimens was extracted under pressure and analysed with an atomic absorption spectrophotometer for $Na^+$ and $K^+$ contents. The cementitious pastes had $Na_2Oeq$ contents ranging from 0.63% (OPC) and 1.25% (i.e. 0.63%, 0.94%, 0.94% + NaOH to reach 1.08 or 1.25%), while the range of cement replacements by GG, SF, MK, FA and BFS was identical to those in the concrete samples. The experimental plan for the paste specimens followed a complete factorial design and the data collected resulted in a surface response that describe the impact of each of the materials in the systems.

The results of the paste specimens' analyses suggest that the composition of the pore solution is not as strongly influenced by GG addition as it would be expected from its high sodic content (about 13% $Na_2Oeq$); also, the $Na_2Oeq$ content of the cement or the addition of NaOH to the system actually modulate the release of sodium ions from GG into solution. For instance, in the case of ternary pastes incorporating SF or MK and a low alkali cement (0.63% of $Na_2Oeq$), raising the GG content from 10 to 30% resulted in an average increase of 67% in the $[Na^+]$ of the pore solution of those pastes. The same increase in GG contents (10 to 30%) for companion pastes made this time with a cement with $Na_2O_{eq}$ content of 0.94% or made with the above cement with added NaOH (to reach 1.25% of $Na_2Oeq$), resulted in an average increase of 102% in the $Na_2Oeq$ in the blend but only 10% increase in $[Na^+]$ in the pore solution.

Greater contents of GG are also associated to lower $[K^+]$ in the pore solution. Once again, the $Na_2Oeq$ content of the cementitious pastes impacts the effect of GG on the pore solution composition since increments of GG (e.g. 10 to 20% and 20 to 30%) are associated to lower $[K^+]$ (especially for pastes with added NaOH). The analysis of the data suggests that the dilution of the potassium-rich cement partially explains the reduction in $[K^+]$ in the pore solution, but other phenomena (such as alkali uptake by the hydrates) also contribute to the observed $[K^+]$ decline.

When summing [$Na^+$] and [$K^+$] to estimate [$OH^-$] of the pore solutions, the results suggest that the GG content has very little influence on [$OH^-$]. What influence the most the [$OH^-$] is rather the content of other SCMs used in the systems analyses, i.e. SF, MK, FA and BFS (inversely correlated) and the $Na_2O$eq content of the cement (directly correlated). In all cases, the impact of GG in raising [$Na^+$] or [$OH^-$] can be counteracted by the use of the other SCMs, e.g : 2.5% SF can counteract the $Na^+$ release of 20% GG. It also worth mentioning that the increase in [$Na^+$] associated to an increase in GG content in the system is somehow masked by NaOH addition used for evaluating the effectiveness of SCMs to prevent ASR in the laboratory in accordance with CSA Standard Practice A23.2-28A (and other similar protocols around the world).

When considering the expansion of concrete specimens subjected to accelerated testing under laboratory conditions (i.e. 38°C and R.H. > 95%), the data suggest that NaOH addition generally enhances the beneficial impact (i.e. pozzolanic activation) of GG in reducing the expansion due to ASR. For instance, the "severity" of the test (i.e. when compared to companion mixtures without NaOH addition) is reduced by NaOH addition for 13/19 mixtures, and increased for 6/19 mixtures. However, for the systems investigated in this study, the NaOH addition rarely influenced the expansion levels obtained to the point that a mix design with NaOH passes the test but failed without NaOH addition. The results obtained in this study showed that GG does not enhance expansion due to ASR in the presence of the highly-reactive Spratt aggregate, both in binary and ternary systems. On the contrary, GG use was found to result in significant expansion reductions and this reduction was enough to meet the 0.040% expansion limit in the case of several of the ternary systems investigated (from 10 to 110%). Unfortunately, the overall expansion reduction potential did not reveal any linear trend, each combination of GG and SF/MK/FA/BFS showing somewhat different behaviors/trends. Hence, GG could be considered similarly to a high alkali FA in the CSA Standard Practice A23.2-27A, which states that a mix design incorporating GG and reactive aggregate (binary or ternary) could be permitted for use in field applications only after satisfying the requirements of performance testing under the auspices of CSA Standard Practice A23,2-28A (expansion below 0.040% at two years). Alternatively, a table with minimal SF, MK, FA and BFS dosages in concrete systems incorporating various contents of GG (10 to 30%) is suggested for designing ternary mixtures incorporating GG and (highly) reactive aggregates. This table was built according to the experimental results presented in this research work. The recommendation are based on the 0.040% limit that correspond to the actual acceptance limite at the time the work was done. Further work is needed to reconsider the limit with less commons test methods and mixtures used in this work.

It is often assumed that pozzolanic materials tend to lower the pH of the pore solution, which limits the dissolution of silica and the production of ASR gel. However, results collected on ternary mixtures incorporating pozzolanic material such as (high-alkali) GG and either SF, MK, FA and BFS, a highly-reactive reactive aggregate and cements of various $Na_2O$eq contents suggest that this rule cannot be simply assumed. For several cementitious

mixtures/systems, the alkalinity of the pore solution of the cementitious pastes investigated (at 182 days) was found to be poorly correlated with the expansion of concrete specimens. For instance, it has been observed that, while NaOH addition enhances [$OH^-$], it reduces concrete prism expansions. This supports the hypothesis that the composition of pore solution is mirrored in the composition of the C-S-H (or C-A-S-H) in the "hydrated" cementitious blends and if the pore solution is punctually concentrated in alkali species, the "pozzolanic" C-S-H would uptake more cations thus lowering their concentration into the pore solution without the production of ASR gel.

Previous research on the chemistry of pore solution of OPC paste systems suggested that the [$OH^-$] is proportional to the $Na_2O_{eq}$ of cement. Despite cases of pessimum effects, the expansion of concrete prisms incorporating reactive aggregates was also found to increase with increasing total alkali content in the concrete. Recent works on binary or ternary mixture incorporating SCMs such as (high alkali) GG, SF, MK, FA and BFS suggested that the expansion in such systems are ruled by hydration processes and ASR, but other reactions such as pozzolanic or alkali activation can also play a role in the behavior observed. Indeed, several hydrates can be formed at a given time according to the local concentration of various species such as $Na^+$, $K^+$, $OH^-$, while the impact of some other ionic species such as $SO_4^{2-}$ or $Al^{3+}$ should not be neglected. These hydrates will influence at the same time the long-term release of chemical species, but also their uptake into the (solid) hydrates. This could explain why the high sodic content of GG is not simply released into the pore solution to simply initiate ASR in the presence of reactive aggregate; more work is needed to confirm such hypotheses.

**Further work**

Some basic information on the chemical "stability" of the GG could be obtained from dissolution work of GG specimens of different composition and in different alkaline solutions (NaOH/KOH, different concentrations, in the presence or not of $Ca(OH)_2$). Also, now that we know that the alkalis from GG were only scarcely released into solution of the various ternary systems selected, microstructural work involving the statistical quantitative analyses of the composition of the solid phases in those paste systems analysed would be very useful to better understand and confirm the results obtained from the pore solution work. It would also be appropriate to examine petrographically several of the concrete prisms showing various levels of expansion to confirm the presence of alkali-silica reaction products in those specimens. Additionally, a complete factorial experimental plan for the concrete specimens is worth considering in order to build more sophisticated trend relating the mixture design and the behavior towards ASR of ternary concrete mixture incorporating GG and reactive aggregates.

In this study, the ternary systems selected were evaluated in the presence of a highly-reactive aggregate, i.e. the Spratt limestone. It would be interesting to evaluate the expansive behavior of a selection of binary and ternary systems when incorporating moderately/marginally-reactive aggregates to determine if the proposed recommendations for minimum SCM contents in combination with GG could be "relaxed" in the presence of less reactive aggregates. Further work is also needed to confirm the impact of the cement alkali content in binary and ternary blends incorporating GG in view of providing robust recommendations for the safe use of GG in concrete incorporating a range of reactive aggregates.

# References


(2003). "Nobel Price in chemistry 2003." Retrieved June 29th 2022, from : https://www.nobelprize.org/prizes/chemistry/2003/summary/

(GCCA) GCCA (2017) Get Numbers Right (GNR). https://gccassociation.org/gnr/. 2020

(OECD) OfEC-oaD, (IEA) IEA (2007) Tracking Industrial Energy Efficiency and CO2 Emissions. International Energy Agency 34 (2):1-12

(WBCSD), W. B. C. f. S. D. (2018). "Technology Roadmap: Low-Carbon Transition in the Cement Industry." Retrieved january 4, 2019, 2018, from https://www.wbcsd.org/Sector-Projects/Cement-Sustainability-Initiative/Resources/Technology-Roadmap-Low-Carbon-Transition-in-the-Cement-Industry.

Afshinnia K, Rangaraju PR (2015) Efficiency of ternary blends containing fine glass powder in mitigatingalkali–silica reaction. Construction and Building Materials 100 (15):234–245

Afshinnia K, Rangaraju PR (2015) Mitigating alkali-silica reaction in concrete: Effectiveness of ground glass powder from recycled glass. Transportation Research Record 2508:65-72. doi:10.3141/2508-08

Afshinnia, K. and P. R. Rangaraju (2015). "Efficiency of ternary blends containing fine glass powder in mitigating alkali–silica reaction." Construction and Building Materials 100(15): 234–245.

Afshinnia, K. and P. R. Rangaraju (2015). "Influence of fineness of ground recycled glass on mitigation of alkali–silica reaction in mortars." Construction and Building Materials **81**: 257-267.

Afshinnia, K. and P. R. Rangaraju (2015). "Mitigating alkali-silica reaction in concrete: Effectiveness of ground glass powder from recycled glass." Transportation Research Record **2508**: 65-72.

Aggregate Reaction in Concrete, Kyoto, Japan.

Allen, N., M. L. Machesky, D. J. Wesolowski and N. Kabengi (2017). "Calorimetric study of alkali and alkaline-earth cation adsorption and exchange at the quartz-solution interface." Journal of Colloid and Interface Science **504**: 538-548.

Association, G. C. a. C. (2019). GCCA Sustainability Guidelines for co-processing fuels and raw materials in cement manufacturing. Sustainability Charter and Guidelines, Global Cement and Concrete Association.

ASTM (2014). Standard guide for reducing the risk of deleterious alkali–aggregate reaction in concrete (ASTM C 1778-14). ASTM International, West Conshohocken, PA, USA.

ASTM C-1260 (2014). Standard Test Method for Potential Alkali Reactivity of Aggregates (Mortar-Bar Method). ASTM International, West Conshohocken, PA, USA.

ASTM C1567 (2021). Standard Test Method for Determining the Potential Alkali-Silica Reactivity of Combinations of Cementitious Materials and Aggregate (Accelerated Mortar-Bar Method). ASTM International, West Conshohocken, PA, USA.

Barnes, B., S. Diamond and W. Dolch (1978). "The contact zone between Portland cement paste and glass “aggregate” surfaces." Cement and Concrete Research **8**(2): 233-243.
Bérubé, M.-A., B. Durand, D. Vézina and B. Fournier (2000). "Alkali-aggregate reactivity in Quebec (Canada)." Canadian Journal of Civil Engineering **27**(2): 226-245.

Bleszynski, R. (2002). “The performance and durability of concrete with ternary blendsof silica fume and blastfurnace slag”. PhD thesis, University of Toronto.
Brown, P. W. (1990). "The System Na2O-CaO-SiO2-H2O." Journal of the American Ceramic Society **73**(11): 3457-3461.

Bussière, I. (2013). Usine de recyclage ferme□e une montagne de verre prend la poussie□re. . Québec, Le Soleil. **2020**.

Carles-Gibergues, A., M. Cyr, M. Moisson and E. Ringot (2008). "A simple way to mitigate alkali-silica reaction." Materials and Structures **41**(1): 73-83.

Carsana, M., M. Frassoni and L. Bertolini (2014). "Comparison of ground waste glass with other supplementary cementitious materials." Cement and Concrete Composites 45 (Supplement C): 39-45.

Cementitious materials compendium A 3000-18. CSA Group, Mississauga, Ontario, Canada, 257p..

Chappex, T. and K. L. Scrivener (2013). "The effect of aluminum in solution on the dissolution of amorphous silica and its relation to cementitious systems." Journal of the American Ceramic Society **96**(2): 592-597.

Charles (2013). Dur coup pour le recyclage du verre. LaPresse. Montréal.

Chen Z, Poon CS (2017) Comparing the use of sewage sludge ash and glass powder in cement mortars. Environmental Technology 38 (11):1390-1398. doi:10.1080/09593330.2016.1230652

Chen, Z. and C. S. Poon (2017). "Comparing the use of sewage sludge ash and glass powder in cement mortars." Environmental Technology **38**(11): 1390-1398.

Cooper, R. J., T. M. Chang and E. R. Williams (2013). "Hydrated alkali metal ions: spectroscopic evidence for clathrates." Journal of Physical Chemistry A **117**(30): 6571-6579.

Cota, F. P., C. C. D. Melo, T. H. Panzera, A. G. Araújo, P. H. R. Borges and F. Scarpa (2015). "Mechanical properties and ASR evaluation of concrete tiles with waste glass aggregate." Sustainable Cities and Society **16**: 49-56.

Criscenti, L. J., J. D. Kubicki and S. L. Brantley (2006). "Silicate Glass and Mineral Dissolution: Calculated Reaction Paths and Activation Energies for Hydrolysis of a Q3 Si by H3O+ Using Ab Initio Methods." The Journal of Physical Chemistry A **110**(1): 198-206.

CSA (2014). Standard Practice for laboratory testing to demonstrate the effectiveness of supplementary cementing materials and lithium-based admixtures to prevent alkali–silica reaction in concrete (CSA A23.2-28A). In CSA A23.2-14 – Test methods and standard practices for concrete. CSA Group, Mississauga, Ontario, Canada, pp. 452–457.

CSA A23.2-14A (2019). Potential expansivity of aggregates (procedure for length change due to alkali-aggregate reaction in concrete prisms at 38 °C). In CSA A23.2-14 – Test methods and standard practices for concrete. CSA Group, Mississauga, Ontario, Canada.

CSA A23.2-25A. Test method for detection of alkali-silica reactive aggregate by accelerated expansion of mortar bars. In CSA A23.2-19 – Test methods and standard practices for concrete. CSA Group, Mississauga, Ontario, Canada.

CSA A23.2-28A (2014). Standard Practice for laboratory testing to demonstrate the effectiveness of supplementary cementing materials and lithium-based admixtures to prevent alkali-silica reaction in concrete. In CSA A23.2-14 – Test methods and standard practices for concrete. CSA Group, Mississauga, Ontario, Canada.

CSA A3000 (2018). Cementitious materials compendium. CSA Group, Mississauga, Ontario, Canada, 257p.

CSI (2009) Cement Industry Energy and $CO_2$ Performance,"Getting the Numbers Right". World Business Council for Sustainable Development

Davraz, M. and L. Gündüz (2008). "Reduction of alkali silica reaction risk in concrete by natural (micronised) amorphous silica." Construction and Building Materials **22**(6): 1093-1099.

Dent Glasser, L. S. and N. Kataoka (1981). "The chemistry of 'alkali-aggregate' reaction." Cement and Concrete Research **11**(1): 1-9.

Dhir, R. K., T. Dyer and M. Tang (2009). "Alkali-silica reaction in concrete containing glass." Materials and structures **42**(10): 1451-1462.

Diamond, S. (1989). ASR-Another Look at Mechanisms. 8th Eight International Conference on Alkali–

Diamond, S. and R. Barneyback Jr (1981). Physics and chemistry of alkali-silica reactions. Master, Purdue University.

Diamond, S. and S. Ong (1994). "Effects of added alkali hydroxides in mix water on long-term SO42− concentrations in pore solution." Cement and Concrete Composites **16**(3): 219-226.

Dove, P. M. and C. J. Nix (1997). "The influence of the alkaline earth cations, magnesium, calcium, and barium on the dissolution kinetics of quartz." Geochimica et Cosmochimica Acta **61**(16): 3329-3340.

Dove, P. M. and S. F. Elston (1992). "Dissolution kinetics of quartz in sodium chloride solutions: Analysis of existing data and a rate model for 25°C." Geochimica et Cosmochimica Acta **56**(12): 4147-4156.

Dove, P. M., N. Han and J. J. De Yoreo (2005). "Mechanisms of classical crystal growth theory explain quartz and silicate dissolution behavior." Proceedings of the National Academy of Sciences **102**(43): 15357-15362.

Dove, P. M., N. Han, A. F. Wallace and J. J. D. Yoreo (2008). "Kinetics of amorphous silica dissolution and the paradox of the silica polymorphs." Proceedings of The National Academy of Sciences **105**(29): 9903-9908.

Du, H. and Tan, K. H. (2017). "Properties of high volume glass powder concrete." Cement and Concrete Composites **75**: 22-29.

Duchesne, J. and E. J. Reardon (1995). "Measurement and prediction of portlandite solubility in alkali solutions." Cement and Concrete Research **25**(5): 1043-1053.

Duchesne, J. and M. A. Bérubé (1994). "The effectiveness of supplementary cementing materials in suppressing expansion due to ASR: Another look at the reaction mechanisms part 2: Pore solution chemistry." Cement and Concrete Research **24**(2): 221-230.

Duchesne, J. and M. A. Bérubé (1994). *"The effectiveness of supplementary cementing materials in suppressing expansion due to ASR: Another look at the reaction mechanisms part 1: Concrete expansion and portlandite depletion."* Cement and Concrete Research **24**(1): 73-82.

Duchesne, J. and M. A. Bérubé (1995). "Effect of supplementary cementing materials on the composition of cement hydration products." Advanced Cement Based Materials 2(2): 43-52.

Duchesne, J. and M.-A. Bérubé (2001). "Long-term effectiveness of supplementary cementing materials against alkali–silica reaction." Cement and Concrete Research 31(7): 1057-1063.

Elsen, J., J. Desmyter and E. Soers (2003). "Alkali-Silica reaction in concrete in Belgium-a review." Aardkundige Mededelingen (Industrial minerals: resources, characteristics and applications) **13**: 73-79.

Fernández, Á., J. L. García Calvo and M. C. Alonso (2018). "Ordinary Portland Cement composition for the optimization of the synergies of supplementary cementitious materials of ternary binders in hydration processes." Cement and Concrete Composites **89**: 238-250

Fily-Paré, I. and Lafrenière, C. (2017), Unpublished

Fily-Paré, I., B. Fournier, J. Duchesne and A. Tagnit-Hamou (2017). "Effect of glass powder on the pore solution of cement pastes". 10th ACI/RILEM International conference on cementitious materials and alternative binders for sustainable concrete, Montréal.

Fily-Paré, I., B. Fournier, J. Duchesne and A. Tagnit-Hamou (2020). "Impact of NaOH addition on the ASR expansion of ternary concrete incorporating Ground Glass (GG)". 16th International Conference on Alkali Aggregate Reaction in Concrete. Lisboa, Portugal.

Fournier, B. and M.-A. Bérubé (2000). "Alkali-aggregate reaction in concrete: a review of basic concepts and engineering implications." Canadian Journal of Civil Engineering **27**(2): 167-191.

Fournier, B., A. Bilodeau, N. Bouzoubaa, P.C. Nkinamubanzi (2018). "Field and Laboratory Investigations on the Use of Fly Ash and Li-Based Admixtures to Prevent ASR in Concrete". Sixth International Conference on the Durability of Concrete Structures, 18-20 July 2018, University of Leeds, Leeds.

Fournier, B., Nkinamubanzi, P.C., Chevrier, R., Ferro, A. (2008): *"Evaluation of the effectiveness of high-calcium fly ashes in reducing expansion due to alkali-silica reaction in concrete".* Electric Power Research Institute (EPRI), Palo Alto (USA), 1014271.

Fournier, B., P.C. Nkinamubanzi, R. Chevrier, R. (2004). "Comparative field and laboratory investigations on the use of supplementary cementing materials to control alkali-silica reaction in concrete". 12th

International conference on Alkali-Aggregate Reaction (AAR) in Concrete, Beijing (China), October 2004, Tang and Deng Editors, International Academic Publishers, Beijing World Publishing Corp., 1: 528-537.

Fournier, B., R. Chevrier, A. Bilodeau, P.C. Nkinamubanzi, and N. Bouzoubaa (2016). "Comparative field and laboratory investigations on the use of supplementary cementing materials (SCMs) to control alkali-silica reaction in concrete". 15th International Conference on alkali-aggregate reaction (AAR) in concrete, July 2016, Sao Paulo (Brazil), 10p.

Gao, X. X., M. Cyr, S. Multon and A. Sellier (2013). "A comparison of methods for chemical assessment of reactive silica in concrete aggregates by selective dissolution." Cement and Concrete Composites **37**(0): 82-94.

Garcia-Diaz, E., J. Riche, D. Bulteel and C. Vernet (2006). "Mechanism of damage for the alkali–silica reaction." Cement and Concrete Research **36**(2): 395-400.

Gholizadeh-Vayghan, A. and F. Rajabipour (2017). "The influence of alkali–silica reaction (ASR) gel composition on its hydrophilic properties and free swelling in contact with water vapor." Cement and Concrete Research **94** (Supplement C): 49-58.

Glasser, L. D. and N. Kataoka (1981). "The chemistry of 'alkali-aggregate'reaction." Cement and Concrete Research 11(1): 1-9.

Glasser, L. S. D. (1979). "Osmotic pressure and the swelling of gels." Cement and Concrete Research **9**(4): 515-517.

Golafshani, E. M. and A. Behnood (2019). "Estimating the optimal mix design of silica fume concrete using biogeography-based programming." Cement and Concrete Composites **96**: 95-105.

Gudmundsson, G. and H. Olafsson (1999). "Alkali-silica reactions and silica fume: 20 years of experience in Iceland." Cement and Concrete Research **29**(8): 1289-1297.

Helmuth, R., D. Stark, S. Diamond and M. Moranville-Regourd (1993). "Alkali-silica reactivity: an overview of research." Contract **100**: 202.

Hong, S.-Y. and F. Glasser (1999). "Alkali binding in cement pastes: Part I. The CSH phase." Cement and Concrete Research **29**(12): 1893-1903.

Hong, S.-Y. and F. P. Glasser (2002). "Alkali sorption by C-S-H and C-A-S-H gels: Part II. Role of alumina." Cement and Concrete Research **32**(7): 1101-1111.

Hou, X., L. J. Struble and R. J. Kirkpatrick (2004). "Formation of ASR gel and the roles of C-S-H and portlandite." Cement and Concrete Research **34**(9): 1683-1696.

Hu, C., B. P. Gautam and D. K. Panesar (2018). "Nano-mechanical properties of alkali-silica reaction (ASR) products in concrete measured by nano-indentation." Construction and Building Materials **158**: 75-83.

Huang W, Kazemi-Kamyab H, Sun W, Scrivener K (2017) Effect of replacement of silica fume with calcined clay on the hydration and microstructural development of eco-UHPFRC. Materials & Design 121:36-46. doi:10.1016/j.matdes.2017.02.052

Idir, R., M. Cyr and A. Tagnit-Hamou (2010). "Use of fine glass as ASR inhibitor in glass aggregate mortars." Construction and Building Materials 24(7): 1309-1312.

Idir, R., M. Cyr and A. Tagnit-Hamou (2011). "Pozzolanic properties of fine and coarse color-mixed glass cullet." Cement and Concrete Composites **33**(1): 19-29.

IEA I, Energy Agency) (2014) Energy Policies of IEA Countries : The United States.

IEA/WBCSD (2009) Cement Technology Roadmap 2009. In: Publication I (ed) Carbon emission reduction up to 2050

Imberti, S., A. Botti, F. Bruni, G. Cappa, M. A. Ricci and A. K. Soper (2005). "Ions in water: The microscopic structure of concentrated hydroxide solutions." The Journal of Chemical Physics **122**(19).

Jiang, W. (1997). Alkali-activated cementitious materials: Mechanisms, microstructure and properties, ProQuest LLC.

Johnston, C. (1974). "Waste glass as coarse aggregate for concrete." ASTM Journal of Testing and Evaluation **2**(5).

Kamali, M. and A. Ghahremaninezhad (2015). "Effect of glass powders on the mechanical and durability properties of cementitious materials." Construction and Building Materials **98**: 407-416.

Kamali, M. and A. Ghahremaninezhad (2016). "An investigation into the hydration and microstructure of cement pastes modified with glass powders." Construction and Building Materials 112: 915-924.

Karamberi, A., E. Chaniotakis, D. Papageorgiou and A. Moutsatsou (2006). ″Influence of glass cullet in cement pastes.″ China Particuology **4**(5): 234-237.

Karamberi,A., Chaniotakis,E., Papageorgiou, D.and Moutsatsou, A. (2006). "Influence of glass cullet in cement pastes." China Particuology **4**(5): 234-237.

Katayama, T. (2012). ASR gels and their crystalline phases in concrete—universal products in alkali–silica, alkali–silicate and alkali–carbonate reactions. Proceedings of the 14th International Conference on Alkali Aggregate Reactions (ICAAR), Austin, Texas.

Katayama, T., T.S. Helgason, and H. Olafsson (1996). Petrography and alkali reactivity of some volcanic aggregates from Iceland. Proceedings of the10th International Conference, Melbourne, Australia.

Ke-rui, Y., Z. Cai-wen Z., Zhi-gang, G. Zhi and N. Cong (2004). A study on alkali-fixation ability of CSH gel. Proceedings of the 12th International Conference on Alkali-Aggregate Reaction in Concrete (ICAAR), Beijing, China **120:** 2.

Kou, S. C. and C. S. Poon (2009). "Properties of self-compacting concrete prepared with recycled glass aggregate." Cement and Concrete Composites **31**(2): 107-113.

Kupwade-Patil, K. and E. N. Allouche (2013). "Impact of alkali silica reaction on fly ash-based geopolymer concrete." Journal of Materials in Civil Engineering **25**(1): 131-139.

Labbez, C., Pochard,I. Jönsson, B. and Nonat, A, (2011). "C-S-H/solution interface: Experimental and Monte Carlo studies." Cement and Concrete Research **41**(2): 161-168.

Lafrenière, C. (2017). "Évaluation du comportement en durabilité de nouvelles matrices cimentaires pour l'obtention de bétons respectueux de l'environnement". Master thesis, Université Laval, https://corpus.ulaval.ca/jspui/handle/20.500.11794/27591.

Lam, C. S., C. S. Poon and D. Chan (2007). "Enhancing the performance of pre-cast concrete blocks by incorporating waste glass – ASR consideration." Cement and Concrete Composites **29**(8): 616-625.

Lane, D. S. and C. Ozyildirim (1999). "Preventive measures for alkali-silica reactions (binary and ternary systems)." Cement and Concrete Research **29**(8): 1281-1288.

Lawson, J. (2014). Design and Analysis of Experiments with R, Taylor & Francis.

Lawson, J. and C. Willden (2016). "Mixture experiment in R using mixexp." Journal of Statistical Software 72.

Lee, G., T.-C. Ling, Y.-L. Wong and C.-S. Poon (2011). "Effects of crushed glass cullet sizes, casting methods and pozzolanic materials on ASR of concrete blocks." Construction and Building Materials **25**(5): 2611-2618.

Leemann, A. and B. Lothenbach (2008). "The influence of potassium–sodium ratio in cement on concrete expansion due to alkali-aggregate reaction." Cement and Concrete Research **38**(10): 1162-1168.

Leemann, A., G. Le Saout, F. Winnefeld, D. Rentsch and B. Lothenbach (2011). "Alkali-Silica Reaction: the Influence of Calcium on Silica Dissolution and the Formation of Reaction Products." Journal of the American Ceramic Society **94**(4): 1243-1249. .

Leemann, A., T. Katayama, I. Fernandes and M. A. T. M. Broekmans (2016). Types of alkli–aggregate reactions and the products formed." Construction Materials **169**(CM3): 117-178.

Lenth, R. V. (2009). "Response-Surface Methods in R, Using rsm." Journal of Statistical software 32(7): 1-17.

Li Z, Thomas RJ, Peethamparan S (2019) Alkali-silica reactivity of alkali-activated concrete subjected to ASTM C 1293 and 1567 alkali-silica reactivity tests. Cement and Concrete Research 123. doi:10.1016/j.cemconres.2019.105796

Lindgård, J., M. D. A. Thomas, E. J. Sellevold, B. Pedersen, Ö. Andiç-Çakır, H. Justnes and T. F. Rønning (2013). "Alkali–silica reaction (ASR)—performance testing: Influence of specimen pre-treatment, exposure conditions and prism size on alkali leaching and prism expansion." Cement and Concrete Research **53**(0): 68-90.

Liu, S., S. Wang, W. Tang, N. Hu and J. Wei (2015). "Inhibitory effect of waste glass powder on ASR expansion induced by waste glass aggregate." Materials 8(10): 6849-6862.

Lu, J.-X., B.-J. Zhan, Z.-H. Duan and C. S. Poon (2017). "Using glass powder to improve the durability of architectural mortar prepared with glass aggregates." Materials & Design **135**: 102-111.

Mahler, J. and I. Persson (2012). "A study of the hydration of the alkali metal ions in aqueous solution." Inorganic Chemistry **51**(1): 425-438.

Maraghechi H, Maraghechi M, Rajabipour F, Pantano CG (2014) Pozzolanic reactivity of recycled glass powder at elevated temperatures: Reaction stoichiometry, reaction products and effect of alkali activation. Cement and Concrete Composites 53 (0):105-114. Doi: http://dx.doi.org/10.1016/j.cemconcomp.2014.06.015

Maraghechi H, Salwocki S, Rajabipour F (2017) Utilisation of alkali activated glass powder in binary mixtures with Portland cement, slag, fly ash and hydrated lime. Materials and Structures 50 (1):16

Maraghechi, H. (2014). "Development and assessment of alkali activated recycled glass-based concretes for civil infrastructure." Ph. D. Thesis, Pennsylvania State University.

Maraghechi, H., F. Rajabipour, C. G. Pantano and W. D. Burgos (2016). "Effect of calcium on dissolution and precipitation reactions of amorphous silica at high alkalinity." Cement and Concrete Research **87**: 1-13.

Maraghechi, H., M. Maraghechi, F. Rajabipour and C. G. Pantano (2014). "Pozzolanic reactivity of recycled glass powder at elevated temperatures: Reaction stoichiometry, reaction products and effect of alkali activation." Cement and Concrete Composites **53**(0): 105-114.

Maraghechi, H., S. Salwocki and F. Rajabipour (2017). "Utilisation of alkali activated glass powder in binary mixtures with Portland cement, slag, fly ash and hydrated lime." Materials and Structures **50**(1): 16.

Maraghechi, H., S.-M.-H. Shafaatian, G. Fischer and F. Rajabipour (2012). "The role of residual cracks on alkali silica reactivity of recycled glass aggregates." Cement and Concrete Composites **34**(1): 41-47.

Matos, A. M. and J. Sousa-Coutinho (2012). "Durability of mortar using waste glass powder as cement replacement." Construction and Building Materials **36**(0): 205-215.

Mejdi, M., W. Wilson, M. Saillio, T. Chaussadent, L. Divet and A. Tagnit-Hamou (2019). "Investigating the pozzolanic reaction of post-consumption glass powder and the role of portlandite in the formation of sodium-rich C-S-H." Cement and Concrete Research 123.

Montgomery, D. C. (2012). Design and Analysis of Experiments, 8th Edition, John Wiley & Sons, Incorporated.

Montgomery, D. C. and G. C. Runger (2010). Applied Statistics and Probability for Engineers, 5th edition.

Mukherjee, P.K. and J.A. Bickley (1986). Performance of glass as a concrete aggregate. 7th international conference on alkali aggregate reaction. Ottawa.

Myers, R. H., D. C. Montgomery and C. M. Anderson-Cook (2011). Response Surface Methodology: Process and Product Optimization Using Designed Experiments, Wiley.

Omran, A. and A. Tagnit-Hamou (2016). "Performance of glass-powder concrete in field applications." Construction and Building Materials 109: 84-95.

Omran, A. F., E. D.-Morin, D. Harbec and A. Tagnit-Hamou (2017). "Long-term performance of glass-powder concrete in large-scale field applications." Construction and Building Materials 135: 43-58.

Omran, A., D. Harbec, A. Tagnit-Hamou and R. Gagne (2017). "Production of roller-compacted concrete using glass powder: Field study." Construction and Building Materials 133: 450-458.

Parghi, A. and M. Shahria Alam (2016). *"*Physical and mechanical properties of cementitious composites containing recycled glass powder (RGP) and styrene butadiene rubber (SBR)*."* Construction and Building Materials **104**: 34-43.

Pereira-de-Oliveira, L. A., J. P. Castro-Gomes and P. Santos (2012). "The potential pozzolanic activity of glass and red-clay ceramic waste as cement mortars components." Construction and Building Materials **31**: 197-203.
Rajabipour, F., E. Giannini, C. Dunant, J. H. Ideker and M. D. A. Thomas (2015). "Alkali–silica reaction: Current understanding of the reaction mechanisms and the knowledge gaps." Cement and Concrete Research **76**: 130-146.

Rajabipour, F., H. Maraghechi and G. Fischer (2010). "Investigating the alkali-silica reaction of recycled glass aggregates in concrete materials." Journal of Materials in Civil Engineering 22(12): 1201-1208.

Rajabipour, F., H. Maraghechi and S. Shafaatian (2012). ASR and its mitigation in mortar containing recycled soda-lime glass aggregates. **.** Proceedings of the 14th International Conference on Alkali Aggregate Reactions (ICAAR), Austin, Texas.

Ramlochan, T., M.D.A. Thomas, K.A. Gruber (2000). "The effect of metakaolin on alkali-silica reaction in concrete". Cement and Concrete Research 30 (3) (2000) 339–344.

Ramsey F, Schafer D (2002) Inference using t distribution. In: Brooks/Cole CL (ed) The statistical sleuth.

Redden, R. and N. Neithalath (2014). "Microstructure, strength, and moisture stability of alkali activated glass powder-based binders." Cement and Concrete Composites **45**: 46-56.

Rehman, S., S. Iqbal and A. Ali (2018). "Combined influence of glass powder and granular steel slag on fresh and mechanical properties of self-compacting concrete." Construction and Building Materials **178**: 153-160.

Rodier, L. and H. Savastano (2018). "Use of glass powder residue for the elaboration of eco-efficient cementitious materials." Journal of Cleaner Production **184**: 333-341.

Rogers, C. A. and R. D. Hooton (1991). *"Reduction in mortar and concrete expansion with reactive aggregates due to alkali leaching."* Cement, Concrete and Aggregates **13**(1): 42-49.

Saccani, A. and M. C. Bignozzi (2010). *"ASR expansion behavior of recycled glass fine aggregates in concrete."* Cement and Concrete Research **40**(4): 531-536.

Saeed, H. (2008). *Glass powder blended cement hydration modelling.* PhD Thesis, Université de Sherbrooke.

Schwarz N, Cam H, Neithalath N (2008) Influence of a fine glass powder on the durability characteristics of concrete and its comparison to fly ash. Cement and Concrete Composites 30 (6):486-496

Scrivener K, Martirena F, Bishnoi S, Maity S (2018) Calcined clay limestone cements (LC3). Cement and Concrete Research 114:49-56. doi:10.1016/j.cemconres.2017.08.017

Serpa, D., A. Santos Silva, J. de Brito, J. Pontes and D. Soares (2013). "ASR of mortars containing glass." Construction and Building Materials **47**(0): 489-495.

Shao, Q., K. Zheng, X. Zhou, J. Zhou and X. Zeng (2019). "Enhancement of nano-alumina on long-term strength of Portland cement and the relation to its influences on compositional and microstructural aspects." Cement and Concrete Composites **98**: 39-48.

Shao, Y., T. Lefort, S. Moras and D. Rodriguez (2000). *"Studies on concrete containing ground waste glass."* Cement and Concrete Research **30**(1): 91-100.

Shayan, A. and A. Xu (2006). "Performance of glass powder as a pozzolanic material in concrete: A field trial on concrete slabs." Cement and Concrete Research **36**(3): 457-468.

Shehata, M. H. (2001). "The effects of fly ash and silica fume on alkali-silica reaction in concrete". Ph.D Thesis, University of Toronto.

Shehata, M. H. (2001). *The effects of fly ash and silica fume on alkali-silica reaction in concrete*. Ph.D PhD Thesis, University of Toronto.

Shehata, M. H. and M. D. A. Thomas (2000). "The effect of fly ash composition on the expansion of concrete due to alkali–silica reaction." Cement and Concrete Research 30(7): 1063-1072.

Shehata, M. H. and M. D. A. Thomas (2002). "Use of ternary blends containing silica fume and fly ash to suppress expansion due to alkali–silica reaction in concrete." Cement and Concrete Research 32(3): 341-349.

Shehata, M. H., M. D. A. Thomas and R. F. Bleszynski (1999). "The effects of fly ash composition on the chemistry of pore solution in hydrated cement pastes." Cement and Concrete Research 29(12): 1915-1920.

Shehata, M.H., M.D.A. Thomas (2002). "Use of ternary blends containing silica fume and fly ash to suppress expansion due to alkali-silica reaction in concrete". Cement and Concrete Research 32 (3): 341–349.

Shevchenko, V. (2012). "ASR effect in glasses used as additives to Portland cement." Glass Physics and Chemistry 38(5): 466-471.

Shi C, Wu Y, Shaob Y, C (2004) Alkali-Aggregate Reaction Expansion of Mortar Bars Containing Ground Glass Powder. Paper presented at the age, Pekin,

Shi, C. and K. Zheng (2007). *"A review on the use of waste glasses in the production of cement and concrete."* Resources, Conservation and Recycling **52**(2): 234-247.

Shi, C., Y. Wu, C. Riefler and H. Wang (2005). *"Characteristics and pozzolanic reactivity of glass powders."* Cement and Concrete Research **35**(5): 987-993.

Shi, C., Y. Wu, Y. Shaob and C. Riefler (2004). "Alkali-Aggregate Reaction Expansion of Mortar Bars Containing Ground Glass Powder". age. Pekin. **20:** 10.

Stade, H. (1989). "On the reaction of C-S-H(di, poly) with alkali hydroxides." Cement and Concrete Research **19**(5): 802-810.
Stanton, T. E. (1940). "Expansion of Concrete through Reaction between Cement and Aggregate." Proceedings of the Americain Society of Civil Engineer **66**(10): 1871-1811.

Struble, L. J. and S. Diamond (1981). "Swelling properties of synthetic alkali silica gels." Journal of the American ceramic society **64**(11): 652-655.

Taha, B. and G. Nounu (2008). *"Using lithium nitrate and pozzolanic glass powder in concrete as ASR suppressors."* Cement and Concrete Composites **30**(6): 497-505.

Team, R. C. (2013). R: A Language and Environment for Statistical Computing, R Foundation for Statistical Computing.

Team, R. C. (2013). R: A Language and Environment for Statistical Computing, R Foundation for Statistical Computing.

Thomas MDA, Fournier B, Folliard KJ (2013) Alkali-Aggregate Reactivity (AAR) Facts Book. U.S. Dept of Transportation edn.,

Thomas, M. (2011). "The effect of supplementary cementing materials on alkali-silica reaction: A review." Cement and Concrete Research **41**(12): 1224-1231.

Thomas, M. D. A., B. Fournier and K. J. Folliard (2013). "Alkali-Aggregate Reactivity (AAR) Facts Book 212.

Thomas, M., B. Fournier, K. Folliard, J. Ideker and M. Shehata (2006). "Test methods for evaluating preventive measures for controlling expansion due to alkali–silica reaction in concrete." Cement and Concrete Research 36(10): 1842-1856.

Thomas, M.D.A. and F.A. Innis (1998). “Effect of slag on expansion due to alkali- aggregate reaction in concrete". ACI Materials Journal 95(6).

U.Laval, D. d. m. e. d. s. d. (2010). "aide-mémoire-stt." Retrieved june, 2018, from https://www.mat.ulaval.ca/fileadmin/mat/documents/CDA/aide-mémoire-mat.pdf.

Vance, K., A. Kumar, G. Sant and N. Neithalath (2013). "The rheological properties of ternary binders containing Portland cement, limestone, and metakaolin or fly ash." Cement and Concrete Research **52**: 196-207.

Vaux, D. L., F. Fidler and G. Cumming (2012). *"Replicates and repeats—what is the difference and is it significant?"* EMBO reports **13**(4): 291-296.

Vézina, D., J. Frenette, M.-A. Bérubé and M. Rivest (2002). *"Measurement of the alkali content of concrete using hot-water extraction."* Cement, concrete and aggregates **24**(1): 28-36.

Viallis,H., Faucon, P., Petit,J.C. and Nonat, A.(1999). "Interaction between Salts (NaCl, CsCl) and Calcium Silicate Hydrates (C−S−H)." The Journal of Physical Chemistry B **103**(23): 5212-5219.

Visser, J. H. M.(2018). "Fundamentals of alkali-silica gel formation and swelling: Condensation under influence of dissolved salts." Cement and Concrete Research **105**: 18-30.

Vollpracht, A., B. Lothenbach, R. Snellings and J. Haufe (2015). "The pore solution of blended cements: a review." Materials and Structures 49(8): 3341-3367.

Wallace, A. F, G.V. Gibbs and P.M. Dove (2010). "Influence of Ion-Associated Water on the Hydrolysis of Si−O Bonded Interactions." The Journal of Physical Chemistry A **114**(7): 2534-2542.

Warner, S., J. Ideker and K. Schumacher (2012). Alkali-silica reactivity and the role of alumina. International Conference on Alkali Reaction. Austin, Texas.

Wikipedia (2019), https://en.wikipedia.org/wiki/Aqueous_solution

Willona S (2019) 2019 Brings New Changes for Municipal Glass Recycling. https://www.waste360.com/glass/2019-brings-new-changes-municipal-glass-recycling.

Wilson, W., L. Sorelli and A. Tagnit-Hamou (2018). "Automated coupling of NanoIndentation and Quantitative Energy-Dispersive Spectroscopy (NI-QEDS): A comprehensive method to disclose the micro-chemo-mechanical properties of cement pastes." Cement and Concrete Research **103**: 49-65.

Wu, Z., K. H. Khayat and C. Shi (2019). "Changes in rheology and mechanical properties of ultra-high performance concrete with silica fume content." Cement and Concrete Research **123**.

Yang, Y., T. Ji, X. Lin, C. Chen and Z. Yang (2018). "Biogenic sulfuric acid corrosion resistance of new artificial reef concrete." Construction and Building Materials **158**: 33-41.

Zhang, L. and Y. Yue (2018). "Influence of waste glass powder usage on the properties of alkali-activated slag mortars based on response surface methodology." Construction and Building Materials **181**: 527-534.

Zhang, L. and Y. Yue (2018). "Influence of waste glass powder usage on the properties of alkali-activated slag mortars based on response surface methodology." Construction and Building Materials **181**: 527-534.

Zhang, S., A. Keulen, K. Arbi and G. Ye (2017). "Waste glass as partial mineral precursor in alkali-activated slag/fly ash system." Cement and Concrete Research 102: 29-40.

Zheng, K. (2016). "Pozzolanic reaction of glass powder and its role in controlling alkali–silica reaction." Cement and Concrete Composites 67: 30-38.

Zhuravlev, L. T. (2000). "The surface chemistry of amorphous silica. Zhuravlev model." Colloids and Surfaces A: Physicochemical and Engineering Aspects **173**(1): 1-38.

Zidol A (2009) Optimisation de la finesse de la poudre de verre dans les systèmes cimentaires binaires. Université de Sherbrooke,